Series II, Volume 4 March 30, 1959 Number 3

BULLETIN

OF THE

AMERICAN PHYSICAL SOCIETY

INCLUDING THE

PROGRAMME OF THE

1959 MARCH MEETING

AT

CAMBRIDGE, MASSACHUSETTS

March 30, 31, and April 1–2, 1959

PUBLISHED BY THE AMERICAN PHYSICAL SOCIETY, COLUMBIA UNIVERSITY, NEW YORK 27, NEW YORK
EIGHT ISSUES EACH YEAR

BULLETIN

of the

AMERICAN PHYSICAL SOCIETY

Published eight times per year

Subscription price: $5.00 per year

Back number prices: $4.00 for the triennial Membership List; $1.00 for other issues.

The Bulletin of the American Physical Society is published eight times a year, once in January, twice in March, once in April, once in June, once in August, once in November, and once in December, at Prince and Lemon Streets, Lancaster, Pennsylvania. Correspondence should be addressed to American Physical Society, Columbia University, New York 27, New York.

Entered as second class matter, December 27, 1949, at the post office at Lancaster, Pa., under the Act of August 24, 1912.

Acceptance for mailing at a special rate of postage provided for in paragraph (d-2), Section 34.40, P. L. & R. of 1948, authorized Nov. 30, 1948.

Table of Contents

Page

Programme of the 1959 "March" Meeting at Cambridge:

Preamble 126

Epitome 128

Main Text 129

Index 190

Announcement of the 1959 Spring Meeting 193

Minutes of the 1958 Meeting of the Division of Fluid Dynamics 193

Calendar of Prospective Meetings and Deadlines 206

Rules and Instructions for the Preparation of Abstracts 206

Map of MIT 207

Reservation forms for the Banquet and Social Hour at Cambridge 209

March 30, 1959 Series II, Vol. 4, No. 3

BULLETIN

OF THE

AMERICAN PHYSICAL SOCIETY

1959 "March" Meeting at MIT, Cambridge, Massachusetts, March 30, 31, and April 1–2, 1959

THE American Physical Society will hold its **1959 "March" meeting** in Cambridge, Massachusetts, in the buildings of the Massachusetts Institute of Technology ("MIT") on Monday, Tuesday, Wednesday, and Thursday, March 30, 31, April 1, and 2. This is called the "March" meeting even though it spreads over into April, for it is one—and, in fact, the tenth—of the March meetings instituted in 1950 by the Council to serve primarily the interests of the Divisions. Those which take advantage of it are, in chronological order of their foundation, the Divisions of High-Polymer Physics, of Solid-State Physics, and of Chemical Physics. This meeting has other anomalies beyond those of its month dates. It is on Monday, Tuesday, Wednesday, and Thursday, not on the last three days of the week as is our usual though not unbroken custom. It is a four-day and yet a three-day convention, for the Division of High-Polymer Physics omits Monday and all the other sessions are over by Wednesday. It is a meeting in which the sessions are in one city and the headquarters hotel in another. Finally (for the moment) it is in number of contributed papers the largest March meeting ever, having crossed the 300 mark which I arbitrarily take as the dividing line between a medium-sized meeting and a big one. The Chairman of the Local Committee for this large enterprise is J. C. Slater of MIT.

The **headquarters hotel** is the Somerset, in *Boston*. Some of our members will be placed in the Kenmore Hotel, others perhaps elsewhere, but all should write to the Somerset for their reservations: do not forget to mention that you are coming to our meeting!

The **registration desk** will be located just inside the main entrance of MIT on Massachusetts Avenue; this area is designated as the lobby of Building T (see map on page 207). Banquet tickets will be sold there, and tickets for the Social Hour. Post-deadline papers, if any, will be announced on a blackboard near the desk. There will be a special blackboard for notice of messages: the privilege of using this is accorded only to those who pay the registration fee. The **registration fee** will be $1.50—one dollar and a half. As our meetings climb in size, they tend to climb faster in expensiveness.

The **invited papers** of this meeting belong to four groups.

The **Oliver E. Buckley Lecture,** to be given by Conyers Herring under the title "Transport Properties of Nearly Pure Semiconductors," constitutes Session LA to begin at 11:15 on Tuesday morning.

Invited papers of the Division of High-Polymer Physics will be found in Sessions N, S, Y, Z, and ZA.

Invited papers of the Division of Chemical Physics are grouped in Session M with the melancholy motive of commemorating William Moffitt, who suddenly departed this life on December 19. It is the firm rule of the Council that not more than one name may be attached to an invited paper, but for two of the papers this rule has been infringed by coupling other names with that of Dr. Moffitt who had collaborated in the work.

Invited papers of the Division of Solid-State Physics constitute the numerous remainder. Eighteen of these are grouped in the five sessions DA, E, L, T, and U, for which no captions were offered nor did the Secretary feel capable of devising any that should be descriptive. Others figure at the beginnings or ends of sessions of contributed papers.

Three hundred and twenty-three contributed papers (the previous record for a March meeting was 260!) are distributed among thirty-four sessions. These also must be characterized in more detail.

The Division of High-Polymer Physics, by special notice to its members, endeavors to have all of the abstracts in its field sent to one of its officers, who arranges them and transmits them to the office of the Society. Such papers will be found in Sessions

N, S, Y, Z, and ZA. But no fewer than fifteen other papers in the field were sent directly to this office, and they posed a problem. The Secretary would not mar the careful interweaving of contributed and invited papers achieved by the Divisional authorities, and so with their approval he has put all of the "nonchanneled" abstracts into a new session called K.

The Division of Chemical Physics asked its members to mark their abstracts for its own sessions. All abstracts so marked are accordingly included in sessions CA, HA, KA, and QA, and so are some others of which the topics seemed to indicate them for these destinations. The arrangement of the abstracts of these sessions was kindly accomplished by R. S. Halford, Vice-Chairman and *de facto* Chairman of the Division.

The Division of Solid-State Physics made no requests of its members. Modifications in the distribution of papers among sessions were made by its Secretary, E. Burstein, to whom the Secretary is indebted for placing the sessions relative to one another and for choosing the chairmen.

For some years the papers in "all the rest of physics"—nuclear and theoretical physics in particular—offered at the March meetings have been steadily waning in number, but now there is a sudden sharp reversal of the trend, partly but not wholly masked by the fact that many such papers have gone into the sessions on chemical physics. The Secretary is ashamed that it took him some time to guess the reason, which is, of course, the fascination of metropolitan Boston.

Another and most welcome oddity of this meeting is the fact that only two abstracts arrived late! The history of one of these is worth telling, to stress the admonition that special-delivery is usually useless and sometimes worse than useless. An envelope containing an abstract, postmarked in Brooklyn on January 15 (day before deadline) and mailed with special-delivery stamp, arrived at this office on January 19 (three days after deadline). It would have been cheaper and quicker to send this abstract by ordinary mail or to bring it by subway.

The **banquet of the Society** will be held on Tuesday evening at seven in the MIT Faculty Club at 50 Memorial Drive, Cambridge. We do not yet know at what hour we shall have to give a guarantee, but the earlier you buy your tickets the better it will be for you and the Local Committee, and better yet will it be to make use of the reservation form printed on page 209. The after-dinner speakers will be announced on the blackboard near the registration desk if not in these pages. The price will be three dollars.

A **social hour** with cocktails, in the MIT Faculty Club at 50 Memorial Drive, will begin at five o'clock on Monday afternoon. The price of participation will be a dollar and a half, and this will entitle the participant to two cocktails. Tickets will be sold at the registration desk; and as all precedents indicate that the demand will be greater than the supply, a prudent member will avail himself of the reservation form on page 209 of this Bulletin.

The **Council of the American Physical Society** will meet at eleven o'clock on Wednesday in the Moore Room, 6-321 (in MIT). It is expected that this will be a brief meeting devoted to routine business.

Business Meetings of the three Divisions are announced in the Epitome and the Main Text.

Post-deadline ten-minute papers, pertaining to very recent achievements of very special importance, will be considered for admission to a special supplementary programme if the abstracts are received at the office of the Society not later than Monday, March 23. The titles of such as are accepted will be displayed on a blackboard near the registration desk, and the papers will be given under the usual ten-minute rule at the end of Session R or perhaps in other places in the programme.

A **preliminary announcement** of the 1959 Spring Meeting at Washington is printed on page 193 of this Bulletin.

On page 206 are published the **calendar of meetings and deadlines for 1959,** and below it the **rules and instructions for the preparation of abstracts** which we commend to the attention of every member. By the way, there was an unusually large percentage of overlong abstracts among those submitted for this meeting. Footnotes had to vanish in such numbers as suggested that many of our members do not realize that a footnote counts as ten words, and there is reason to fear that the climaxes of some of the abstracts have vanished along with them.

Errata pertaining to the contents of this issue will be published in a later issue of this Bulletin if received not later than Monday, April 13, by Miss Ruth Bryans, American Institute of Physics, 335 East 45th Street, New York 17, N. Y. Do not send in your abstract marked with corrections! Write out the corrections in the form "Instead of . . . read . . . ." Add nothing.

KARL K. DARROW, *Secretary*
American Physical Society
Columbia University
New York 27, New York

EPITOME OF THE 1959 "MARCH" MEETING AT CAMBRIDGE

(Personal names are those of invited speakers. DSSP stands for Division of Solid-State Physics, DHPP for Division of High-Polymer Physics, DCP for Division of Chemical Physics.)

Monday Morning

10:00 A. Solid-state theory I (electron gas, bands). 10–250.
10:00 B. Toupin; mechanical properties of solids. 4–270.
10:00 BA. Braunstein; compound semiconductors. 4–370.
10:00 C. Irradiation effects I (metals). 6–120.
10:00 CA. General chemical physics. 26–100.
10:00 D. Cosmic rays; nuclear physics I. Kresge Little Theater.
10:00 DA. DSSP: Foner, Walsh, Nethercot, Arrott. Kresge Auditorium.

Monday Afternoon

2:15 E. DSSP: Pratt, Marshall, Freeman, Riste. Kresge Auditorium.
2:00 EA. Lundqvist: solid-state theory II. 6–120.
2:00 F. Impurities in semiconductors. 26–100.
2:00 FA. Wiegand; alkali halides and AgCl, including irradiation effects II. 4–270.
2:00 G. Matthias; cryogenics. 10–250.
2:15 H. Nuclear physics II; plasma physics. Kresge Little Theater.
2:15 HA. Chemical physics: experimental spectroscopy. 4–370. Social hour. MIT Faculty Club at 5:00

Tuesday Morning

9:30 I. Excitons. Kresge Little Theater.
9:30 IA. General theoretical physics. 6–120.
9:30 J. General solid-state physics. 4–270.
9:30 JA. Irradiation effects III: quartz, silica, etc. 10–250.
9:30 K. Polymeric papers not channeled via the Division. 26–100.
9:30 KA. Chemical physics of solids. 4–370.
10:00 L. DSSP: Bloembergen, Anderson. Kresge Auditorium.
11:15 LA. Oliver E. Buckley Lecture by Herring. Business Meeting of DSSP. Kresge Auditorium.

Tuesday Afternoon

2:15 M. DCP: Symposium in memory of William Moffitt: Gouterman-Moffitt, Moffitt-Goodman, Meyer, Van Vleck, Wilson. Kresge Auditorium.
2:00 N. DHPP: High-Polymer physics I; Rivlin, Gibbs. 26–100.
2:15 NA. Magnetic resonance. Kresge Little Theater.
2:15 O. Cohen; electronic properties of metals. 6–120.
2:15 P. Gibbs; dislocations and other defects. 10–250.

Tuesday Evening

7:00 Banquet of The American Physical Society. MIT Faculty Club.

Wednesday Morning

10:00 Q. Diffusion in metals. Kresge Little Theater.
10:00 QA. Chemical physics: theoretical. Business Meeting of DCP. 10–250.
10:00 R. X-ray and optical properties of metals; post-deadline papers, if any. 4–270.
10:00 RA. Magnetism I. 6–120.
10:00 S. DHPP: High-polymer physics II; Coleman, Maxwell. Business Session of DHPP. 26–100.
10:00 SA. General semiconductor physics. 4–370.
10:00 T. DSSP: Herman, Phillips, Marcus, Kaus. Kresge Auditorium.

Wednesday Afternoon

2:15 U. DSSP: Reitz, Fan, Overhauser, Lax. Kresge Auditorium.
2:00 UA. Thermal effects and order-disorder in metals. 6–120.
2:00 V. Magnetism II; ferroelectricity; Chynoweth. 10–250.
2:00 VA. Steele; transport phenomena in semiconductors. 4–270.
2:00 Y. DHPP; High-polymer physics III; Nielsen, Douglass. 26–100.

Thursday Morning

9:30 Z. DHPP: High-polymer physics IV; Krimm, Stein. 26–100.

Thursday Afternoon

2:00 ZA. DHPP: High-Polymer physics V; Flory, Hoeve, Zimm. 26–100.

PROGRAMME

MONDAY MORNING AT 10:00

Room 10–250

(J. M. LUTTINGER presiding)

Solid-State Theory I; Electron Gas, Bands

A1. Variational Principle and Transport Equations. G. E. TAUBER, *Western Reserve University and Franklin Institute Laboratories.*—It is known that the Boltzmann transport equation is equivalent to a variational principle, for which the variational function is simply related to the rate of change of the H function. The Boltzmann equation itself can be derived from Liouville's equation under special assumptions by a series of integrations in phase space. An appropriate generalization of the H function permits one then to express the reduced equations of motion also in terms of a variational principle. In quantum statistics Liouville's equation is replaced by $d\rho/dt=(\rho\mathbf{H}-\mathbf{H}\rho)$, where ρ is the density matrix and $\mathbf{H}$ the Hamiltonian of the system. From the density matrix a distribution function in phase space can be constructed, in terms of which the equations of motion in quantum statistics can be obtained. By a suitable definition of the H function an equivalent variational principle can be formulated for that case also.

A2. Synchronous Ensemble Theory. P. J. PRICE, *IBM Watson Laboratory.*—The steady nonequilibrium state of (e.g.) electrons in a crystal is conventionally represented by $f(\mathbf{p})$, the distribution function of the ensemble of all electrons at an arbitrary instant. Instead one may work with f_a, representing the ensemble of electron states immediately after a scattering, and f_b, representing the ensemble of states immediately before a scattering. It can be shown that f_b/f is proportional to the scattering frequency and that

$$f_a=\mathcal{L}^*f_b, \quad f_b=Q^*f_a,$$

where $\mathcal{L}^*$ and Q^* are integral operators previously defined.[1] Iterations of $\mathcal{L}^*Q^*$, starting with a "delta function" distribution, give the ensemble of possible "histories" of an electron, synchronized to successive collisions as a time scale. The theory promises to be useful for "hot electron" situations where surfaces of constant f deviate appreciably from surfaces of constant energy. It might be used to calculate the "differential mean free path."[1,2]

[1] P. J. Price, IBM J. Research Develop. 2, 200 (1958). The * signifies the operator's adjoint, defined in reference 8.
[2] P. J. Price, "On the theory of strong-field conduction," Proceedings of the 1958 International Conference on Semiconductors (to be published).

A3. Variational Approach to Hot Electrons. I. ADAWI, *RCA Laboratories.*—Kohler's variational method[1] has been extended to higher orders in the field for a nondegenerate electron gas using perturbation theory. Consequently, solution for the distribution function reduces to solving sets of linear algebraic equations. Therefore, corrections to Ohm's law can be given in terms of infinite determinants. It is shown that the "popular" Maxwellian distribution (with a new temperature) is nothing but a rough variational solution and cannot therefore, be reliable in general. The method has been applied to obtain deviations from Ohm's law in nonpolar crystals including scattering by optical and acoustical modes of lattice vibrations and ionized impurities. The E^3 term in the conductivity is given as the ratio of two infinite determinants. For many interesting situations, the elements of these determinants can be expressed in terms of the Bessel's functions K_0 and K_1 and other elementary functions.

[1] A. H. Wilson, *Theory of Metals* (Cambridge University Press, New York, 1954), second edition, Chap. X. References to original papers will be found there.

A4. Self-Consistent Field Approach to the Electron-Correlation Problem. H. EHRENREICH, *General Electric Research Laboratory,* AND MORREL H. COHEN, *University of Chicago.*—Lindhard's approach of describing a many-electron system by a time-dependent interaction of a single particle with a self-consistent electromagnetic field is shown to be equivalent to the treatment given by Sawada and Brout. To prove this, one considers the Liouville equation, $i\hbar\partial\rho/\partial t=[H,\rho]$ with $\rho=\rho_0+\rho_1$ and $H=p^2/2m+V$. One linearizes the problem by neglecting terms $\rho_1 V$ and determines the self-consistent potential V from Poisson's equation $\nabla^2 V=-4\pi e^2 Tr\{\delta(x_s-x)\rho_1\}$. The resultant equation of motion of the matrix elements $\langle k|\rho_1|k+q\rangle$ taken with respect to plane-wave states, is then found to be the same as that of the pair-creation operators $a_{k+q}^\dagger a_k$ in the many-electron formalism when the approximations characteristic of the Sawada-Brout scheme are made. These approximations are seen to correspond to (1) factorization of the two-particle density matrix and (2) linearization with respect to off-diagonal components of the one-particle density matrix. The present approach permits a straightforward calculation of the frequency-dependent dielectric constant, which is shown to be equivalent to that of Nozières and Pines in the random phase approximation. When applied to plasma oscillations in real solids, this approach yields very simply the results of the Nozières-Pines and other previous treatments.

A5. Exchange Energy of an Electron Gas in a Strong Magnetic Field.* G. DRESSELHAUS, *Cornell University.*—The magnetic field variation of the exchange energy of a free electron gas is calculated by deriving the form of the "Fermi hole" around each electron. The wave functions which are used exactly diagonalize the kinetic energy. The exchange energy, which for the alkali metals is larger in magnitude than the kinetic energy, is found to show the same periodicity in the reciprocal magnetic field which is displayed by the kinetic energy. The de-Haas-van-Alphen effect thus shows the same gross features which are derived considering only the oscillatory behavior of the kinetic energy alone.

* Supported in part by the Office of Naval Research.

A6. Theory of Bloch Electrons in a Magnetic Field: Effective One-Band Hamiltonian.* WALTER KOHN, *Carnegie Institute of Technology.*—The Hamiltonian of a Bloch electron in a static magnetic field is $H=\frac{1}{2}\mathbf{P}^2+V(\mathbf{r})$, where $V(\mathbf{r})$ is the periodic potential, $\mathbf{P}=\mathbf{p}+(1/c)\mathbf{A}$, and $\mathbf{A}$ is the vector potential giving rise to the magnetic field $\boldsymbol{\kappa}$. We consider the case of a a nondegenerate band m. It is then shown that, with an error vanishing with κ like κ^{N+1} (N arbitrary), the eigenstates of H can be calculated from an equivalent Hamiltonian $\tilde{H}_m(\mathbf{P})$ with the following properties. (1) It is a one-band Hamiltonian,

obtained by transforming away all relevant interband matrix elements. (2) It depends only on the gauge covariant operators P^{α}. (3) It has the periodicity property $\bar{H}_m(\mathbf{P}+\mathbf{K}_r)=\bar{H}_m(\mathbf{P})$, where $\mathbf{K}_r$ is an arbitrary reciprocal lattice vector. (4) It can be written as a series $\bar{H}_m(\mathbf{P})=\sum s^i \bar{H}_{m;i}(\mathbf{P})$ (summed over i from 0 to N) where $s=\kappa/c$ and the functions $\bar{H}_{m;i}(\mathbf{P})$ are completely symmetrized in the noncommuting operators P^{α}. Properties (3) and (4) can also be summarized in the equations $\bar{H}_m(\mathbf{P})=\sum a^{(l)} \exp[iR^{(l)}]\cdot P$, where the $R^{(l)}$ are lattice vectors and the $a^{(l)}$ can be expanded as $a^{(l)}=\sum s^i a_i^{(l)}$. An algorithm is given for the construction of the $\bar{H}_{m;i}$ and carried through for $i=0,1,2$. The formalism is not restricted to the neighborhood of the bottom and top of the band.

* Supported in part by the Office of Naval Research.

A7. Calculation of Wave Functions in Diamond- and Zinc-Blende-Type Crystals.* L. KLEINMAN† AND J. C. PHILLIPS,‡ *University of California, Berkeley.*—The method for calculating wave functions in metals and semiconductors which is based on the introduction of an effective potential to represent the interaction of valence electrons with the core is here applied to the calculation of energy bands and wave functions for diamond- and zinc-blende-type crystals. The term levels of the effective potential are compared with the free-atom term levels. The crystal potential is then represented as a superposition of atomic potentials. Results of the calculations for several crystals including diamond, Si, and AlP will be presented.

* Supported in part by the National Science Foundation.
† National Science Foundation Predoctoral Fellow.
‡ National Science Foundation Postdoctoral Fellow.

A8. Energy Bands in Alkali Metals. FRANK S. HAM, *General Electric Research Laboratory.*—Energy bands for all of the alkali metals have been calculated using the quantum defect method[1] and the variational procedure of Kohn and Rostoker.[2] These results confirm the anticipated efficiency of the Kohn-Rostoker procedure for calculations on one simple solid for several values of the lattice constant, or on several solids of similar lattice type, once tables of "structure constants" have been prepared, and provided that the approximation of the "muffin-tin" potential (potential constant outside the sphere inscribed in the cell and spherically symmetric inside) can be corrected for by perturbation theory. In particular, the convergence of the method is excellent. Calculations are therefore feasible not only at symmetry points but also at interior points of the Brillouin zone. Our calculations have been for points along the 100, 110, and 111 axes, and we find that in the conduction band and lower excited bands it suffices to limit the wave function expansion to terms with angular momentum $L=0,1,2,3$. Coefficients in this expansion can be obtained with fair accuracy.

[1] H. Brooks and F. S. Ham, Phys. Rev. 112, 344 (1958).
[2] W. Kohn and N. Rostoker, Phys. Rev. 94, 1111 (1954).

A9. Energy Bands in Potassium for Several One-Electron Potentials. LELAND C. ALLEN, *OMRO and MIT.*—A program for the Augmented Plane Wave method which exists for the MIT digital computer, Whirlwind, has been used to investigate the effect of modification of the assumed one-electron potential. Calculations were carried out for a number of states at each of the points Γ, H, P, and N in the Brillouin zone. The potentials used were those determined by Callaway[1] and comprised a Coulomb potential formed from the Hartree-Fock K^+ free ion solution as well as those made by the addition of several different exchange corrections. States at Γ were also obtained for a considerably reduced lattice parameter.

[1] J. Callaway, Phys. Rev. 103, 1219 (1956).

A10. Energy Bands in Iron.* J. H. WOOD, *MIT.*—Energy bands have been calculated for fcc and bcc iron using Slater's original augmented plane wave method.[1] Programs developed by M. M. Saffren for the Whirlwind computer allow one to obtain energy levels at any point in the Brillouin zone in a completely automatic fashion. The band structures have been calculated using the one-electron potential of Manning and Greene[2] using a maximum angular momentum $l=12$ in the expansion of the wave functions. A convergence study was also made of one of the d levels; here a maximum $l=19$ was used.

* Research supported by the Office of Naval Research.
[1] J. C. Slater, Phys. Rev. 51, 846 (1937).
[2] M. F. Manning, Phys. Rev. 63, 203 (1943).

A11. On the Band Structure of the bcc Transition Elements.* JOHN B. GOODENOUGH, *MIT.*—Cubic fields are assumed to split the d levels into a triply degenerate t_{2g} level with orbitals directed toward near neighbors, a doubly degenerate e_g level with orbitals directed toward next-near neighbors. If the t_{2g} orbitals are half-or-less filled, the direct exchange interactions are antiferromagnetic and it is assumed that the t_{2g} band is split into a bonding and an antibonding band. Further, intra-atomic exchange is assumed to stabilize a bonding s-p band so that there are approximately three s-p electrons/atom. If intra-atomic and near-neighbor exchange interactions are stronger than next-near-neighbor exchange interactions, interacting, next-near-neighbor e_g-electron spins are forced to be parallel; therefore e_g electrons are localized and the ferromagnetic, simple-cubic sublattices couple antiferromagnetically. With a very small overlap of e_g and bonding t_{2g} bands, the physical properties of the bcc phases of Ti, Zr; V, Nb, Ta; Cr, Mo, W; and Mn can be consistently interpreted. If the t_{2g} orbitals are more-than-half filled, a polarizable, metallic-type t_{2g} band is formed which is essentially ferromagnetic. Such ferromagnetism inhibits the formation of a bonding s-p band and couples localized e_g electrons ferromagnetically. The bcc Fe-Co alloys are discussed as illustrations of this situation.

* The work reported here was performed at Lincoln Laboratory, a technical center operated by MIT, with the joint support of the U. S. Army, Navy, and Air Force under contract.

A12. Approximate Band Structure of Beta Brass. M. F. AMSTERDAM, *Temple University and Frankford Arsenal* (introduced by L. Muldawer).—An approximation is obtained for the band structure of beta brass along five directions of high symmetry inside and on the surface of the Brillouin zone. The results should be correct to proper orders of magnitude, so that they should be useful in describing a model in terms of which experimental data may be meaningfully interpreted. The $3d$ bands are in effect calculated, using the tight-binding approximation, by adapting the two center integrals computed by Fletcher and Wohlfarth for the $3d$ bands of nickel in a manner similar to that demonstrated by Slater and Koster for iron. The $4s$-$4p$ bands are estimated by considering the perturbing effect of the periodic lattice potential on the energy bands for an "empty" cubic lattice. Essential features exhibited by this approximation include a splitting of the ten $3d$ bands into two sets of five, the deeper set being very narrow, and, in the valence bands, the possibility of certain transitions from the Fermi level to higher energy states. These transitions are between bands whose separation decreases with increasing magnitude of wave vector. It is possible to account for some observed optical properties of beta brasses in terms of absorbtion induced transitions between these bands.

A13. Random Walk Model for Excitation Transfer. HERBERT B. ROSENSTOCK, *U. S. Naval Research Laboratory.*—Consider a particle performing a random walk on a lattice. Let the lattice sites be of two kinds, "ordinary" sites and "absorb-

ing" sites, the latter having the property of terminating the walk by absorption if the particle chances upon it. Further, ascribe to the particle a definite probability per step of leaving the lattice abruptly by emission. We ask for the emission probability as a function of the concentration of "absorbing" sites. The problem can be straightforwardly solved for one-dimensional lattices,[1] but only under certain restrictions for two- and three-dimensional ones.[1,2] An inverse square dependence of the emission probability on the concentration of absorbing sites for high concentration of the latter is found, independent of dimensionality. The physical significance of the problem is in the decrease of luminescence of certain organic phosphors after damage by radiation.[3] Agreement with experiment[4] can be obtained only if the probability of absorption by an "absorbing" site is itself taken as smaller than one.

[1] W. Feller, *Introduction to Probability Theory* (John Wiley and Sons, Inc., New York, 1957), second edition, Chaps. 13 and 14.
[2] W. H. McCrea and F. J. W. Whipple, Proc. Roy. Soc. (Edinburgh) **60**, 281 (1940).
[3] H. B. Rosenstock and J. H. Schulman, J. Chem. Phys. **30**, 116 (1959).
[4] J. B. Birks and F. A. Black, Proc. Phys. Soc. (London) **A64**, 511 (1951); E. R. Hardwick and W. G. McMillan, J. Chem. Phys. **26**, 1463 (1957); Schulman, Etzel and Allard, J. Appl. Phys. **28**, 792 (1957).

MONDAY MORNING AT 10:00

Room 4–270

(CHARLES S. SMITH presiding)

Invited Paper

B1. Mathematical Foundations of Stress-Strain Relations in Classical Elasticity. R. A. TOUPIN, *U. S. Naval Research Laboratory.* (30 min.)

Mechanical Properties of Solids

B2. Comparison of the Debye θ Determined from Elastic Constants and Calorimetry. J. R. NEIGHBOURS AND G. A. ALERS, *Ford Motor Scientific Laboratory.*—In principle the lattice specific heat near 0°K can be calculated from the simple Debye model using the low-temperature elastic constants. The validity of such a calculation and the temperature range over which it might apply has been a subject of theoretical discussion. Actual experimental testing of the model has been delayed because of a lack of low-temperature elastic constant data. Within the past year a large number of elasticity measurements have been reported for a wide variety of materials for which accurate low-temperature specific heat data are also available. Various methods of calculating θ_0 from these elastic constant data have been used and compared with one another as well as with the calorimetric results. For the cubic metals examined (Cu, Ag, Au, Ni, Al) the agreement with specific heat measurements is excellent up to temperatures of the order of $\theta/60$. The alkali halides also show excellent agreement where there is sufficient calorimetric data below $\theta/60$. The hexagonal metals (Zn and Mg) do not show this agreement. In these cases it appears that temperatures below $\theta/150$ may be necessary in order for the Debye model to be appropriate.

B3. Temperature Dependence of Elastic Constants of Dilute Alloys of Maganese in Copper. D. L. WALDORF, *Ford Motor Scientific Laboratory* (introduced by J. R. Neighbours).—Measurements of the elastic constants of dilute copper-manganese alloys down to low temperatures were undertaken to compare the temperature dependence of dilute alloys with that of pure copper and to provide data for the calculation of the lattice specific heat. The elastic constants C, C', and $\frac{1}{3}(C_{11}+C_{12}+2C_{44})$ were measured in the region from 4.2°K to room temperature by the ultrasonic pulse-echo method. It was found that a plot of any of the measured moduli *vs* temperature is essentially parallel to that of pure copper[1] and decreased by an amount depending upon the manganese concentration. At any temperature the decrease in the moduli is initially linear with increasing manganese concentration. Of the three modes C' shows the greatest change and C the least. This is consistent with the findings of other investigators.[2] At higher manganese contents the C' dependence upon concentration was no longer linear, in contrast with the other two moduli. The Debye temperature was insensitive to manganese concentration.

[1] W. C. Overton, Jr., and J. Gaffney, Phys. Rev. **98**, 969 (1955).
[2] J. R. Neighbours and C. S. Smith, Acta Met. **2**, 591 (1954).

B4. Elastic Constants of Nickel from 4.2° to 750°K. G. A. ALERS, J. R. NEIGHBOURS, AND H. SATO. *Ford Motor Scientific Laboratory.*—The elastic constants C, C', and $\frac{1}{3}(C_{11}+C_{12}+2C_{44})$ of nickel have been measured from 4.2°K to more than 100°K above the Curie temperature in a magnetic field high enough to saturate the sample. All three constants decrease almost linearly with temperature except near 0°K and near the Curie temperature. An extrapolation to lower temperatures from the paramagnetic range indicates that all three constants are increased by the presence of ferromagnetism. A Debye θ_0 of 476.2°K was calculated from the 4.2°K elastic constants. This value is in satisfactory agreement with the calorimetric data of Rayne and Kemp.[1] In units of 10^{12} dynes cm^{-2}, the adiabatic elastic constants of nickel are (at 10 kilo-oersted).

temp.	C	C'	$\frac{1}{3}(C_{11}+C_{12}+2C_{44})$
295°K	1.237	0.5045	3.242
4.2°K	1.317	0.5525	3.377

[1] J. A. Rayne and W. R. G. Kemp, Phil. Mag. **1**, 918 (1956).

B5. Pressure Variation of the Elastic Constants of Sodium.* W. B. DANIELS, *Case Institute of Technology* (introduced by Charles S. Smith).—The pressure variation of the single-crystal elastic constants of sodium has been measured at room temperature using a modified ultrasonic pulse-echo method. The values found for the pressure derivatives of the elastic constants are $dC/dP=1.63$, $dC'/dP=0.226$, $dB_s/dP=3.60$. The notation $C=C_{44}$, $C'=(C_{11}-C_{12})/2$, and $B_s=(C_{11}+2C_{12})/3$ has been used. The results are interpreted in terms of Fuchs' theoretical calculation of the Coulomb contribution to the shear stiffnesses of the alkali metals. The results indicate that as the metal is compressed, the electron charge density at the boundaries of the cellular polyhedra increases more rapidly than e/Ω where Ω is the volume of the atomic polyhedron.

* Research supported in part by the Office of Naval Research and the National Carbon Company.

B6. Pressure Derivatives of the Elastic Constants of Aluminum and Magnesium. RICHARD E. SCHMUNK, *Phillips Petroleum Company*, AND CHARLES S. SMITH, *Case Institute of Technology*.—The pressure derivatives of the elastic stiffness constants of aluminum and magnesium have been measured using a pressure range from 0 to 6500 bars, by a modified ultrasonic pulse-echo method. The values found are

	dC/dP	dC'/dP	dB_s/dP		
Al	2.31	1.62	5.19		
	dC_{11}/dP	dC_{33}/dP	dC/dP	dC'/dP	dC_H/dP
Mg	6.11	7.22	1.58	1.36	13.7

The notation, $C=C_{44}$, $C'=(C_{11}-C_{12})/2$, $B_s=(C_{11}+2C_{12})/3$ and $C_H=C_{11}+C_{12}+2C_{33}-4C_{13}$ has been used. The pressure data for aluminum have been interpreted in terms of Leigh's theory for the elastic stiffnesses themselves, and the magnesium data in terms of the similar theory of Reitz and Smith. Variation of the effective charge density at the boundary of the atomic polyhedron under volume strain causes the electrostatic contribution to the shear stiffnesses to vary approximately as r^{-6} instead of r^{-4} for both metals. Electron transfer from states overlapping one type of Brillouin zone face to states overlapping another type of face under volume strain contributes appreciably to the variation of the Fermi shear stiffness contribution with pressure.

B7. High-Temperature Damping of Ta, Re, and W. R. SCHNITZEL, *Westinghouse Electric Company, Bloomfield* (introduced by C. Wert).—The conventional torsion pendulum of Ke (sic) has been limited largely to about 1000°C or less by design features. A pendulum of new design has been constructed which removes some of these limitations; with it measurements have been made to temperatures in excess of 2000°C. This equipment uses two identical wire specimens which are heated by an electric current. The specimens hang vertically, one above the other; the pendulum bob is held between them. Since most of the heat loss at high temperatures is by radiation, the temperature in the specimens is quite constant over most of their length. With this equipment the grain boundary damping peaks have been measured for some of the refractory metals. Data for polycrystals and single crystals of W and Ta will be reported. The grain boundary peaks for these two metals occur at about 1250°C and 1100°C, respectively, for a frequency of about 1 cps. For polycrystalline Re a peak at about 1300°C has been observed. This is presumed to be the grain boundary peak although no data for a single crystal are available to verify this. Possible use of this equipment for measurements of other materials will be discussed.

B8. The Role of Vacancies in an Unusual Anelastic Phenomenon. B. S. BERRY, *IBM Yorktown Research Center* (introduced by A. S. Nowick).—Consideration is given to the internal friction results obtained by Entwistle[1] from a number of quench aging Al-rich alloys. Two transient contributions to the internal friction were observed on aging duralumin near room temperature, and the second of these was shown to be due to the appearance of an inelastic internal friction peak characterized by an activation energy of 13.5 kcal/mole. The relaxation is thought to arise from a stress induced rearrangement of small groups of solute atoms containing vacant lattice sites as an integral component of their structure. This model successfully explains the salient experimental results, and leads directly to the interpretation of the activation energy as that for vacancy motion. The sequence of changes observed during aging suggests that the relaxation centers are formed by a spontaneous rearrangement within the G.P. zones.

[1] K. M. Entwistle, J. Inst. Metals 82, 249 (1953–1954); 85, 425 (1956–1957).

B9. Temperature Dependence of the Flow Stress of Cu Single Crystals. J. DIEHL* AND R. BERNER, *Max-Planck Institut fuer Metallforschung, Stuttgart* (introduced by T. H. Blewitt).—Previous measurements of the temperature dependence of some work-hardening parameters of Cu (99.98%) single crystals between 78 and 300°K showed an unexpected behavior of the critical shear stress of undeformed crystals: a relatively strong rise with decreasing temperature below ~165°K and a fairly sharp bend at this temperature. In the same temperature range, the flow stress of work-hardened crystals depends only weakly upon the temperature, showing, however, a small step between about 195 and 240°K. To clear up this anomaly, more detailed measurements of the reversible change of the flow stress due to changes in the deformation temperature have been performed, especially at small deformations. A constant ratio of the flow stresses of two temperatures, as otherwise reported, could be found only at higher stresses and in relatively small intervals. The results, extrapolated to $\epsilon=0$, support the critical shear-stress data, whereas for higher prestrains a fairly good agreement with the aforementioned flow-stress measurements could be established. Apparently the steep part of the flow-stress-temperature curves becomes shifted to higher temperatures and its relative magnitude decreases with increasing work hardening. Both effects can be interpreted in terms of Seeger's theory of the flow stress.

* Present address: Oak Ridge National Laboratory.

B10. Pressure Dependence of Mechanical Properties.* K. L. DEVRIES, H. T. HALL,† G. S. BAKER, AND P. GIBBS, *University of Utah*.—A vessel has been designed and built, for measuring mechanical properties of crystals up to 1000°C and 20 000 atmospheres in argon. The sample chamber is large enough (1 in. diam×4 in. long) to accommodate a torsional pendulum. Six electrical leads are provided. Extensional creep will be studied where stress is applied by controlled thermal expansion of a linkage assembly inside the vessel. It is estimated that changes of more than an order of magnitude in vacancy concentration may be explored. Results will be presented.

* This research was supported in whole or in part by the U. S. Air Force monitored by the Aeronautical Research Laboratory, Wright Air Development Center.

† Permanent address: Brigham Young University.

B11. Permanent Set, Creep, and Hysteresis in Carbon and Graphite at Room Temperature.* J. F. ANDREW, D. C. WOBSCHALL, AND J. OKADA, *University of Buffalo*.—An apparatus has been developed for measuring the elastic moduli of graphite in bending and torsion, in which the specimen can be stressed in either of two opposite directions. Forces and deflections are measured with high precision using linear variable differential transformers and approximate electronic circuits. It was found that permanent set and creep in commercial graphite depend logarithmically on time. The slope of the lines decreases as the sample is worked back and forth. Hysterisis loops are observed in both force-deflection and torque-twist measurements, the successive loops becoming more and more narrow. Crackling noises are detected when carbon specimens are strained for the first time beyond the limits of previous deflection. The permanent set is very small in baked carbon rods but becomes increasingly larger with increase of the heat-treatment temperature. For soft filler-soft binder rods both Young's modulus and the modulus of rigidity first increase with baking temperature for temperatures between 500°C–1100°C, then decrease in the range of heat treatments 1100°C–2000°C, reach a minimum at about 2000°C followed by a maximum at 2500°C, and finally decrease gradually up to the highest heat treatments used (3100°C).

* Supported by the U. S. Air Force, through the Wright Air Development Center.

B12. Ultrasonic Attenuation in Carbon Rods.* D. WOBSCHALL AND H. HAMMILL, *University of Buffalo.*—The attenuation and velocity of sound waves transmitted through specially prepared carbon rods were measured as a function of frequency, from about 100 kc to 1000 kc. Young's modulus calculated from the sound velocity is found to be close to, but slightly higher than, the measured static values. The ultrasonic attenuation increases with increasing frequency and with increase in size of coke particles used in preparation of the carbon. The relative contribution of the scatter and absorption will be discussed.

* Supported by the U. S. Air Force, through the Wright-Patterson Air Development Center.

MONDAY MORNING AT 10:00

Room 4–370

(R. H. BUBE presiding)

Invited Paper

BA1. Spin-Orbit Splitting of Valence Bands. R. BRAUNSTEIN, *RCA Laboratories.* (30 min.)

Compound Semiconductors

BA2. Infrared Faraday Rotation in InSb.* RICHARD N. BROWN AND BENJAMIN LAX, *MIT.*—The Faraday effect was investigated in n-type InSb at room temperature at wavelengths between 9 and 21 μ. Magnetic fields up to 21 kilogauss were obtained from a Bitter-type solenoid. Material with carrier concentrations approximately 2.5×10^{16} cm^{-3} showed λ^2 dependence at long wavelengths and a linear field dependence at low magnetic fields, in accordance with theory. Departure from linear behavior was observed at higher magnetic fields. A value of the effective mass was obtained from the Faraday rotation and the determination of the electron concentration by Hall measurements. The value obtained for the effective mass was $(0.021\pm0.002)m_0$, in good agreement with the results of Smith and Moss[1] for similar electron concentrations.

* The work reported here was performed at Lincoln Laboratory, a technical center operated by MIT with the joint support of the U. S. Army, Navy, and Air Force, under contract.

[1] S. D. Smith and T. S. Moss, Brussels Solid State Congress, (1958).

BA3. Infrared Transmission Properties of Indium Arsenide in the Absorption Edge Region. JACK R. DIXON, *U. S. Naval Ordnance Laboratory.*—Optical absorption constants, α, in the wavelength region of the absorption edge (2 to 5 μ) have been determined as a function of impurity content for temperatures ranging from 5°K to 300°K. The absorption edge at room temperature for n-type material having a carrier concentration of 4×10^{16} cm^{-3} was located at an energy, E, of 0.35 ev as determined from an α^2 *vs* E plot.[1] The position of the absorption edge of this material increased linearly with decreasing temperature by 3.1×10^{-4} ev/°K for temperatures ranging from 300°K to approximately 80°K, but became relatively independent of temperature below 80°K. At a given temperature it is found that the transmission edge of n-type material of low-compensation shifts to higher energies as the concentration of n-type impurities is increased, in agreement with the results of previous work.[2] For highly compensated material the positon of the transmission edge varies in a similar manner with carrier concentration, but for a given carrier concentration the edge is at a lower energy than that of material of low compensation. This effect is attributed to a narrowing of the energy gap due to shifts of the band edges by impurity levels.[3]

[1] Bardeen, Blatt, and Hall, *Photoconductivity Conference* (John Wiley & Sons, Inc., New York, 1956), p. 146.
[2] F. Stern and R. M. Talley, Phys. Rev. 100, 1638 (1955).
[3] F. Stern and J. R. Dixon, J. Appl. Phys. (to be published).

BA4. Optical Constants of the Semiconductor SnSe.* D. L. MITCHELL† AND H. LEVINSTEIN, *Syracuse University.*—Tin selenide has a sheet like crystal structure, behaving much the same as mica. This is an orthorhombic structure with the cleavage planes perpendicular to the "c" axis. The index of refraction was measured from 1–15 μ for the two directions of polarization perpendicular to the "c" axis. The values found were $n_1=4.6\pm0.1$ and $n_2=5.0\pm0.1$ at 2.5 μ. The intrinsic absorption coefficient of 1000Ω cm material was measured over the range of 1–10^5 cm^{-1}. Two components were observed in the region of indirect transitions which extended to 10^3 cm^{-1}. The two coefficients for the indirect transitions and also the coefficient for the direct transitions exhibited the expected energy dependence. The energy separations were 0.90 and 0.86 ev for indirect and 1.2 ev for direct transitions. The free carrier absorption was measured for "p" type material. This followed a $\lambda^{3/2}$ dependence to 10 μ and then asymptotically approached a limiting value. This is due to the short relaxation time which was found to be 1.0×10^{-14} second. An estimate for the effective mass of holes of 0.15 m_e may be obtained from the free carrier absorption and the dc conductivity.

* This work was supported by the Office of Ordnance Research.
† Now at Utica College of Syracuse University.

BA5. Some Optical Properties of Cadmium Telluride. P. W. DAVIS AND T. S. SHILLIDAY, *Battelle Memorial Instute.*—Some optical properties of CdTe samples having a carrier concentration of 10^{18}/cc were measured. The index of refraction in the near infrared was determined to be 2.56. Values of the absorption coefficient as a function of frequency were obtained at various temperatures. By plotting $(\alpha)^{\frac{1}{2}}$ and α^2 against frequency, it was found that the room temperature value for the direct transitions was 1.505 ev and that for the indirect transitions 1.440 ev. Their temperature dependencies between 77°K and 394°K are given by $(1.66-5.32\times10^{-4}T)$ ev direct transitions, $(1.56-4.08\times10^{-4}T)$ ev indirect transitions.

BA6. Semiconducting Properties of the Compound CsAu. W. E. SPICER, A. H. SOMMER, AND J. WHITE, *RCA Laboratories.*—The spectral distribution of optical absorption and the magnitude of the resistivity indicate that the compound CsAu is a semiconductor. The optical absorption edge seems to occur at about 2.6 ev. Exciton absorption coefficients are in the range of 10^5/cm. The conductivity of the thin

layers studied is about 100 (ohm-cm)$^{-1}$ and is constant within about 50% between 4°K and 410°K. Thus the material seems either to be a degenerate semiconductor or to have an impurity band. Photoemission measurements indicate that the material is n type with an electron affinity of about 1.6 ev. The crystal structure is of the ordered CsCl type and the lattice volume is 24% smaller than that calculated from the metallic volumes of Cs and Au; therefore, it appears that CsAu has a certain degree of ionic binding with Au representing the negative component.

BA7. Electrical Conductivity of CdSb. J. YAHIA AND R. OVERSTREET, *U. S. Naval Ordnance Laboratory.*—Measurements of the resistivity as a function of temperature have been made in the range 77° to 700°K on polycrystalline samples of both n- and p-type CdSb. The results indicate that the samples studied are degenerate; maxima occur in the conductivity curves and the position of the maxima is a function of the impurity concentration. For the n-type sample investigated this maximum occurred at about 320°K and for the p-type sample it occurred at about 135°K. Using the conductivity formulas for a degenerate semiconductor,[1] the values in Table I were obtained for the density of carriers at 290°K, the density

TABLE I.

	No. of carriers (cm^{-3})	No. of impurities (cm^{-3})	ΔE_1, ΔE_2 (ev)
n type	6.4×10^{19}	5.3×10^{20}	0.05
p type	1.05×10^{19}	6.94×10^{19}	0.02

of impurities, and the position of the impurity centers below the bottom of the conduction band for the n-type sample (ΔE_1) and above the top of the valence band for the p-type sample (ΔE_2). The energy gap, as calculated from the intrinsic slope, was found to be 0.49 ev for the n-type sample and 0.37 ev for the p-type sample.

[1] E. H. Putley, Proc. Phys. Soc. (London) **A62**, 284 (1949).

BA8. Some Electrical and Thermal Properties of $InAs_{1-x}P_x$. R. BOWERS, J. E. BAUERLE, AND A. J. CORNISH, *Westinghouse Research Laboratories.*—Measurements have been made between 350°C and 800°C of the electrical resistivity, the Seebeck coefficient (thermoelectric power) and the thermal conductivity of n-type $InAs_{1-x}P_x$, with x varied from 0 to 0.4. These measurements extend earlier data of Weiss[1] to higher temperatures. On the whole, our results agree with reasonable extrapolations of the data of Weiss, except at $x=0$, where we obtain somewhat higher Seebeck coefficients. The electrical properties of these alloys show qualitatively a similar temperature dependence to those of InAs, but the magnitude of the resistivity and Seebeck coefficient increase with increasing x in the intrinsic range because the addition of phosphorus increases the energy gap.[2] Our thermal conductivity data exhibit a sum of a $1/T$ behavior due to the phonon-phonon scattering and a temperature-independent contribution due to phonons scattered by the phosphorus added. No anomalous behavior of the thermal conductivity was found at high temperatures. The value of this ternary system for thermoelectric power generation will be discussed.

[1] H. Weiss, Z. Naturforsch. 430 (1956), and unpublished work.
[2] H. Welker and H. Weiss, *Solid State Physics* (Academic Press, Inc., New York, 1956), Vol. 3, p. 1.

BA9. Measurements of Thermal Diffusivity in Semiconductors: InSb and Mg_2Sn.* I. I. SOCHARD† AND J. H. BECKER, *National Bureau of Standards.*—Accurate measurements of thermal diffusivity k in metals have been made from analysis of temperature waves due to periodically heating one end of an effectively semi-infinite rod.[1] Generally low-frequency heat pulses ($f\sim1/100$ cps) and large samples (~25 cm long) are employed. In contrast, with smaller semiconductor samples ($\sim0.5\times1\times10$ mm) we use higher frequency heat pulses ($f\sim10$–1000 cps) obtained by chopping light which is strongly absorbed at a large area surface of the specimen; temperature waves are deduced from thermoelectric power, Nernst, or bolometric steady-state voltages produced by the sample. Sandblasting reduces undesired photosignals. To calculate k from the bolometric and Nernst effects the ambipolar diffusion constant is required,[2] with thermoelectric power voltages V, k is obtained from the slope of $\log V(f)^{\frac{1}{2}}$ *vs* $(f)^{\frac{1}{2}}$. Results on intrinsic samples at 300 and 400°K agree with calculations from known thermal constants, however, for InSb an anomalous nonlinearity appears when measuring the magnetic field dependence of the Nernst effect.

* Research supported by the U. S. Air Force.
† Present address: Diamond Ordnance Fuze Laboratories.
[1] P. H. Sidles and G. C. Danielson, J. Appl. Phys. 25, 58 (1954).
[2] I. I. Sochard and J. H. Becker, Bull. Am. Phys. Soc. Ser. II, 3, 114 (1958).

BA10. Thermal Properties of Cadmium Antimonide. GEORGE G. KRETSCHMAR AND ROY F. POTTER, *U. S. Naval Ordnance Laboratory.*—A number of samples of cadmium antimonide have been tested for thermal power by measuring the potential difference developed across the sample when the ends were in contact with a cooled copper plate on one side and a heated copper on the other. For a number of specimens of both p- and n-type material the thermal power measured was approximately 100 to 200 μv per degree. For some samples, however, which had been remelted in argon gas, and which were highly crystalline in character, the thermal power was much higher, approximately 500 μv per degree. These values are for the specimen temperatures between zero and 100°C. The thermal conductivity of some samples of cadmium antimonide has been determined by a modified Fitch[1] method which permits rapid measurements of good accuracy. Preliminary results indicate that solid ingots of cadmium antimonide have a thermal conductivity of 5×10^{-3} calorie cm/sec cm^2 at room temperature.

[1] A. L. Fitch, Am. J. Phys. 3, 135 (1935).

BA11. Photoconductivity in Gallium Selenide Crystals. EDWARD L. LIND AND RICHARD H. BUBE, *RCA Laboratories.*—Single crystals of GaSe have been prepared by reaction of the elements, followed by gradient freeze crystallization. Crystals as grown were p type, with hole mobility of 15 cm^2/volt sec and hole concentration of 10^{16} cm^{-3}. Conductivity *vs* temperature data give 0.12 ev as the acceptor impurity ionization energy, probably Cu. The absorption edge of GaSe is at 6310 A, corresponding to a band gap of 1.97 ev; the temperature coefficient of band gap is 3×10^{-4} ev/deg. Insulating and photosensitive GaSe crystals can be prepared by compensating the acceptor impurities by incorporated donors from Groups VII or IV. Below the temperature at which thermal quenching of photoconductivity occurs, the sensitivity is within the range of sensitive CdS or CdSe. Rectification tests of photoconductivity suggest that holes may be the photocurrent carriers. Thermal quenching of photoconductivity corresponds to an ionization energy of 0.5 ev, whereas optical quenching gives 1.0 ev. This large difference in thermal and optical energies suggests either a large Franck-Condon shift or a center with multiple levels. A capture cross-section ratio of 3×10^6 is found for the sensitizing centers. Crystals of Ga_2Se_3 (band gap = 1.88 ev) and of solid solutions of $GaSe(x)GaS(x)$ have also been prepared.

BA12. Composition Limits of Stability of Crystalline PbTe. R. F. BREBRICK, R. S. ALLGAIER, AND G. L. HAMMOND, *U. S. Naval Ordnance Laboratory.*—The composition of a binary crystal in equilibrium with liquid and vapor phases of the two elements of the crystal will be one of the two limiting

stable compositions, depending on which element is in excess in the liquid. We have applied this principle to PbTe at temperatures between 600° and 830°C. The crystals were originally about 6×10^{18} p type. Scanning freshly cleaved faces of treated crystals with a thermoelectric probe showed that the changes in carrier concentration were associated with a diffusion process to or from the crystal surface. Crystals which had come to equilibrium with tellurium-rich liquid were close to 10^{19} p type with only a small dependence on the equilibrium temperature. The carrier concentrations for these crystals were determined from the Hall constant measured at 77.4°K, assuming one carrier, degenerate statistics, and the ⟨111⟩ many valley model with a mass ratio of 5.[1] We experienced difficulties in obtaining uniform, stable n-type crystals, but it appears that the limit of stability on the n-type side is closer to 10^{18}.

[1] Deduced from room temperature magnetoresistance measurements on [110]-oriented p-type PbTe crystals [R. S. Allgaier (unpublished)].

MONDAY MORNING AT 10:00

Room 6–120

(A. I. SCHINDLER presiding)

Irradiation Effects I (Metals)

C1. Liquid Helium Cryostat for Reactor Irradiation of Metals. C. E. KLABUNDE, R. R. COLTMAN, AND T. H. BLEWITT, *Oak Ridge National Laboratory.**—The study of neutron irradiation effects in metals at low temperatures has been extended to 4.2°K by the addition of a liquid helium cryostat to the previous helium-refrigerated cryostat in Hole 12 of the Oak Ridge Graphite Reactor. The system involves continuous liquefaction through Joule-Thomson expansion of a small recirculating stream of helium gas. The one-half inch diameter sample tube which dips into the "pot" of liquid thus formed at the center of the reactor allows full control over sample environment (vacuum, helium gas or liquid, or a separate vacuum-jacketed gas chamber). Cooling capacity and system stability are adequate to make full-power bombardments (4×10^{17} n/cm^2 per week) at sample temperatures of 3.9–4.2°K, while the gamma ray heating is 0.005 watt/g. *In-situ* experiments have been carried out to measure radiation-induced resistivity changes and the thermal behavior (annealing) of these up as high as room temperature. Annealing while the reactor is off is by the pulse technique where the temperature is returned to the reference value, say 3.6°K, for each resistivity reading.

* Oak Ridge National Laboratory is operated by Union Carbide Corporation for the U. S. Atomic Energy Commission.

C2. Low-Temperature Radiation Damage in Metals. R. R. COLTMAN, T. H. BLEWITT, C. E. KLABUNDE, AND J. K. REDMAN, *Solid State Division, Oak Ridge National Laboratory.** —High-purity specimens of many metallic elements have been bombarded at 4°K in the graphite reactor at Oak Ridge National Laboratory to a flux of 4×10^{17} nvt. The damage rates of these materials as measured by changes in residual resistivity are linear and vary widely from the lowest rate of about 1×10^{-26} ohm cm/neutron/cm^2 for Cu to 10^4 times this rate for Bi. Isochronal annealing studies of many of these materials have been made following bombardment. Measurable annealing has been found in Cu as low as 7.2°K and other materials show evidence of annealing at 10°K and possibly lower. Pt, Ag, and Cu show similar large annealing peaks centered at 20, 27, and 38°K, respectively. These annealing peaks, which are found also in other materials at different temperatures are generally preceded and followed by a continuous or "garbage" type annealing. Au appears to be anomalous in that it is the only face centered cubic material studied, which shows no large annealing peak. It has also been found that the damage rate at 4°K in cold worked Cu is greater than in annealed Cu. Differences of 30% have been observed. In addition, the large annealing peak at 38°K in cold worked Cu appears to be slightly surpressed.

* Oak Ridge National Laboratory is operated by Union Carbide Corporation for the U. S. Atomic Energy Commission.

C3. Annealing Kinetics of Irradiated Copper and Aluminum. T. H. BLEWITT, R. R. COLTMAN, C. E. KLABUNDE, J. K. REDMAN, AND J. DIEHL, *Oak Ridge National Laboratory.**—The annealing kinetics of copper and aluminum following a neutron dose of 5×10^{17} nvt at 3.9°K in the Oak Ridge Reactor, hole No. 12 facility were studied by measuring the recovery of radiation-induced resistivity. In the range of temperature from 9°K to 20°K a series of sequential isothermal annealing curves were determined with each isothermal curve increasing about 1°K in temperature. The apparent activation energies determined from the change in slope induced by the increase in temperature were found to increase with slight evidence of uniquely activated processes for both metals. At higher temperatures the apparent activation energy was determined from the relaxation time of nonsequential isothermal annealing curves taken at 36.5°K and at 38.7°K as well as by the sequential method. These results suggest a nonunique activation energy in this region. The model of a continuous spectrum of activation energies of the first order used to analyze earlier data[1] is clearly inapplicable here as the high activation energies (twice those found earlier) implies a jump frequency many magnitudes greater than the atomic frequency factor.

* Oak Ridge National Laboratory is operated by Union Carbide Corporation for the U. S. Atomic Energy Commission.

[1] G. D. Magnuson *et al.*, Phys. Rev. **109**, 1990 (1958).

C4. Radiation Effect in Copper Irradiated with 50–350-kev Protons at 115°K.* EDGAR A. PEARLSTEIN AND BRUCE E. ANSPAUGH, *University of Nebraska.*—Electrical resistivity measurements were made for proton bombardments at various energies between 50 and 350 kev, in order to test the energy dependence of radiation damage. Irradiations and measurements were made at about 115°K on copper foils ¼ mil thick. Although this thickness is greater than the range of the protons, so that the measured resistance is that of irradiated and nonirradiated material in parallel, data can be interpreted straightforwardly as long as the irradiation is small. Measured energy dependence is compared with calculated energy dependence, using the cross section formulas of Seitz and Koehler[1] and energy loss data of Whaling.[2] The measurements give a straight line graph of resistance change *vs* energy, while the calculation gives a graph which is concave toward the energy axis. Perhaps this apparent discrepancy can be accounted for by the fact that the range of the lowest energy

protons is comparable to the mean free path of conduction electrons. An experimental test of this would be to irradiate at oblique incidence, thus effectively shortening the range of the protons without changing their energy.

* This work is supported in part by the U. S. Atomic Energy Commission.
[1] F. Seitz and J. Koehler in *Solid State Physics* edited by Seitz and Turnbull (Academic Press, Inc., New York, 1956), Vol. 2.
[2] W. Whaling, *Handbuch der Physik* (Springer-Verlag, Berlin, 1958), Vol. 34.

C5. Etch Pits and Dislocations in Irradiated Copper. F. W. YOUNG, JR, *Oak Ridge National Laboratory.**—Crystals of 99.999% copper were etched to reveal the dislocations as etch pits before and after irradiation in the Oak Ridge graphite reactor (up to 6×10^{17} nvt). There was no evidence of the production of dislocations by irradiation. The dislocation patterns produced by hardness indentations were observed on unirradiated and irradiated crystals. Copper crystals doped with about 0.05% tellurium were irradiated and etched. No additional etch pits were observed after irradiation, but after subsequent annealing additional pits were found, the number being a function of the time and temperature of annealing, and the position of the pits being a function of the substructure of the crystals.

* Oak Ridge National Laboratory is operated by Union Carbide Nuclear Corporation for the U. S. Atomic Energy Commission.

C6. Effect of Neutron Bombardment at Various Temperatures upon the Young's Modulus and Internal Friction of Copper. D. O. THOMPSON AND V. K. PARÉ, *Oak Ridge National Laboratory.**—It has been shown[1] that during room-temperature irradiation of copper crystals there occurs an increase of elastic modulus and a decrease of internal friction which are well described by a simple theory of pinning of dislocation loops by radiation-induced defects. Similar runs have now been made at various constant temperatures between 90°K and 300°K. It is found that changes in irradiation temperature alter somewhat the shapes of the curves of modulus and decrement *vs* irradiation time, and influence greatly the rate at which dislocation pinning occurs. Relative to the room-temperature value, the rate is 23% at 145°K and 5% at 94°K. In the warmup which follows each irradiation, two features are evident: (1) There is usually a sharp maximum in the decrement and modulus curves in the vicinity of 210°–230°K. This peak probably does not represent a simple defect stress relaxation process since the modulus data are not consistent with this interpretation. (2) Starting at approximately 260°K, the modulus and decrement rapidly approach their "saturation" values. Presumably defects, stored in the lattice due to a lack of thermal mobility at the irradiation temperature, become mobile and move to the dislocation lines.

* Oak Ridge National Laboratory is operated by Union Carbide Corporation for the U. S. Atomic Energy Commission.
[1] D. O. Thompson and D. K. Holmes, J. Appl. Phys. **27**, 713 (1956).

C7. Radiation Hardening in Copper Single Crystals.* I. G. GREENFIELD AND H. G. F. WILSDORF, *The Franklin Institute Laboratories* (introduced by N. Fuschillo).—The effect of neutron bombardment on the mechanical properties of copper single crystals has been investigated. Long crystals of various orientations were cut into two specimens; one part was subjected to an irradiation of 10^{18} nvt, and the other was used in the annealed condition as a comparison specimen. Each pair of crystals was deformed in tension so that the resulting properties would be representative of stage *I*, *II*, or *III* of the stress-strain curve. It was found that neutron bombardment increased the critical resolved shear stress from 0.2 kg/mm² of the annealed copper to about 1.6 kg/mm². Irradiated crystals had an extended easy glide range in which the stress-strain curve exhibited discrete serrations. Electron micrographs of this region showed nearly evenly spaced clusters of very fine slip lines separated by large slip free areas, while the non-irradiated material contained elementary structure characteristic of small deformation in copper. The initial part of the linear work hardening curve contained little or no serrations although an increase in the number of clusters was noted. In addition, cross slip became detectable. At higher strains, fine slip lines appeared between the clusters.

* Work supported by the U. S. Atomic Energy Commission.

C8. Energy Dependence of the Recovery in Irradiated Copper. R. M. WALKER AND J. W. CORBETT, *General Electric Research Laboratory.*—Stage *I* recovery in electron irradiated copper consists of five substages labeled I_A-I_E in order of increasing temperature.[1] We have measured the shift in the populations of I_A-I_E as a function of the energy of the bombarding electrons. The sum $I_A+I_B+I_C$ is observed to increase with decreasing energy, as does the ratio I_D/I_E. These data are interpreted as additional confirmation of previously proposed model for stage *I* recovery.[2] In this model I_A-I_C are due to close pairs. I_D and I_E are due, respectively, to the correlated and uncorrelated diffusion of interstitials. The measured population shifts are small. This fact will be discussed in terms of the recoil energy spectra, and it will be shown that the most likely interpretation is that the average separation between a primary recoil and its vacancy does not vary rapidly with energy, near threshold.

[1] J. W. Corbett and R. M. Walker, Phys. Rev. 110, 767 (1958).
[2] Corbett, Smith, and Walker (to be published).

C9. Irradiation and Quenching Experiments on Cu-Al. R. H. KERNOHAN AND M. S. WECHSLER, *Oak Ridge National Laboratory.**—Previous experiments on α-phase Cu-Al (15 at. % Al) have indicated that the alloy as normally prepared is in a metastable state at room temperature. Upon irradiation at temperatures above 0°C, a decrease in resistivity (~0.2 μohm-cm) takes place[1] and the metastability is erased. Also, upon quenching,[2] the extent of the metastability is increased. A study has been made of the combined effect of irradiation and quenching treatments. Specifically, isothermal and isochronal annealing experiments were performed on (1) samples quenched from 450°C and (2) samples quenched from 450°C followed by irradiation at −120°C. It was found that the irradiation causes the quench annealing to be accelerated in the early stages of the annealing. However, at longer times and higher temperatures, the quench annealing is more sluggish for the irradiated samples. Two other types of experiments will be described; (1) irradiation experiments at higher temperatures, and (2) an interrupted irradiation experiment in which the sample was withdrawn to the edge of the reactor.

* Oak Ridge National Laboratory is operated by the Union Carbide Corporation for the U. S. Atomic Energy Commission.
[1] M. S. Wechsler and R. H. Kernohan, J. Phys. Chem. Solids **7**, 307 (1958).
[2] M. S. Wechsler and R. H. Kernohan, Bull. Am. Phys. Soc. Ser. II, **3**, 118 (1958).

C10. Effects of Fast Neutron Irradiation on Cu-Fe Precipitation-Hardening Alloys.* A. BOLTAX, *Nuclear Metals, Inc.* (introduced by W. B. Nowak).—The effects of fast neutron irradiation at several integrated fluxes, were investigated on solution treated and aged Cu-1.7 w/o Fe precipitation-hardening alloys using electrical resistivity and saturation induction measurements. The present data, in agreement with the results obtained previously,[1] indicate that the behavior of aged samples under irradiation can be described by competitive processes of irradiation-induced precipitation and resolution as functions of precipitate particle size. The solution-treated samples showed an irradiation-induced aging similar to Cu-Be alloys. The behavior of the aged samples under irradiation was a function of the aging temperature, which in turn determined the precipitate particle size. Samples aged below 500°C showed an increase in electrical resistivity consistent with the mechanism of irradiation-induced resolution, whereas samples aged

above 500°C showed a decrease in electrical resistivity consistent with the irradiation-induced aging. The results suggest that resolution takes place by localized homogenization due to Brinkman type displacement spikes which affect 5×10^2 to 20×10^2 atoms per spike. Simultaneously, about 50 to 100 atoms precipitate per incident neutron, probably by enhanced diffusion due to the excess vacancies and interstitials introduced by irradiation.

* Work supported by the U. S. Atomic Energy Commission.
[1] A. Boltax, ASTM Special Tech. Publ. 208, 183 (1957).

C11. Irradiation Induced Magnetic Changes in Cu-Ni Alloys.* F. M. Ryan, E. W. Pugh, and R. Smoluchowski, *Carnegie Institute of Technology*.—The effect of neutron irradiation on copper-nickel alloys has been investigated by means of magnetic susceptibility measurements. The susceptibilities were measured by the Gouy method between 300°K and 2.0°K for a series of alloys ranging from 17.22 to 46.5 atomic percent nickel. The samples were exposed to neutron fluxes at the Brookhaven reactor, ranging up to 2.2×10^{19} neutrons/cm^2 while at 80°C and the magnetic susceptibilities were found to increase following the irradiation. The increase was easily observable due to its strong temperature dependence and was greatest for the samples with the highest nickel content and neutron fluxes. The susceptibilities of the alloys returned to their original values following an anneal in or above the temperature range corresponding to the activation energy for self-diffusion, while no changes in the susceptibilities were observed following anneals at lower temperatures. It is suggested that the copper-nickel system is not a perfect random solid solution but tends toward segregation, and that the neutron irradiation enhances diffusion toward a true equilibrium at room temperature. This is in a qualitative agreement with several other observations.

* This research was supported by an U. S. Atomic Energy Commission contract.

C12. Recovery Processes in Electron Irradiated Gold.* J. A. Tesk, J. B. Ward, H. L. Kohn, and J. W. Kauffman, *Northwestern University*.—Gold samples were irradiated with electrons at various energies from 2 Mev to 2.6 Mev and over a range of fluxes. The samples were held near liquid nitrogen temperature during irradiation; since the high temperature annealing was of interest in this experiment it was not necessary to irradiate at liquid helium temperature. Subsequent to the irradiation, the specimens were isothermally or isochronally annealed. The annealings were carried out until complete recovery was obtained. Activation energies using the slope intersection method and the order of the reactions were determined. A considerable fraction of the residual resistivity produced by the irradiation annealed out between 10°C and 60°C with an activation energy of 0.86 ± 0.07 ev. This value agrees with that found for quenched gold samples when the quenching is performed in such a way as to produce dilute concentrations of defects.[1] This annealing process was approximately a first-order reaction but showed some deviation from first order. A portion of the residual resistivity annealed out below room temperature with a range of activation energies considerably lower than the 0.86 ev found in the room temperature range.

* This research was partially supported by the U. S. Atomic Energy Commission.
[1] J. E. Bauerle and J. S. Koehler, Phys. Rev. 107, 1493 (1957).

C13. Electron Microscope Observation of Radiation Damage in Gold Films. T. S. Noggle, *Oak Ridge National Laboratory** (introduced by F. W. Young).—Gold films have been examined in transmission in the electron microscope and a fine structure associated with the radiation damage introduced by pile irradiation has been observed. The structure observed appears as small spots 50–200 A in size. It is probable that this apparent size is not simply related to the size of the damaged region, but arises from local disturbances in the diffraction process in the crystal. The observed density of this structure (less than 1% of primary knock-ons) seems too small to be associated with the damage produced directly by fast neutrons and probably arises from clustering of lattice defects produced by irradiation and which are mobile at the irradiation temperature.

* Oak Ridge National Laboratory is operated by Union Carbide Corporation for the U. S. Atomic Energy Commission.

C14. Nuclear Irradiation Effects on Permanent Magnet Materials. R. S. Sery, D. I. Gordon, and R. H. Lundsten, *U. S. Naval Ordnance Laboratory*.—Permanent magnet materials exposed to nuclear reactor radiation showed no measurable changes in magnetic properties. This result, though negative, is consistent with that for soft magnetic materials[1,2] given the same irradiation, i.e., for the soft materials, those with lowest coercive force showed drastic changes, while those with higher coercive forces showed negligible changes. In the permanent magnet experiment, the following materials were irradiated to 10^{17} epicadmium neutrons/cm^2 in 12 days in the BNL reactor: 3½ Cr steel, 36 Co steel, Alnico II, V, and XII, Cunico, Cunife, Silmanal, fine irons, platinum-cobalt, and unoriented and oriented barium ferrites. Pre- and post-irradiation measurements of (a) demagnetization curves and (b) open magnetic circuit induction values were made on test samples and unirradiated control samples. The controls were held in a furnace for 12 days at the reactor hole temperature of 90°C. Because of induced radioactivity, post-irradiation measurements were made remotely in the NRL hot-cell facility. Within the accuracy of the measurements (which is $\mp2\%$ for open circuit induction, $\mp3\%$ for residual induction, and $\mp10\%$ for coercive force), there were no changes attributable to radiation.

[1] Sery, Fischell, and Gordon, *Conference on Magnetism and Magnetic Materials, October 1956* (American Institute of Electrical Engineers, February, 1957).
[2] R. S. Sery and D. I. Gordon, Bull. Am. Phys. Soc. Ser II, 3, 117 (1958).

Monday Morning at 10:00

Room 26–100

(R. S. Mulliken presiding)

General Chemical Physics

CA1. Brownian Motion.* Gerald Mandel and Frank Collins, *Polytechnic Institute of Brooklyn*.—A theory of Brownian motion has been presented[1] with the starting assumption that the ensemble average force acting on a molecule is proportional to its velocity at low velocities in a system otherwise at equilibrium. It is now shown that the

assumption is superfluous as this condition follows as a necessary consequence of the form of the equation for the ensemble average time derivative of the frictional force. The latter equation is rederived with some gain in rigor. The frictional coefficient is used to derive a mean correlation length which has the statistical significance of the mean free path in gases, except that it does not depend on a collisional model. It is numerically equal to the mean free path corrected for persistence of velocity in dilute gases and has a value of the order of 0.24 A in liquid argon. Brownian motion in pair space is re-examined and the frictional coefficient for relative motion is obtained. At short intermolecular distances, it is given only approximately as the sum of the independent singlet coefficients.

* Supported by the Wright Air Development Center, U. S. Air Force.
[1] F. C. Collins and H. Raffel, J. Chem. Phys. 29, 699 (1958).

CA2. Electrophoretic Velocity of Spherical Lyophobic Colloid Particles.* A. L. Loeb and P. H. Wiersema, *MIT*, and J. T. G. Overbeek, *University of Utrecht*.—The speed, U, of colloid particles in an external electric field depends upon the electrical potential, ζ, at the interface between particles and liquid. A relationship[1] between U and ζ, based on a series expansion in ζ was previously established, but it is valid only for low values of ζ. The present approach is based upon the Gouy-Chapman distribution of charge and potential and its perturbation by the applied electric field. The resulting nonlinear system of five simultaneous transcendental equations has been evaluated by electronic computation,† and the results are found to agree with those of Overbeek[1] for low values of ζ. Special attention is given the relaxation effect in electrophoretic transport.

* This work supported in part by the Departments of the U. S. Army, the U. S. Navy and the U. S. Air Force, and by the Stichting Fundamenteel Onderzoek der Materie of The Netherlands.
[1] J. T. G. Overbeek, Advances in Colloid Sci. 3, 97 (1950).
† Computer time made available by the MIT Computation Center.

CA3. Scattering of High-Velocity Neutral Particles.* I. Amdur and M. S. Longmire, *MIT*, and E. A. Mason, *University of Maryland*.—Total collision cross sections have been measured for beams of neutral helium atoms, with energies between 500 and 2100 ev, scattered in CH_4, CH_3F, CH_2F_2, CHF_3, and CF_4, all at room temperature. The cross sections, which depend on apparatus geometry, show the following behavior: (1) For the He-CH_4 system, they decrease from about 17 A^2 at 500 ev to about 12.5 A^2 at 2100 ev. (2) For the He-CF_4 system, they decrease from about 23.5 A^2 at 500 ev to about 19 A^2 at 2100 ev. (3) For all the systems, there is a systematic trend characterized by an increase in cross section of about 1.6 A^2, independent of energy, for each substituent fluorine atom. The scattering results are discussed in terms of the average intermolecular potentials for the five systems.

* Supported by the Office of Naval Research.

CA4. Scattering of Metastable Helium Atoms in Helium, Neon, and Argon.* G. M. Smith† and E. E. Muschlitz, Jr., *University of Florida*.—Measurements of total cross sections for the scattering of 2^1S and 2^3S excited helium atoms in helium, neon, and argon have been made by utilizing a thermal-energy molecular beam in which a fraction of the atoms are excited by electron bombardment. The singlet to triplet ratio in the beam is changed by varying the bombarding electron energy. The excited particles are detected by measuring the secondary electron emission from metal surfaces. By utilizing a suitable draw-out potential, positive ions produced by ionizing collisions may be measured separately. The total cross sections for the scattering of the triplet atoms are larger than for the singlet in each case. For neon the difference is considerably greater than the estimated experimental error. The ionization cross section for either metastable atom in argon is $(8\pm3)\times10^{-16}$ cm^2. The effect of angular resolution on the total cross sections has been investigated to angles of 1.4°. These results indicate essential agreement with the work of Stebbings.[1]

* Supported by the National Science Foundation.
† Now located at Los Alamos Scientific Laboratory.
[1] R. E. Stebbings, Proc. Roy. Soc. (London) A241, 270 (197).

CA5. Chemical Reactions in the Wake of a One-Dimensional Blast Wave. James L. Lauer, *Sun Oil Company*.—A *tee*-type, electric-discharge-driven shock tube was set up in a way similar to that described by Kolb.[1] It was found that the relationship of Harris,[2] *viz.* $t=Ax^1$, between time and shock radius, applied in nitrogen at pressures below 10 mm. At higher pressures and distances over 30 cm the exponent was 5/4. The shock velocity at any point was calculated by differentiating this expression, and from it the temperature profile was obtained. By placing a barrier against the shock front, reflected shocks could be produced whose characteristics were a function of barrier distance. The temperature above which chemical reactions yielding stable products would proceed during the time of the shock pulse was estimated from the barrier distance at which measurable (by mass spectrometer) product was obtained. The method was applied to the pyrolysis of methane where hydrogen, acetylene, and carbon were the principal products.

[1] A. C. Kolb, *Magnetohydrodynamics* (Stanford University Press, Stanford University, California, 1957), p. 76.
[2] E. G. Harris, NRL Report 4859 (1956).

CA6. Equilibrium Properties of a Multicomponent Ionized Gas.* Gilda Maki, *University of California, Livermore*.—A method has been developed for the calculation of the equilibrium properties of an ionized gas consisting of many nuclear and molecular species. An essential feature of the present calculation is that it explicitly considers more than one ionic species per atom and therefore applies to partially ionized atoms and molecules. Free and bound electrons are distinguished by counting as bound electrons all those in the ground state of each ionic species. Molecular species with internal degrees of freedom are also included. The additivity of kinetic and potential energy is assumed, a classical electrostatic potential of interaction is used, and electron degeneracy is included only in the kinetic energy terms. The Helmholtz free energy of the system is minimized with respect to the concentration of each species assumed present, thus determining the equilibrium composition of the system as a function of temperature and volume. The thermodynamic quantities of interest are then calculated for an appropriate temperature-volume grid. This method thus allows the effect of the variation of composition on the equation of state to be determined, as well as the delineation of regions in PVT space where the electron degeneracy and electrostatic interaction each becomes important.

* This work was performed under the auspices of the U. S. Atomic Energy Commission.

CA7. Interaction of Oxygen with Clean Silicon Surfaces. K. H. Maxwell and Mino Green, *Zenith Radio Corporation* (introduced by R. Seiwatz).—The adsorption of oxygen on virgin silicon surfaces produced by crushing *in vacuo* has been examined in the pressure range 30–200 μ Hg of oxygen at room temperature. The experimental techniques are those previously described for germanium.[1] The initial adsorption to the extent of about a monolayer was very rapid, kinetics were obtained for the subsequent slow adsorption. The results show that the slow uptake *cannot* be expressed in any simple mathematical form (e.g., Elovich's equation does *not* apply). The adsorption process is found to terminate at an oxygen uptake equivalent to about 1.6 oxygen atoms per surface silicon atom. The surface areas were measured by krypton adsorption at liquid nitrogen temperature.

[1] Green, Kafalas, and Robinson, *Semiconductor Surface Physics*, edited by R. H. Kingston (University of Pennsylvania Press, Philadelphia, Pennsylvania, 1956), p. 349.

CA8. Interaction of Hydrogen with Tungsten. T. W. HICKMOTT, *General Electric Research Laboratory.*—The kinetics of chemisorption of hydrogen on tungsten, and its desorption, have been measured under ultrahigh vacuum conditions. A lanthanum boride-coated tantalum filament replaced the conventional tungsten ionization gauge cathode to minimize contaminant effects due to atomic hydrogen produced by operation of the gauge.[1] The sticking probability for chemisorption at $T=77°K$ is 0.09, and no state of binding that desorbs above 1100°K is found if contaminant is absent.[1] On raising the filament temperature to 1100°K, only the evolution of molecular hydrogen is detected; evaporation is second order in the concentration of adsorbed atoms, n_a, showing that chemisorbed hydrogen is atomically bound, and the rate equation at low coverage ($n_a<30\times10^{13}$ molecules cm^{-2}) is $dn_a/dt=-(3\times10^{-2})\exp(-35\,000/RT)n_a^2$. Production of atomic hydrogen is detectable for filament temperatures greater than 1100°K, using liquid nitrogen cooled glass as a trap for the free atoms formed. At high temperatures ($T>1500°K$) and low pressures ($p<5\times10^{-8}$ mm) the probability of formation of atomic hydrogen from molecular hydrogen is 0.07. Combining data on the rate of production of atomic hydrogen, and on the desorption and sticking probability of molecular hydrogen, the rate equation for evaporation of hydrogen from tungsten as atoms is $dn_a/dt=-(5\times10^{13})\times\exp(-72\,000/RT)n_a$.

[1] T. W. Hickmott and G. Ehrlich, J. Phys. Chem. Solids 5, 47 (1958).

CA9. Comparison of Residual Gases in Ion-Getter and Oil Pumped Vacuum Systems. R. L. CHRISTENSEN AND I. AMES, *IBM Research Laboratory, Poughkeepsie.*—Analyses of constituent gases within two unbaked glass-metal vacuum systems have been made by an Omegatron mass spectrometer (partial pressure sensitivity limit about 2×10^{-9} mm Hg, resolution about 10%). One system was conventionally pumped by a GF-25 diffusion pump with Octoil-S, backed by a mechanical force pump. The other was evacuated by an ion-getter ("Vac-Ion") pump after being roughed out by cryogenic pumping.[1] Spectra were taken, within a range of total pressure (measured by WL-5966 ion gauge) from 3×10^{-6} to 3×10^{-6} mm Hg, primarily to demonstrate the difference in background vapors between the systems. At 2×10^{-7} mm Hg under conditions found preferentially to reduce hydrocarbons relative to mass 28 in the oil-pumped system (liquid nitrogen trapped, pump input power reduced), peaks corresponding to masses 42, 58, 72, and roughly, 100 to 128 are present with amplitudes about one-half that of mass 28. However, in the ion-getter pumped system at the same total pressure, these resonances, while not totally absent (as evidenced by their appearance if the envelope is heated) are less than 1% as large as that of mass 28.

[1] Ames, Christensen, and Teale, Rev. Sci. Instr. 29, 736 (1958).

CA10. Mass Spectrometer Study of the Vaporization of Certain Refractory Compounds. P. O. SCHISSEL AND W. S. WILLIAMS, *National Carbon Company Research Laboratories.*—A mass spectrometer has been used with a high-temperature Knudsen cell to study the vaporization of BN, AlN, and TiB_2 in vacuum. No mixed gaseous species were found. The following heats of formation were obtained: BN, $\Delta H_{298}\sim-60$ kcal/mole; AlN, $\Delta H_{298}\sim-63$ kcal/mole; TiB_2, $\Delta H_{298}\sim32$ kcal/mole. These BN and AlN heats agree with other recent determinations, but the TiB_2 heat obtained is a factor of two less than that reported by Brewer[1] and by Samsonov.[2] The heat of sublimation of boron was found to be 129 ± 5 kcal/mole, leading to an equilibrium vapor pressure of boron approximately a factor of ten higher than tabulated by Stull and Sinke.[3] The value 129 kcal/mole also has been obtained by Chupka in a similar experiment.[4]

[1] L. Brewer and H. Haraldsen, J. Electrochem. Soc. 102, 399 (1955).
[2] G. V. Samsonov, Zhur. Priklad. Khim. 28, 919 (1955).
[3] D. Stull and G. Sinke, "Thermodynamic properties of the elements." Advances in Chem. Ser. No. 18 (1956).
[4] W. Chupka (private communication).

CA11. Functional Representation of Sintering Severity.* BENNETT BOVARNICK, *Watertown Arsenal.*—The results of an experimental investigation of the sensitivity of the electrochemical potential of sintered iron to the degree of sintering has been previously reported.[1] Carbonyl iron powder specimens were sintered to conditions constituting 40 different treatments for study. The specimens were shown to have a decreasing potential depending upon the severity of the treatment. In order to provide a basis for a correlation of these results with recognized characteristics, specimens have been tested for mechanical strength. It was found that the strength increases uniformly with severity of the sintering treatment. The potential and strength are linear with respect to each other with a high statistical correlation coefficient. Based on the principles of rate process theory, a sintering severity function was derived in the form $P=(d/d_a)t^{1/7}T^2e^{-Q/RT}$, where the variables are the sintering conditions; relative density, time, and temperature. Both the electrochemical potential and strength were found to have linear dependence on the sintering parameter, P, with high statistical correlation coefficients.

* Supported by Ordnance Corps; Ph.D. thesis, Boston University, 1958.
[1] B. Bovarnick, Bull. Am. Phys. Soc. Ser. II, 1, 381 (1956).

MONDAY MORNING AT 10:00

Kresge Little Theater

(V. F. WEISSKOPF presiding)

Cosmic Rays; Nuclear Physics I

D1. Cosmogenic Noble Gases in the Washington County Meteorite.* DAVID E. FISHER AND OLIVER A. SCHAEFFER, *Brookhaven National Laboratory.*—An iron object that had been found sometime about 1916 embedded in the soil of Washington County was examined mass spectroscopically to determine if noble gases originating from cosmic ray induced spallation effects were present. There had previously been a question as to whether or not the object in question was a meteorite, the over-all appearance suggesting that it might have been machined and the presence of voids throughout the mass having been observed. In the present experiment $2\text{–}4\times10^{-6}$ grams per cc of helium-3 was found. Such a large quantity must be cosmogenic in origin, establishing definitely a meteoric origin. Values for the helium-3 content of various iron meteorites established in this and other laboratories range from 0.1×10^{-6} to 4×10^{-6} grams per cc. In addition to the helium-3 content, numbers are presented for helium-4, for the neon isotopes 20, 21, and 22, and for argon-36 and argon-38. It is concluded from a helium-4/helium-3 ratio of 2900, approximately five times higher than values reported

for similar meteorities, that there is present an excess of radiogenic over cosmogenic helium. Previous considerations ruling invalid uranium-helium age determinations are not significant in this case. It is calculated that sufficient uranium is present to make feasible its determination by neutron activation.

* Research performed under the auspices of the U. S. Atomic Energy Commission.

D2. Production of Helium and Neon in Aluminum by 700-Mev Protons and the Rare-Gas Contents of Stony Meteorites.* OLIVER A. SCHAEFFER AND DAVID E. FISHER, *Brookhaven National Laboratory.*—In the study of the rare gases produced in meteorites by cosmic rays, it is of interest to have information concerning the production cross sections of the rare gases from proton irradiated targets. Such measurements have been made for iron targets which can be compared to the rare-gas contents of iron meteorities. For stony meteorites the measured rare gases should be compared to a target of lower Z. Aluminum is a target in the range of the elements found in stones and the production cross sections were measured. It was found that for 700-Mev protons $\sigma_{He^3}=35$ mb, $\sigma_{He^4}=320$ mb, $\sigma_{Ne^{20}}=18$–23 mb, $\sigma_{Ne^{21}}=21$ mb, and $\sigma_{Ne^{22}}=14$ mb. The target was irradiated at the 700-Mev Berkeley synchrocyclotron and the rare-gas products measured with a high sensitivity mass spectrometer. Using the tritium production cross section[1] of 30 mb, $\sigma_{He^3}/\sigma_T=1.15$ and $(\sigma_{He^3}+\sigma_T)/\sigma_{He^4}=0.20$. So that if aluminum is representative of stony meteorites only 55% of the He^3 is directly produced rather than 70% as previously found for iron meteorites. The He^3-T exposure ages of stony meteorites will than require a much smaller correction for directly produced He^3.

* Research performed under the auspices of the U. S. Atomic Energy Commission.
[1] Currie, Libby, and Wolfgang, Phys. Rev. **101**, 1557 (1956).

D3. Absence of Cosmogenic Gases in a Tektite.* J. H. REYNOLDS AND G. C. FORD, *University of California, Berkeley.*—A search has been made for cosmic-ray produced He^3 and Ne^{21} in a tektite. Most of a 35-g specimen from Kalgoorlie, Western Australia, was digested in molten NaOH without having been preheated. The helium and neon evolved were purified and analyzed in a sealed-off mass spectrometer to which "spikes" of He^3 and Ne^{22} were later added so as to determine the amounts of gas by isotope dilution. To within experimental accuracy the gases were of atmospheric composition. The excess Ne^{21} was less than 14×10^{-12} cc STP per g; the excess He^3 was less than 1.6×10^{-13} cc STP per g. The tektite was dated by the K-A method and an age of $0.8\pm0.2\times10^6 y$ obtained, although this age remains to be confirmed. The diffusion coefficients for He and Ne in Kalgoorlie tektite glass are being determined. Preliminary data indicate that the 35-g specimen should have retained neon for a time of the order of 10^7 years. The neon datum thus points to a "flight time" of less than about 10^6 years. It appears then that the rare-gas data will neither confirm nor deny the extra-terrestrial origin of tektites, although by using latest techniques there should be no appreciable difficulty in obtaining reliable K-A ages for tektites.

* Work supported by the U. S. Atomic Energy Commission.

D4. Apparatus for Semiautomatic Ionization Measurements in Emulsion. F. W. O'DELL, M. M. SHAPIRO, B. STILLER, AND R. C. WADDEL, *U. S. Naval Research Laboratory.*—A semi-automatic device has been constructed for enhancing the precision and efficiency of gap-type ionization measurements in nuclear emulsions. The instrument incorporates a *variable*-speed motor drive for the microscope stage, and a pulsing system that delivers a fixed number of pulses per unit of stage travel independently of the speed at which the stage is moved. The variable-speed capability allows the observer to speed up the stage movement over long blobs or gaps. Conversely, the stage can be slowed down markedly as the edge of a blob or gap is approached. This minimizes the setting error incurred in signaling the instant at which the edge of a blob crosses a fiducial line in the field of view. The device records the integrated gap length, the number of gaps, the gap size distribution, and the length of track over which the measurements are made. Data are presented illustrating the range of ionizations over which the device has been used in Ilford G-type emulsions for inferring the charges of relativistic heavy primary nuclei.

D5. Variation of the Heavy Primary Flux with the Solar Cycle. HERMAN YAGODA, *Air Force Cambridge Research Center.*—The omnidirectional flux of heavy primaries ($Z\geq6$) as measured in emulsions flown in rockets at White Sands, New Mexico ($\lambda=41°$N) exhibits an appreciable diminution in intensity following the solar sunspot cycle. On a Viking rocket launched December 15, 1952, the flux J^0 was 7.0 ± 0.8 (m² sec sterad)$^{-1}$. Two similar rockets flown in May, 1954, gave J^0 values of 5.38 and 5.67. During a period of maximum sunspot activity (July, October, 1957) the fluxes measured on two Aerobee rockets averaged 4.98 ± 0.65 about 20% smaller than the mean for the 1952–1954 flights. Measurements of the number of heavy primaries which reach the end of their range in emulsions (P_t cc^{-1} d^{-1}) flown at balloon elevations ($\lambda=55°$N) confirm this time variation and indicate the existence of a much larger effect for the less energetic components. At 80 000-ft elevation where the air cutoffs for M and H nuclei are 430 and 900 Mev per nucleon, respectively, P_t shows insignificant variations during 1951 to 1958. In a recent exposure (August, 1958) at 112 000 ft permitting the termination of carbon nuclei with $\epsilon_0\geq160$ Mev per nucleon the P_t intensity is 3 times smaller than at equal altitude in 1953 and 1955 flights.

D6. Helium Flux in the Cosmic Radiation at Geomagnetic Latitude 3°N. B. HILDEBRAND, F. W. O'DELL, M. M. SHAPIRO, AND B. STILLER, *U. S. Naval Research Laboratory.*—600 μ Ilford G-5 nuclear emulsions were exposed on a Skyhook balloon flight near Guam (geomagnetic latitude $\approx3°$N) at an altitude corresponding to a residual atmosphere of 10 g/cm². Fast He nuclei were identified by scanning for 3–4.5 times plateau-ionization tracks and measuring their multiple Coulomb scattering. In this way one could discriminate against protons, deuterons, and tritons. Since the geomagnetic cutoff energy at $\lambda=3°$N is ~7 Bev/nucleon for helium, scattering measurements on the tracks of these particles yield mean deflections indistinguishable from "noise." On the other hand, tracks due to singly-charged particles with the same rate of ionization loss, have measurable scattering angles. This permits the use of a large scattering cell, 500 μ, and a small minimum track length, 4 mm. Preliminary analysis, based upon measurements of 800 tracks, resulted in classifying 195 of the particles as helium nuclei. By selecting tracks* with zenith angle $<30°$, we deduce a provisional flux *at altitude* of 11 peters (particles/m² sec sterad). Measurements are continuing, and intensity values based on improved statistics will be reported.

* 123 tracks were found in this interval.

D7. Energy Distribution of Li^8 Fragments at Various Excitation Energies.* A. G. BARKOW, *Marquette University,* G. KANE, *Manhattan College,* R. E. MCDANIEL, *New Mexico College of A and M. A.,* AND Z. O'FRIEL, *St. Bonaventure University.*—A preliminary report on the analysis of Li^8 fragments from stars produced at excitation energy of 140 Mev (stopped π^-), 400 Mev, 1 Bev, 4.5 Bev, 6.3 Bev, and cosmic rays. The emission of Li^8 in stopped π^- stars favors the three prong stars. The proton energy distribution of Li^8 is

highly peaked at the low energies for low excitation. The apparent discrepancies between the distribution of Li^8 and $Li^{6,7}$ is strictly due to the inability of identifying $Li^{6,7}$ tracks of ranges less than 40 μ. At high energies the distribution is dependent on the nuclear temperature (T) and potential barrier (V). The energy distribution of Li^8 was found to be independent of the size of the parent star.

* Work supported by the National Science Foundation.

D8. Angular Correlation between the Pions in a Photoproduced Pair.* D. D. ELLIOTT AND M. SANDS, *California Institute of Technology*.—The angular correlation between the two pions from the reaction $\gamma+P \rightarrow P+\pi^+ +\pi^-$ has been studied by observing coincidences between the two pions produced simultaneously in a hydrogen target in the 1.1-Bev x-ray beam of the CalTech synchrotron. The negative pion was detected in a magnetic spectrometer set to accept 150-Mev pions at an angle, θ_-, of 35° with respect to the x-ray beam. The positive pion was detected in a telescope which was set at several angles, θ_+, with respect to the x-ray beam, with azimuthal angles, ϕ_+, of 0°, 90°, 180° (with respect to the azimuthal angle of the negative pion). For each set of angles the absorbers in the telescope were chosen so that the photon responsible for the pair reaction was in the energy interval 650–825 Mev. In the c.m. system the cross section shows no azimuthal dependence within the statistical error of about 20% at either of the two c.m. angles $\theta_+' = 70°$ and 120°. For $\phi_+' = 180°$ the cross section appears to be independent of zenith angle, θ_+', except at the most forward point ($\theta_+' = 35°$) where the measurement shows a cross section about 30% larger than that observed at other angles.

* This work was supported in part by the U. S. Atomic Energy Commission.

D9. Measurement of the Deuteron Binding Energy by Direct Crystalline Diffraction of the Gamma Ray from $H^1(n,\gamma)H^2$.* E. L. CHUPP, J. W. M. DUMOND,† R. JEWELL, AND HANS MARK,‡ *University of California*.—It has recently been demonstrated[1] that a two-meter-radius bent-quartz-crystal photographic spectrograph could be used to record gamma rays of energy >1 Mev. It was therefore evident that this technique could be used to measure the energy of the gamma ray from the reaction $H^1(n,\gamma)H^2$. The LPTR, a 1-mw research reactor at the Livermore laboratory, was used to provide a source of 1500 curies of the deuteron formation gamma ray. By diffracting from the two sides of the crystalling planes it is possible to record symmetrically, with respect to the zero wavelength point of the instrument, both deuteron formation gamma rays and both of the Au^{198} 411.77-kev calibration lines. A preliminary wavelength value for the deuteron formation gamma ray is 5.567 ± 0.015 x units which, when corrected for the deuteron recoil, gives 2.224 ± 0.008 Mev for the deuteron binding energy.

* This work was performed under the auspices of the U. S. Atomic Energy Commission.
† California Institute of Technology.
‡ Massachusetts Institute of Technology.
[1] Chupp, DuMond, and Mark, Rev. Sci. Inst. **29**, 1153 (1958).

D10. (n,p) Cross Sections near $Z=20$.* M. R. ZATZICK AND H. P. EUBANK, *Brown University*.—Forward differential (n,p) cross sections have been measured with a counter telescope for 14.1-Mev neutrons on the following elements, all of natural isotopic abundance: $_{12}$Mg, $_{18}$A, $_{21}$Sc, $_{22}$Ti, $_{23}$V, $_{24}$Cr, and $_{28}$Ni. The measurements cover the proton energy range 4–14 Mev. Differential cross sections assigned are Mg: 10.7 mb/sterad; A: <1 mb/sterad; Sc: 28 mb/sterad; Ti: 3.5 mb/sterad; V and Cr: <1 mb/sterad; Ni: 32 mb/sterad. Angular distributions (0–80°) have been made of Mg, Sc, and Ni which exhibit an anisotropy of no more than 50% in the case of Mg and Sc and less than 20% in the case of Ni. This is consistent with the work of others in this mass region,[1,2] and is in marked contrast to angular distribution from nuclei in the vicinity of $Z=50$.[1-3] The large (n,p) cross section at $Z=21$ is analogous to that found following shell closure at $Z=50$[3].

* Supported in part by the U. S. Atomic Energy Commission.
[1] Verbinski, Hurlimann, Stephens, and Winhold, Phys. Rev. **108**, 779 (1957).
[2] D. L. Allan, Proc. Roy. Soc. (London) **A70**, 195 (1957).
[3] Eubank, Peck, and Al-Kital, Bull. Am. Phys. Soc. Ser. II, **3**, 269 (1957).

D11. Isomer Ratios in Alpha-Induced Reactions.* T. MATSUO AND T. T. SUGIHARA, *Clark University*.—The ratio of sections for forming 2.4-day $Sc^{44m}(6,7+)$ and 3.9-hr $Sc^{44g}(2,3+)$ has been measured for the reaction $K^{41}(\alpha,n)$. Stacked-foil techniques were used in the energy range 6 to 30 Mev, and the isomer ratio and the excitation function for the (α,n) reaction were measured. The results are shown in Table I.

TABLE I. Mean alpha energy in thin target (Mev).

	6	11	16.5	20.3	20.8	23.9	25.8	27.7	29.9
Ratio (m/g) (I 5%)	0.30	0.34	0.74	1.10	1.56	1.60	2.00	1.83	1.45

These data will be compared with similar results[1] obtained in the reaction $Sc^{45}(p,pn)$ and with the calculated distribution of angular momentum states in the compound nucleus.

* Supported in part by the U. S. Atomic Energy Commission.
[1] Meadows, Diamond, and Sharp, Phys. Rev. **102**, 190 (1956).

D12. Electron Microscope Observation of Fission Tracks in UO_2 Films. J. O. STIEGLER AND T. S. NOGGLE, *Oak Ridge National Laboratory** (introduced by F. W. Young).—Thin films of UO_2 irradiated in the graphite reactor at Oak Ridge National Laboratory have been examined in the electron microscope and a line structure associated with fission has been observed. Comparison of the density of this structure in films formed with natural uranium and with enriched uranium indicates that the tracks observed are associated with the U_{235} present in the film and hence with fission. Comparison of the observed density with simple calculations relating geometry of the observational system, cross section for fission, and thermal flux indicates that there is substantially a one to one relationship between the number of events observed and number expected. It is suggested that this technique offers promise as a method of measuring the range of fission fragments and cross sections for fission processes.

* Oak Ridge National Laboratory is operated by Union Carbide Corporation for the U. S. Atomic Energy Commission.

MONDAY MORNING AT 10:00

Kresge Auditorium

(B. LAX presiding)

Invited Papers of the Division of Solid-State Physics

DA1. High Field Antiferromagnetic Resonance. S. FONER, *Lincoln Laboratory.* (30 min.)

DA2. Stress and Temperature Dependence of Electron Spin Resonance. WALTER M. WALSH, JR., *Harvard University.* (30 min.)

DA3. Antiferromagnetic Resonance in MnF_2. A. H. NETHERCOT, JR., *Columbia University.* (30 min.)

DA4. Competition between Ferromagnetic and Antiferromagnetic Exchange Interactions in Alloys. A. ARROTT, *Ford Motor Scientific Laboratory.* (30 min.)

MONDAY AFTERNOON AT 2:15

Kresge Auditorium

(C. G. SHULL presiding)

Invited Papers of the Division of Solid-State Physics

E1. Optical Properties of Antiferromagnetic Salts. G. W. PRATT, JR., *Lincoln Laboratory.* (30 min.)

E2. Covalency Effects in Mainly Ionic Crystals. W. MARSHALL, *Harvard University.* (30 min.)

E3. Neutron and X-Ray Scattering from Electrons in Crystalline Fields. A. J. FREEMAN, *Ordnance Materials Research Office, MIT.* (30 min.)

E4. Inelastic Scattering of Neutrons by Spin Waves. T. RISTE, *Joint Establishment for Nuclear Energy Research, Norway.* (30 min.)

MONDAY AFTERNOON AT 2:00

Room 6–120

(R. F. WALLIS presiding)

Invited Paper

EA1. Calculations of Lattice Vibrations in Alkali Halides. STIG LUNDQVIST, *Universities of Uppsala and Pennsylvania.* (30 min.)

Solid-State Theory II

EA2. Specific Heats and Vibration Spectra of Alkali Halides.* J. C. PHILLIPS,† *University of California, Berkeley.*—A method is presented for inverting specific heat data to obtain frequency distributions for lattice vibrations. The "singularity" method is sufficiently simple that it is easy to fit specific heat data within 0.2% as well as estimate the uncertainties in the resulting frequency distributions. In this way frequency distributions are constructed for KCl, KBr, KI, NaCl, and NaI. These distributions reproduce the specific heats which have been measured with an experimental uncertainty of 0.2% to within that limit. From these frequency distributions dispersion curves can be deduced. The results show systematic variations with relative size of the halide ion. Deviations from the sum rule recently derived by Brout[1] on the assumption of nearest-neighbor repulsive forces only indicate the increasing importance of halide-halide repulsive forces with increase of relative size of the halide ion.

* Supported in part by the National Science Foundation.
† National Science Foundation Postdoctoral Fellow.
[1] R. Brout, Phys. Rev. (to be published).

EA3. Fundamental Lattice Absorption Frequency in NaCl and KCl. MARVIN HASS, *U. S. Naval Research Laboratory.*—The far infrared absorption spectra of thin films of NaCl and KCl were obtained at liquid nitrogen temperature. Maximum absorption occurs at 171 cm^{-1} for NaCl and 147 cm^{-1} for KCl. These values can be used to check the semiempirical Lundqvist[1] modification of the Szigeti[2] formula relating the absorption frequency and compressibility. The Lundqvist formula takes into account the failure of the Cauchy relations. Since the Cauchy relations are not satisfied for NaCl at low temperatures,[3] it is of interest to compare the experimental value with the Lundqvist value of 182 cm^{-1}.

[1] S. Lundqvist, Arkiv. Fysik **9**, 435 (1955).
[2] B. Szigeti, Proc. Roy. Soc. (London) **A204**, 51 (1950).
[3] W. C. Overton, Jr., and R. T. Swim, Phys. Rev. **84**, 758 (1951).

EA4. Energy Expansions in a Sodium Chloride Type Lattice.* R. D. HATCHER,† AND G. J. DIENES, *Brookhaven National Laboratory.*—The calculation of equilibrium arrangements in a solium chloride type lattice, when an additional

neutral ion is added, has been carried out by making expansions for the electrostatic, polarization, and repulsive energy terms. These expansions have been made in terms of the displacements of the regular ions from their normal positions; and for the additional ion in terms of its displacement from an arbitrary position in the lattice. For small displacements these approximate expansions are found to be sufficient to represent the energy when carried to the second order in the coordinates of the displacements. Using the equilibrium conditions that the derivative of the energy with respect to each coordinate is zero, a set of simultaneous linear equations are obtained which can be solved uniquely for the displacements. An application has been made to the case of NaCl with an additional Cl^0 ion present to determine the equilibrium arrangement and the mobility of the Cl^0 ion under the assumption that no additional types of forces are necessary.

* Assisted by the U. S. Atomic Energy Commission.
† Permanent address: New York University.

EA5. Theory of Anharmonic Vibrations in Crystals. L. A. GIRIFALCO, *National Aeronautics and Space Administration.*—A statistical thermodynamic theory of crystals has been developed which includes the anharmonic contribution to the thermodynamic properties. The first step in this theory is a calculation of the energy levels of the crystals by perturbation theory, using a potential that includes the cubic terms in the atom displacements, with the result that the energy of the crystal is quadratic in the quantum number. These energy levels are then substituted into the equation for the partition function of the crystal. The harmonic and anharmonic contributions to the partitions function can be separated, so that by applying the usual thermodynamic formulas it is possible to obtain equations that exhibit the harmonic and anharmonic contributions to the thermodynamic properties separately. The theory is a generalization of previous work in that the quantum mechanical energy levels of the crystal are used in the partition function.

EA6. Anharmonic Lattice Vibration Absorption in a One-Dimensional Diatomic Lattice. A. A. MARADUDIN* AND R. F. WALLIS, *U. S. Naval Research Laboratory.*—Using the Born-Huang[1] theory of optical absorption in anharmonic lattices, calculations have been made of the optical absorption coefficient of a one-dimensional diatomic lattice with nearest neighbor interactions for which the potential energy has been expanded up to cubic terms in the atomic displacements. For this model it is possible to obtain exact expressions in closed form for the absorption coefficient in both the low- and high-temperature limits. The frequency dependent damping constants in this theory vary as the cube of the absolute temperature at high temperatures in contrast with the linear dependence obtained from the classical treatments of Blackman[2] and Neuberger.[3]

* Permanent address: University of Maryland.
[1] M. Born and K. Huang, *Dynamical Theory of Crystal Lattices* (Oxford University Press, New York, 1954), p. 341.
[2] M. Blackman, Z. Physik **86**, 421 (1933).
[3] J. Neuberger, AFCRC-TR-57-353 (New York University, 1957), p. 189.

EA7. Vibrational Frequency Spectra of Two-Dimensional Lattices with Coulomb Interactions.* J. A. DAVIES AND A. A. MARADUDIN, *University of Maryland* (introduced by R. D. Myers).—The frequency spectra of a 2-*D* monatomic lattice with Coulomb interactions plus nearest neighbor repulsive forces have been calculated for the cases of one and two degrees of freedom per lattice point. In the former case the vibrations are taken to be normal to the plane of the lattice. The frequency spectrum contains two logarithmic infinities and a discontinuity in slope not found in short-range force models. The latter singularity is associated with a critical point at which grad $\omega^2 \neq 0$. The second model differs from that studied by Smollett[1] only in the range of the non-Coulomb forces. The constant frequency curves are qualitatively the same as obtained by Smollett, but the frequency spectrum contains a logarithmic infinity, two jump discontinuities not located at the end points, and a discontinuity in slope in addition to the singularities found by Smollett.

* This work was supported by the U. S. Air Force.
[1] M. Smollett, Proc. Phys. Soc. (London) **A65**, 109 (1952).

EA8. Vibration Frequencies of Defect Modes for Lattices with Coupled Displacement Components.* J. MAHANTY† AND A. A. MARADUDIN, *University of Maryland* (introduced by R. D. Myers).—All calculations up to the present time of the frequencies of localized modes of vibration associated with defects in a crystal have been carried out either for the longitudinal vibrations of linear chains[1] or for physically unrealistic models of two- and three-dimensional lattices where the x, y, and z-components of displacement are uncoupled.[2] The usual methods[1] for calculating these frequencies cannot be used in the case of lattices with coupled displacement components. The frequencies of the localized modes due to a light isotope defect in a monatomic linear chain in which the particles have coupled longitudinal and transverse displacement components have been calculated by a study of the analytic properties of the secular determinant in the complex frequency plane. A single frequency emerges from the top of each of the two bands of the frequency spectrum, and each varies quadratically with the strength of the defect. Applications of this method to two- and three-dimensional lattices will be discussed.

* This work was partially supported by the U. S. Air Force.
† Bell Telephone Laboratories Fellow.
[1] E. W. Montroll and R. B. Potts, Phys. Rev. **100**, 525 (1955).
[2] Maradudin, Mazur, Montroll, and Weiss, Revs. Modern Phys. **30**, 175 (1958).

EA9. Theory of Dielectric Constant of LiF. E. R. LEVIN, *Frankford Arsenal,* AND E. L. OFFENBACHER, *Temple University.*—A theory for the dielectric constant of LiF has been developed from the standpoint of wave mechanics, using a Heitler-London model in which the wave functions of the outermost ($2p$) electrons of the F^- ion are distorted in an electric field, while the Li^+ ion and the inner-core electrons of the F^- ion retain their normal configurations. A variational form is assumed for the distorted wave functions of the $2p$ electrons, which remain orthogonal to the inner core electrons, and the change in energy resulting from application of the field is determined. Energy terms are grouped according to whether they involve interactions (a) between the external field and the lattice, (b) within a single ion, or (c) between ions in the lattice. The distorted ions interact with the uniform external field as simple dipoles. Intraionic terms (b) yield energy contributions of significant magnitude for both Coulomb and exchange interactions, and for the kinetic energy. The terms (c) are analyzed on the basis of Löwdin's expression for the cohesive energy of a crystal. The Madelung energy and portions of the overlap energy are readily evaluated in terms of first and second moments of the distorted wave function.

EA10. On the Stability of Lattice Defects. J. W. CORBETT AND D. W. HARRIS, *General Electric Research Laboratory.*—The stability of the equilibrium position[1] of the crowdion and the body-centered interstitial is examined by considering the second derivative of the potential energy of a central defect atom due to the Born-Mayer type repulsive interaction of the first and second nearest neighbors. In both cases the solutions given[1] are found to represent stable equilibrium positions with respect to displacements in *all* three major displacement directions. The present calculations do not consider the contribution of the elasticity theory solutions associated with

the more remote neighboring atoms, nor the contribution of the change in condition electron energy. The interstitialcy will also be discussed.

[1] L. Tewordt, Phys. Rev. 109, 61 (1958).

EA11. Divacancy in Copper. V. G. WEIZER AND L. A. GIRIFALCO, *NASA Lewis Research Center.*—An accurate calculation of the binding energy and equilibrium configuration is performed for copper using Morse type pairwise potentials. The model used is a 20- by 20- by 20-atom lattice with two vacancies, separated by one nearest neighbor distance, imbedded in the center of it. A process of successive approximations is employed to find the relaxation energy and equilibrium configuration. The actual calculations are performed on a high-speed digital computer. The results are discussed and compared to previous efforts. This work is the first step in the solution of the problem of the interaction of two vacancies as a function of their separation.

MONDAY AFTERNOON AT 2:00

Room 26–100

(H. Y. FAN presiding)

Impurities in Semiconductors

F1. Spin Resonance of Iron-Acceptor Complexes in Silicon. G. W. LUDWIG, R. O. CARLSON, AND H. H. WOODBURY, *General Electric Research Laboratory.*—Association of iron with the shallow acceptors, boron, gallium, aluminum, and indium, has been detected in silicon by spin-resonance techniques. Samples were prepared by diffusing iron at ~1300°C into crystals containing $\sim 10^{16}/cm^3$ acceptors. If one uses boron- or gallium-doped silicon, pairs are formed with iron. It is believed that the boron or gallium occupies a substitutional site in the lattice and the iron is interstitial. The spectrum of any one pair shows axial symmetry about a (111) axis ($g_{\parallel}=2.069$, $g_{\perp}=4.089$ for Fe–B; $g_{\parallel}=5.087$, $g_{\perp}=2.530$ for Fe–Ga). The B^{10}, B^{11}, and Fe^{57} hyperfine structure has been studied in Fe–B doped silicon utilizing enriched isotopes. In Fe–Ga doped silicon the Fe^{57} hyperfine structure is not resolved. However, Fe^{57}, as well as Ga^{69} and Ga^{71}, double resonance has been observed. In both pairs the quadrupole interaction of the acceptor appears to be comparable to its magnetic hyperfine interaction. The spectra in aluminum- and indium-doped crystals are more complicated, and the composition of the complexes is not yet known. In indium-doped crystals the principal axes of the spectra are two (110) axes and a (001) axis, having g values of 3.78, 4.40, and 2.07, respectively.

F2. Electron Spin Resonance of Donor and Acceptor States in Diamond. W. V. SMITH, I. L. GELLES, AND P. P. SOROKIN, *IBM Research Laboratory, Poughkeepsie.*—Room-temperature paramagnetic resonance spectra have been observed in the majority of a surveyed lot of approximately 50 natural, unirradiated diamonds.[1] Except for a few samples with a single line at $g=2$, as yet not analyzed, the diamonds display either the paramagnetic resonance spectrum of bound substitutional aluminum acceptors[2] or a spectrum believed to be due to bound substitutional nitrogen donors. The observed absence of a sample with both spectra simultaneously present can be explained by a simple impurity compensation argument. The g factor of the donors is isotropic, but one of the C–N bond directions is a hyperfine axis with constants $|A|=40.8$ oersted, $|B|=29.3$ oersted. There are thus four types of donor impurity centers, equally abundant. There is no evidence of rapid reorientation of the donor hyperfine axes. No effects due to an interaction with the nuclear quadrupole moment of nitrogen are seen, in sharp contrast to the acceptor resonance case.[2] The extremely small line width of $\leqq 0.3$ oersted for both donor and acceptor resonances probably represents hyperfine broadening of the lines by the 1.1% abundant C^{13} isotope.

[1] The diamond samples were kindly made available to us by Mr. Bart Van Berg of the Rough Diamond Company.
[2] Smith, Gelles, and Sorokin, Phys. Rev. Letters 2, 39 (1959).

F3. Spin Resonance in SiC. H. H. WOODBURY, R. I. SCACE, AND G. W. LUDWIG, *General Electric Research Laboratory.*—Spin resonance absorption in n-type and p-type single crystals of SiC has been observed. Crystals are prepared by heating silicon with the doping material in a graphite tube to a temperature of 2700°C under 35 atmos pressure. The SiC is formed by reaction of the silicon with the graphite tube. Some undoped runs contain nitrogen as an accidental impurity and are n type. Boron has been added producing p-type crystals. The spin resonance spectra of the n-type samples containing nitrogen are similar to those observed by van Wieringen.[1] The spectra of the boron-doped samples are anisotropic, and show considerable structure which is believed to be B^{11} hyperfine structure. Samples have been studied doped with enriched B^{10}. In the latter samples, the structure is only poorly resolved. There may be more than one type of boron site, each of which has a distinct spectrum.

[1] J. S. van Wieringen in *Semiconductors and Phosphors*, edited by M. Schön and H. Welker (Interscience Publishers, Inc., New York, 1958), p. 367.

F4. Zeeman Effect of Donors in Silicon. I. Theory.* WALTER H. KLEINER, RICHARD N. BROWN, AND BENJAMIN LAX, *MIT.*—The theory is considered neglecting spin in the one-valley effective mass approximation for the states with envelope functions which are $2p$-like and $3p$-like in zero field. The effective mass Hamiltonian matrix is set up for these states with approximate zero-field envelope functions. An analysis is made of the relations among the matrix elements arising from symmetry. Hydrogen-like zero-field functions with modified exponentials of the form $\exp|-[B^2(x^2+y^2)+D^2z^2]^{\frac{1}{2}}|$ are used to evaluate the matrix. The energy levels *vs* magnetic field obtained with parameters determined variationally and with $B=D$ show, as expected, the Zeeman splitting of the $2p_{\pm}$- and $3p_{\pm}$-like levels, the anisotropic dependence on field orientation, and for large fields, the upward shift with field and the repulsion between levels arising from different zero-field levels. Results obtained from this approximation and two others characterized by different choice of the parameters B and D will be examined to indicate the effect of varying the zero-field functions.

* The work reported here was performed at Lincoln Laboratory, a technical center operated by Massachusetts Institute of Technology with the joint support of the U. S. Army, Navy, and Air Force, under contract.

F5. Zeeman Effect of Donors in Silicon. II. Experiment.* SOLOMON ZWERDLING, KENNETH J. BUTTON, AND BENJAMIN LAX, *MIT.*—Experiments were conducted using a low-temperature infrared magneto-spectrophotometric system[1] to observe the Zeeman effect of impurity levels in* silicon. Double-pass KBr prism dispersion (resolution $\sim 2\times10^{-4}$ ev) was used. For the donor impurity, bismuth, the zero-field results are in good agreement with previous work.[2] The Zeeman spectrum was interpreted in accordance with the theory developed.[3] For **B**//[110], only four of six ellipsoidal energy surfaces contribute to a splitting of the $2p_{\pm}$ level of 1.7×10^{-3} ev at 38.9 kilogauss, within 10% of the calculated value. Polarization with **E**//**B** and **E** $\perp$ **B** was used, as for measurements of the $2p_0$, $3p_0$, and $3p_{\pm}$ levels. For these p_0 levels, theory predicted a small quadratic shift with field. Splitting of the $3p_{\pm}$ level was observed, but the absorption had much lower intensity than for $2p_{\pm}$. For the sample used (9×10^{14} imp/cm^3; $t=6$ mm), additional lines not previously reported[2] were found. One showed a $p_{\pm}$-like behavior and the other two, a p_0-like behavior with field. Preliminary measurements of acceptor levels were also made (gallium, $\sim10^{16}$ imp/cm^3) with **B**//[111]. The spectrum contained two lines which split and shifted with field, respectively.

* The work reported here was performed at Lincoln Laboratory, a technical center operated by Massachusetts Institute of Technology with the joint support of the U. S. Army, Navy, and Air Force, under contract.

[1] Zwerdling, Lax, Roth, and Button, Phys. Rev. (to be published).
[2] H. J. Hroetowski and R. H. Kaiser, J. Phys. Chem. Solids **4**, 315 (1958).
[3] Kleiner, Brown, and Lax (preceding abstract).

F6. Hall Effect and Impurity Levels in Phosphorus-Doped Silicon. DONALD LONG AND JOHN MYERS, *Honeywell Research Center.*—Careful measurements of the Hall coefficient R and Hall mobility between 25°K and 300°K were made on a set of phosphorus-doped silicon samples of widely varying impurity content and compensation in an attempt to test the Kohn-Luttinger theoretical energy level model for donors in silicon. According to this model, failure of the effective mass theory of donor states near the impurity ion causes a depression of one of the six (excluding spin) ground states relative to the remaining five. The depressed state gives the 0.044-ev ionization energy. The separation Δ between the singly and fivefold degenerate levels can be measured by comparing carrier concentration n *vs* temperature T curves corresponding to this energy level scheme with experimental curves derived from Hall data. The n *vs* T curves for our samples all agree well with the Kohn-Luttinger model for values of Δ between 0.009 and 0.012 ev. To calculate n from R, we estimated the temperature dependence of the factor $r(n=r/Re)$ for each sample from its mobility data and the Brooks-Herring impurity scattering formula. Actually, the apparent magnitude of Δ proves quite insensitive to the values of r used, although uncertainty about the precise relation between n and R at all temperatures precludes a meaningful resolution of any further splitting of the fivefold degenerate level.

F7. Infrared Absorption of Group III Impurities in Germanium.* P. FISHER AND H. Y. FAN, *Purdue University.*—The excitation spectrum of each of the impurities, B, In, Ga, and Tl, in germanium is characterized by a pair of adjacent strong lines, These lines occur at 143 and 155.7 μ for B, 126 and 135.5 μ for In, 134.5 and 147 μ for Ga, and 109 and 116.5 μ for Tl. Several weak lines are observed on either side of the strong lines. The energy separation of the two strong lines is consistent to within a few percent for the different impurities. Comparison with the effective mass calculation given by Kohn leads to the assignment of the two strong lines to the $1s-2p^{(3)}$ and $1s-2p^{(3)}$ transitions. With a magnetic field applied parallel to the [111] direction, the line assigned to the $1s-2p^{(2)}$ transition is observed to split into two lines, the separation of which is linear with field strength to within experimental accuracy. The line $1s-2p^{(3)}$ is shifted to higher energy with evidence of a much smaller splitting than for the other line. The effect of magnetic field on the ionization absorption has also been observed and seems to be caused by Landau levels of the light hole band.

* Work supported by the Office of Naval Research.

F8. Theory of Valence Band Structure and Photoionization of Acceptor Impurities in Germanium in Magnetic Fields. R. F. WALLIS AND H. J. BOWLDEN,* *U. S. Naval Research Laboratory.*—The energies of the magnetic subbands of the valence band in germanium have been calculated as a function of k_z, the propagation constant parallel to the external magnetic field. The theory of Luttinger[1] was employed with the assumption that $\gamma_2=\gamma_3$. The 1^+ and 2^+ light hole subbands and the 2^- heavy hole subbands have minima at $k_z=0$ and show quantum effects in their curvatures near the valence band edge. The 1^- heavy hole subbands show very marked quantum effects, their minima occurring at values of k_z different from zero. The results of the magnetic subband calculation have been used to investigate the photoionization absorption spectrum of acceptor impurities in germanium in magnetic fields. The peculiar nature of the 1^- magnetic subbands may introduce additional peaks into the spectrum.

* Permanent address: National Carbon Research Laboratories.
[1] J. M. Luttinger, Phys. Rev. **102**, 1030 (1956).

F9. Effect of Pressure on the Impurity Levels in Gold-Doped Germanium.* M. G. HOLLAND, *Harvard University and Raytheon Manufacturing Company,* AND WILLIAM PAUL, *Harvard University.*—The pressure coefficient of the four impurity energy levels in gold-doped germanium has been estimated from resistivity measurements at discrete temperatures (between 45°K and 195°K) for which the statistics can be easily analyzed. The changes of the mobility and the density of states with pressure are taken into account. Results for the four levels are: (1) for the donor level, $E_1-E_v=0.04$ ev, $\alpha_1=0.1$, (2) for the acceptor level, $E_2-E_v=0.15$ ev, $\alpha_2=0.6$, (3) for the acceptor level, $E_3-E_v=0.55$ ev, $\alpha_3=2.1$, (4) for the highest acceptor level, $E_4-E_v=0.71$ ev, $\alpha_4=2.9$, where $\alpha_i=(d/dP)(E_i-E_v)$ in units of 10^{-6} ev/kg/cm^2. For comparison the total gap coefficient is 5.0×10^{-6} ev/kg/cm^2. For all four levels the percentage change of the level is greater with respect to the conduction band edge than the valence band edge. Evidence for an explicit temperature dependence which is greater than the volume derived temperature dependence will be presented.

* Supported by the Office of Naval Research.

F10. Lithium Oxygen Complexes in Germanium. W. W. TYLER, *General Electric Research Laboratory.*—The complicated behavior of oxygen in silicon has been the subject of many investigations. Preliminary studies suggest that the behavior of oxygen in germanium is similarly complex. Crystals grown from melts doped with GeO_2 contain oxygen in at least two forms, one electrically active,[1] the other inactive. Hall measurements indicate that electrically active sites, attributed to oxygen, act as double donors and may be present in concentrations as high as 5×10^{16} cm^{-3}. The presence of electrically inactive imperfections associated with oxygen is inferred from Li precipitation studies. Certain oxygen doped crystals which contain $<10^{14}$ cm^{-3} electrically active sites, contain $>10^{17}$ cm^{-3} stable donor Li$-$O complexes after the Li diffusion cycle. This behavior is analogous to that observed by Pell[2] for Li and oxygen in Si. The nature of the active and inactive oxygen sites and the Li$-$O complexes is not understood in detail. Infrared absorption and heat treatment studies are in progress. The presence of electrically inactive sulfur in Ge at concentrations as high as 10^{17} cm^{-3}

has also been inferred from donor complex formation in Li precipitation studies.

[1] G. Elliott, Nature **180**, 1350 (1957).
[2] E. M. Pell, Bull. Am. Phys. Soc. Ser. II, **3**, 128 (1958).

F11. Theory of the Energy Level Structure of Associated Donor-Acceptor Pairs. FERD E. WILLIAMS, *General Electric Research Laboratory.*—The donor-acceptor pair which is a two-particle system consisting of an electron and a positive hole bound in the field of a finite dipole is examined theoretically in a way similar to the Heitler-London treatment of the hydrogen molecule. The two-particle wave function is taken as a single product of separated hydrogen atom-like donor and acceptor wave functions. For the donor-acceptor pair no exchange integral arises, and the Coulomb integral is opposite in sign to the Coulomb integral of the hydrogen molecule. The energy for total ionization decreases with increasing degree of association. The analysis is generalized to pairs whose electron and hole masses are unequal and to pairs in polar media. The radiative transition energies involved in the creation and evolved in the annihilation of these bound electron-hole pairs are calculated. The effect of the state of ionization on the energies of the electron and hole levels is determined. In highly associated pairs the ionization of the electron or hole greatly reduces the ionization energy of the remaining particle. The analysis is applied to zinc sulfide containing Group IIIB donors and Group IB acceptors. Other possible applications of the theory are suggested.

F12. Dependence of Hole Ionization Energy on Copper Proportion in CdS:Ga:Cu Photoconducting Powders. RICHARD H. BUBE AND ARTHUR B. DREEBEN, *RCA Laboratories.*—The variation of hole ionization energy with copper proportion has been measured using photoconductivity in a series of CdS:Ga:Cu powders. The Cu concentration varies from 4×10^{17} to 2×10^{20} cm^{-3}, and each sample was prepared with a Cu-concentration to Ga-concentration ratio of 1.05. The hole ionization energy decreases from about 1.0 ev for low Cu concentrations to about 0.3 ev for 2×10^{20} Cu cm^{-3}. Measurements of photoconductivity *vs* Cu concentration at fixed temperature are exactly analogous to measurements of photoconductivity *vs* temperature at fixed Cu concentration. Invariance of the long wavelength cutoff of photoconductivity with Cu concentration indicates that the initial level does not move with increasing concentration, but that other levels are interposed between the initial level and the top of the valence band to facilitate hole escape. These results help to clarify other recent findings of a decrease in hole ionization energy with high sensitizing level concentration, both in CdSe:Cu crystals and in defect-sensitized CdS crystals.

F13. Equilibrium Vacancy Concentration in Ge at the Melting Point. A. G. TWEET, *General Electric Research Laboratory.*—Studies of dislocation-free Ge crystals have led us to the hypothesis that vacancies are incorporated into the crystal during growth, and precipitate during some stage of cooling of the crystal to room temperature,[1] possibly into prismatic dislocations formed from collapsed vacancy disks. We have attempted to determine the density of these vacancies by a Cu decoration technique in which we take advantage of the fact that Cu diffuses into Ge interstitially, but is electrically active only when it is substitutional.[2] Evidence is presented indicating that diffusing Cu into a dislocation-free Ge slab results in dissolution of the cluster, the individual vacancies combining with interstitial Cu atoms to form substitutionals. These latter can be counted by measuring the electrical conductivity. Such measurements indicate that the equilibrium concentration of vacancies grown into a Ge crystal at the melting point is $2.9\text{–}3.9\times10^{15}$/cm^3, and that heat treatment of dislocation-free crystals during normal growth permits vacancies to diffuse to the surface. If too much Cu is used in the decoration process, electrically inactive aggregates of unknown composition are formed.

[1] A. G. Tweet, J. Appl. Phys. **29**, 1520 (1958).
[2] C. S. Fuller and J. A. Ditzenberger, J. Appl. Phys. **28**, 40 (1957).

F14. Interaction of Diffusants in Germanium. J. O. MCCALDIN, *Hughes Semiconductors.*—The usual diffusion experiments employing impurities from columns III and V in a germanium or silicon medium are not designed to show any deviations from simple Fick's law distributions. Under some experimental conditions, however, interaction between two diffusing species can be exhibited. Reiss *et al.*[1] have shown pronounced effects for the case of lithium, which behaves as a positively charged ion, in doped silicon. Experiments in this laboratory show analogous behavior in germanium for column V impurities. In one experiment, two planar diffusion fronts, the one formed by a relatively rapid diffusant like arsenic and the other by an aluminum regrowth, intersect at 90°, and the progress of the fronts at 800°C is followed by metallography. In other experiments, the two fronts are parallel and their progress is followed by sheet conductance measurements as well as metallography. The experiments show that column V impurities in germanium are attracted to regions of heavy aluminum doping.

[1] Reiss, Fuller, and Morin, Bell System Tech. J. **35**, 535 (1956).

MONDAY AFTERNOON AT 2:00

Room 4–270

(W. W. TYLER presiding)

Invited Paper

FA1. Low-Temperature Annealing of Defects in Alkali Halides. D. A. WIEGAND, *Carnegie Institute of Technology.* (30 min.)

Alkali Halides and AgCl, including Irradiation Effects II

FA2. Detection of the Vacancies Created in Synthetic and Natural NaCl by High-Energy Radiation. H. W. ETZEL AND J. G. ALLARD, *U. S. Naval Research Laboratory.*—The growth of the *F*-band absorption produced by ultraviolet light has been measured in synthetic and natural crystals of NaCl before and after exposure to high-energy radiations. From previous work[1] it is known that vacancies are produced in synthetic NaCl by soft x-rays. It has been established recently[2] that synthetic NaCl contains hydroxyl ions which affect the production of *F* centers by ionizing radiations. The

present work indicates that the sensitization (colorability by ultraviolet light after exposure to high-energy radiation relative to colorability before exposure) is due to the production of U centers by the photochemical dissociation of hydroxyl ions by the high-energy radiation.

[1] H. W. Etzel, Phys. Rev. 100, 1643 (1955).
[2] H. W. Etzel and D. A. Patterson, Bull. Am. Phys. Soc. Ser. II, 3, 272 (1958).

FA3. γ-Ray Coloration of NaCl and KCl at 4°K and 300°K. HERBERT RABIN AND CLIFFORD C. KLICK, *U. S. Naval Research Laboratory.*—The growth of the F band under x-ray irradiation in a number of impurity-doped and undoped NaCl and KCl crystals has been measured at low temperature and at room temperature. Earlier measurements performed on these NaCl crystals suggested considerable variation in their initial negative ion vacancy concentrations and dislocation densities. The results of the present investigation indicate that although there is sizable variation in the magnitude of the x-ray coloration at room temperature (a factor of at least ten for the NaCl crystals and a factor greater than two for the KCl crystals), at approximately 4°K the coloration growth rate is identical to within 20% for all specimens of the same crystal. Since the coloration growth at 4°K is dependent only on the type of crystal and not on the impurity, vacancy or dislocation content, it appears likely that the production of negative ion vacancies (and hence F centers) occurs as a result of the formation of Frenkel defects in the negative ion sublattice. Furthermore, since the low-temperature coloration is independent of the initial concentration of vacancies, it may be supposed that vacancies originally contained in the crystal are clustered or in some configuration which does not permit the direct production of F centers at low temperature.

FA4. Some Low-Temperature Properties of the R, M, and N Centers in KCl and NaCl. CLIFFORD C. KLICK AND W. DALE COMPTON, *U. S. Naval Research Laboratory.*—Temporary changes in the absorption spectrum of a colored NaCl crystal can be produced at 77°K and 4°K by irradiating the crystal with a strong auxiliary light. The changes in the absorption spectrum indicate that the R, M, and N centers are not randomly distributed but are located near each other. It is concluded that previous arguments based upon less complete observations are not valid and that one cannot decide from this type of experiment whether the R_1 and R_2 bands arise from transitions in two distinct centers or from two transitions in the same center. Measurements of the degree of polarization of the emission excited with R_1- or R_2-band light indicate that the concentration of other centers probably affects this number. It is concluded that this measurement may not determine the symmetry of these centers. Measurements of the temperature dependence of the half-widths of the absorption and emission bands of the M center indicate that the optical transition is primarily influenced by local interactions of the center with neighboring ions and not by interactions with the long-range phonons of the lattice.

FA5. Optical Bleaching of Color Centers in KCl. W. E. BRON AND A. S. NOWICK, *IBM Yorktown Research Center.*—Thin specimens of Harshaw KCl were irradiated for various periods of time with filtered x-rays so as to obtain uniformly colored samples. Observations were made at room temperature on the optical absorption due to F, R, M, N, and V_3 centers as a function of F-light illumination. Throughout the bleaching period, the V_3 absorption remains essentially constant, indicating that all changes involve only electron centers. As observed by others, the F band bleaches in two stages, rapidly at first, and more slowly thereafter. The M band rises rapidly to a maximum in the range in which the F band bleaches rapidly. It then decreases slowly during the period when the F band bleaching is slow, and maintains a constant ratio to the F band. The R bands also go through a maximum, though at a later time than the M band. Examination of the bleaching data for lightly and heavily x-irradiated samples leads to the conclusion that the rapid stage of bleaching is closely connected with the first stage[1] of coloration. An anomaly exists, however, in that the initial bleaching rate of F centers is somewhat smaller for the more heavily irradiated samples. These results are valid for deformed as well as for annealed crystals.

[1] A. S. Nowick, Phys. Rev. 111, 16 (1958).

FA6. Excitation Spectra of KCl:Tl. D. A. PATTERSON, *U. S. Naval Research Laboratory.*—A series of potassium chloride single crystals with various amounts of thallium chloride have been grown in an argon atmosphere by the Kyropoulos technique. The thallium concentrations cover a considerable range corresponding to optical absorption coefficients at the peak of the 247-mμ thallium band of 1 to 230 cm^{-1}. The excitation spectra of these crystals have been measured at room temperature from 200 to 290 mμ. Results will be presented showing the growth, with increasing thallium concentration, of subsidiary bands on the long-wavelength sides of the primary thallium excitation peaks.

FA7. Alternative Configuration Coordinate Model for KCl:Tl. P. D. JOHNSON AND FERD E. WILLIAMS, *General Electric Research Laboratory.*—The 1960-A and 2470-A absorption bands and the 3050-A and 4750-A emission bands of thallium-activated potassium chloride have been interpreted on the basis of a configuration coordinate model including the effect of the crystalline field on spin-orbit interaction.[1] The discovery of a predicted emission band at 2470 A tends to confirm the model. We now propose a possible alternative model having a simpler theoretical basis but not as yet explaining all experimental data. In this model the two excited states are roughly parallel, the upper state being predominantly singlet, the lower, triplet. The 1960-A absorption and 2470-A emission can be attributed to transitions between the ^1S ground state and the upper excited state; 2470-A absorption and 3050-A emission, to transitions between ground and lower excited state, in accord with approximate theoretical calculations. In contrast to the earlier model, the pure $^1P^0$ and $^3P^0$ spin states do not cross: thereby we avoid spin-dependent crystalline interactions which vary rapidly with configuration coordinate. We are exploring modifications of the model to account for 4750-A emission. Experimental data and theoretical considerations will be discussed to determine the relative validities of the two models.

[1] F. E. Williams and P. D. Johnson, Phys. Rev. (to be published).

FA8. Isothermal Changes in Ionic Conductivity of Gamma-Irradiated NaCl.* H. S. INGHAM, JR., AND R. SMOLUCHOWSKI, *Carnegie Institute of Technology.*—A previous report[1] has been given on the isothermal changes in the dc ionic conductivity of NaCl after exposure to 10^5 roentgens of Co^{60} gamma rays. The results were interpreted as a clustering of the positive ion vacancies (presumed to be the current carriers) with other point imperfections, "traps," at a rate controlled by the diffusion of these vacancies. It is proposed that the traps are negative ion vacancies and small vacancy clusters which are created during irradiation. The experimental evidence suggests that the number of traps approaches a saturation value and the primary effect of further irradiation is to increase their average size and charge. Several specific trapping centers are deduced which include F centers and M centers. A suggested mechanism for creating these traps involves the formation of vacancy pairs by the Seitz mechanism. These mobile pairs cluster with each other or with existing imperfections.

The clusters become ionized by the irradiation and may then break up again, forming the traps and color centers.

* This research was supported by a U. S. Atomic Energy Commission contract.

[1] H. S. Ingham, Jr., and R. Smoluchowski, Bull. Am. Phys. Soc. Ser. II, 3, 143 (1958).

FA9. Formation of Defects in LiF, NaCl, and KCl by Ionizing Radiation.* D. A. WIEGAND AND R. SMOLUCHOWSKI, *Carnegie Institute of Technology.*—Several types of measurements, such as growth and regrowth curves of color centers and of volume changes, annealing studies, and energy absorbed per F center have been made on LiF, NaCl, and KCl crystals in an effort to determine the types of defects introduced by ionizing radiation and also to clarify the mechanism by which these defects are created. Annealing and regrowth data indicate two important annealing processes in LiF which can be associated with the motion of interstitials and vacancies respectively. Similar data have been taken on NaCl. Damage rates have also been investigated as a function of several parameters such as temperature, intensity, and plastic deformation. The results will be discussed in relationship to the various possible mechanisms of defect generation.

* This research supported by a U. S. Atomic Energy Commission contract.

FA10. Yield Point Effects in Silver Chloride Crystals.* M. N. KABLER AND L. M. SLIFKIN, *University of North Carolina.*—Plasticity of AgCl single crystals (Harshaw) has been investigated by repeated straining in tension in a "hard" machine in the vicinity of room temperature. Each test produces a strain of the order of 0.002. Samples of differing orientations all cut from the same crystal show different extents of easy glide; this can be correlated with slip line patterns. Aging at room temperature or higher produces an upper and lower yield point effect, the magnitude of which is characteristic of the crystal from which the specimen was cut. Attempts to correlate this with purity by means of electrical resistivity measurements are underway. Specimens cut from a crystal which exhibits pronounced age hardening show an interesting phenomenon: whereas the enhancement of the flow stress upon aging increases monotonically with aging time, the subsequent drop in stress after yielding *vs* aging time goes through a maximum. Thus, long anneals (one day at room temperature) enable the network produced to attain considerable stability against further applied stress. An investigation of the effect of internal print-out silver, produced by the Haynes-Shockley sweeping technique, on the yield point effect is currently in progress.

* Supported by the Office of Ordnance Research, U. S. Army.

FA11. Effects of Heat Treatment and Mechanical Deformation on Dark Conductivity of AgCl Crystals.* H. P. LAYER, L. M. SLIFKIN, AND R. C. HUDSON, *University of North Carolina.*—The structure-sensitive region of dark (ionic) conductivity of AgCl crystals has been studied as a function of thermal history and during plastic deformation. The room temperature conductivity (approximately $10(-8)$/ohm-cm) of an as-received Harshaw crystal was increased 40% by careful annealing in air at 420°C. This annealed value is decreased by a factor of 2.3 if the hot crystal is rapidly cooled (20 min). Further annealing increases the conductivity toward its highest value. These results may be understood in terms of a polyvalent negative ion which tends to segregate at dislocations and sub-boundaries. A rapid plastic extension of several percent produces a transient increase in conductivity over and above the relatively permanent effect due to excess dislocations and studied by W. G. Johnston. This pulsed conductivity follows the strain rate pulse even at liquid nitrogen temperatures indicating a relaxation time of no more than 0.02 sec. The effect is presumably due to excess interstitial silver ions. Quantitative evaluation of the conductivity increase per unit strain rate, the effect of dislocation content on the pulse magnitude, and extension of the experiment to lower temperatures are in progress.

* Work supported by the U. S. Atomic Energy Commission and Office of Ordnance Research, U. S. Army.

MONDAY AFTERNOON AT 2:00

Room 10–250

(D. E. MAPOTHER presiding)

Invited Paper

G1. Superconductivity and Electron Ferromagnetism. BERND MATTHIAS, *Bell Telephone Laboratories.* (30 min.)

Cryogenics

G2. Time Reversal and Superconductivity in Imperfect Crystals. P. W. ANDERSON, *Bell Telephone Laboratories.*—A remarkable fact about superconductivity is its insensitivity to amounts of crystal imperfection which scatter the electrons so rapidly that the energy uncertainty $\hbar/\tau$ of a plane wave function must be greater than the gap E_0, or even the Debye energy. This contrasts with the fact that the critical temperature decreases rapidly with the first small amount of scattering. The energy eigenfunctions in the presence of large amounts of elastic scattering are not Bloch waves but complicated linear combinations $\psi_{n\sigma}$ of them. If the scattering is nonmagnetic the time-reversed function $(\psi_{n,\sigma})^*$ is also an exact eigenfunction. We show that the BCS interaction transforms into an attractive interaction between pairs in these two functions ψ_n and $(\psi_n)^*$ which is close in value to the *average* BCS interaction between plane waves at the same energy. This interaction is more obviously unique here because in the absence of momentum conservation other matrix elements are smaller. The solution of the equation for E_0 will always be slightly smaller for this averaged interaction than for Bloch waves, which explains the initial T_c decrease. This decrease is expected to stop when $\hbar/\tau \sim E_0$. The considerable anisotropy in the energy gap expected from the plane wave theory will be absent, which may help to explain the failure so far to observe this.

G3. Millimeter Wave Measurements of the Energy Gap in Superconducting Aluminum. MANFRED A. BIONDI AND M. P. GARFUNKEL, *Westinghouse Research Laboratories.*—Recent experiments[1-3] concerning the absorption of electromagnetic

energy in the frequency range $h\nu \sim kT_c$ (the millimeter microwave and far infrared regions) have given direct evidence for the existence of an energy gap in the electronic energy spectrum of superconductors. We have extended our calorimetric measurements[2] to lower temperatures ($T=0.38$°K) and to shorter wavelengths ($\lambda=3.2$ mm) to determine the value of the energy gap at absolute zero in superconducting aluminum ($T_c=1.178$°K). The experimental value $E_g=3.2^{5}_{\pm 0.1}kT_c$ is in reasonable agreement with the theoretical value of $3.52\ kT_c$.[4] Furthermore, the variation of E_g with temperature exhibits the same shape as that given by the theory. The observed temperature dependences of the absorption curves are in good agreement with theory[4] provided that the experimentally determined value of $E_g(0)$ is used.

[1] R. E. Glover and M. Tinkham, Phys. Rev. **104**, 844 (1956); **108**, 243 (1957).
[2] Biondi, Garfunkel, and McCoubrey, Phys. Rev. **108**, 495 (1957); Biondi, Forrester, and Garfunkel, Phys. Rev. **108**, 497 (1957).
[3] P. L. Richards and M. Tinkham, Phys. Rev. Letters **1**, 318 (1958).
[4] Bardeen, Cooper, and Schrieffer, Phys. Rev. **108**, 1175 (1957).

G4. Superconducting Energy Gap Measurements by Direct Photon Absorption.* P. L. RICHARDS,† *University of California, Berkeley.*—Our measurements[1] of the onset of far infrared absorption, which occurs when the incident photon energy becomes large enough to excite electrons across the energy gap, have been extended to a variety of superconductors. These measurements are limited to superconductors with high critical temperatures, for which the absorption edge lies in the available wavelength range from ~0.15 to 2 mm and for which temperatures $T \ll T_c$ can be reached with liquid helium. The observed absorption edge is very sharp in pure superconductors, giving widths of the energy gap at absolute zero of $4.1\pm0.2\ kT_c$ for lead, $4.7\pm0.2\ kT_c$ for mercury, and $3.4\pm0.3\ kT_c$ for tin. These results indicate a departure from the law of corresponding states that is not a simple function of T_c/Θ_D. Preliminary measurements of the temperature dependence of the absorption edge have been made, which indicate the temperature dependence of the energy gap.

* Supported in part by the Office of Naval Research, the National Science Foundation, and the Alfred P. Sloan Foundation.
† National Science Foundation Predoctoral Fellow.
[1] P. L. Richards and M. Tinkham, Phys. Rev. Letters **1**, 318 (1958).

G5. Changes in the Superconductive State Resulting from an Interaction between Conduction Electrons and 4*f* Electrons.* J. PERETTI AND A. A. MARADUDIN, *University of Maryland* (introduced by R. D. Myers).—It has been found by B. T. Matthias and others[1] that alloying lanthanum with the paramagnetic rare earth metals decreases the superconductive transition temperature by an amount ΔT_c which depends on the concentration and the total spin of the solute atom. The same phenomenon occurs[2] in the systems $(Ce,Pr)Ru_2$ and $(Ce,Gd)Ru_2$. In this case an initial increase in the transition temperature is related to the increase in the number of conduction electrons and consequently of the density of states at the Fermi level. Our object is to explain such a behavior by considering the Coulomb (direct and exchange) interaction of conduction electrons with the 4*f* inner electrons of the solute atoms. Various effects of this interaction are taken into account. The result is that ΔT_c is nearly proportional to the solute concentration and depends on the total spin in a rather complicated way.

* This work was supported by the U. S. Air Force.
[1] Matthias, Suhl, and Corenzwit, Phys. Rev. Letters **1**, 92 (1958).
[2] Matthias, Suhl, and Corenzwit, Phys. Rev. Letters **1**, 449 (1958).

G6. Superconductive Transition Rates of Thin Films.* FREDERICK W. SCHMIDLIN AND ARTHUR J. LEARN, *Space Technology Laboratories, Inc.*, AND E. C. CRITTENDEN, JR., AND JOHN N. COOPER, *U. S. Naval Postgraduate School.*—In a thin indium film the superconducting to normal state transition initiated by fast current pulses exhibits three distinct types of behavior depending on the magnitude of the pulse. Typically, for a film 30 μ wide, 0.2 μ thick, and 350 μ long at 2.295°K and for a current somewhat larger than dc critical (73 ma), the transition involves a few mμsec nucleation process at an imperfection followed by a long delay (300 μsec); after which the bulk of the film resistance is restored by propagation of the phase boundary along the length of the film. Below the λ point of the helium bath the long delay disappears. At larger pulse heights (90–110 ma) the phase boundary propagates along the film's length with little initial delay at the imperfection. The switch times (3−0.03 μsec) are then proportional to length as verified by measurements on films of different lengths. Still larger current pulses result in faster switching of the film simultaneously along its length. Dependence on film width and thickness and type of substrate will also be discussed.

* Work supported in part by the Office of Naval Research.

G7. Critical Currents for Superconducting Transitions in Thin Films.* E. C. CRITTENDEN, JR., AND JOHN N. COOPER, *U. S. Naval Postgraduate School*, AND FREDERICK W. SCHMIDLIN AND ARTHUR J. LEARN, *Space Technology Laboratories, Inc.*—For thin films of indium deposited at 80°K and annealed at 300°K, dc current-induced transition occurs first near imperfections. For polished glass substrates near the critical temperature, and below the He λ point, these transformed regions are stationary until the current is increased to the "dc critical current," at which I^2R heating leads to propagation of the boundaries. For intermediate temperatures the boundaries immediately move by heating after triggering at an imperfection. The dc critical current shows a large discontinuity at the λ point, but is still heat determined below this, even though the helium has high conductivity. For pulses (rise time 10^{-9} sec) the pulse height I needed to produce simultaneous switching all along the specimen can be identified. These pulse heights follow $I/I_0=1-(T/T_c)^4$. The switch delay time, which is constant for this entire curve for a given specimen, varies with thickness, but not with width. At 0.1 μ it is 6×10^{-9} sec; at 0.4 μ, 12×10^{-8} sec. Films deposited on polished crystalline quartz (heat conductivity 5000 times greater) show dc critical currents with a smaller discontinuity.

* Work supported in part by the Office of Naval Research.

G8. Thermal Conductivity of Normal and Superconducting Aluminum. C. B. SATTERTHWAITE, *Westinghouse Research Laboratories.*—The thermal conductivity of pure aluminum has been measured in both the normal and superconducting states between 0.35°K and the transition temperature. By the technique used it was possible to obtain the ratio of the conductivity in the superconducting state to that in the normal state, K_s/K_n, more accurately than either of these quantities separately. Because of its high Debye Θ and low transition temperature, aluminum represents an excellent example of the case where the thermal conductivity is predominantly electronic and the scattering is predominantly by static imperfections. The ratio K_s/K_n for aluminum is in general agreement with the Heisenberg[1] treatment and the more recent treatment of Bardeen, Rickayzen, and Tewordt[2] for this case based on BCS. The temperature dependence of this ratio is also similar to that found experimentally for tin.[3]

[1] W. Heisenberg, Z. Naturforsch. **3a**, 65 (1948).
[2] Bardeen, Rickayzen, and Tewordt (to be published).
[3] J. K. Hulm, Proc. Roy. Soc. (London) **A204**, 98 (1950).

G9. Quenched-in Defects in Tin and the Superconducting Transition Temperature. WARREN DESORBO, *General Electric Research Laboratory.*—Wire specimens of tin quenched from a temperature T_Q, ($420°K < T_Q < T_{m.p.}$), exhibit a resistivity component, $\Delta\rho_0$, which disappears on annealing at lower temperatures. It is inferred that this increase in resistivity is

the result of quenched-in defects. For a specimen with $\alpha = R_{273°K}/R_{4.2°K} = 1.4\times10^{3}$, it is deduced that the activation energy of motion of the defects is 0.68 ± 0.06 ev. From the dependence of $\Delta\rho_0$ on T_Q, the activation energy of formation of the defects is 0.50 ± 0.05 ev. If the assumption is made that the defects involved are vacancies, the activation energy for self-diffusion in tin is approximately 1.2 ev. This compares favorably with the measured value 1.1 ev.[1] However, for a given T_Q, $\Delta\rho_0$ at 4.2°K decreases with increasing purity of tin; e.g., $\alpha = 1.4\times10^{3}$, $\Delta\rho_0 = 2.22\times10^{-8}$ ohm-cm; $\alpha = 1.3\times10^{4}$, $\Delta\rho_0 = 0.17\times10^{-9}$ ohm-cm. The superconducting critical temperature T_c decreases as $\Delta\rho_0$ increases; $\Delta\rho_0 = 2.22\times10^{-8}$ ohm-cm, $\Delta T_c = -3.0\pm0.2$ millidegree; $\Delta\rho_0 = 0.17\times10^{-9}$ ohm-cm, $\Delta T_c = -0.8\pm0.2$ millidegree. This variation in T_c is similar to that observed upon addition of small amounts of chemical impurities to tin.[2]

[1] J. D. Meakin and E. Klokholm, Fall Meeting of the Am. Inst. Mining Met. Engrs., Cleveland, October 30, 1958.
[2] Lynton, Serin, and Zucker, J. Phys. Chem. Solids **3**, 165 (1957).

G10. Variation of Low-Temperature Heat Capacity with Hardness in an Aluminum Alloy.* F. A. Otter and D. E. Mapother, *University of Illinois.*—The specific heat of a dilute alloy of Mg (0.7%) and Si (0.3%) in aluminum has been measured down to 1.8°K. The hardness and mechanical strength of this alloy varies with the degree of precipitation of Mg_2Si from supersaturated solution and can be controlled by heat treatment. Measurements have been made in the annealed and fully hardened conditions. From 1.8 to 4.2°K, the specific heats of hard or annealed specimens can be represented by $C = \gamma T + 1.944\times10^{+6}(T/\theta_D)^3$ mj/mole deg with $\gamma = 1.33\pm0.02$ mj/mole deg[2] and $\theta_D = 430\pm4$°K for the case of the annealed specimen (whose behavior closely approximates that of pure Al). In this temperature range both γ and θ_D increase for the alloy in the hardened condition, the changes being $d\gamma/\gamma = 1.1\pm0.4\%$ and $d\theta_D/\theta_D = 1.3\pm0.6\%$. These results will be discussed in connection with previous superconducting critical field measurements on the same alloy,[1] using an approach based upon Morel's[2] application of the BCS theory[3] to the pressure effect. In the range from 10 to 20°K no difference in γ or θ_D between the hardened and annealed specimens was detected.

* Supported by the Office of Ordnance Research, U. S. Army.
[1] R. E. Mould and D. E. Mapother, Phys. Rev. **96**, 797 (1954).
[2] Pierre Morel, Phys. Rev. Letters **1**, 244 (1958).
[3] Bardeen, Cooper, and Schrieffer, Phys. Rev. **108**, 1175 (1957).

G11. Electronic Specific Heat of γ-Mn. J. E. Zimmerman and H. Sato, *Ford Motor Scientific Laboratory.*—In order to investigate the electronic structure of face-centered-cubic transition metals as a function of the number of *d* electrons, we have attempted a determination of the electronic specific heat of fcc manganese. Since the fcc form of pure manganese is not stable at low temperatures, a series of copper-manganese alloys was prepared with copper contents up to 30 atomic percent. These were water-quenched from the γ region to retain the fcc form. Owing to the antiferromagnetic transition the alloys are actually slightly tetragonal at low temperature. The specific heats at liquid helium temperatures were measured and the electronic components were extrapolated to zero copper content. The value thus derived for pure γ-Mn is 11.8 mj/mole deg[2]. This is high compared to the values for Co and Ni but is comparable to the value for a γ-phase Fe Mn alloy reported by Goldman and Guthrie.[1]

[1] J. E. Goldman and G. L. Guthrie. Bull. Am. Phys. Soc. Ser. II, **1**, 148 (1956)

G12. Effect of Gaseous Impurities on the Residual Resistivity of Copper. J. K. Redman, R. R. Coltman, T. H. Blewitt, and C. E. Klabunde, *Oak Ridge National Laboratory.**—The residual resistivity at 4.2°K of a large number of copper single crystals prepared from ASR high-purity copper have been studied. It has recently been found that small amounts of oxygen and chlorine will substantially reduce the residual resistivity. For example, samples with a resistivity of 2×10^{-8} were reduced to 9×10^{-10} after annealing for 1 hr at 900°C with 20 μ of air pressure. On the other hand, this sample resistivity returned to 1×10^{-8} after a 1-hr anneal at 900°C in a hard vacuum (5×10^{-6} mm of Hg). Similar results were found for atmospheres of oxygen and chlorine, whereas nitrogen atmosphere had no effect. Data will be presented showing the diminution of resistivity as a function of time when annealed at 700°C in an atmosphere of air at 30 μ pressure. This apparent interaction of chlorine and oxygen with metallic impurities, probably iron, illustrates the unreliability of using resistivity as a measure of purity. It is also suggested that this interaction may greatly reduce the anomalous resistivity minimum of impure copper.

* Oak Ridge National Laboratory is operated by Union Carbide Corporation for the U. S. Atomic Energy Commission.

G13. Nuclear Spin Relaxation in the He^3-He^4 Solutions.* Robert H. Romer and William M. Fairbank, *Duke University.*—We are making a study of the nuclear spin relaxation time T_1 of He^3 nuclei in dilute solution in liquid He^4 at various concentrations and temperatures. We measure T_1 by the standard procedure of observing the growth of the absorption signal after saturation by a strong rf field. At a temperature of 1.25°K we find T_1 to be approximately 90 min for a 3.5 atomic % solution of He^3 and approximately 120 min for a 1.7% solution. The samples were condensed into a Pyrex bulb of about 175 mm^3 volume. In order to see whether relaxation processes at the walls are affecting the results, we are making further measurements in bulbs of different sizes. In some previous experiments[1] on pure liquid He^3, various values for T_1 were observed, up to 200 sec, depending on the container used. Since diffusion measurements[2,3] in solutions below the λ point indicate that a He^3 nucleus in the present bulb will diffuse to the wall in a few seconds, the wall relaxation processes, if any, in the present experiment, must be extremely slow.

* Supported by the Office of Ordnance Research, U. S. Army.
[1] Fairbank, Ard, and Walters, Phys. Rev. **95**, 566 (1954).
[2] R. L. Garwin and H. A. Reich, Bull. Am. Phys. Soc. Ser, II, **3**. 133 (1958).
[3] Fairbank and Walters, Proceedings of the Ohio State Symposium on He^3, 1957.

Monday Afternoon at 2:15

Kresge Little Theater

(Martin Deutsch presiding)

Nuclear Physics II; Applied Plasma Physics

H1. Decay of "Anomalous" Inelastic Alpha-Particle States. M. Crut and N. S. Wall, *MIT.**—We have observed coincidences between the inelastic alpha particles leading to the 5-Mev anomalous structure in the spectrum of 30-Mev alpha particles on Ni and de-excitation gamma rays.[1] Measurements indicate a significant fraction of the anomalous states

so formed decay through the emission of a gamma ray of energy greater than 3.4 Mev. The experimental techniques as well as the significance of this measurement will be discussed.

* This work supported in part by a joint program of the U. S. Atomic Energy Commission, Office of Naval Research, and U. S. Signal Corps.
[1] D. R. Sweetman and N. S. Wall (to be published).

H2. Lifetime of the 3.56-Mev State in Li^6. LESLIE COHEN AND RALPH TOBIN, *U. S. Naval Research Laboratory.*—Nuclei of Li^6 were excited to the 3.56-Mev state by irradiating a disk of enriched lithium metal with the x-rays from the U. S. Naval Research Laboratory betatron, operated at an energy of 6.5 Mev. The gamma radiation from the de-excited nuclei was detected with a shielded 4-in.-diam×4-in. NaI(Tl) crystal placed at an angle of 130° with respect to the x-ray beam. The observed nuclear radiation consisted solely of 3.56-Mev gamma rays. The gamma-ray yield from the scatterer was observed with and without a second enriched lithium metal disk alternately interposed in the primary beam. Assuming a spin assignment $J=0$ for the 3.56-Mev state,[1] and a Debye temperature of 430° for lithium metal,[2] an analysis of the data gives a value of $\Gamma=(8.2\pm1.7)$ ev for the width of the excited state. This result yields a mean lifetime, $\tau=\hbar/\Gamma$, of $(8.0\pm1.3)\times10^{-17}$ sec.

[1] Stoltzfus, Friichtenicht, and Nelson, Bull. Am. Phys. Soc. Ser. II, 1, 329 (1956).
[2] M. Blackman, *Handbuch der Physik* (Springer-Verlag, Berlin, 1955), Vol. VII, Part I, Crystal Physics Sec. 1, p. 364.

H3. Proportional Counter Measurement of L/K-Capture Ratios.* J. SCOBIE AND R. W. FINK, *University of Arkansas.*—A multiwire proportional counter system similar to that described by Drever and Moljk[1] has been constructed for use in orbital electron capture studies. Initially, measurements are being made of the L/K-capture ratio in Fe^{55} decay. The radioactive iron is introduced into the counter in the form of ferrocene vapor. Preliminary work with nonradioactive ferrocene has shown that the counter operates satisfactorily with as much as 50 mg of the compound mixed with the normal argon-methane filling. Preliminary results will be presented.

* Supported by the National Science Foundation.
[1] R. W. P. Drever and A. Moljk, Phil. Mag. 2, 427 (1957).

H4. K Capture to Positron Branching Ratios in the Decay of Ga^{68}.* M. K. RAMASWAMY,† *The Johns Hopkins University* (introduced by L. Madansky).—K capture to positron branching ratios have been measured in the decay of Ga^{68} to Zn^{68} using coincidence scintillation spectrometer techniques. The measured values are 1.28 ± 0.12 (to the 1.07-Mev level) and 0.10 ± 0.02 (to the ground state). Assuming these decays to be pure Gamow-Teller transitions, the Fierz interference terms are computed to be $b_{G\,T}=-0.03\pm0.02$ and $\pm0.03\pm0.01$, respectively (the uncertainty in the latter result arising from uncertainty in N_β, the source strength). The ratio of positrons to the first excited state and ground state of Zn^{68} has been found to be $(1.76\pm0.22)\times10^{-3}$. A search for a possible low-lying O^+ state in Ga^{68} was made through the decay of Ge^{68} using x-ray-x-ray and x-ray-γ-ray coincidences employing NaI(Tl) crystals. Besides the 9-kev K x-ray, annihilation radiation and the known γ ray in Ga^{68} whose energy was measured to be 1.067 ± 0.035 Mev, no other γ ray was observed ($<8\%$ of 1.07 γ). The number of positrons per 1.07 γ quantum was determined as 19.47 ± 2.10 by comparison with Na^{22}. An upper limit of 0.4% per decay was set on positron emission by Ge^{68}.

* Supported in part by the U. S. Atomic Energy Commission.
† On leave from Mysore University, India.

H5. Activity of Rh^{101} and Neutron Cross Section of Ru^{100}. B. L. SHARMA AND M. L. POOL, *The Ohio State University.*—$Ru^{101}+p$ was observed to emit 75-, 310-, 545-kev gamma rays, each decaying on a 4.4-day half-life. A weak 235-kev radiation was in coincidence with the 310-kev emission previously assigned to Rh^{101}. The latter is not in coincidence with the 545 kev. After the decay of the 4.4-day activity, gamma rays of 127 and 198 kev were observed to be in coincidence and have a very long half-life. The 127-kev radiation is identified with Rh^{101} from the reported Coulomb excitation of Ru^{101} and the decay of Tc^{101}. A Ru+d sample, allowed to decay for 13 years, strongly shows the 127- and 198-kev radiations. A decay scheme having levels at 127, 310, 235, and 545 kev will be presented. Enriched Ru^{104} was exposed to a thermal neutron flux of 1.2×10^{14} cm^{-2} sec^{-1}. After the decay of the 40-day Ru^{103}, the silver impurity was removed and the contributions from Co and Eu were subtracted. The 513- and 621-kev gamma rays of Rh^{106} were then verified to be in coincidence. The thermal neutron activation cross section of Ru^{105} was calculated to be 0.20 barn from the gamma-ray intensities.

H6. Nuclear Spin of Cr^{51}.* W. J. CHILDS, L. S. GOODMAN, AND L. J. KIEFFER, *Argonne National Laboratory.*—The atomic-beam magnetic-resonance technique[1,2] has been used to determine the nuclear spin of 28-day chromium-51. The measured value of $\frac{7}{2}$ is in agreement with the single-particle model from which one would expect the configuration $\pi(f_{\frac{7}{2}})^4$, $\nu(f_{\frac{7}{2}})^7$. Since the total electronic angular momentum is integral (3), only multiple-quantum transitions can be "flopped" in with the present geometry. The sample, which was produced by neutron capture in the MTR, was heated in a graphite oven to produce the atomic beam.

* Work performed under the auspices of the U. S. Atomic Energy Commission.
[1] J. R. Zacharias, Phys. Rev. 61, 270, (1942).
[2] L. S. Goodman and S. Wexler, Phys. Rev. 99, 192, (1955).

H7. Series Expansion Methods for Inferring Radial Distributions. A. E. S. GREEN,* *Los Alamos Scientific Laboratory*, U. MEYER-BERKHOUT,† *Stanford University*, AND K. W. FORD,‡ *Los Alamos Scientific Laboratory.*—When the Born approximation is valid, it is possible to apply simple series techniques to infer directly the radial distribution functions without presupposing an analytical form. We assume that experimental information gives a structure function $F(q)$ which is related to the charge distribution $\rho(r)$ in the usual way. It can readily be shown that $r\rho(r)$ and $qF(q)$ are simply the usual Fourier sign transforms of each other. When the radial function falls rapidly toward zero as $r\to\infty$, one might assign a cutoff radius, (b) and expand $r\rho(r)$ in a Fourier series in the interval 0 to b. The analysis then permits an immediate determination of the Fourier amplitudes directly from the values of the structure function at certain critical values of q. When the cutoff assumption is questionable, a second-series expansion technique involving, for example, Hermite functions and utilizing matrix methods is available which does not require the cutoff assumption. This second method also leads to a simple inversion of the Fourier transform. These series methods shed light on a question of what is determined physically by the experimental data.

* Present address: Florida State University.
† Present address: University of Heidelberg.
‡ Present address: Brandeis University.

H8. Analysis of High-Energy Electron Scattering from 1p-Shell Nuclei. U. MEYER-BERKHOUT,* *Stanford University*, AND K. W. FORD† AND A. E. S. GREEN,‡ *Los Alamos Scientific Laboratory.*—Elastic scattering data from six 1p-shell nuclei (Li^6, Be^9, B^{11}, C^{12}, N^{14}, O^{16}) at energies of 160 to 420 Mev have been analyzed. No "reasonable" spherically symmetric charge densities account for the scattering from N^{14} and B^{11}. If quadrupole and/or magnetic moment effects are not too large, the spherically symmetric part of the charge density may still be deduced. Some conclusions are: The maximum charge

density in each of these nuclei is $(8\pm1)\times10^{37}$ protons/cm^3, the same as in heavier nuclei. The "half-density" radius, defined by $\rho=4\times10^{37}$ protons/cm^3, varies regularly from $0.79\times10^{-13}A^{\frac{1}{3}}$ cm for Li^6 to $1.04\times10^{-13}A^{\frac{1}{3}}$ cm for O^{16}. The rms radius decreases from 2.80 for Li^6 to 2.45 for C^{12}, increasing to 2.65 for O^{16} (in units of 10^{-13} cm). The quadrupole moment of N^{14} can be inferred only roughly, and probably lies between 2 and 3×10^{-26} cm^2.

* Present address: University of Heidelberg.
† Present address: Brandeis University.
‡ Present address: Florida State University.

H9. Stability of Plasma Confinement by Electromagnetic Field Pressure.* J. W. BUTLER, *Argonne National Laboratory* (introduced by A. J. Hatch).—A perfectly conducting compressible fluid with finite extension in one direction may be held in equilibrium against its internal pressure by a rigid wall on one side and a resonant electromagnetic field at the other boundary. The stability of the fluid-field interface can be simply investigated if the electromagnetic field frequency is assumed high enough so that only time average forces need be considered. A typical result is that, in the case of a circularly polarized field, the equilibrium is unstable for periodic boundary perturbations with wave numbers p in the interval $k^2<p^2<2k^2$. Here k is the wave number $2\pi/\lambda$ of the rf field. Acoustic resonance effects occur if the sound speed in the fluid is finite. For other field polarizations, the unstable wave number range is reduced by a properly oriented steady magnetic field parallel to the boundary.

* This work performed under the auspices of the U. S. Atomic Energy Commission.

H10. Radio-Frequency Fields in rf Plasmas and Plasmoids.* ALBERT J. HATCH, *Argonne National Laboratory*.—A probe method has been developed for measurement of rf electric fields within rf excited plasmas. A single wire sensing probe is inserted into the plasma and attached directly to the pickup probe of an oscilloscope. The observed wave forms are analyzed harmonically. The method has been used to measure the attenuation of the exciting rf field inside a plasma excited by a 10-Mc potential applied to plane parallel metal electrodes. At pressures below 10^{-4} mm Hg where the multipacting plasma mechanism dominates, the applied rf field is not appreciably attenuated within the plasma. In the nominal pressure range of 10^{-4} to 3×10^{-2} mm where various high-frequency plasmoids are observed, the applied rf field is strongly attenuated inside the plasmoids. As pressure is increased above 3×10^{-2} mm where electron diffusion becomes the controlling plasma mechanism, the attenuation of the applied rf field within the plasma gradually decreases. A second harmonic signal detected by the probe is attributed to electron bunches sweeping past the probe twice during each cycle of the applied fundamental rf potential. The amplitude and phase of this harmonic partially characterize the electron motion within the plasma and plasmoids.

* This work performed under the auspices of the U. S. Atomic Energy Commission.

H11. Steady-State Plasma Distribution in a Rotating Electromagnetic Field.* A. J. ULRICH AND J. W. BUTLER, *Argonne National Laboratory*.—In a cavity composed of the space between two perfectly conducting parallel planes of infinite extent in x and y, the two cutoff modes, one involving electric and magnetic fields E_z and B_y, and the other involving E_y and B_z, are excited in time quadrature. The result is a standing wave with $E\times B=0$ rotating about the z direction. In such a cavity, a steady-state plasma density exists depending only on z. It is assumed that the plasma is neutral and that rf forces on the ions are negligible. A steady B_z is included. Because the magnitude of the filed vectors is constant in time rather than alternating,[1-3] this solution gives electron fluid velocities which exactly satisfy the hydromagnetic plasma equations. A steady-state solution is also possible with charge separation present. Individual electron motions without B_z can be found from the solution of only one second-order differential equation.

* Work performed under the auspices of the U. S. Atomic Energy Commission.
[1] F. B. Knox, Australian J. Phys. **10**, 565 (1957).
[2] Boot, Self, and Harvie, J. Electronics and Control **4**, 434 (1958).
[3] E. S. Weibel, ARL-57-1026, Ramo-Wooldridge Corporation, 1957.

H12. Coulomb Scattering in a Very Strong Magnetic Field. L. M. TANNENWALD, *Lockheed Aircraft Corporation*.—Various transition probabilities for collisions of a spiraling charged particle with a fixed charge are presented. The equivalent results in the relative coordinate system of two identical particles are shown. The existence of an adiabatic cutoff distance in the interaction and its influence on plasma properties is pointed out. The utility of working with a quantum-mechanical description is explained.

MONDAY AFTERNOON AT 2:15

Room 4–370

(W. A. KLEMPERER presiding)

Chemical Physics: Experimental Spectroscopy

HA1. Infrared Spectrum of Methyl Bromide near 2.2 Microns.* R. G. BROWN AND T. H. EDWARDS, *Michigan State University*.—The infrared absorption in this region consists, in the main, of three overlapping perpendicular bands, which have been tentatively assigned to $\nu_3+\nu_4$, $\nu_4+\nu_5$, and $\nu_1+\nu_3+\nu_6$. One band, $\nu_4+\nu_5$, is comparatively weak, but has sharp Q branches from which the analysis was made. The expected weak parallel component was not observed. The other two bands have broad Q branches (as much as 2 cm^{-1}) rendering direct measurement of their frequencies meaningless. However, under high resolution ($\sim$0.07 cm^{-1}), many of the lines in the P and R branches of the subbands were resolved, enabling more certain assignment of quantum numbers, more accurate determination of the "A" term, and, in addition, determination of the B's.

* Supported by the National Science Foundation.

HA2. Absorption Spectra of Nitrogen. P. G. WILKINSON, *University of Chicago*.—Four bands belonging to the forbidden $a'\,{}^1\Sigma_u^- \leftarrow X\,{}^1\Sigma_g^+$ system of nitrogen have been analyzed. The agreement of the rotational constants and the vibrational intervals with those of Lofthus[1] leaves no doubt as to the identity of the upper state. The rotational line intensities are proportional to $S_R(2J+1)\exp-[B_0''J(J+1)hc/kT]$, where B_0'' is 1.9898 cm^{-1}. $S_R=J^2$ in agreement with theory for this type of forbidden transition. T_{00} of $a'\,{}^1\Sigma_u^-$ is now known

precisely as 8.398 ev. The T_{0c} energies of the other "floating" states of nitrogen may now be given with high precision: $w\ ^1\Delta_u$, 8.889 ev; $x\ ^1\Sigma_g^-$, 14.036 ev; $y\ ^1\Pi_g$, 14.154 ev. Besides the $a'-X$ bands, weak bands of two other forbidden systems, $A\ ^3\Sigma_u^+-X$ (Vegard-Kaplan system), and $^3\Delta_u-X$ or $^3\Sigma_u^--X$, have been found for the first time in absorption. From appearance pressures and auxiliary data on the mean life of a $^1\Pi_g$, the mean lifetimes of other metastable states of nitrogen may be deduced as follows: $A\ ^3\Sigma_u^+$, $1.2.10^{-2}$ sec; $a'\ ^1\Sigma_u^-$, $1.4.10^{-2}$ sec; $^3\Sigma_u^-$, $1.4.10^{-2}$ sec.

[1] A. Lofthus, J. Chem. Phys. **25**, 494 (1956).

HA3. Approximate Normal Coordinate Treatment of Propane. W. T. KING* AND B. L. CRAWFORD, JR., *University of Minnesota*.—Force constants for propane are found by solution of approximate vibrational secular equations, using the infrared spectra of C_3H_8, $(CH_3)_2CD_2$, $(CD_3)_2CH_2$, and C_3D_8, reported by McMurray and Thornton.† To simplify the calculations the following approximation method is used. Normal coordinates for the modes characteristic of methyl and methylene groups are estimated and used to construct an orthogonal coordinate transformation which approximately factors the vibrational secular equation into two equations of reduced order, one yielding the group frequencies and the other the remaining "framework" frequencies. Using a simplified potential function, thirteen force constants that reproduced the fundamentals of propane satisfactorily were computed from the reduced secular equations by a least-squares adjustment method. As a further test of these force constants and the approximation methods used, the fundamentals of $(CH_3)_4C$ and $(CD_3)_4C$ were calculated and compared with the observed infrared spectra.

* Now at Brown University.
† H. L. McMurray and V. L. Thornton, J. Chem. Phys. **19**, 1014 (1951).

HA4. Magnetic Rotation Spectra of NO in the near Infrared.* C. D. HAUSE AND GLEN A. MANN, *Michigan State University*.—The magnetic rotation spectra associated with the (3–0) and (2–0) absorption bands of NO at 1.8 and 2.7 μ, respectively, have been observed in some detail. With fields of 2400 gauss and an absorbing path of 5 meter-atmos the first line in the Q branch of the $^2\Pi_{\frac{1}{2}}$ component shows strong rotation. On the other hand magnetic rotation of the P and R branches can be observed only with small absorbing paths, ~0.4 meter-atmos. P- and R-branch lines in rotation have been obtained for both components of the $^2\Pi$ state in the (3–0) band up to $J=31/2$. The direction and degree of rotation have been established.

* Supported by the National Science Foundation.

HA5. Doublet and Quartet States of O_2^+ and the Spin-Orbit Interactions. KATSUNORI HIJIKATA, *University of Oklahoma*.—The coupling constants of spin-orbit interactions for the lower II states ($^2\Pi_g$, $^2\Pi_u$, and $^4\Pi_u$) cannot be explained by simple molecular orbital theory. One of the reasons is that the orbital energies of $2p\pi_u$ and $2p\sigma_g$ are very close. We calculated the energies of these lower II states by ASMO with CI, using the effective nuclear charges 2.30 for $2s$ and $2p$ and 7.65 for $1s$. These values were determined by minimizing the total energy of the atomic constituents at infinite separation. The energy levels of O_2^+, the ionization potential of O_2, and the Rydberg series are also discussed. The coupling constants in these states were calculated (1) by semiempirical method, (2) by the straightforward application of ASMO method, and (3) by substituting HF AO's into the molecular WF's calculated by ASMO.

HA6. Microwave Spectrum, Nature of the Ring Puckering Vibration and Structure of Trimethylene Oxide. WILLIAM D. GWINN, JOHN ZINN,* AND JOSE FERNANDEZ-BERTRAM,† *University of California, Berkeley*.—From the analysis of the microwave spectra of $(CH_2)_3O$, $(CH_2CHDCH_2)O$, $(CD_2CH_2CD_2)O$, and $(CH_2)_3O^{18}$, the complete structure of trimethylene oxide has been determined. It has been found to be

$$d_{C-C'}=1.55\text{ A};\quad d_{C'-C}=1.44\text{ A};\quad d_{C-H}=1.08\text{ A};$$
$$\angle H-C-H=111°;\quad d_{C'-H}=1.09\text{ A};\quad \angle H-C'-H=110°;$$
$$\angle C'-C-C'=84°,\quad \text{and}\quad \angle C'-C'-H_2=4°.$$

The primes on the carbons refer to the carbons adjacent to the oxygen.

From an analysis of the Stark effect and the satellite lines arising from the ring puckering vibrations, it is concluded that the four-membered ring is essentially planar. From the vibration-rotation interaction resulting from the ring puckering vibrational mode, it was possible to conclude that the potential function does have a very small maximum corresponding to the planar configuration. This maximum is approximately the energy of the zero vibrational level and consequently the vibrational levels are nearly evenly spaced and there is no inversion doubling.

* John Zinn is now at Los Alamos.
† Jose Fernandez-Bertram is on leave from Universidad de Oriente, Santiago de Cuba, Cuba.

HA7. Electronic g Factors for Free Atomic States—Cl^{35}.* G. J. WOLGA AND M. W. P. STRANDBERG, *MIT*.—The magnetic hyperfine energy levels of the $2P_{\frac{1}{2}}$ free atomic ground state of Cl^{35} have been investigated by the method of paramagnetic resonance. The atomic Cl^{35} was produced in a microwave gas discharge at 3000 Mc. A flow system enabled observation of the atomic state before recombination. Absorptions corresponding to the $\Delta M_J=\pm1$, $\Delta M_I=0$ selection rules were observed between the hyperfine states of both Cl^{35} and Cl^{37}. The two isotopes were distinguished by the relative intensities of the lines. The transitions occurred at 8993 Mc within the range 4600–5000 gauss. Numerical solutions of the secular equations were used with atomic beam[1] values of a and b to obtain the atomic g_J factor for Cl^{35}. The result is $g_J=1.33376\pm0.00007$. This is to be compared with the value $g_J=1.3341$ assuming L-S coupling in the $2P_{\frac{1}{2}}$ state with $g_L=1.0000$, $g_S=2.0023$.

* This work was supported in part by the U. S. Army (Signal Corps), the U. S. Air Force (Office of Scientific Research, Air Research and Development Command), and the U. S. Navy (Office of Naval Research).
[1] Davis, Feld, Zabel, and Zacharias, Phys. Rev. **76**, 1076 (1949).

HA8. Molecular Complexes between Iodine and *N*, *N*-Dimethylaniline and its Derivatives. H. TSUBOMURA, *University of Chicago*.—The visible absorption spectra of the charge transfer complexes of iodine with N, N-dimethylaniline and its methyl derivatives were studied in the n-heptane solutions. All complexes have strong, broad absorption bands which begin to absorb the light at about 400 mμ. Owing to the strong absorption of the bases, it was impossible to find the peaks of these absorption bands. From the measurement of the change of the intensities of these bands, however, the equilibrium constants and the heat of formation of the complexes were obtained as follows: For I_2 and N, N-dimethylaniline, $K(11°C)=41.0$, $\Delta H=-8.2$ kcal; for I_2 and N, N-dimethly-p-toluidine, $K(12°C)=65.7$, $\Delta H=-8.3$ kcal; for I_2 and N, N-dimethyl-o-toluidine, $K(17°C)=2.49$, $\Delta H=-2.3$ kcal. The ΔH for N, N-dimethylaniline lies between those for triethylamine and pyridine. This is quite parallel to the pK values of these bases. Therefore it can be concluded that the nitrogen atom of dimethylaniline acts as an attracting center toward the iodine molecule. The weak binding strength of N, N-dimethyl-o-toluidine can be explained by the twisting of the dimethylamino group of this compound which is caused by the steric hindrance between the methyl groups.

HA9. Wave Shape Recorder with Accurate Reproduction of Fractional Microsecond, Noise Limited Signals. S. NUDELMAN

AND J. T. HICKMOTT, *University of Michigan, Willow Run Laboratories.*—A recording system has been developed permitting precise wave shape reproduction of repetitive signals, even with ratios of S/N less than one. The equipment resolution is of the order 2×10^{-9} sec (comparable to a 15-megacycle oscilloscope). With a S/N voltage ratio (peak to peak) of 0.1, the accuracy of trace reproduction is within two percent. The electronics for this operation consists of a periodically driven blocking oscillator providing narrow gating pulses to a box car circuit (functioning as an electronic switch), followed by an RC integrator, a cathode follower, and recorder. The gating time is small compared to the signal time. Therefore, it permits a periodic sampling of a small portion of the signal voltage. The output is then fed to the integrator, where noise is reduced by averaging. If the gate is slowly and uniformly retarded in phase with respect to the initiation of the signal for successive periodic cycles, then an accurate recorder reproduction of the signal wave shape is obtained. Our application of this device is in the measurement of the photoresponse of infrared detectors, and the wavelength dependence of this response. However, it is useful for the study of any low level electronically induced wave forms.

MONDAY AFTERNOON AT 5:00

Social Hour in MIT Faculty Club

TUESDAY MORNING AT 9:30

Kresge Little Theater

(A. W. OVERHAUSER presiding)

Excitons

I1. Exciton Spectrum of ZnO. D. G. THOMAS, *Bell Telephone Laboratories.*—The reflection and absorption spectra of ZnO crystals near the band edge have been measured. The results may be obscured by improper surface treatment. Near 4°K there are three sharp reflectance peaks X, Y, Z at 3.374, 3.382, and 3.421-ev photon energies, respectively. X and Y are active in light polarized with $E\perp$ hexagonal C axis, and Z with $E\|C$. Analysis of the reflectance reveals three corresponding but displaced absorption peaks, in which α approaches 10^6 cm^{-1}. Z has an oscillator strength near 0.014 and X and Y each has a strength of 0.007. Similar behavior occurs at 78°K, but at 300°K two broad maxima are seen. The peaks correspond to the direct, allowed formation of three exciton states. The absorption spectra in crystals about 10^{-3} cm thick are steep but show structure at 4°K. The absorption and structure depend on the polarization. For $E\|C$ there is an absorption line corresponding to peak X but not Y. By using this "wrong" mode of polarization,[1] an excited exciton state may be observed. Other lines which probably involve excitons associated with impurities are also found.

[1] J. J. Hopfield, Bull. Am. Phys. Soc. Ser. II, 4, 154 (1959), following abstract.

I2. Theory of Exciton Fine Structure in Hexagonal ZnO and CdS. J. J. HOPFIELD, *Bell Telephone Laboratories.*—It is shown that the exciton fine structure and polarization phenomena observed in hexagonal ZnO is consistent with the assumption of a split P-type valence band. The dominant splitting in ZnO is due to the crystal field. A weak spin-orbit splitting is also present. Direct excitons exhibit the polarization phenomena and energy shifts characteristic of the valence band. Weak spin-orbit coupling mixes slightly certain of the $P_\perp$ and $P_\|$ states. This weak mixing makes it possible to study some of the strongly absorbing exciton lines ($\alpha\approx10^6$ cm^{-1}) in the "wrong" (weakly active) mode of polarization in relatively thick ($\approx10^{-3}$ cm) crystals. A rough estimate from the model of the oscillator strength of the exciton ground state absorption line as observed in the "wrong" mode of polarization is in reasonable agreement with experiment. The magnitude of the exciton binding energy (0.024 ev), mean reduced mass (0.13 m), and the valence band splittings have been estimated from the data of Thomas.[1] It is shown that the exciton singlet-triplet splitting can be observed optically in ZnO. The same kind of valence band splitting is expected in CdS, although spin-orbit effects should be much more important in this case.

[1] D. G. Thomas, Bull. Am. Phys. Soc. Ser. II, 4, 154 (1959), preceding abstract.

I3. Fine Structure in the Magneto-Absorption Spectrum of Germanium.* D. F. EDWARDS, R. W. TERHUNE, AND MARTHA BRUEMMER, *Willow Run Laboratories* AND C. W. PETERS, *The University of Michigan.*—Additional fine structure[1] has been observed in the magneto-absorption spectrum of germanium. The measurements were made on an intrinsic single-crystal sample about 5 μ thick and at a temperature of 22°K with $\mathbf{B}$ along a [110] direction. Plane polarized radiation was used with $\mathbf{E}\perp\mathbf{B}$ and $\mathbf{E}\|\mathbf{B}$ for magnetic fields up to 24 kilogauss. The sample was in the exit optics of a high-resolution laboratory grating spectrometer having a resolving power of 0.65 cm^{-1}, as determined from the half-width of the central image. From the transmission data it is apparent that each of the absorption minima is composed of multiple lines. A preliminary identification has been made of the lower Landau lines by a correlation with the theoretical Landau spectrum. The ground state of the exciton is observed to be a doublet, with two levels indicated at $\mathbf{B}=0$. The width of the narrowest absorption line indicates that the spectrum is limited by the monochromator resolution.

* Work was supported by Project MICHIGAN (administered by the U. S. Signal Corps).

[1] Zwerdling, Roth, and Lax, Phys. Rev. 109, 2207 (1958).

I4. Fine Structure in the Zeeman Effect of the Direct and Indirect Excitons in Germanium.* KENNETH J. BUTTON, SOLOMON ZWERDLING, AND BENJAMIN LAX, *MIT.*—The exciton observed in the experimental study[1] of the indirect

transitions in Ge showed two strong absorptions at zero magnetic field and developed additional structure in the form of a series of absorption edges which moved toward higher energy as the magnetic field intensity was increased. The analysis of the transmission spectrum in the region of exciton absorption will be discussed, and it will be shown that the fine structure is resolved for polarized incident radiation with $\mathbf{H}\|[100]$ and $\mathbf{H}\|[111]$. The phenomenological "spin Hamiltonian"[2] $\mathcal{H}=A\mathbf{J}\cdot\mathbf{H}-\frac{1}{3}\Delta(J_z^2-J^2)+\mathbf{S}\cdot\mathbf{B}\cdot\mathbf{H}+CH^2$, which predicts eight discrete absorption lines in the exciton spectrum for $\mathbf{H}\|[100]$, has been fitted to the experimental data by variation of the four adjustable coefficients. The term CH^2 becomes significant at fields above 10 000 oersteds. At 38 900 oersteds, electron spin splitting is about 4×10^{-4} ev, and the splitting caused by the linear Zeeman effect for the hole is about 6×10^{-4} ev. The zero-field splitting is 10^{-3} ev. The direct exciton[1] can be analyzed similarly; here the orbital splitting is estimated to be 8×10^{-4} ev and the electron spin splitting is 5×10^{-4} ev at 38 900 oersteds.

* The work reported here was performed at Lincoln Laboratory, a technical center operated by MIT with the joint support of the U. S. Army, Navy, and Air Force, under contract.

[1] Zwerdling, Lax, Roth, and Button, Phys. Rev. (to be published).

[2] L. M. Roth and W. H. Kleiner, Bull. Am. Phys. Soc. Ser. II, 4, 155 (1959), following abstract.

I5. Theory of the Zeeman Effect of Excitons in Semiconductors.* LAURA M. ROTH AND WALTER H. KLEINER, *MIT.*—The Zeeman effect for the lowest states of the indirect exciton in Ge or Si has been studied. The effects which must be taken into account are (1) the Zeeman effect of the hole due to a combination of spin and orbital angular momentum corresponding to $J=\frac{3}{2}$, (2) the zero field splitting of the acceptor-like ground state due to the inclusion of the anisotropic electron kinetic energy operator in the "reduced" effective mass equation, (3) the magnetic splitting due to the conduction electron spin, which has an anisotropic g factor, and (4) diamagnetic effects. These effects can be treated by means of a spin Hamiltonian whose form can be obtained from symmetry considerations. The four effects are included (in order) in the Hamiltonian $A\mathbf{J}\cdot\mathbf{H}-\frac{1}{3}\Delta(J_z^2-J^2)+\mathbf{S}\cdot\mathbf{B}\cdot\mathbf{H}+CH^2$, where z is the direction of the ellipsoid. While this is not the most general form, it was found to fit the experimental results of Button, Zwerdling, and Lax[1] in Ge. The parameters in the spin Hamiltonian, and the relative intensities of the lines, will be compared with theoretical estimates. Similar considerations can be applied to the direct exciton.

* The work reported here was performed at Lincoln Laboratory, a technical center operated by Massachusetts Institute of Technology with the joint support of the U. S. Army, Navy, and Air Force, under contract.

[1] Button, Zwerdling, and Lax, Bull. Am. Phys. Soc. Ser. II, 4, 154 (1959), preceding abstract.

I6. Ground-State Energy of Charged, Effective-Mass Particle Complexes. MURRAY A. LAMPERT, *RCA Laboratories.*—In a number of III–V compounds the effective mass of the electron is isotropic and substantially smaller than the average effective mass of the hole. In such cases the dissociation energy D of the "excitonic ion" $++-$ (i.e., the bound aggregate consisting of two holes and an electron) is an appreciable fraction of the binding energy of the exciton $(+-)$. Being charged and mobile these excitonic ions can be detected in cyclotron resonance if a sufficient density of them can be generated in a sample held at helium temperature (and if the complex has sufficiently high mobility). Since the density which can be generated depends on the magnitude of D, it would be useful to know the latter quantity accurately. A variational calculation of D has been formulated for the ground state of the almost identical, but simpler, complex $\oplus+-$ ($\oplus$ a substitutional donor ion) in the framework of the effective-mass approximation. A four-parameter (two-electron, two-hole parameters) product wave function of Born-Oppenheimer type is employed. The electron function is a slight modification of the Guillemin-Zener function for H_2^+ and the hole function is a simple Gaussian. Machine calculations are in progress for a wide range of m_h/m_e values exceeding unity. Available results will be presented.

I7. Interaction of Excitons with Conduction Electrons.* P. R. ZILSEL AND J. D. NIXON, *Western Reserve University.*—We have considered the interaction of mobile (Wannier) excitons with conduction electrons (concentration n_e, mobility μ_e) in an electric field E. Excitons acquire momentum, P_x, parallel to the electron current j_e at the rate $dP_x/dt=(j_e/e)m_r u_e \sigma_P$ (m_r=reduced mass; u_e=thermal electron velocity; σ_P=momentum transfer cross section). Since $j_e\sim E$, the exciton may be considered as having an "effective charge" $q_x=n_e\mu_e m_r u_e \sigma_P$. One can (under) estimate σ_P by Born approximation for a screened Coulomb interaction with screening radius $a_x\approx\epsilon a_0$ (ϵ=dielectric constant) to be of the order $5a_x^2$. In synthetic CdS with $n_e\approx10^{16}$ cm^{-3}, $\mu_e\approx8\times10^4$ esu, at room temperature, this gives $q_x\approx10^{-2}e$. This means that, *if* it is possible in CdS to observe *exciton diffusion* over several millimeters,[1] it should be possible to observe *exciton drift* in moderate electric fields. The Einstein relation gives $L_E/L_D=(q_x/e)(eV/kT)L_D/d$ for the lifetime drift distance, L_E, in a field V/d, compared to the diffusion length L_D.

* Supported in part by the U. S. Army Office of Ordnance Research.

[1] M. Balkanski and R. D. Waldron, Phys. Rev. 112, 123 (1958); G. Diemer and W. Hoogenstraaten, J. Phys. Chem. Solids 2, 119 (1957).

TUESDAY MORNING AT 9:30

Room 6–120

(G. E. UHLENBECK presiding)

General Theoretical Physics

IA1. Scattering of Electrons with an Electric Dipole Moment. S. ROSENDORFF, B. MARGOLIS, AND A. SIRLIN, *Columbia University.*—The elastic scattering of electrons with a small intrinsic electric dipole moment (e.d.m.) by spinless targets is discussed in the first and second Born approximations. For large momentum transfer ($q\sim500$ Mev/c) the e.d.m. contribution to the elastic scattering cross section becomes important even for values $\lambda\sim10^{-3}$ (where λ is the e.d.m. in units of e times the Compton wavelength of the electron). Thus, it seems likely that experiments involving high-energy electrons may give valuable information on the hypothetical existence and upper limit of the e.d.m. interaction. It is also found, in the first Born approximation, that at sufficiently high energies the existence of the e.d.m. can change the polarization of the electron beam from longitudinal to transverse. Finally, asymmetry effects which appear in the

second Born approximation are discussed in detail. Detection of these asymmetries or of the spin correlation effects of the first Born approximation mentioned above would imply the noninvariance of the electromagnetic interactions under parity and time reversal.

IA2. Quasi-Elastic Scattering in the Optical-Model.* B. J. MALENKA, *Tufts University*.—The quasi-elastic scattering of high-energy protons by a nucleus has been calculated by methods analogous to the deuteron pickup problem.[1] The procedure followed is to rewrite the steady-state integral equation in a form more suitable for the usual approximation in which the proton and the struck nucleon scatter primarily through a direct two-body interaction inside the nucleus. The interactions of the scattered nucleon with the rest of the nucleus before and after direct collision are then included in the optical model approximation. The resulting expressions are similar to those obtained by the impulse approximation,[2] however the relation to the optical model parameters is specifically exhibited. The connection of the results with nuclear momentum distribution, and the possible consequences of using polarized beams will be discussed.

* Supported in part by the U. S. Atomic Energy Commission.
[1] K. R. Greider, University of California Radiation Laboratory Report UCRL-8357 (1958).
[2] Maris, Hillman, and Tyren, Nuclear Phys. **7**, 1 (1958).

IA3. Calculation of the Structure of a Finite Nucleus.* ANDREW M. LOCKETT III AND MANUEL ROTENBERG,† *Los Alamos Scientific Laboratory*, AND K. A. BRUECKNER, *University of Pennsylvania*.—A theory of finite nuclei, based on the reaction matrix theory of the nuclear many-body system has been described previously.[1] It consists of essentially a Hartree-Fock treatment in which the effective potential is the nonlocal reaction matrix of the infinite nuclear medium[2] appropriate to the local density. The calculations of the properties of the nucleus Ca^{40} in its ground state have been carried out with the IBM 704 computing machines of the Los Alamos Scientific Laboratory. The results of these calculations will be presented. These include (a) the total binding energy, (b) the particle density profile, (c) the single-particle energies, wave functions, and effective potentials, and (d) the contributions from the Coulomb, spin-orbit, and rearrangement energies.

* Supported in part by the U. S. Atomic Energy Commission.
† Now at the University of Chicago.
[1] Brueckner, Gammel, and Weitzner, Phys. Rev. **110**, 431 (1958).
[2] K. A. Brueckner and J. L. Gammel, Phys. Rev. **109**, 1023 (1958).

IA4. Solution of a Reduced Bethe-Salpeter Equation.* E. M. MACKINNON† AND Z. V. CHRAPLYVY, *Saint Louis University*.—One test of the validity of the Bethe-Salpeter (B.S.) equation and especially of the ladder approximation is its capability of reproducing the Dirac results for the H atom. This is examined theoretically by using Salpeter's three-dimensional form of the B. S. equation[1] and reducing it to an equivalent one body form similar to the Dirac equation. This is solved in momentum space by the Fock-Lévy method.[2] The reduced B.S. equation reproduces the Dirac eigenvalues to the order of accuracy of the fine-structure splitting (order α^4). The principal (order 1 and α) terms in the eigenfunctions are reproduced but not the higher coefficients (of order α^2 and α^3).

* This research was supported in part by the U. S. Air Force Office of Scientific Research, Air Research and Development Command.
† This work is based on a dissertation submitted to the Department of Physics, Saint Louis University in partial fulfillment of the requirements for the degree of Doctor of Philosophy. Present address: Weston College.
[1] E. E. Salpeter, Phys. Rev. **87**, 328 (1952).
[2] M. Lévy, Proc. Roy. Soc. (London) **A204**, 154 (1951).

IA5. Two-Electron Wave Functions.* P. N. ARGYRES AND L. EYGES, *MIT*.—We consider a two-electron problem (e.g., He atom, H molecule, two electrons in a periodic lattice) for which we assume we can find one-electron orbitals, i.e., wave functions when the repulsion e^2/r_{12} between the electrons is neglected. We investigate the possibility of taking the repulsion into account and finding the perturbed wave function to the first power of e^2, hence the energy to the third power, by calculating directly from the inhomogeneous differential equation that is given by first-order perturbation theory. To do this we convert the differential equation to an integral equation for the momentum space wave function $\varphi(\mathbf{k}_1,\mathbf{k}_2)$. Expanding this wave function in spherical harmonics of both $\mathbf{k}_1$ and $\mathbf{k}_2$ leads to an infinite set of coupled integral equations for the radial parts of this wave function. In practical cases the set can be truncated in good approximation, and the small number of equations that remain appear tractable for machine calculation. Numerical examples will be discussed.

* The work reported here was performed at Lincoln Laboratory, a technical center operated by Massachusetts Institute of Technology with the joint support of the U. S. Army, Navy, and Air Force, under contract.

IA6. Reduction of the Ground-State *N*-Body Problem for Two-Body Operators to a Two-Body Problem.* T. L. GILBERT, *Argonne National Laboratory*.—Let $H^{(N)}=\Sigma_{i=1}^{N} H^{(N)}(i)+\Sigma_{i<j=1}^{N}H^{(N)}(ij)$ be an N-body Hamiltonian containing one- and two-body interactions only, and let $\mathbf{D}^{(N)}$ be any non-negative Hermitian operator in the $\binom{Z}{N}$-dimensional N-body space spanned by all Nth order Slater determinants constructed from Z spin orbitals. Imposing the constraint $Trace\ \mathbf{D}^{(N)}=1$, the $\mathbf{D}^{(N)}$ operators which satisfy $\delta\,[Trace\,\mathbf{H}^{(N)}\mathbf{D}^{(N)}]=0$ and are invariant under the symmetry operations of the system are proportional to the projection operators for the manifolds spanned by eigenvectors of the distinct eigenvalues of $\mathbf{H}^{(N)}$. This N-body variational problem can be reduced to a two-body problem by using the identity $Trace\,\mathbf{H}^{(N)}\mathbf{D}^{(N)}=Trace\,\mathbf{H}^{(2)}\mathbf{D}^{(2)}$, where $\mathbf{H}^{(2)}=(N-1)^{-1}\,\Sigma_{i=1}^{2}\,\mathbf{H}^{(2)}(i)+\mathbf{H}^{(2)}(12)$ is a Hamiltonian in the $\binom{Z}{2}$-dimensional two-body space and $\mathbf{D}^{(2)}$ is a Hermitian operator with $Trace\ \mathbf{D}^{(2)}=\binom{N}{2}$ and diagonal elements which must lie between zero and unity in any configuration representation. If the only constraints on $\mathbf{D}^{(2)}$ were that $0\leq d_i\leq 1$ and $\Sigma_i d_i=\binom{N}{2}$, where d_i are the eigenvalues of $\mathbf{D}^{(2)}$, then the invariant $\mathbf{D}^{(2)}$ operator for the ground state would be $\mathbf{D}^{(2)}=\Sigma_1^{\,n}\,\mathbf{\Gamma}_i^{(2)}+d\,\Sigma_{n+1}^{\,n+q}\,\mathbf{\Gamma}_i^{(2)}$, where $\mathbf{\Gamma}_1^{(2)},\cdots,\mathbf{\Gamma}_n^{(2)}$ are projection operators for all $n\leq\binom{N}{2}\leq n+q$ eigenstates of $\mathbf{H}^{(2)}$ which belong, in complete sets, to the lowest eigenvalues.

* Based on work performed under the auspices of the U. S. Atomic Energy Commission.

IA7. On Some Relations Connecting the Mass Differences of the Chief Isotopes of Elements Belonging to the Inert Gas Periods. N. EFREMOV, *1061 Intervale Avenue, New York, New York*.—The algebraic sums of the numbers representing the mass differences of the chief isotopes of elements of the inert gas periods are a constant number equal to 15. Therefore these numbers representing the mass differences of the chief isotopes belonging to the He period can be changed into the numbers representing the mass differences of the chief isotopes of any other inert gas period (Ne, A, Kr, etc). That is done by means of certain series of numbers to be added[1]:

From He to Ne period:	0, −1, 1, 0, 1, −1, 0
From He to A period:	−4, −1, 3, 2, 1, −1, 0
From He to Kr period:	−2, 1, −1, 0, 1, 3, −2 etc.

The algebraic sum of the numbers of each series is equal to 0. Successive addition of the corresponding "addition numbers" (e.g., 0, −1, 1, 0, 1, −1, 0) to the numbers representing the mass differences of the chief isotopes of elements of the He period[2] (3,2,2,1,2,2,3) gives us the numbers of the mass differences of the chief isotopes of the Ne period (3,1,3,1,3,1,3) etc. The above regularities allow us to explain some deviations from the Mattauch's rules[3] concerning isotopes.

[1] Cf. the method of "addition numbers" used in Bode's law.
[2] N. Efremov, Bull. Am. Phys. Soc. Ser. II, **4**, 66 (1959).
[3] J. Mattauch, Z. Physik **91** (1934), Naturwissenschaften **25** (1937).

TUESDAY MORNING AT 9:30

Room 4–270

(E. E. LOEBNER presiding)

General Solid-State Physics

J1. Diffusion of Phosphorus in SiO_2 Film. C. T. SAH, H. SELLO, AND D. A. TREMERE, *Shockley Transistor Corporation.*—The diffusion of phosphorus in SiO_2 film from a P_2O_5 gaseous phase in an open-tube diffusion system is investigated. SiO_2 films of thickness from 0.08 to 0.9 μ are grown on p-type optically polished single crystal silicon surface of (100) orientation at 1200°C and 1300°C in a wet oxygen atmosphere. The p-type silicon beneath the SiO_2 film is used as a "phosphorus detector." Experimental relationships are obtained for diffusion temperature, diffusion time, and oxide thickness at the point where the oxide film fails to mask against P_2O_5. Over the temperature range of 900°C to 1250°C, it is found that the masking boundary condition has an activation energy of 1.5 ev. The experimental results are discussed in terms of a simple diffusion mechanism.

J2. Molecular Transport in Liquids and Glasses. MORREL H. COHEN, *University of Chicago,* AND DAVID TURNBULL, *General Electric Research Laboratory.*—We have derived, using simple considerations, a relation between the diffusion constant D in a liquid of hard spheres and the "free volume," v_f. This derivation is based on the concept that statistical redistribution of the free volume occasionally opens up voids large enough for diffusive displacement. The relation is $D=A\exp[-\gamma v/v_f]$ where v is the minimum required volume of the void and A and γ are constants. This equation is of the same form as Doolittle's[1] empirical relation between the fluidity ϕ of simple hydrocarbons and their free volume. It has been shown[2] that the Doolittle equation also can be adapted to describe the abrupt decrease in molecular kinetic constants with decreasing temperature that accompanies the glass transition in certain liquids. Our result predicts that even the simplest liquids would go through this glass transition if sufficiently undercooled and crystallization did not occur. The problem of transport in actual simple and network liquids also will be discussed.

[1] A. K. Doolittle, J. Appl. Phys. **22**, 1471 (1951).
[2] Williams, Landel, and Ferry, J. Am. Chem. Soc. **77**, 3701 (1955).

J3. Conduction in Silver Azide. D. A. YOUNG,* *Imperial College, London* (introduced by G. H. Vineyard).—The orthorhombic body-centered form of silver azide stable at room temperature undergoes an apparently irreversible transformation to a form of lower symmetry at 190°C. The crystals shatter during the transition. Additionally, decomposition into nitrogen and silver occurs at a measurable rate above 160°C. Optical absorption spectra of the partially decomposed material (fractional decomposition ~0.1%) suggest the presence of colloidal silver in both high- and low-temperature forms, particularly in well-annealed specimens. In this condition both forms exhibit marked photoconductivity extending to the near infrared. The dark conductivity of both freshly prepared and partially decomposed samples was studied at the transition point and during the annealing and sintering processes which occur on thermal cycling at various rates between room temperature and 210°C. These results were compared with thermoelectric power and Hall-effect measurements made under similar conditions. From this comparison it was possible to propose that the current carriers in partially decomposed silver azide are interstitial cations and electrons from the collodial centers.

* Now Guest Scientist at Brookhaven National Laboratory, on leave of absence from Atomic Energy Research Establishment.

J4. Intrinsic and Impurity Absorption Spectra in Rutile. ARTHUR LINZ, JR., *National Lead Company.*—Reflection measurements on single crystals and transmission measurements on thin films of rutile TiO_2 in the ultraviolet indicate a large intrinsic absorption peak at 4.1 ev (3000 A) which shifts to longer wavelengths as the temperature decreases, with smaller temperature independent peaks at 4.6 ev (2700 A) and 5.6 ev (2200 A), and a long wavelength tail extending to the previously observed absorption edge in the neighborhood of 3 ev. Measurements with polarized light show that the absorption edge and the first reflection maximum occur at shorter wavelengths when the electric vector of the incident radiation is parallel to the optic axis of the crystal. An average value of the index of refraction in the ultraviolet region was calculated from the data. Niobium and beryllium doped rutile crystals show a broad absorption at about 0.8 ev (1.6 μ) similar to that found in "reduced" crystals containing oxygen vacancies or interstitial hydrogen ions and also exhibited similar "n" type conductivity with a low-temperature coefficient of resistivity. Tungsten-doped crystals show a steep negative temperature coefficient of resistivity and an optical absorption at 1.4 ev (0.9 μ). These impurity absorption peaks all shift to longer wavelengths when the temperature is decreased. The data can be interpreted in terms of a model suggested by Morin involving narrow conduction bands formed by overlapping titanium 3d levels.

J5. Absorption Edge in Single Crystals of Alloys of ZnS CdS. LAWRENCE C. GREENE AND DAVID L. KINGSTON, *Wright-Patterson Air Force Base.*—Single crystals of ZnS CdS alloys have been grown using the vapor phase technique of Greene, Reynolds, Czyzak, and Baker[1] for the growth of single crystals of cadmium sulfide and zinc sulfide. Large bulk crystals of a wide range of compositions have been produced by this method. The absorption edge has been measured as a function of composition by means of optical transmission measurements. These results are compared with those obtained from diffuse reflectance measurements made on pellets of compressed microcrystalline material.

[1] Greene, Reynolds, Czyzak, and Baker, J. Chem. Phys. (to be published).

J6. On the Efficiency of Electroluminescence in ZnS. G. F. NEUMARK, *Sylvania Research Laboratories.*—For a model of impact ionization in a barrier one can show that the best theoretical efficiency is proportional (to a good degree of approximation) to the ratio of the number of electrons created in the barrier to the number penetrating the barrier. This ratio can be obtained from the ionization rate. This rate has here been calculated for ZnS by applying to this material a theory developed for Ge and Si.[1] In this theory, two parameters are of main importance. These are the ionization threshold and the mean free path for electron-lattice interaction.[1] For both parameters, ranges that appeared appropriate for ZnS were selected; the former, on the basis of the energy gap and the latter by using an expected similarity between the Ge and Si values and the ZnS value. The efficiency can then be obtained. By considering its voltage dependence it can then be maximized with respect to the voltage. This maximum efficiency, which now no longer involves the electron-lattice interaction, is ≈80 lumens/watt times the ratio of the barrier

voltage to the total voltage. It appears adequate to account for efficiencies reported to date.

[1] P. A. Wolff, Phys. Rev. 95, 1415 (1954).

J7. Flash Evaporation.* HOWARD SALTSBURG, *General Electric Company.*—Thin films of Cd, deposited upon a *W* ribbon, have been caused to evaporate in the form of a vapor pulse by rapidly heating the ribbon to temperatures in excess of the conventional boiling point of Cd. The velocity of the emitted vapor pulse has been measured, in vacuum, using a time-of-flight technique involving the sequential scattering of two fixed electron beams. The dependence of the velocity has been measured as a function of the calculated adiabatic ribbon temperature. An analysis of the data, based upon a study of the shape of the observed scattering signal due to the vapor pulse, suggests that the condensed phase of Cd is superheated to the *W* ribbon temperature. Further, the vapor pulse formed has a temporal distribution in density, at some distance from the ribbon, which is equivalent to a molecular velocity distribution of a modified Maxwell-Boltzmann type, characteristic of an equilibrium molecular beam of Cd at the *W* ribbon temperature.

* Supported by U. S. Air Force.

J8. Transmission Coefficients of Sound at a Quartz-Zinc Single Crystal Interface. ROBERT A. ARTMAN,* *Ford Motor Company.*—In the pulsed ultrasonic technique of measurement of the elastic constants of a hexagonal crystal, one shear wave velocity measurement must be made with the direction of sound propogation not in a pure mode direction. Under these conditions three waves, one quasi-transverse, one pure transverse, and one quasi-longitudinal, are generated in the sample, and three waves are reflected into the quartz driver. The general solution of reflection and transmission coefficients of a *BT*-cut quartz transducer coupled to a hexagonal single crystal has been determined. Curves of the six coefficients *vs* orientation for a zinc sample crystal have been computed. The amplitude of the desired shear mode in the zinc varies from 90% to 118% of the incident amplitude, whereas the unwanted quasi-longitudinal mode can have an amplitude as large as 28% of the incident. The unwanted pure shear mode never exceeds 2% of the incident amplitude. The introduction of the two additional modes does not offer serious complications. However, due attention must be given to orientation since the energy flux vector can deviate from the propagation direction by as much as 30°.

* Now at Bucknell University.

TUESDAY MORNING AT 9:30

Room 10–250

(A. SMAKULA presiding)

Irradiation Effects III; Quartz, Silica, etc.

JA1. The Importance of Thermal Spikes Produced in Quartz and Vitreous Silica by Positive Ion Bombardment.* R. L. HINES AND R. ARNDT, *Northwestern University.*—Comparison of bombardments by positive ions of different masses can be used to determine experimentally the effect of the local temperature produced when an energetic atom (10–50 kev) is stopped in a solid. Bombardments of polished quartz and vitreous silica samples by 10-kev He^+, 39-kev Ne^+, and 50-kev A^+ ions produce similar changes in refractive index of the bombarded region except for differences in the magnitude of the integrated flux. At these energies the ions will loose almost all of their energy in displacement collisions and very little in ionization. Since the ion energies are chosen to give the same ion penetration of 10^{-5} cm, the He^+ ions will give the lowest local temperature and the A^+ ions will give the highest local temperature. However, the product of ion energy times the integrated flux required to produce a given change in refractive index is the same for all bombardments within a factor of 2. This suggests that only the total energy dissipated per unit volume in displacement collisions is important and that the localization of energy on individual energetic atoms is of minor importance.

* Work supported by the U. S. Atomic Energy Commission.

JA2. *E* Band in Silica and Quartz. C. M. NELSON AND R. A. WEEKS, *Oak Ridge National Laboratory.*—The appearance of the *E* band[1] (7.5 ev) has been observed in fused silica and crystalline quartz after both Co^{60}-γ and fast neutron irradiations. No *D* band (7.1 ev) was observed even with very light γ irradiations in the very-high-purity materials available. Impurities seem to play an important role in the development of coloration in the vacuum ultraviolet region particularly with ionizing radiation and short neutron bombardments. The *E* band was shown to be related to a previously described electron spin resonance (ESR) line by using different materials with different irradiation conditions, followed by annealing and bleaching studies. In addition, an attempt was made to find a correlation between the *E* band and one or more of the other absorbing centers. The *C* and *E* bands develop and disappear quite independently of each other. Though ESR measurements indicate the *C* band is a trapped electron and the *E* band a hole trapped on an interstitial oxygen, our results show there is no simple relation between them. Possible models to explain these results will be discussed based on a strained bond picture.

[1] E. W. J. Mitchell and E. G. S. Paige, Phil. Mag. 1, 1085 (1956).

JA3. Radiation Effects in Silica at Low Temperatures. GEORGE W. ARNOLD AND W. DALE COMPTON, *U. S. Naval Research Laboratory.*—Optical absorption measurements of silica irradiated at low temperatures have revealed several facts. Bombardment and measurement of Corning fused silica 7940 with 2-Mev electrons at 77°K give an absorption coefficient at 2150 A (*C* band) about 10 times (α=93/cm) that at room temperature. Warming to room temperature and remeasuring at 77°K bleaches the absorption by about one-half. A similarly strong band at 2570 A has negligible absorption when remeasured at 77°K after warming. Crystalline synthetic quartz (Clevite) has 15 times less absorption at 2150 A than does 7940 silica for 5 times the electron flux. Corning fused silica 7943,[1] which has at least 100 times less OH^- content than does 7940 silica, has about 3.5 times as much 2150-A absorption for equal flux values (α=61/cm *vs* α=18/cm). The absorption at 2570 A is down by a factor of at least 10 in the 7943 material. For equivalent absorbed energy the 2150-A band in *x*-irradiated 7940 silica is about 10 times less than that obtained for electron bombardment. Curves of absorption

coefficient *vs* flux for 0.5–2 Mev electron energies for both the 2150-A and 2570-A bands (7940 material) show increasing damage with decreasing electron energy.

[1] Corning fused silica 7943 supplied through courtesy of Corning Glass Works, Corning, New York.

JA4. Mechanism of Radiation Damage in Silica at Low Temperatures. W. DALE COMPTON AND GEORGE W. ARNOLD, *U. S. Naval Research Laboratory.*—The growth of the 2150-A absorption band (*C* band) in fused silica with neutron irradiation is thought to result from the displacement of oxygen ions from their lattice sites and the subsequent trapping of an electron by the vacancy.[1] Data obtained by electron irradiation at 77°K (previous abstract) are not in agreement with the simple theory of the displacement of oxygen ions; e.g., (1) damage induced in Corning 7940 silica cannot be fitted to a theoretical curve of cross-section *vs* electron energy; (2) damage induced in Corning 7943 silica can only be fitted to the theoretical cross-section curve if the energy for displacement of an oxygen ion is about 7 ev. In this case, agreement between the calculated number of displaced ions by 2-Mev electrons and the area under the 2150-A band is found only if an oscillator strength of about 25 is taken for the center. (3) Agreement is not improved by considering displacements produced by a rapidly moving oxygen ion or displacements by secondary electrons. Since ionization and excitation are not the predominant mechanisms, it is concluded that the simple pictures of damage are inadequate to account for the observed effects.

[1] E. W. J. Mitchell and E. G. S. Paige, Phil. Mag. 1, 1085 (1956).

JA5. Irradiation Effects and Short-Range Order in Silica and Quartz. R. A. WEEKS AND C. M. NELSON, *Oak Ridge National Laboratory.*—The crystalline order in the region of one of the defects of the quartz structure produced by irradiation of silica and quartz crystals has been examined by electron spin resonance. In a single crystal its g tensor has eigenvalues $g_1=2.0003$, $g_2=2.0006$, $g_3=2.0018$. Taking $S=\frac{1}{2}$, $I=0$ (Si^{29}: $I=\frac{1}{2}$, 4.7% abundant)[1] the shape of the envelope of the single crystal lines was calculated for random orientation. Good agreement of the calculated line shape with that in γ-irradiated Corning silica was found. The line shape in reactor-irradiated Corning silica and in a heavily irradiated single crystal was not in agreement. The line shape in a "waterless" silica (Corning 7943) was found to be similar to the shape in heavily irradiated silica and quartz crystal. Other indications of a structural difference are: (1) the optical absorption edge in the "waterless" is ~1.0 ev below the "normal" silica and (2) its density is 0.5% higher. The agreement of calculated and observed line shape in the γ-ray irradiated "normal" silica indicates that the crystalline order around the defect in the silica is similar to that in the single crystal. It is suggested that an ordered region, similar to the single crystal, around each defect in the "normal" silica has a diameter of ~30 A.

JA6. Annealing Characteristics of the Color Centers Formed by Radiation Damage in Single Crystals of Al_2O_3 and Pure Fused Silica.* PAUL W. LEVY, *Brookhaven National Laboratory.*—Previously we have shown that when Linde crystalline Al_2O_3 is irradiated in a reactor color centers are produced, in particular one at 204 mμ that cannot be formed by purely ionizing radiation. Similarly the color centers induced in Corning pure fused silica such as the one at 218 mμ are formed readily in a reactor and very slowly in purely ionizing radiation. Reactor colored samples of both materials have been subjected to isochronal pulse anneals in which the temperature is increased the same amount at each step. In both materials any coloring removed by annealing Al_2O_3 to approximately 450°C and fused silica to approximately 270°C can be restored by Co^{60} gamma-ray irradiation while annealing above these temperatures removes coloring that is not restored by subsequent Co^{60} irradiation. Thus, in these materials annealing can occur in two steps, the first being uncoloring of the centers by "electronic" process while the second involves destruction of the center colored or uncolored such as that expected, for example, when vacancy interstitial recombination occurs. Presumably the fast reactor neutrons form centers by radiation damage processes which are then colored by ionization processes. By application of this technique these two processes may be separated.

* Work performed under auspices of the U. S. Atomic Energy Commission.

JA7. Spin Resonance in Silicon Electron Irradiated at Low Temperatures. G. D. WATKINS, J. W. CORBETT, AND R. M. WALKER, *General Electric Research Laboratory.*—We have studied the spin resonance spectrum in silicon at 20°K after room-temperature, 78°K, and 20°K irradiations with 1.5-Mev electrons. The change in the spectrum during the annealing of a low-temperature irradiation has also been studied. The dominant center observed after a room-temperature irradiation of phosphorus-doped silicon is that previously described.[1] This anisotropic center, composed of a central group plus satellites arising from hyperfine interaction with one Si^{29} atom,[1] is found to have additional weak satellites. Analysis shows that the center must be composed of *two* equivalent silicon atoms, the additional satellites arising from the 0.22% abundant center for which both atoms are Si^{29}. The production rate of this center in irradiations at 20°K is $<\frac{1}{4}$% of that in room-temperature irradiations. The number of these centers increases during subsequent annealing, but after annealing at room temperature, the number is still only ~2% of that of a corresponding room-temperature irradiation. Possible models for this two-silicon center will be discussed in the light of the above production and annealing experiments. Other spectra are also observed and will be discussed.

[1] Bemaki, Feher, and Gere, Bull. Am. Phys. Soc. Ser. II, 3, 135 (1958).

JA8. Paramagnetic Resonance in Neutron-Irradiated Silicon.* M. NISENOFF AND H. Y. FAN, *Purdue University.*—Spin resonance in neutron-irradiated silicon is investigated.[1] Both n- and p-type samples are studied, the resistivity of which reached about 10^4 ohm-cm after the irradiation. Near 4°K, the relaxation time is of the order of seconds. The steady-state dispersion signal has $g=2.0061$ and 16-oersted half-width. At room temperature the relaxation time is short, and the derivative of absorption observed showed a number of peaks. The integrated curve agrees with the signal observed at the low temperature. The pattern is anisotropic with orientation of the magnetic field. With annealing at temperatures up to 470°C, the pattern gradually simplifies, showing that the original signal is produced by more than one type of center. The simplest pattern shows one line for $H\|\langle 100\rangle$ with $g=2.0078$ and half-width of 4 oersted, there are several peaks for $H\|\langle 110\rangle$ and $H\|\langle 111\rangle$. The pattern becomes more complicated after annealing at still higher temperatures, indicating the formation of new types of defects. Samples having lower resistivities after irradiation give different types of signals, depending on the Fermi level.

* Work supported by Signal Corps Contract.
[1] Schulz-DuBois, Nisenoff, Fan, and Lark-Horovitz, Phys. Rev. 98, 1561 (1955).

JA9. Infrared Absorption and Photoconductivity of Irradiated Silicon.* A. K. RAMDAS AND H. Y. FAN, *Purdue University.*—Irradiation by high-energy neutrons or 4.5-Mev electrons produces in n-type silicon an absorption band with peak at 3.3 μ,[1] provided the Fermi level does not become too low in the irradiated sample. At low temperatures, the absorption

band resolves into three sharp bands at 3.61, 3.45, and 3.31 μ with small peaks discernable at shorter wavelengths. The relative strengths of the three bands do not change appreciably in samples of different Fermi levels, indicating that the bands correspond to transitions from the ground level to various excited states of a defect center. The spacings between the bands are close to four times the spacings between the $(2p,0)$, $(2p, \pm 1)$, and $(3p, \pm 1)$ levels of group V impurities in silicon. Thus the absorption could be the excitation spectrum of He^+-like defects. Measurements show that the absorption is not associated with photoconductivity. The 3.9-μ absorption band observed in p-type irradiated samples[1] and the 1.8-μ band first found in irradiated silicon do not show structure at low temperatures. The 3.9-μ band is associated with photoconductivity and should correspond to ionization of bound holes.

* Work supported by a Signal Corps contract.
[1] H. F. Fan and A. K. Ramdas, Bull. Am. Phys. Soc. Ser. II, 3, 129 (1958).

JA10. Recovery of Electron Bombardment Damage in InSb.* F. H. EISEN, *North American Aviation.*—The recovery of electron bombardment damage in n-type InSb (about 2×10^{16} carriers/cc) has been studied by isothermal and isochronal annealing of samples irradiated between 80° and 90°K. The electrical conductivity and Hall coefficient of the sample were measured during the irradiation and subsequent annealing. At 400 kev the change in the reciprocal of the Hall coefficient is approximately linear with the integrated beam current. The damage recovers in a single stage centered at 150°K with an activation energy of 0.58 ev. Damage produced at other bombarding electron energies recover partially in this stage, but some recovery is also observed at other temperatures, depending on the energy of bombardment. A discussion of the interpretation of the isothermal recovery data, and the difficulties involved in its interpretation is presented.

* This work was supported by the U. S. Atomic Energy Commission.

TUESDAY MORNING AT 9:30

Room 26–100

(L. A. WOOD presiding)

Polymeric Papers Not Channeled via the Division

K1. Imperfectly Flexible Molecular Chains at Finite Extensions. R. A. SACK,* *British Rayon Research Association* (introduced by R. S. Mulliken).—The statistical properties of imperfectly flexible chains are usually discussed in terms of Kuhn's model of the equivalent random chain. The effect of short-range correlation can be explicitly calculated by means of the theory of Markoff chains.[1,2] As the resulting series expansions are cumbersome and poorly convergent, numerical calculations were carried out on EDSAC II at the University of Cambridge to determine the behavior at arbitrary extensions of a linear chain model with tetrahedral bond angles and free rotation about bonds. For extensions of up to 70% of the contour length, the deviations of the mechanical properties from those of the equivalent Gaussian chain are approximately $\frac{3}{4}$ times as big for the tetrahedral chain as for the equivalent Kuhn chain. The discrepancies are more pronounced for the mean birefringence.

* Present address: University of Chicago.
[1] H. M. James and E. Guth, J. Chem. Phys. 11, 531 (1943).
[2] R. Kubo, J. Phys. Soc. Japan 2, 47, 51, 84 (1947); *ibid.* 3, 119 (1948).

K2. Correspondence Principles Relating Certain Steady Flows in General Incompressible Viscoelastic Fluids. BERNARD D. COLEMAN, *Mellon Institute,* AND WALTER NOLL, *Carnegie Institute of Technology.*—Solutions have been obtained by Rivlin[1] for certain steady flows in the Rivlin-Ericksen theory which deals with fluids of the differential type. These solutions are shown to be valid for the most general fluids; i.e., fluids for which the stress is an arbitrary functional of the deformation history. Using appropriate coordinate systems, it is shown that the following steady flows are equivalent for all fluids: simple shear between two parallel plates, flow between two fixed parallel plates, Poiseuille flow, and Couette flow. From a measurement of the shearing and normal stresses in any one of these flows, it is possible to predict the stresses and velocity profiles in each of the others without approximations. For a general incompressible fluid, simple transformations can be derived which relate the following measureable functions: shearing traction *versus* velocity gradient in simple shear, discharge rate *versus* pressure head in Poiseuille flow, and flow between two fixed plates, and angular velocity *versus* torque in Couette flow.

[1] R. S. Rivlin, J. Rational Mech. Anal. 5, 179 (1956).

K3. Effects of Pressure upon the Phase Separation of Polymer Solutions.* JOE S. HAM, *A and M College of Texas.*—The molecular weight fractionation of a polymer is commonly carried out with a phase separation achieved either by increasing the concentration of nonsolvent or by cooling a dilute solution of the polymer. In the literature, there seems to have been no discussion of the use of pressure to carry out this phase separation. To anticipate the magnitude of the pressure effects, some rough calculations have been made. These computations attempt to compute the pressure dependence of Flory's theta temperature both from experimental volumes of mixing and from the pressure dependence of the solubility parameters. A discussion is given of the reliability of the assumptions made in the computations. The results indicate a wide variety of behavior is to be expected for various polymer-solvent pairs and suggest that experimental studies of the pressure effects will be worthwhile.

* Supported by the Robert A. Welch Foundation.

K4. Thermal Diffusion in Dilute Polymer Solutions near the Theta Temperature.* FRANK C. WHITMORE AND JOE S. HAM, *A and M College of Texas.*—According to the theory of thermal diffusion in dilute polymer solutions proposed by Emery and Drickamer,[1] $\alpha/\alpha_0 = [X_p(\partial\mu_p/\partial X_p)]^{-1}$, where X_p is the mole fraction of the polymer, μ_p the excess chemical potential of the polymer, and α_0 the thermal diffusion ratio at infinite dilution. At the theta temperature of the solution, the solvent-segment interaction vanishes and $[X_p(\partial\mu_p/\partial X_p)] = (1-\phi_p^2)(1+m\phi_p^2)$, where ϕ_p is the volume fraction of the polymer and m is the ratio of the molar volume of the polymer to that of the solvent. Thus, at sufficiently low concentrations, $(\alpha/\alpha_0) = (1+m\phi_p^2)^{-1}$. Measurements of the thermal diffusion ratio for several solutions near the theta temperature will be presented and compared with this theory.

* Supported by Convair.
[1] A. H. Emery and H. G. Drickamer, J. Chem. Phys. 23, 2252 (1955).

K5. Spherulitic Crystallization in Polypropylene. F. J. PADDEN, JR., AND H. D. KEITH, *American Viscose Corporation.*—Spherulites in thin films of polypropylene crystallized from the melt have been studied with the polarizing microscope over a range of crystallization temperatures from 120°C to 148°C. Four types of spherulites may be distinguished: (I) coarse-textured spherulites exhibiting positive birefringence and growing preferentially in the temperature range 120–132°C; (II) coarse-textured negative spherulites growing preferentially in the range 138–148°C; (III) fine-textured negative spherulites, about eight times as birefringent as (I) or (II), growing in the range 120–128°C under conditions of rapid cooling from the melt; (IV) negative spherulites of relatively high birefringence exhibiting dark rings of extinction between crossed Nicols, and growing in a narrow temperature interval around 130°C. Spherulites grown in the range 134–138°C show predominantly a mixture of positively and negatively birefringent material. The exceptionally large dimensions of spherulites which may be obtained in this polymer and the pronounced cracks which form at inter-spherulite boundaries permit separation of the spherulites for individual study. The density of individual spherulites extracted from solid plugs has been measured at three crystallization temperatures.

K6. Evidence for a Second Crystal Form of Polypropylene. H. D. KEITH, F. J. PADDEN, JR., N. M. WALTER, AND H. W. WYCKOFF, *American Viscose Corporation.*—X-ray diffraction patterns have been obtained from selected areas of the four principal types of spherulite in polypropylene discussed in the preceding paper. The x-ray reflections from spherulites of types I and II are consistent with the structure proposed by Natta. Despite their difference in optical sign, however, the same preferred molecular orientation, in which the b axis (=20.95 A) and the c axis (=6.50 A) of the monoclinic unit cell lie approximately normal to the radius, appears to occur in both types. Spherulites of type IV give a completely different pattern with strong reflections corresponding to a lattice-plane spacing of 5.54 A and indicative of a hexagonal packing of the helical molecular chains. The possibility of a second crystal form in this polymer had previously been suspected[1] from the appearance of extraneous x-ray reflections of variable intensity, depending on sample history. There is now good reason to believe that such a phase, which can be isolated in the form of discrete spherulites and is probably monoclinic with a hexagonal basal projection, does exist.

[1] N. M. Walter (unpublished results).

K7. Polyethylene Specific Volume, Crystallinity, and Glass Transition. PAUL R. SWAN, *Union Carbide Plastics Company.*—The determination of polymer crystallinity by a combination of specific volume and x-ray unit cell measurements requires in general only the basic assumptions common to all polymer crystallinity determinations, namely, the existence of only two distinct, well-characterized phases and the requirement that their volumes be additive. For polyethylene, however, the inability to obtain a direct measurement of the amorphous specific volume requires additional assumptions, usually those involving a linear extrapolation of the melt specific volume to room temperature. An alternative method is proposed similar to that used[1] by Hoffman and Weeks which utilizes the temperature derivatives of the specific volume and of the crystalline specific volume, but which requires that the crystallinity be constant over some temperature range. The results of applying this method to a linear polyethylene will be discussed. During this work, specific volume data obtained by Quinn and Mandelkern[2] were analyzed by an apparently new technique which provides an unambigious demonstration of a second-order transition in linear polyethylene at −130°C.

[1] J. D. Hoffman and J. J. Weeks, J. Research Natl. Bur. Standards **60**, 465 (1958).
[2] F. A. Quinn, Jr., and L. Mandelkern, J. Am. Chem. Soc. **80**, 3178 (1958).

K8. Solution Grown Crystals of an Acetal Resin. P. H. GEIL, JR., N. K. J. SYMONS, AND R. G. SCOTT, *E. I. du Pont de Nemours and Company.*—Single crystals of polyoxymethylene have been grown from solution. They consist of hexagonal lamellae, often thickened by growth from spiral dislocations. The chain axes are normal to the lamellae which are 100 A thick. Thus, it is suggested that the chains have a folded conformation. In many of the crystals, double Bragg reflections were found in the electron diffraction patterns, resulting from rotation of the lamellae during growth from the dislocation. Dark field electron microscope photographs of these crystals exhibit moiré patterns.

K9. g-Anisotropy and Line Width of Electron Spin Resonance in a C_3O_2-Polymer Char.* S. MROZOWSKI, *University of Buffalo.*—Studies of resonance in chars of several simple substances indicated that the width of the lines in the higher heat-treatment range (from 700°C up) depends on the degree of compaction of the original material. It was found recently that small flakes of a C_3O_2-polymer char (the polymer prepared in a special way was kindly given to us by Dr. H. P. Boehm in Darmstadt) heat treated to about 750°C show a remarkable anisotropy: instead of a single absorption line in some cases as much as four or five lines are seen, the lines shifting in position relative to each other, as the flakes are rotated (period 180°). Only a sharp single line ($\leq 0.5G$) is observed if the flake was finely ground *before* heat treatment, but a wide line ($1.5G$ or more) corresponding to the averaged out multicomponent structure is obtained when the flake was ground *after* the heat treatment. One concludes that the observed widths (at least in the latter, but possibly also in the former case) represent a statistical distribution of the g values and do not give information as to the spin-spin relaxation time. The variation in the g value might possibly be the result of bond strains introduced by the anisotropic shrinkage of the flakes during heat treatment.

* Work supported by the Office of Naval Research.

K10. Polymers as Pile Radiation Detectors. D. BINDER, W. K. KIRKLAND, AND R. L. TOWNS, *Oak Ridge National Laboratory.**—Polymers of different hydrogen contents were irradiated both in a cobalt gamma-ray source and in a pile to determine their neutron sensitivity. In pile irradiation of polymers, only the hydrogen recoil has sufficient energy to compare with the gamma-ray effect. The polymer reactions are listed in Table I along with in-pile, calorimetric measurements

TABLE I.

Substance	Reaction	δ_γ	H_c	H_s
Teflon	Density increase	0.45×10^6 R/hr	0.000	...
Lucite	Viscosity decrease	0.86	0.148	2.6×10^6 R/hr
Polyisobutylene	Viscosity decrease	1.05	0.250	2.3
Graphite	Heat absorbed	0.48	0.000	...
Nylon	Heat absorbed	1.41	0.178	5.2
Allyl diglycol carbonate	Gassing	1.6 ± 0.2	0.124	9 ± 1
Nylon	Gassing	2.4	0.178	11
Polyethylene	Gassing	2.3 ± 0.3	0.250	8 ± 1

of the heat absorbed in graphite and nylon. The "gamma equivalent" δ_γ is the cobalt gamma-ray intensity equivalent to the pile, H_c is the ratio of the number of hydrogen atoms to the number of electrons in the molecule, and H_s is the part of the gamma equivalent due to hydrogen *per unit hydrogen content* H_c.

* Oak Ridge National Laboratory is operated by Union Carbide Nuclear Corporation for the U. S. Atomic Energy Commission.

K11. Apparatus for the Measurement of Normal Stress Distribution in Adhesive Bonds during Peel. E. G. JOHNSON AND D. H. KAELBLE, *Minnesota Mining and Manufacturing Company.*—The theoretical distribution of normal stresses in an adhesive bond in the region ahead of the failure line during stripping tests has been derived by G. J. Spies[1] for a 90° angle of peel. This stress distribution has never been measured. An apparatus has been developed, utilizing a stripping plate with a split beam attached to a differential transformer, with which direct measurements of the normal stress distribution can be made. Such data provides new, independent information concerning the bond response during peel. The apparatus will be described, and some preliminary data involving bonds with viscoelastic interlayers will be presented to illustrate its applicability. The stress distribution predicted by theory is substantiated.

[1] G. J. Spies, Aircraft Eng. 30 (1953).

K12. Effect of Reactor Irradiation on the Mechanical Strength of Drawn and Undrawn Nylon.* Y. C. DAS AND C. C. HSIAO, *University of Minnesota.*—Samples of 610 drawn and undrawn nylon-filament irradiated in a nuclear reactor to accumulated perturbed thermal neutron doses from 4×10^{17} nvt to as high as 1.3×10^{19} nvt have been studied by static tension at room temperature. The tensile strength of the undrawn nylon decreases markedly upon receiving a thermal neutron dose of about 6×10^{17} nvt as compared with that of the drawn nylon. However, at higher levels of neutron irradiation the tensile strength of the undrawn nylon increases while that of the drawn nylon decreases. Beyond a thermal neutron dose of 10^{19} nvt the tensile strength of both types of samples drops sharply.

* Supported by the U. S. Atomic Energy Commission.

K13. Theory of Mechanical Breakdown and Molecular Orientation of Linear Polymers.* C. C. HSIAO, *University of Minnesota.*—A theory of the molecular orientation dependance of mechanical breakdown is presented for some linear high polymers. A microscopic molecular model is first introduced. After simplification an approximation is then considered. For one directional orientation the result indicates a rapid increase in the fracture strength as the degree of molecular orientation increases. The maximum fracture strength obtainable on the basis of the theory is nearly six times that of the unoriented strength.

* Supported in part by the U. S. Atomic Energy Commission.

TUESDAY MORNING AT 9:30

Room 4–370

(W. H. STOCKMAYER presiding)

Chemical Physics of Solids

KA1. Hyperfine Structure of Trapped Hydrogen Atoms.* F. J. ADRIAN, *Applied Physics Laboratory, The Johns Hopkins University.*—Hydrogen atoms stabilized in solid matrices at liquid helium temperatures exhibit small shifts in the hyperfine structure splitting (~0.5%) from the free atom value.[1] It is assumed that the perturbing effect of the matrix consists of Van der Waals interactions and the overlap or Pauli exclusion forces. These two effects are treated separately and added to get the net result. The Van der Waals effect, which is treated by perturbation theory, leads to a reduction in the hfs constant. The overlap effect, which is accounted for by requiring that the hydrogen atom wave function be orthogonal to the wave functions of the matrix particles, leads to an increase in the hfs constant. For a specific model of a hydrogen atom a distance R from six nearest-neighbor matrix particles one obtains the following results: For H in H_2, $\delta\psi^2/\psi^2=-0.13\%$ at $R=6.8a_0$; for H in A, $\delta\psi^2/\psi^2=-0.34\%$ at $R=6.5a_0$. These results are in qualitative agreement with experiment.

* Work supported by the Bureau of Ordnance, Department of the Navy.
[1] Jen, Foner, Cochran, and Bowers, Phys. Rev. 104, 846 (1956); also Phys. Rev. (to be published).

KA2. Nuclear Resonance Spectra of Hindred Rotators.* J. S. WAUGH AND R. W. FESSENDEN,† *Massachusetts Institute of Technology.*—Chemical shifts and spin-spin coupling constants observed in most substituted ethanes are averages over internal rotation. In molecules of sufficiently low symmetry they are experimentally temperature-dependent and reflect the degree of rotational hindrance. By means of suitable approximations one can thus estimate the relative stabilities of rotational isomers. It is found, for example, that the two distinct isomers of $CHCl_2-CClF_2$ differ in energy by about 2.2 kcal/mole. The assumptions required in such measurements will be discussed, with reference to CH_2Br-CF_2Br[1] and $CHClBr-CF_2Br$ as further examples.

* This work was supported in part by a grant from the Alfred P. Sloan Foundation and in part by the U. S. Army (Signal Corps), the U. S. Air Force (Office of Scientific Research, Air Research and Development Command), and the U. S. Navy (Office of Naval Research).
† Now at the California Institute of Technology.
[1] D. M. Graham and J. S. Waugh, J. Chem. Phys. 27, 968 (1957).

KA3. Slow-Neutron Scattering by Rotators. H. C. VOLKIN, *NASA Lewis Research Center.*—The methods of Zemach and Glauber[1] for treating the scattering of low energy neutrons by molecules were confined for the rotational degrees of freedom to the case of a linear molecule. Their results can be most readily generalized to any type of rotator by employing the angular momentum commutation relations and the description of the rigid rotator system in their full generality. This enables the use of simple operator identities and state vector properties to carry the calculations as far as possible before introducing any particular coordinate representation. The simplicity of the operator and state vector properties is obscured by too early an introduction of the rotator wave functions in Euler angle coordinates in the form in which they are usually found in the literature. The formalism has been applied to the derivation of generalized differential cross sections for rotator scattering corresponding to the different regions of validity given by Zemach and Glauber, namely in the limits of high and low energy and the more general development in powers of the mass ratio.

[1] A. C. Zemach and R. J. Glauber, Phys. Rev. 101, 118, 129 (1956).

KA4. Rotational Energy Levels in Diatomic Molecular Crystals.* BARBARA J. CASTLE, *University of Maryland* (introduced by R. D. Myers).—Crystals of CO and N_2 exhibit transitions from one solid form to another at 61.6°K and

35.6°K, respectively. The prediction of these transition temperatures on the basis of classical self-consistent calculations employing the intermolecular potential has been discussed by Jansen and de Wette[1] whose results are in good agreement with experiment. The Schrödinger equation for the rotational eigenstates of the molecules in the low-temperature structures, with the inclusion of a potential which is believed to be a good representation of the crystal field, has as eigenfunctions oblate spheroidal wave functions. The separation for the lowest lying rotational energy levels is not small enough to justify the assumption of a Boltzmann distribution for the diatomic rotors below the transition point. The partition function for the rotational states has therefore been calculated quantum mechanically for the region in which the classical approximation is deemed invalid, taking two shells of neighbors about a central molecule into account, and including the effect of nuclear spin in the case of N_2. The results for the transition temperatures will be discussed.

* This work was supported by the U. S. Air Force.
[1] L. Jansen and F. W. de Wette, Physica 21, 83 (1955); de Wette, Physica 22, 644 (1956).

KA5. Interaction of Excitation Waves in a One-Dimensional Molecular Crystal.* R. E. MERRIFIELD, *E. I. du Pont de Nemours and Company.*—The interaction of two Frenkel excitons in a molecular crystal is discussed in terms of the stationary two-quantum excited states of an idealized one-dimensional crystal. If only a single molecular excited state is considered, the wave functions and energy levels of the two-quantum states may be obtained directly from those of the corresponding one-quantum problem with the proviso that the exciton be regarded as a fermion. If, in addition, a second molecular excited state is considered, there may exist states in which the two excitons remain bound to each other as they propagate through the crystal.

* Contribution No. 494.

KA6. Solid-Solid Phase Transitions and Compressibilities of CH_4, CD_4, and O_2 at Low Temperature.* JOHN W. STEWART, *University of Virginia.*—Relative volumes of samples of these solidified gases have been measured as functions of pressure and temperature by the piston displacement technique over the ranges 0–19 000 atmos and 4°K–120°K. Phase transitions appear as discontinuities either in the PV curves themselves or in their slopes. While both methanes exhibit three distinct solid phases, there are qualitative differences between the isotopes. At atmospheric pressure CH_4 shows only one of the two rotational transitions (20.4°K), whereas CD_4 shows both (22.2°K, 27.1°K). Hysteresis effects prevent unequivocal determination of the order of these transitions. Our phase diagram for CH_4 disagrees with that of Stevenson.[1] The two first-order transitions in solid oxygen have been traced to high temperature and pressure. Both have positive slopes in the PT plane. Agreement with earlier work is excellent.[2] Relative volume decreases at 19 000 atmos for CH_4 (77°K), CD_4 (77°K), and O_2 (51°K) are 0.30, 0.29, and 0.30, respectively.

* Supported by Office of Ordnance Research, U. S. Army.
[1] R. K. Stevenson, J. Chem. Phys. 27, 656 (1957).
[2] R. K. Stevenson, J. Chem. Phys. 27, 673 (1957).

KA7. Structure and Bonding in Transition-Group Intermetallic Phases.* DAVID P. SHOEMAKER, CLARA B. SHOEMAKER, AND YUKITOMO KOMURA,† *MIT.*—The crystal structures of the P phase (Mo–Ni–Cr, Pbnm, $a_0=9.070$ A, $b_0=16.983$ A, $c_0=4.752$ A, $Z=54$ atoms) and of the R phase (Mo–Co–Cr, $R\bar{3}$, $a_0=9.011$ A, $\alpha=74°\ 27.5'$, $Z=53$ atoms) have been determined. They are found to be closely related to the previously determined structures of the σ phase (e.g., Fe–Cr), the μ phase (e.g., Mo–Co), the Laves-Friauf phases, and to some extent α-manganese or the χ phase (Mo–Fe–Cr). Common features of these structures are generally tetrahedral packing, coordination polyhedra limited to four types (CN 12 = icosahedral; CN 14, 15, and 16 polyhedra with both 5- and 6-fold vertices), and "kagomé" nets. Bond radii appear to conform to the symmetries of the idealized coordination polyhedra. Splittings of atomic orbital energies in these symmetries have been examined. No splitting of s, p, or d exists in CN 12; the $3d$ level is perhaps filled. Splitting in the other coordinations corresponds roughly to the formation of strong bonds to the 2, 3, or 4 nearest neighbors, in CN 14, 15, and 16, respectively.

* Sponsored by the Office of Ordnance Research (U. S. Army).
† Present address: Osaka City University, Japan.

TUESDAY MORNING AT 10:00

Kresge Auditorium

(J. H. VAN VLECK presiding)

Invited Papers of the Division of Solid-State Physics

L1. Cross Relaxation in Spin Systems. N. BLOEMBERGEN, *Harvard University.* (30 min.)
L2. Collective Excitations in Superconductors. P. W. ANDERSON, *Bell Telephone Laboratories.* (30 min.)

TUESDAY MORNING AT 11:15

Kresge Auditorium

(G. E. UHLENBECK presiding)

1959 Oliver E. Buckley Lecture

LA1. Transport Properties of Nearly Pure Semiconductors. CONYERS HERRING, *Bell Telephone Laboratories.* (45 min.)

Business Meeting of the Division of Solid-State Physics

TUESDAY AFTERNOON AT 2:15

Kresge Auditorium

(E. BRIGHT WILSON presiding)

Symposium of the Division of Chemical Physics

(Organized in Memory of William Moffitt)

M1. Origin of Zero-Field Splittings in Triplet States of Aromatic Hydrocarbons. MARTIN GOUTERMAN AND †WILLIAM MOFFITT, *Harvard University.* (30 min.)

M2. Colors of the Transition Metal Hexafluorides. †WILLIAM MOFFITT, GORDON GOODMAN, AND MARK FRED, *Harvard University.* (30 min.)

M3. Magnetic Resonance of O and N_2 in a Clathrate Compound. HORST MEYER, *Harvard University.* (30 min.)

M4. Magnetic Susceptibility of O_2 and NO in a Clathrate Compound. J. H. VAN VLECK, *Harvard University.* (30 min.)

M5. Nonresonant Microwave Absorption in Polyatomic Molecules. E. BRIGHT WILSON, JR., *Harvard University.* (30 min.)

TUESDAY AFTERNOON AT 2:00

Room 26–100

(H. LEADERMAN presiding)

High-Polymer Physics I

N1. Dynamic Mechanical Properties of a Model Filled System: Polyisobutylene—Glass Beads. II. Behavior at Long Times. ROBERT F. LANDEL, *California Institute of Technology* (introduced by Thor L. Smith).—In Part I, the dynamic mechanical properties of three dispersions of 40-micron-diameter glass beads in NBS polyisobutylene were studied in the rubber-to-glass transition zone. These studies have now been extended to longer times—through the rubbery plateau to the region of viscous flow. The experimental method was that of tensile creep under constant load. The filler increased both the modulus and the steady-flow viscosity by the same factor. The concentration dependence of this factor is better represented by the Eilers-van Dyck equation,

$$F=\left[\frac{1+k\varphi}{1-S'\varphi}\right]^2, \qquad (1)$$

than by the Guth-Smallwood equation,

$$F=1+2.5\varphi+14.1\varphi^2, \qquad (2)$$

where φ is the volume fraction of filler, $2k$ is the Einstein viscosity constant 2.5, and $1/S'$ can be interpreted as a sedimentation volume.

N2. Stress Relaxation in Polystyrene Film. I. L. HOPKINS AND R. P. WENTZ, *Bell Telephone Laboratories* (introduced by W. P. Slichter).—A simple technique, requiring no special equipment, is presented for testing the stress relaxation of polystyrene film in flexure. The results obtained at different temperatures may be combined by the method of reduced variables to form a master curve; the activation energy for the relaxation process varies from about 50 kcal at 85°F to 80 kcal at 150°F. Brief exploratory tests show that the relaxation is highly sensitive to the amount of volatile matter in the film.

N3. Creep of a Pure-Gum Rubber Vulcanizate from −60° to +50°C. LAWRENCE A. WOOD, *National Bureau of Standards.*—Shear creep data of Leaderman on a pure-gun vulcanizate of natural rubber subjected to a constant shear stress of 0.75 kg/cm² at temperatures from −60° to +50°C covering times from 5 sec to 5 min can be represented by a single sigmoid curve. The data are subjected to two successive operations: (1) compliance values are multiplied by a factor proportional to the absolute temperature T and (2) an arbitrary amount is added to the logarithm of the time at each temperature until the revised values agree. The amount of arbitrary shift in the logarithm of the time at each temperature is in quite good agreement with that predicted by the equation of Williams, Landel, and Ferry. It has been found possible to represent the sigmoid curve by two empirical equations covering different ranges. For the higher values of equivalent time, the applicable equation predicts linearity of compliance with the logarithm of the time, with a slope of a few percent per decade, as normally observed. The 1-min compliance at 25° corresponds to a shear modulus $G=4.59$ kg/cm². The empirical representation can be used over the entire range of times and temperatures in which observations can be made without appreciable degradation and flow.

N4. Experimental Tests of Symmetry Conditions in Laminar Flow. WLADIMIR PHILIPPOFF, *The Franklin Institute* (introduced by G. P. Wachtell).—The development of deformational mechanics for large deformations has led to somewhat of a controversy over the symmetry conditions: equality or nonequality of forces in the plane normal to the direction of shear (2–3 plane). Experimental checks of this equality have been performed by Roberts and Pilpel. We have designed a capillary experiment in which polarized light is transmitted axially through a capillary. The occurrence of birefringence in the 2–3 plane during flow decides on the presence of symmetry of forces. Numerous tests on polymer solutions gave no trace of birefringence; however, vanadium pentoxide gave an effect. We further subjected bubbles and drops in a gel to a shearing motion in the 1-direction, we

found that in the 1–2 and 1–3 plane the spherical bubbles form an ellipse but, viewed in the shear direction, they remain circular. Subsequently, we used a sphere of cardboard layers and sheared it. The center plane of the ellipse remains circular, and there is a circle viewed in the 2–3 plane as well. Thus it seems that direct experiments of the symmetry of deformation in plane shear substantiates the equality of forces normal to the direction of shear in the 2–3 plane.

Invited Papers

N5. Some Recent Advances in Mathematical Rheology. R. S. RIVLIN, *Brown University.* (40 min.)

N6. Chain Stiffness and Transitions in Polymers. J. H. GIBBS, *American Viscose Corporation.* (30 min.)

TUESDAY AFTERNOON AT 2:15

Kresge Little Theater

(M. W. P. STRANDBERG presiding)

Magnetic Resonance

NA1. Noise Characteristics of Infrared Quantum Counters. N. BLOEMBERGEN, *Harvard University.*—A recent proposal for a solid-state infrared quantum (IQ) detector[1] showed that spontaneous emission noise is absent, if the device is operated at $T=0°K$. At a temperature $T \ll h\nu/k$ the equivalent Johnson noise input power in a band width $\Delta\nu$ is $N(T_2/T_1) \times \exp(-h\nu/kT)\Delta\nu$, where N is total number of ions in a detector of area A and with a thickness comparable to the optical absorption length. $(\frac{1}{2}\pi T_2)$ is the width of the infrared absorption line of frequency, T_1^{-1} is the probability for the emission of a phonon by an excited ion in the crystal. In practice the background count from the incident optical pumping flux is likely to be much higher than the fundamental Johnson noise. Fluctuations in the photomultiplier should also be referred to the input. Finally the fluctuations in the incident background radiation over the band width $(\frac{1}{2}\pi T_2)$ should be considered. The proposed IQ detector will be compared with Masers, and with photoelectric and blackbody radiation detectors.

[1] N. Bloembergen, Phys. Rev. Letters (to be published).

NA2. Extension of the Spin Hamiltonian in Paramagnetic Salts. G. F. KOSTER, *MIT*, AND H. STATZ, *Raytheon Manufacturing Company.*—In the literature on paramagnetic resonance one finds statements that the conventional spin Hamiltonian formalism is sometimes inadequate or inaccurate in describing the measured spectrum. We have reinvestigated the applicability of the spin Hamiltonian from rather general symmetry considerations. We start from the exact eigenstates of the ion in the absence of a magnetic field and include the effect of the magnetic field through the perturbation $H_1=\beta H\cdot(L+2S)$. In the resultant Hamiltonian matrix, we investigate all restrictions imposed on the matrix elements resulting from the symmetry of the lattice, from the symmetry of the wave functions, and from time inversion symmetry. In general, we find fewer restrictions than those imposed by the conventional spin Hamiltonian. A few examples will be compared explicitly. We have evaluated certain matrices which make it possible to write down any Hamiltonain matrix for any crystal symmetry and for any wave function. Work has been initiated to compare the more general theory with experiment.

NA3. Paramagnetic Resonance Spectrum of Cr^{+++} in TiO_2.* H. J. GERRITSEN, S. E. HARRISON, H. R. LEWIS, AND J. P. WITTKE, *RCA Laboratories.*—Paramagnetic resonance of Cr^{+++} in TiO_2 has been observed at X band and K band. The concentration of Cr^{+++} was 0.12 atomic percent and the half-widths of the resonance lines were narrow enough so that the hyperfine structure was easily observed. The observed fine and hyperfine spectra can be described by a spin Hamiltonian of the form

$$W=\beta g\mathbf{H}\cdot\mathbf{S}+D[S_z^2-\tfrac{1}{3}S(S+1)]+E(S_x^2-S_y^2)+A\mathbf{I}\cdot\mathbf{S},$$

with $g=1.97$, $D=0.55$ cm^{-1}, $E=0.27$ cm^{-1}, and $A=0.0015$ cm^{-1}. Both g and A are isotropic. The spin lattice relaxation times are found to be $1.5\times10^{-2}-3.0\times10^{-2}$ sec at 4.2°K.

* Partially supported by the Signal Corps.

NA4. Approach to Spin Temperature Equilibrium in a Quadrupolar Solid.* WALTER I. GOLDBURG, *Carnegie Institute of Technology.*—A single crystal of $NaNO_3$ is oriented in an external magnetic field at an angle (θ_1) for which the quadrupole splitting is large. With radio-frequency radiation a pair of Zeeman levels of the sodium spin system $(J=\frac{3}{2})$ is saturated. Then the crystal is quickly rotated to an angle where the inequality of the level spacings is a minimum (approximately $\frac{1}{3}$ the line width) and where spin mixing can take place. The crystal is then quickly returned to θ_1 where, by nuclear resonance pulse techniques, the populations of the four sodium levels can be determined. This sequence of operations is completed in a time short compared to T_1. When the $m=\pm\frac{1}{2}$ levels are initially saturated, the spin system rapidly comes to the expected spin temperature $T_S=10/9$ the lattice temperature. When the outer satellites are saturated, however, the resulting equilibrium populations of the levels are not those of a Boltzmann distribution. Also measured was the rate of approach of the spin system to equilibrium for various larger splittings. For splittings of the order of the line width an unexpected plateau appears in the spin mixing rate. A qualitative discussion of the experimental results will be given.

* Supported in part by the National Science Foundation.

NA5. Analysis of Paramagnetic Resonance Absorption in Irradiated Molecular Crystals.* P. E. WIGEN, J. A. COWEN, AND PAUL M. PARKER, *Michigan State University.*—The paramagnetic resonance spectrum in irradiated hydrated molecular crystals of the form $XSO_4\cdot nH_2O$ in general arises from the breaking of a covalent bond in the SO_4^{-2} group. It appears that normally the center is created in the neighborhood of the sulfate oxygen which is hydrogen bonded to the water molecule; thus all spectra which have been observed exhibit hyperfine structure due to the neighboring protons as well as a g-factor variation due to local crystalline fields. For

the case $S=\frac{1}{2}$ and $I=\frac{1}{2}$ or 1, a Hamiltonian of the form

$$\mathcal{H}=\beta_e S\cdot g^0 H+\hbar^2\gamma_e\gamma_n I_e S_e\left[\frac{16\pi}{3}|\psi(0)|^2+2\langle r^{-3}\rangle(3\cos^2\vartheta-1)\right],$$

has been applied to obtain the principal values and axes of the g tensor as well as position of the paramagnetic electron with respect to the proton. In general the principal axes of the g tensor and the hfs interaction are oriented differently in the crystal so that it is necessary to choose the coordinate axes for the hfs interaction and then diagonalize the g tensor obtained in this system to obtain the principal values and axes.

* Supported by a grant from the National Science Foundation.

NA6. Calculation of Cross-Relaxation Times in Spin Systems. PETER S. PERSHAN,* *Harvard University.*—Several workers[1,2] have observed that two spins with different magnetic resonance frequencies can exchange energy if their frequencies are sufficiently close together. Using conventional perturbation theory, expressions are derived that predict the rate of transfer of energy, described by the cross-relaxation time T_{21}. It is shown that the simplest mechanism for exchange, where two spins make opposite flips, is not always the most probable, and sometimes one must consider processes involving more than two spins. In order to obtain numerical results, certain simplifying assumptions are made as to the form of the frequency distribution function that appears in the expression for T_{21}; the more rigorous procedure is exceedingly lengthy and will only be outlined. The results are in reasonable agreement with experimental data. It is interesting to note that the calculation predicts T_{21} should vary with crystal orientation.

* National Science Foundation Predoctoral Fellow.
[1] A. Abragam and W. G. Proctor, Phys. Rev. **109**, 1441 (1958).
[2] Robert T. Schumacher, Phys. Rev. **112**, 837 (1958).

NA7. Effects of Pressure on Proton Spin-Lattice Relaxation in Several Organic Liquids.* A. W. NOLLE AND P. P. MAHENDROO, *The University of Texas.*—The spin-lattice relaxation time, T_1, is measured in a field of 6800 oe, in the pressure range one to 1400 atmos. Various temperatures are used from -10 to 50°C. The concentration of gaseous paramagnetic impurities in the samples is sufficiently reduced, by repeated freezing and pumping, and by the addition of magnesium filings, that paramagnetic contributions to relaxation are not dominant. The liquids studied are methyl iodide, toluene, benzene, *n*-heptane, chloroform, 1,1,1-trichloroethane, and cyclohexane (the latter being a solid in part of the experimental range). Comparison with earlier results by Benedek shows that T_1 may become much more pressure dependent when paramagnetic impurities are removed, but that the pressure dependence of $1/T_1$ still fails to follow that of the viscosity. An exception occurs for chloroform, which was not studied earlier, where relaxation is necessarily intermolecular, and $1/T_1$ follows the viscosity.

* Supported by the Office of Naval Research.

NA8. Nuclear Magnetic Resonance in Beta Brass. P. L. SAGALYN AND J. A. HOFMANN, *Ordnance Materials Research Office.*—We have observed the nuclear magnetic resonances of Cu^{63} and Cu^{65} in beta brass. Absorption signals were obtained at room temperature with a Numar spectrometer. A preliminary value for the Knight shift in beta brass is 0.15% for both isotopes, as compared with 0.23% in pure copper. The line width in beta brass is about 3 gauss, measured between points of maximum amplitude on the derivative curve, as compared with 6 gauss in pure copper. The integrated intensity in beta brass is strongly dependent on heat treatment. The maximum integrated intensity per copper atom obtained at writing is about one-half that found in pure copper. Measurements of the effects of composition and temperature are in progress.

NA9. Nuclear Magnetic Resonances in Sodium Tungsten Bronzes. R. G. BARNES, R. A. HULTSCH, AND W. H. JONES, JR., *Iowa State College.**—The nonstoichiometric sodium tungsten bronzes, Na_xWO_3, having the cubic perovskite structure for x values in the range $0.3<x<1.0$, are known to be good metallic conductors.[1,2] Various researches have shown the electrical conductivity[1,2] and paramagnetic susceptibility[3] to be consistent with a free electron model in which each sodium atom contributes one electron. We find that the Na^{23} nuclear magnetic resonance shows essentially zero Knight shift (-0.003 ± 0.003%) for x values of 0.56, 0.65, 0.73, 0.75, 0.78, 0.81, and 0.89. A rough determination of the spin lattice relaxation time T_1 shows it to be large, consistent with the negligible Knight shift. These results may be interpreted as signifying that the conduction electron wave function vanishes at the sodium positions. This could be the case if the wave function were a 5*s* or 6*s* function centered on the tungsten atom at the center of the crystalline unit cell so that a radial node in the function occurs at the sodium positions.

* Work performed in the Ames Laboratory of the U. S. Atomic Energy Commission.
[1] B. W. Brown and E. Banks, Phys. Rev. **84**, 609 (1951).
[2] W. R. Gardner and G. C. Danielson, Phys. Rev. **93**, 46 (1954).
[3] F. Kupka and M. J. Sienko, J. Chem. Phys. **18**, 1296 (1950).

NA10. Nuclear Magnetic Resonance in Alkali Metal Alloys.* L. RIMAI† AND N. BLOEMBERGEN, *Harvard University.*—The Na^{23} and Rb^{87} resonances in Na-K and Na-Rb systems have been observed. The solid solubility is small, but the components are completely miscible in the liquid phase. The Knight shifts in the liquid phases are linear functions of the relative concentration. Let K_0 be the Knight shift in the pure metal, K in the alloy with a solute concentration c. The value of $K_0^{-1}(\delta K/\delta c)$ is $+0.30$ for Na in NaK, $+0.51$ for Na in NaRb, and -0.27 for Rb^{87} in NaRb. These results agree rather well with recent theories.[1] The line width of Na^{23} increases on alloying, whereas the Rb^{87} line width decreases with increasing c. Saturation data indicate that T_1 is proportional to T_2. The change in T_1 calculated from the Korringa relation is much smaller than the observed change. The results can be explained if the effect of the spin-exchange interactions $A\mathbf{I}(\mathrm{Na})\cdot\mathbf{I}(\mathrm{Rb})$ and $A'\mathbf{I}(\mathrm{Rb}^{85})$. $\mathbf{I}(\mathrm{Rb}^{87})$ on T_1 and T_2 is taken into account.

* Supported by a Joint Services contract.
† Union Carbide and Carbon Predoctoral Fellow.
[1] Blandin, Daniel, and Friedel, Phil. Mag. (to be published).

NA11. Nuclear Magnetic Resonance in $KMnF_3$. R. G. SHULMAN, K. KNOX, AND B. J. WYLUDA, *Bell Telephone Laboratories.*—The F^{19} nuclear magnetic resonance has been measured in single crystals of $KMnF_3$. At arbitrary orientations of the external magnetic field three separate F^{19} resonances are observed as is expected. For the particular case of $[111]\|H_0$ only one resonance line is observed as predicted from the cubic perovskite structure. From the angular dependence of the resonance frequency in the (110) plane as measured at 90°K and 16 Mc/sec the isotropic, A_s, and the anisotropic, A_σ, parts of the hyperfine interaction are calculated. These are $A_s=15.5\pm0.5\times10^{-4}$ cm^{-1} and $A_\sigma=1.27\pm0.13\times10^{-4}$ cm^{-1} for each antibonding electron. From these values the character of the antibonding electron can be calculated[1] to be (0.48 ± 0.02)% 2*s* and (1.32 ± 0.2)% 2*p*. The relation between the antibonding electrons and those in the bonding orbitals will be discussed in terms of orthogonalized molecular orbitals. At 88.3°K the resonance pattern changes character. The results are consistent with an antiferromagnetic transition at this temperature where the two Mn^{++} ions adjacent to each fluoride site have their spins aligned antiparallel.

[1] R. G. Shulman and V. Jaccarino, Phys. Rev. **108**, 1219 (1957).

NA12. Absorption Spectra of MnF_2 and $KMnF_3$. H. J. HROSTOWSKI AND R. H. KAISER, *Bell Telephone Laboratories.*—The visible and ultraviolet absorption spectra of single crystals of MnF_2 and $KMnF_3$ have been obtained at temperatures between 300 and 4.2°K. Although the symmetry of the Mn^{++} sites is O_h in $KMnF_3$ and V_h in MnF_2, the spectra at 300°K are very similar. Eight bands were observed at approximately 19.2, 23.1, 25.2, 28.2, 30.1, 32.8, 38.5, and 41.3×10^3 cm^{-1}. These results indicate that the energy level splittings in the crystal field are only slightly influenced by the different environments of the Mn^{++} ion in the two materials. The value of Dq determined from the energy level diagram of Orgel[1] is 830 cm^{-1}. At lower temperatures fine structure is resolved in most of the bands. The separation of absorptions within a band is of the order of 100 cm^{-1} at 4.2°K. The similarity of the absorption patterns of different bands suggests that the fine structure can be attributed to vibrational-electronic transitions.

[1] L. E. Orgel, J. Chem. Phys. **23**, 1004 (1955).

NA13. Infrared Absorption from $L\cdot S$ Splittings in Co^{2+} Salts. R. NEWMAN AND R. M. CHRENKO, *General Electric Research Laboratory.*—A line absorption spectrum is observed in the 0.09- to 0.16-ev region in $CoCl_2$, $CoBr_2$, and CoO. The isomorphic Mn^{2+} and Ni^{2+} salts are transparent in this range. At 300°K lines are found at 0.147 and 0.114 ev for $CoCl_2$ and 0.140 and 0.105 ev for $CoBr_2$. In each case the higher energy line is more intense. The intensity of the lower energy lines is strongly temperature dependent, decreasing with decreasing temperature. This dependence suggests that the lower energy lines result from transitions involving thermally excited initial states 0.03–0.04 ev above the ground states. For the halides, the crystal field is trigonal. However, the observed frequencies are approximately those calculated for the spin-orbit splitting of the lowest orbital state of a Co^{2+} ion in a cubic field.[1,2] For both halides there is a sharp temperature independent line at 0.09 ev which may result from non cubic terms. In cubic CoO a single broad line is found at 0.156 ev just above the onset of the lattice vibration absorption.

[1] A. Abragam and H. M. L. Pryce, Proc. Roy. Soc. (London) **A206**, 173 (1951).
[2] W. Low, Phys. Rev. **109**, 256 (1958).

TUESDAY AFTERNOON AT 2:15

Room 6–120

(R. W. MORSE presiding)

Invited Paper

O1. Magnetic-Field Dependence of Ultrasonic Attenuation by Electrons. MORRELL H. COHEN, *University of Chicago.* (30 min.)

Electronic Properties of Metals

O2. Oscillatory Magneto-Acoustic Effect in Metals. T. KJELDAAS, JR., AND T. HOLSTEIN, *Westinghouse Research Laboratories.*—The effect of a static magnetic field on ultrasonic attenuation in metals has been computed for the case in which the field is perpendicular to both the propagation and polarization directions, the latter being either parallel (Case I) or perpendicular (Case II) to each other. The treatment, like that of Rodriguez[1] is based on the free-electron model. The attenuation is given in terms of conductivity coefficients, σ_{ij}, relating the internal electron current to the ultrasonic deformation field. The expressions for the σ_{ij} involve Anger-Weber functions; their series expressions are identical with those of Rodriguez. Nevertheless, our conclusions differ in that substantial oscillations in the attenuation *vs* field curve are found for both cases, particularly when the electron mean-free path is large compared to the wavelength. The oscillations are of the general type suggested by Pippard[2]; however, their detailed shape is not in accord with his predictions. The limiting behavior at high fields is also in disagreement with Rodriguez; in particular, it is found that for Case II, the attenuation goes to zero $\sim 1/H^3$.

[1] S. Rodriguez, Phys. Rev. **112**, 80 (1958).
[2] A. B. Pippard, Phil. Mag. **2**, 1147 (1957).

O3. Magnetic Oscillations of Ultrasonic Attenuation in Copper. J. D. GAVENDA AND R. W. MORSE, *Brown University.*—The magnetic field dependence of ultrasonic attenuation has been measured in a single crystal of copper where the condition $kl>1$ is amply satisfied at liquid helium temperatures (k being the ultrasonic propagation constant and l the electron mean free path). At frequencies around 70 Mc/sec several distinct maxima and minima in attenuation are found, the oscillations being in H^{-1}. With a longitudinal wave propagated along the (0,0,1) direction and H directed perpendicularly, pronounced anisotropic effects are found as H is rotated about the (0,0,1) direction. These presumably reflect anisotropy of the Fermi surface. When H is along (1,0,0) or (0,1,0) well-defined oscillations are found, which, however, are largely suppressed for H along a 45° direction such as (1,1,0). This suppression is probably a result of the Fermi surface touching the zone boundaries in the (1,1,1) direction as suggested by Pippard.[1] The period of the oscillations should be related directly to the Fermi momentum and reasonable values are found using a simple model. Shear waves show a pronounced phase change of the oscillations as H is rotated with respect to the direction of polarization, the effect being similar to that previously observed in a polycrystal.[2]

[1] A. B. Pippard, Trans. Roy. Soc. (London) **A250**, 325 (1957).
[2] Morse, Bohm, and Gavenda, Phys. Rev. **109**, 1394 (1958).

O4. Magnetic Dependence of Ultrasonic Attenuation in Tin. T. OLSEN AND R. W. MORSE, *Brown University.*—The ultrasonic attenuation due to electron interaction has been measured as a function of magnetic field in single crystals of tin where the electron mean free path is much longer than the wavelength at liquid helium temperatures. Frequencies around 50 Mc/sec give pronounced oscillations from which several periods (periodic in H^{-1}) can be distinguished. These oscillations are highly anisotropic and should be related directly to the Fermi momentum. Another anisotropic effect occurs

at fields of several kilogauss.[1] For some cases we find a general decrease in the attenuation with increasing field as would be expected from a simple theoretical model. However, for several orientations of the field the attenuation increases rapidly and levels off at a value higher than the one at zero field. It is felt that this anomalous increase with H may be related to the occurrence of open orbits for certain directions; i.e., the Fermi surface touches the zone boundaries in such a way that increasing H does not lead to localization of these electrons. An attempt will be made to deduce features of the Fermi surface of tin from these results.

[1] Morse, Bohm, and Gavenda, Bull. Am. Phys. Soc. Ser. II, 3, 44 (1958).

O5. Oscillatory Dependence of Temperature with Magnetic Field in Bismuth. J. E. KUNZLER AND W. S. BOYLE, *Bell Telephone Laboratories.*—Temperature oscillations in a thermally isolated single crystal of bismuth have been observed when the sample was rotated in a constant magnetic field or when the field was fixed along a particular crystal direction and the magnitude of the field was varied. At 1.5°K the maximum temperature changes were a few thousandths of a degree and differences of about 10^{-5} degree were observable by using a carbon resistor as the thermal sensing element and an amplifier-recorder combination to observe the resistance variations. In these preliminary observations, it has been convenient to observe the angular dependence at a series of fixed fields and it is found that the polar plots have a number of features that are reproduced periodically in $1/H$. From these data the cyclotron effective masses along principal crystal directions can be obtained in terms of the Fermi energy. These oscillations are similar in nature to the de Haas-van Alphen oscillations but the method of observation appears to be much simpler.

O6. Mean Free Path of Carriers in Bismuth at 4.2°K. A. N. FRIEDMAN, J. J. HALL, AND S. H. KOENIG, *IBM Watson Laboratory.*—The mean free path of carriers in bismuth has been an object of much speculation. The cyclotron resonance work of Aubry and Chambers[1] and Dexter and Lax[2] at 4.2°K leads to an estimate of the mean free path of electrons of ~0.01 mm and a mean free path of holes of ~0.1 mm. More recently Reneker[3] in his ultrasonic attenuation experiments observed a magneto-acoustic resonance at 12 Mc which indicated a mean free path of the carriers involved of 0.6 mm. Preliminary results have been obtained in an experiment measuring the dc resistivity of single crystal Bismuth rods as a function of diameter using a 4 contact method of measurement and repeated etching. These measurements indicate (using Sondheimer's calculations of the size effect[4] and making no corrections for anisotropic effective mass) a mean free path at 4.2°K, at least of the order of 0.5 mm. It is not certain whether this mean free path corresponds to electrons or holes. Future Hall effect measurements should determine this. Measurements at 77°K show no size effects down to 0.3-mm diam crystals.

[1] Aubry and Chambers, J. Phys. Chem. Solids 3, 128–132 (1957).
[2] R. N. Dexter and B. Lax, Phys. Rev. 100, 1216–1218 (1955).
[3] D. H. Reneker, Phys. Rev. Letters 1, 440–442 (1958).
[4] E. H. Sondheimer, Advances in Phys. 1, 13 (1952).

O7. Seebeck Coefficient of Single Crystals of Bismuth. B. S. CHANDRASEKHAR, *Westinghouse Research Laboratories.*—The Seebeck coefficient S was measured as a function of orientation and temperature, up to the melting point, for single crystals of 99.999% pure bismuth. The values of $S_{\parallel}$ and $S_{\perp}$, parallel and perpendicular to the trigonal axis, were computed from these data using Kohler's formula. The results indicate that the pronounced maximum, just above room temperature, in the S *versus* T curve for polycrystalline bismuth observed by T. Sato cannot be due to the difference in the temperature dependences of $S_{\parallel}$ and $S_{\perp}$. Using the results of Abeles and Meiboom on the mobilities and concentrations of the current carriers, the separate contributions to S from the holes and the electrons are obtained. From these the average effective masses of the carriers are calculated, and compared with the results of cyclotron resonance measurements by Aubrey and Chambers, and Brailsford and Galt.

O8. Least-Square Analysis of de Haas-van Alphen Data. J. W. MCCLURE AND L. B. SMITH, *National Carbon Research Laboratories.**—Valuable information about the conduction electrons in solids in provided by the de Haas-van Alphen effect and by other magneto-oscillatory effects. The information is contained in the parameters of the experimental curves, such as periods of oscillations and damping rates. When more than one type of carrier is present, the process of obtaining the values of the parameters is difficult and tedious. The IBM-704 computer has been programed to fit the experimental curves by the method of least squares, and thereby to determine the best values of the parameters. Two types of carriers can be handled, each represented by a fundamental and a second harmonic term. The period of oscillation and the mass of each carrier, and the amplitude and phase of each term are varied independently to achieve the best fit. Results are presented for the magnetic susceptibility of graphite,[1,2] where masses of 0.038 m_0 and 0.057 m_0 are found for electrons and holes, respectively.

* National Carbon Company.
[1] D. Shoenberg, Phil. Trans. Roy. Soc. London 245, 1 (1952).
[2] T. G. Berlincourt and M. C. Steele, Phys. Rev. 98, 956 (1955).

O9. c-Axis Magnetoresistance of Graphite Crystals.* MANUEL A. KANTER AND WILLIAM PRIMAK, *Argonne National Laboratory.*—The resistivity along the c axis of graphite crystals has been measured as a function of magnetic field strength and orientation in the magnetic field from 500–10 000 gauss at 4°K, 78°K, and 300°K. The transverse magnetoresistance was found to have a normal dependence on magnetic field, i.e., $\Delta\rho/\rho = aH^n$ where n ranges from 1.6 to 2.0 for the various crystals. The longitudinal effect exhibited an "anomalous" dependence on magnetic field similar to that reported for antimony,[1] bismuth,[2] and InSb,[3] i.e., the longitudinal magnetoresistance exhibited a maximum which shifts to lower magnetic field as the temperature is lowered. Negative values were observed at the higher fields. Measurements in magnetic fields up to 22 000 gauss will be given. The "anomalous" effect in the longitudinal magnetoresistance will be discussed.

* Work performed under the auspices of the U. S. Atomic Energy Commission.
[1] M. C. Steele, Phys. Rev. 97, 1720 (1955).
[2] J. Babiskin, Phys. Rev. 107, 981–992 (1957).
[3] H. P. R. Frederikse and W. R. Hosler, Phys. Rev. 108, 1136–1151 (1957).

O10. Effect of Absorbed Hydrogen on the Low-Temperature Electrical Resistivity of Palladium and Palladium-Nickel Alloys. A. I. SCHINDLER AND R. J. SMITH, *U. S. Naval Research Laboratory.*—Palladium is well known for its ability to absorb interstitially large amounts of hydrogen. In order to explain magnetic susceptibility data of this system Mott[1] has proposed that the dissolved hydrogen atoms are completely ionized, and their electrons are used to fill states in the d band. The filling of the d band should result in not only a change in the electrical resistivity but also in $d\rho/dT$, the variation of the resistivity with temperature. In order to test this hypothesis, electrical resistivity measurements were made between 4.2°K and 240°K on palladium and two palladium rich nickel-palladium alloys which had been electrolytically saturated with hydrogen. As a result of this treatment the resistivity of the palladium sample was found to increase by a factor of 75 at 4.2°K. In addition a maximum at approximately 45°K and a minimum at 90°K were found in the resistivity-temperature curve. The two

hydrogen charged palladium-nickel alloys exhibited similar but less drastic variations.

[1] N. F. Mott, Proc. Phys. Soc. (London) **47**, 571 (1935).

O11. Lattice Parameters and Zone Overlap in Solid Solutions of Lead in Magnesium.* C. B. WALKER AND M. MAREZIO, *University of Chicago.*—Lattice parameters have been measured as a function of composition for solid solutions of lead in magnesium with a relative precision of 1:25 000. Both parameters vary smoothly with composition, with no sign of a break or rapid change in slope, and thus give no evidence of any onset of electron overlap across faces of the Brillouin zone, contrary to the results of Raynor. Further consideration of the various lattice parameter data in the literature for five other dilute solid solutions in magnesium suggests that in none of these particular solid solutions do the lattice parameter data give satisfactory evidence of the onset of overlap.

* Research supported partly by the Office of Ordnance Research, U. S. Army.

TUESDAY AFTERNOON AT 2:15

Room 10–250

(A. NOWICK presiding)

Invited Paper

P1. Macroscopic Flow of Impurity along Dislocations (with movies). P. GIBBS, *University of Utah.* (30 min.)

Dislocations and Other Defects

P2. Macroscopic Flow of Impurity along Dislocation.* H. B. VANFLEET, G. S. BAKER, AND P. GIBBS, *University of Utah.*—It has been suggested that impurity from the ambient may penetrate Al_2O_3 crystals along dislocation lines at room temperature, and give rise to prominent electrical effects.[1] Ag ions (*et al.*) from an evaporated film can evidently be drawn through the crystal by a charged (negative 300 v with respect to metal film) microprobe 1 μ in diam, above about 500°C.[2] The effects will be reviewed, and a motion picture presented showing the impurity emerging from dislocation termini.

* Supported by the Office of Naval Research.

[1] R. N. Tucker and P. Gibbs, J. Appl. Phys. **29**, 1374 (1958); *ibid.* **29**, 1375 (1958). See also P. Gibbs, *Kinetics of High Temperature Processes*, edited by W. D. Kingery (John Wiley and Sons, Inc., and MIT Technology Press, Cambridge), Chap. IV.

[2] Vanfleet, Baker, and Gibbs, Bull. Am. Phys. Soc. Ser. II, **3**, 359 (1958); *ibid.* **3**, 414 (1958).

P3. Dislocation Pinning by Point Defects.* A. SOSIN AND L. L. BIENVENUE, *North American Aviation.*—Young's modulus measurements have been made on annealed 99.999% polycrystalline copper foils following electron irradiation and thermal treatment. The modulus increases with electron irradiation carried out at either −190°C or 0°C, faster at the more elevated temperature. Initially the modulus rises rapidly but saturates as the electron flux is increased. If the irradiation at −190°C is interrupted somewhat before saturaion and the sample warmed, a thermally induced increase is found to occur, starting at about −80°C, which also brings the modulus to a saturated value. If the irradiation at −190°C is interrupted very early and the sample warmed, the thermally induced increase described above occurs but does not bring the modulus value up to full saturation. Continued warming results in further increases toward saturation, starting most strongly at about +80°C. If the irradiation at 0°C is interrupted and the sample warmed, the increase at +80°C is again observed. Modulus increases in all cases are presumed to be due to dislocation pinning by points defects. The thermally induced increases also require defect migration.

* This work was supported by the U. S. Atomic Energy Commission.

P4. Lattice Resistance for a Screw Dislocation with Small Burger's Vector. A. GRANATO, *University of Illinois.*—An attempt is made to separate the influence of finite strains from the atomic structure of a solid in determining the lattice resistance for a screw dislocation. This is done by restricting consideration to a unit cell of rectangular dimensions a, b, and c, where b is the Burger's vector and is small enough so that all strains are small. The atomic structure is taken into account by using the energy density of anisotropic continuum elasticity theory evaluated and summed over the lattice points. The critical shear stress σ_c is found to be $\sigma_c = (2\beta C_{44} b/a)\exp(-\pi m\beta)$, where the anisotropy constant β^2 is given by $\beta^2 = C_{55}/C_{44}$, C_{55}, and C_{44} are the elastic constants for shear waves polarized along the a and c directions, respectively, and $m = c/a$. The result shows that the anisotropy has a strong influence on the critical shear stress, and that very large critical shear stresses are possible for small strains. The appearance in the exponential of the factor β, which is in general a function of temperature, permits the possibility of a change in slip plane with temperature.

P5. Equilibrium Shape of a Dislocation under an Applied Stress in an Elastically Anisotropic Crystal. G. DE WIT AND J. S. KOEHLER, *University of Illinois.**—The differential equation of equilibrium is derived for a dislocation pinned at two points in the same glide plane in an elastically anisotropic crystal with an applied stress. It is assumed that the dependence of the dislocation energy on the geometry of the dislocation line is accounted for by using an energy per unit length E which for fixed Burger's vector is a function only of φ, the angle between the Burger's vector and the dislocation segment. A parametric solution of the differential equation is found in terms of E and its derivatives. Numerical work done for several real fcc crystals indicates that the first few terms in a Fourier expansion give a good fit to E. Using this expansion, the solution of the differential equation is plotted in such a way that only one curve is needed to obtain the equilibrium shape of the dislocation for all values of the stress. Appreciable deviation from a circle is found. In this formulation, if $E + d^2E/d\phi^2 < 0$ for some values of φ, certain straight dislocations would be unstable. This case requires more careful consideration.

* Work partially supported by the Office of Naval Research.

P6. Fine Structure of Dislocation Motion. ROBB THOMSON, *University of Illinois.*—The uniform motion of dislocations has been treated by many authors in the past with the resulting picture that a dislocation has some of the attributes of a particle with relativistic mass dilatation, etc. These theories show that the dislocation has little interaction with a radiation field and contributes little to sound scattering, etc., until the velocity of the dislocation approaches the velocity of sound. On the other hand, when it is remembered that the dislocation is not in a real continuum, but that specific core effects due to the discrete crystal structure are present, some of the results of the continuum theory must be modified. If we imagine a dislocation moving through the crystal with a certain average velocity v as the core moves over the Peierls valleys of the crystal, the real motion of the core is rather more like that of a roller coaster than a uniformly moving particle. Some consequencies of this motion fine structure on the mobility of a thermally fluctuating dislocation under an external stress will be presented.

P7. Dislocations in Two Types of CdS Crystals. D. C. REYNOLDS, *Aeronautical Research Laboratory,* AND S. J. CZYZAK, *University of Detroit.*—CdS crystals grown in a static system are of two types depending upon position in the system where nucleation occurs. One type grows in the form of hexagonal prisms. Growth surface in this type coincide with the crystalline plane. The other type grows on a seed plate and the growth surface makes an angle with the c axis of the crystal. One method of comparing crystalline perfections is to determine the dislocation densities. This has been done using an HCl vapor etch which develops hexagonal etch pitch in the direction of the c axis. The etch is preferential in the direction of the a axis and has little effect in the direction of the c axis, unless there is some disturbance in the plane normal to the c axis. The etch, therefore, shows up the dislocations by etching down the core of the dislocation. The dislocation densities determined from etch pit studies on a number of crystals of both types vary from less than 10 per cm^2 to approximately 10^7 per cm^2. However, in the prism type growth larger number of low-angle boundaries are observed and, also, there is a greater tendency toward twinning.

P8. Interaction of interstitial Carbon and Nitrogen with Dislocations in Iron.* K. KAMBER AND C. WERT, *University of Illinois.*—An internal friction peak has long been known to exist in solid solutions of C and N in undeformed α-iron; it is found near room temperature for both C and N with a frequency of 1 cps. An extra peak, occurring around 200°C, has also previously been observed in deformed iron containing C or N. The present paper is a further study of this second peak. The peak does not develop immediately after deformation; some time is required for the interstitials to diffuse to the newly formed dislocations. This time is much longer for Fe−C alloys than for Fe−N alloys. This fact is not explained simply; a rather involved explanation is required. The peaks themselves are not stable, they disappear upon prolonged aging at moderate temperatures. They largely disappear, for example, in a few weeks at 359°C. The entire process of trapping of C and N by dislocations in iron is thus seen to be a complicated one. It appears, in particular, that internal friction measurements of this peak do not offer the possibility of determination of the binding energy.

* Supported by the Office of Ordnance Research, U. S. Army.

P9. Study of the Dislocation Distribution in Single Crystals of α Brass.* J. D. MEAKIN AND H. G. F. WILSDORF, *The Franklin Institute Laboratories* (introduced by A. E. Berkowitz).—A decoration technique capable of revealing individual dislocations in α brass has been used to study the dislocation distribution in the easy-glide range. Doped single crystals strained in tension and aged at 200°C were electro-polished and etched in a phosphoric acid solution, the dislocations being then revealed as small, crystallographic etch pits. The minimum resolvable distance between dislocations is limited by the size of the pits and is generally of the order of 500 A. The method has been used to study dislocations within the bulk of the crystal by careful sectioning and polishing after the aging treatment. In addition to the expected glide on the primary system, there is clear evidence of slip on secondary systems although all crystals were oriented for single slip. The observations furnish direction evidence of the difficulty experienced by dislocations in cutting through intersectioning systems, and these results will be discussed in the light of current theories of work hardening.

* Research supported by U. S. Air Force Office of Scientific Research.

P10. Dislocation Groups and Pile-Ups in Lightly Deformed α-Brass.* H. G. F. WILSDORF AND J. D. MEAKIN, *The Franklin Institute Laboratories* (introduced by A. E. Berkowitz).—Dislocation patterns in α-brass, as revealed by a decoration technique, exhibit the presence of discrete dislocation groups. If these groups are lying not too close to other dislocations, the spacings between dislocations are as predicted by theory. Pile-ups in heavily deformed regions show deviations from the spacings which had been expected theoretically, indicating the strong influence of neighboring groups. In addition, there is direct experimental information on the dislocation density before and after plastic deformation, the number of dislocations per group and the density of the groups. Making use of slip-line data, the average glide length of a dislocation, the average distance between groups on a single slip line, and the number of groups per line have been calculated. Possible mechanisms of dislocation pinning will be discussed.

* Research supported by U. S. Air Force Office of Scientific Research.

P11. Diffusion of Interstitial Atoms near Dislocations. D. N. BESHERS, *Columbia University.*—One of the essential features of a dislocation is that stresses exist in its vicinity. This has important consequences for internal friction observations. The well-known Snoek peak is the result of carbon jumping between several interstitial sites, the reorientation of the anisotropic stress field of the carbon resulting in a relaxing of the external stresses. The stresses near a dislocation result in a preferred position for the carbon atoms, i.e., they relax part of the carbon stress field, and thus jumping to other types of sites becomes energetically unfavorable. The result is a reduction in the contribution of such carbon atoms to the height of the internal friction peak. In particular, the damping peak observed at 220°C in cold-worked iron, which has a relaxation strength per atom nearly equal to that of the Snoek peak,[1] cannot be due to the jumping of isolated interstitial atoms near the dislocation if there is 10% strain there. An alternative mechanism for the damping peak will be suggested.

[1] Köster, Bangert, and Hahn, Arch. Eisenhüttenw. 25, 569 (1954).

P12. Work-Hardening in Sodium Chloride Crystals. B. H. KEAR, *The Franklin Institute Laboratories,* AND P. L. PRATT, *University of Birmingham, England* (introduced by C. T. Chase).—Further insight into the nature of work hardening in sodium chloride has been gained by examining the influence of a controlled distribution of dislocations on the plastic properties of crystals. It was found that following a prestrain in one system the stress required to start slip in an intersecting system was increased by $\Delta\sigma$. The value of $\Delta\sigma$ increased steadily with prestrain up to about 2%, but thereafter remained fairly constant at about 330 g/mm^2. The variations of $\Delta\sigma$ with prestrain were correlated with changes in the shape of the stress/strain curve. Slip bands in the intersecting system were

seen to grow in the direction perpendicular to the glide direction, which is evidence that screw dislocations are more reluctant to cut through a forest of intersecting dislocations than are edge dislocations. From these and other observations it is concluded that the onset of work hardening, following a period of easy glide in a primary system, is associated with the initiation of secondary slip between the primary glide lamellae. The dislocation reaction, $(a/2)[\bar{1}01]+(a/2)[0\bar{1}\bar{1}] \rightarrow (a/2)[\bar{1}\bar{1}0]$, is believed to play an important role in work hardening of sodium chloride crystals.

P13. X-Ray Investigation of Imperfections in Silicon Single-Crystals.* LEONID V. AZÁROFF, *Illinois Institute of Technology*, AND ROBERT H. BRAGG, *Armour Research Foundation*.—The determination of dislocation densities in single crystals using an extension of the Guinier-Tennevin transmission arrangement has been reported previously.[1] It since has been found that significant results can be obtained only if x-radiations having wavelengths shorter than 0.70 A are employed in such investigations. This is consistent with the earlier results of Allison and Parratt who observed that diffraction intensities from freshly cleaved calcite crystals agreed with calculations based on the ideally perfect crystal for $\lambda > 0.70$ A but not for shorter wavelengths. A possible reason for this is the dependence of extinction on wavelength. It can be shown that the geometry of the diffraction arrangement does not impose stringent restrictions on the thickness of the crystal used so that the bulk rather than the surface of a crystal can be investigated. Variations in the dislocation density from 10^6 to 10^8 cm^{-2} have been observed in regions of the same silicon crystal separated by only a few millimeters. These results are in accord with lifetime and noise measurements made on the same crystals. It has also been found that commercial x-ray tubes and diffractometers, with minor modifications, can be used to obtain quantitative results.

* This research was supported in part by the U. S. Air Force monitored by AFOSR of ARDC.

[1] L. V. Azároff and R. H. Bragg, Bull. Am. Phys. Soc. Ser. II, **3**, 111 (1958).

TUESDAY EVENING AT 7:00

MIT Faculty Club

(G. E. UHLENBECK presiding)

Banquet of the American Physical Society

After-dinner speakers to be announced.

WEDNESDAY MORNING AT 10:00

Kresge Little Theater

(D. LAZARUS presiding)

Diffusion in Metals

Q1. Diffusion of Ga, As, Cd, and Hg in Cu.* C. T. TOMIZUKA AND D. L. GARRETT, *University of Chicago*.—The diffusion of various types of impurities in single crystals of copper was studied with the standard technique of radioactive tracers and lathe sectioning. The activation energies and the frequency factors are determined over a temperature range of 700°–1040°C. The results indicate that the electronic screening does not necessarily account for the observed change in the activation energy. They also suggest that it is impossible to isolate the effect of excess electronic charge from that of the elastic strain introduced by the impurities.

* Supported in part by the Office of Scientific Research, Air Research, and Development Command.

Q2. Atomic Mobility in Body-Centered-Cubic Li-Mg Solid Solution. D. P. SERAPHIM AND A. S. NOWICK, *International Business Machines Corporation*.—Internal friction peaks were measured* for single crystal rods of Li-57 atomic % Mg oscillated in flexure and in torsion by the magnetic drive method (300 to 2000 cps). An Arrhenius plot of relaxation time provides an activation energy $H=0.93\pm0.02$ ev and a frequency factor of $10^{-15.7}$ sec. The ratio $H/KTm \approx 13$, where Tm is the solidus temperature. This ratio like that for β-brass is distinctly lower than the corresponding ratio for diffusion or for relaxation in fcc alloys. The quantity τ_0 is, however, of the same order of magnitude in all solid solutions.

* The measurements on which this work is based were made while the authors were at Yale University and were supported by the Office of Ordnance Research, U. S. Army.

Q3. Self-Diffusion in Tin Single Crystals.* E. KLOKHOLM AND J. D. MEAKIN, *The Franklin Institute Laboratories*.—The self-diffusion of tin has been measured in single crystals using a plating and sectioning technique. The diffusivity along the a axis has been shown to be about two times greater than along the c axis in marked variance with the results of P. Fensham,[1] but in general agreement with the value predicted from a vacancy model of diffusion. The activation energy of self-diffusion along both axes is of the same order as published values for high-temperature creep of tin,[2] and the results also show reasonable agreement with previous diffusion measurements of indium in tin.[3]

* Supported by the U. S. Atomic Energy Commission.

[1] P. Fensham, Australian J. Sci. Research **3A**, 91 (1950).

[2] Wiseman, Sherby, and Dorn, Trans. Am. Inst. Mech. Engrs. **204**, 57 (1957).

[3] A. Sawatzky, J. Appl. Phys. **29**, 1303 (1958).

Q4. Effect of Simultaneous Torsional Strain on Self-Diffusion in Silver.* J. B. DARBY, JR., *Argonne National*

Laboratory, C. T. TOMIZUKA, *University of Chicago*, AND R. W. BALLUFFI, *University of Illinois*.—The effect of deformation on silver self-diffusion, previously investigated for extension and compression,[1] was studied during torsion. Polycrystalline rods of high-purity silver with an initial grain size $\simeq(\frac{1}{2}$–3 mm) were plated with Ag^{110} and were simultaneously twisted and diffused in the range 790–800°C. The penetration curves were obtained by sectioning. No enhancement of diffusion was observed within the estimated experimental error in the diffusivity ($\pm 20\%$). Strain rates between 1.6×10^{-5} and 14×10^{-5} sec^{-1} and strains $\leqslant 0.5$ were employed. These results are consistent with the previous data[1] which indicate that the effects of plastic deformation are small at these relatively high temperatures. The results disagree markedly with those of Lee and Maddin[2] who report enhancements two orders of magnitude larger than the present results under comparable experimental conditions. The results will be compared with those of other workers in the field. Further work at lower temperatures is continuing.

* Supported by the U. S. Air Force Office of Scientific Research
[1] Darby, Tomizuka, and Balluffi, Bull. Am. Phys. Soc. Ser. II, 3, 124 (1958); J. Appl. Phys. (to be published).
[2] C. H. Lee and R. Maddin, J. Metals 10, 93 (1958).

Q5. Self-Diffusion of Silver and Gold in Silver-Gold Alloys.* W. C. MALLARD,† R. BASS, AND L. M. SLIFKIN, *University of North Carolina*.—Tracer diffusion measurements have been made for each component of the Ag−Au system in the concentration range 8 to 66 atomic percent Au. Five different compositions were studied over the temperature range 635 to 950°C. The activation energy and pre-exponential factor D_0 were found to decrease monotonically over the concentration range studied for the diffusion of Ag^{110}. Preliminary Au^{198} diffusion measurements and Franklin Institute data on the diffusion of Au in Ag do not indicate this simple dependence on concentration. Further studies which will clarify this dependence are now in progress and will be described.

* Supported in part by the U. S. Atomic Energy Commission.
† Now at Emory University, Atlanta, Georgia.

Q6. Marker Motion in Current-Carrying Gold Wires.* H. B. HUNTINGTON AND A. R. GRONE, *Rensselaer Polytechnic Institute*.—The motion of markers on the surface of gold wires carrying a current density of about 7×10^3 amp/cm^2 has been observed for periods of several days. Light transverse scratches were used for markers. Clear evidence for an "electron drag" effect was shown by the direction of the motion—several microns a day toward the cathode. The ends of the wires were held near room temperature in pin vises floating on mercury, whereas the temperature of the center of the wire was varied from 850 to 1000°C. In contrast to the results reported for copper, the transport number increased monotonically with temperature, apparently controlled by an activation energy close to that of self-diffusion. On the basis of a naive model a relationship has been developed between the marker velocity/current density and the product of the diffusivity and the specific resistivity of the lattice defect corresponding to the activated complex for diffusion. On the basis of our measurements the specific resistivity is about 0.5 μohm cm/percent of defects which is smaller than most of the calculated values for the specific resistivities of lattice point defects. Reasons why this experiment might be expected to give a lower limit will be discussed.

* Supported by the U. S. Atomic Energy Commission.

Q7. Annealing of Defects Resulting from Quenched-In Vacancies.* M. MESHII AND J. W. KAUFFMAN, *Northwestern University*.—Recovery of the residual electrical resistivity together with yield stress was used to study processes occurring above room temperature involving defects produced by vacancy migration. Quench hardening is very persistent below 600°C and appreciable resoftening occurs above it with a strong temperature dependent rate. The time to reach half-recovery was 9.8 hr at 612°C, 3.8 hr at 627°C, 1.2 hr at 642°C, and $\frac{1}{4}$ hr at 657°C, which gives a phenomenological activation energy of 4.7 ev. The residual resistivity due to quenching and still remaining after an hour aging at 100°C was close to $1.5\cdot10^{-9}$ ohm-cm for all specimens tested. Isochronal recovery of this resistivity is a two-step process. Two-thirds of this resistance recovered gradually with rising temperature below 600°C. On the other hand, the last one-third of this recoverable disappeared suddenly around 630°C. The estimated activation energy of resistivity recovery at lower temperature is the order of that for self-diffusion or less, but the sharp drop for the second step suggests a much higher activation process than that for the first step. The second step of resistivity recovery is accompanied by resoftening of the quench hardening, whereas the earlier recovery corresponded to no detectable resoftening.

* This research was partially supported by the Office of Naval Research.

Q8. Kinetics of Annihilation of Point Defects in High-Purity Aluminum. WARREN DESORBO AND DAVID TURNBULL, *General Electric Research Laboratory*.—The rate of annealing out of point defects (in the temperature range 273–295°K) from high-purity aluminum ($\alpha = R_{273°K}/R_{4.2°K} = 4200$) quenched from $T_Q = 550$–600°K was investigated by the resistivity method. At defect concentrations less than 1.0×10^{-6} atom fraction the annealing rates are independent of T_Q and described by a first-order rate equation. The activation energy for the process is 0.67 ± 0.06 ev which is 0.15 ev higher than that found for less pure aluminum[1] ($\alpha = 800$). This may indicate some trapping of defects by impurities. The results are interpreted on the basis of the Koehler-Seitz-Bauerle[2] dissociative mechanism.

[1] W. DeSorbo and D. Turnbull, Acta Met. (to be published).
[2] Koehler, Seitz, and Bauerle, Phys. Rev. 107, 1499 (1957).

Q9. Theoretical Evaluation of the Mechanism and Effect of Strain on Diffusion. HUBERT H. GRIMES, *National Aeronautics and Space Administration*.—Recent theoretical considerations[1] have led to an expression for the magnitude of the effect of strains on solid-state diffusion. For static strains this dependence has been found to be explicitly related to the geometry, strain, and rate of change of the potential energy with strain of a lattice containing a diffusing atom in an activated position. Utilizing the Morse potential function, this last quantity has been calculated for the sodium self-diffusion system for which an experimental estimate of this term is available for comparison and satisfactory agreement was found. In addition to determining the influence of strain on the diffusion coefficient these calculations also permit the evaluation of the activation energy for diffusion for a given transport mechanism. Comparison of this calculated energy with experimental values helps to elucidate the actual diffusion mechanism operative, which in the case of body-centered-cubic metals appears to be the vacancy mechanism.

[1] L. A. Girifalco and H. H. Grimes, National Advisory Committee for Aeronautics, Tech. Note 4408, 1958.

Q10. Bardeen-Herring Correlation Factor in Crystalline Diffusion. ALAN SCHOEN, *Convair Scientific Research Laboratory*.—Published values[1] of the Bardeen-Herring correlation factor[2] f for self-diffusion by the vacancy mechanism in cubic crystals are too small. The reduction in the tracer self-diffusion coefficient resulting from correlation is shown to be a few times smaller than these published values imply. Correct values for f may be derived by including the probability (<1) that a particular vacancy performing a random walk in a cubic crystal will visit a given lattice site more than once. Similar considerations apply to the evaluation of f for self-

diffusion by the interstitialcy mechanism. With a corrected value for f for the collinear-jump interstitialcy mechanism, the measurements of Compton and Maurer[3] of ionic conductivity and diffusion in AgCl may be brought into better agreement. The relation between correlation and the isotope effect for diffusion[4] will also be discussed on the basis of a revised treatment of f.

[1] K. Compaan and Y. Haven, Trans. Faraday Soc. **52**, 786 (1956).
[2] J. Bardeen and C. Herring, *Atom Movements* (American Society for Metals, Cleveland, 1951).
[3] W. D. Compton and R. J. Maurer, J. Phys. Chem. Solids **1**, 191 (1956).
[4] A. H. Schoen, Phys. Rev. Letters **1**, 524 (1958).

Q11. Resistivity of Cold-Worked Copper and Silver Alloys.* F. J. BLATT, L. J. CURTIS, M. GARBER, AND R. H. KROPSCHOT,† *Michigan State University.*—We have measured the resistance ratio $p=R_{4.2}/(R_{273}-R_{4.2})$ of pure copper and silver and of copper and silver alloys containing 1 atomic percent Ge, In, Sn, and Sb. The samples were severely deformed at room temperature by cold rolling. Subsequently the samples were annealed at temperatures ranging between 450°C and 850°C for periods between 8 hr and 3 hr. Samples were annealed in vacuum and also in an atmosphere of helium. In every instance annealing caused the resistance ratio of the pure samples to decrease as expected. The residual resistivities of the pure cold-worked metals were of the magnitude consistent with a dislocation density of approximately 10^{11} lines/cm^2. The residual resistivities of the dilute alloys, however, *increased* upon annealing in every instance. A tentative explanation of the anomalous behavior of the alloys will be presented.

* Supported in part by the Office of Ordnance Research, U. S. Army.
† Present address: National Bureau of Standards, Boulder.

WEDNESDAY MORNING AT 10:00

Room 10–250

(A. A. FROST presiding)

Chemical Physics: Theoretical

QA1. Resonance Interaction of Normal and Excited Atoms. R. S. MULLIKEN, *University of Chicago.*—According to King and Van Vleck,[1] the interaction energy at large distances between an atom in an S and a like atom in a P state is $+2C/R^3$; $+C/R^3$; $-C/R^3$; $-2C/R^3$, respectively, for the resulting $^1\Sigma_g^+$ and $^3\Sigma_g^+$; $^1\Pi_u$ and $^3\Pi_u$; $^1\Pi_g$ and $^3\Pi_g$; $^1\Sigma_u^+$ and $^3\Sigma_u^+$ potential curves. Here $C=\mu_{SP}^2$, μ_{SP} being the dipole moment of the $S\rightarrow P$ transition for (say) $\Delta M_L=0$. A reconsideration shows that, while these results are correct for the singlet curves (and in agreement with experimental evidence from Na_2, Cd_2, and Hg_2 spectra[1]), one must replace C by $-C$ for the triplet states in the case of a ^3S plus a ^3P atom, and by zero in the ^1S plus ^3P case (except insofar as, for $^3P_1$, spin-orbit coupling mixes ^1P into it). Thus for two H or two Na atoms one has $+2C/R^3$ for $^1\Sigma_g^+$ and $^3\Sigma_u^+$, $+C/R^3$ for $^1\Pi_u$ and $^3\Pi_g$, $-C/R^3$ for $^1\Pi_g$ and $^3\Pi_u$, $-2C/R^3$ for $^1\Sigma_u^+$ and $^3\Sigma_g^+$. For the Π states of H+H, the correct results were given by Eisenschitz and London in 1930.

[1] G. W. King and J. H. Van Vleck, Phys. Rev. **55**, 1165 (1939).

QA2. Ground-State Wave Function for the μ-Mesonic Molecule.* C. C. J. ROOTHAAN, W. KOLOS,† AND R. A. SACK,‡ *University of Chicago.*—The ground-state wave functions for μ-mesonic molecules ($pp\mu$, $pd\mu$, $dd\mu$) depends only on the interparticle distances. Accordingly, the wave functions was put forward as $\exp(-\zeta_{13}r_{12}-\zeta_{13}r_{13}-\zeta_{23}r_{23})P(r_{13},r_{13},r_{23})$, where P is a polynomial with adjustable coefficients, and ζ_{ij} are additional parameters. The best wave function of this type is determined by minimizing the energy evaluated with the full three-particle Hamiltonian. This wave function is a generalization of the Hylleraas function for He, and is expected to yield an energy of high accuracy, after sufficient experimentation with the polynomial length and ζ values. This method avoids the difficulty encountered with the Born-Oppenheimer approximation, due to the relatively large muon-proton mass ratio. The method also enables one to calculate the ground state of helium-like systems with the mass polarization included, rather than computing the latter by a perturbation method. Applications to other three-particle systems, like $e^+e^-e^-$, are being studied.

* Work supported by Wright Air Development Center, U. S. Air Force, the Office of Naval Research, and the National Science Foundation.
† On leave of absence from Institute of Physics, Polish Academy of Sciences.
‡ On leave of absence from British Rayon Research Association.

QA3. Hartree-Fock and Correlated Orbital Calculations for the Ground State of Helium-Like Systems.* A. W. WEISS AND C. C. J. ROOTHAAN, *University of Chicago.*—Ground-state wave functions of the types (1) $\varphi(r_1)\varphi(r_2)$, (2) $\varphi(r_1)\psi(r_2)+\psi(r_1)\varphi(r_2)$, (3) $\varphi(r_1)\varphi(r_2)\chi(r_{12})$, (4) $[\varphi(r_1)\psi(r_2)+\psi(r_1)\times\varphi(r_2)]\chi(r_{12})$, have been determined for helium and a number of isoelectronic ions; φ and ψ were put forward as an exponential times a polynomial, χ as a polynomial. The best values for the parameters were determined by the variation principle; this was done for many different ions, and in each case for various expansion lengths for φ, ψ, χ. The results indicate that expansion lengths of at most five terms yield the same energies, to about six figures, as those obtainable with completely flexible variational functions φ, ψ, χ. The difference between the energy calculated with the functions (1)–(4) and the exact eigenvalue is almost constant over the range $1\leqslant Z\leqslant 10$, or from H^- to Ne^{+8}, namely about 1.1, 0.8, 0.15, and 0.015 ev, respectively. Considering that this corresponds to total energies ranging from about 0.5 to 2550 ev, this is a remarkable result, which may form a basis for empirical correlation corrections in many-electron cases.

* Work assisted in part by Wright Air Development Center, U. S. Air Force, and the National Science Foundation.

QA4. New Digital Computer Program (1103A) for Computing Molecular Electronics Repulsion Integrals.* A. D. MCLEAN, *University of Chicago,* AND J. J. SINAI, *Purdue University.*—Recent work on multicenter electronic repulsion integrals involving Slater orbitals using techniques not yet

reported in the literature will be presented, including details of performance of a machine program in operation on a Scientific Univac 1103A Computer. The method involves computation of the potential of the charge distribution of the first electron as a function of the coordinates of the second electron using either the Laplace or Neumann expansion for r_{ij}^{-1}, followed by integration over the coordinates of the second electron by straightforward numerical techniques.

* Work supported in part by National Science Foundation and in part by Wright Air Development Center, U. S. Air Force.

QA5. Electronic Properties of Selected First Row Diatomic Molecules in LCAO-MO-SCF Approximation.* BERNARD J. RANSIL, *University of Chicago.*—Ground-state wave functions, total energies, and ionization potentials for selected first row diatomic molecules (LiH, BH, NH, HF; Li_2, Be_2, C_2, N_2, F_2; LiF, CO) have been computed in LCAO-MO-SCF approximation for their respective spectroscopic internuclear distances. Corresponding dipole moments and population analyses were computed. These calculations utilized inner and valence shell Slater type AO's of the atoms involved. For some calculations (LiH, HF; Li_2, F_2; LiF, CO) the wave functions are being improved by varying the orbital exponents to achieve minimum energy and/or utilizing an extended basis set, i.e., introducing supervalence shell AO's. The results to date will be discussed with the (possibly mutually exclusive) desiderata in mind: (1) accuracy of wave function—where possible comparison of the most recent available calculations and experiment will be made; (2) simplicity of mathematical form, able to lend itself to quantum-chemical interpretations; (3) computing ease and economy.

* Work supported in part by the National Science Foundation and by Wright Air Development Center, U. S. Air Force.

QA6. Hartree-Fock, Correlated Orbital, and Extended James and Coolidge Wave Functions for H_2.* W. KOLOS AND C. C. J. ROOTHAAN, *University of Chicago.*—The ground-state energy of the H_2 molecule was calculated using wave functions of the types (1) $\varphi(1)\varphi(2)$, (2) $\varphi(1)\psi(2)+\psi(1)\varphi(2)$, (3) $\varphi(1)\varphi(2)\chi(r_{12})$, (4) $[\varphi(1)\psi(2)+\psi(1)\varphi(2)]\chi(r_{12})$, and (5) an extended James and Coolidge type wave function. Simple 5-term expansions in elliptic coordinates were used for φ and ψ, and the correlation function χ was a 3-term polynomial. For the binding energy (experimental value 4.7467 ev) the following results were obtained: (1) 3.6345, (2) 3.8589, (3) 4.6955, (4) 4.7062, (5) 4.7445. This compares with Coulson's result of 3.623 for (1) and James and Coolidge's[2] result of 4.720 for (5). Computation of the potential energy curve with the extended James and Coolidge type wave function is in progress.

* This work was supported in part by the Polish Academy of Sciences and in part by the National Science Foundation and Wright Air Development Center, U. S. Air Force.

[1] C. A. Coulson, Proc. Cambridge Phil. Soc. **34**, 204 (1938).
[2] H. M. James and A. S. Coolidge, J. Chem. Phys. **1**, 825 (1933).

QA7. On the Theory of Electron Transfer Processes. R. A. MARCUS, *Polytechnic Institute of Brooklyn.*—When two species interact weakly electronically in a condensed phase, a reorganization of the atomic configuration is necessary for an electron transfer to occur between them. The system passes through a configuration lying at the intersection of two electronic energy surfaces in many-dimensional atomic configuration space. A system on one of these surfaces has the charge distribution of the initial state and on the other that of the final one. The degeneracy at the intersection is removed by the weak interaction, and an electron transfer results if the system stays on the lowest surface on moving across the intersection line. This event occurs adiabatically or nonadiabatically, depending on the extent of the interaction. In this paper, expressions are deduced for the probability of attaining configurations on the intersection line and, thereby, for the over-all rate of electron transfer. Changes in interatomic distances nearest the two transfer sites are expressed in terms of structural properties while the other part of the system is regarded as a dielectric continuum. In computing the latter, special methods are needed because of the unusual probability charge distribution in the intersection region. These methods have been presented in earlier papers of the author.

QA8. Specific Charge Fluctuation Interactions. JERROLD M. YOS AND HERBERT JEHLE, *University of Nebraska.**—It has been shown that charge fluctuation forces, in particular the London force, provide for preferential association of identical molecules as nearest neighbors if a mixture of different types of molecules is imbedded in a liquid medium. We may name this effect "specific London-van der Waals attraction." A characteristic mutual orientation of the identical nearest neighbor molecules ensues. Specific London attraction is of prime importance for understanding the association of identical molecules during crystal formation and it often determines the mutual orientation of these molecules. This effect with all its implications of mutual orientation manifests itself of course only if it is not overshadowed by other types of intermolecular interactions. In order to illustrate such overshadowing, consider e.g., situations in which altogether only London-van der Waals interactions play a role. The general London-van der Waals attraction prefers crystal structures which provide for maximum space-filling: Crystals of identical molecules are formed whose molecular orientations differ from the orientations discussed in the foregoing (which usually do not correspond to closest fitting of molecules), or crystals are formed from mixtures of molecules or atoms which fit together in a complementary fashion.

* Research supported by Research Corporation and National Cancer Institute.

QA9. Biological Implications of Charge Fluctuation Interactions. HERBERT JEHLE,* *University of Nebraska.*†—The preferential nearest neighbor association of identical molecules due to specific London-van der Waals attraction[1] is proposed to be the basic mechanism which provides for the selection of the proper sequence of filial amino acids in the formation of a filial peptide chain (protein synthesis) from information provided by a parental peptide chain (usually mounted on a nucleic acid). All the variety of filial amino acids is supplied from the surrounding medium, carried around by Brownian motion, and then retained (by the specific London force) next to those parental amino acids which are identical with the respective filial amino acids. Molecule models show the compatibility of proposed schemes with steric requirements (slides).

* On leave of absence at George Washington University.
† Research supported by the Research Corporation and National Cancer Institute.

[1] Jehle, Yos, and Bade, Phys. Rev. **110**, 793 (1958); J. M. Jos, *ibid.*, p. 800.

Business Meeting of the Division of Chemical Physics

(To be held during the session whenever the Chairman elects.)

WEDNESDAY MORNING AT 10:00

Room 4–270

(C. G. SHULL presiding)

X-Ray and Optical Properties of Metals

R1. Vacuum Soft X-Ray Spectrometer Using a Flow Proportional Counter. J. E. HOLLIDAY, *U. S. Steel Corporation.*—A soft x-ray spectrometer has been built for the study of the electronic structure of metals and alloys. The spectrometer covers a wavelength region from 40 A to 500 A. The grating is lightly ruled in glass with 30 000 lines per in. and a radius of curvature of 1 m. In order to detect radiation down to 40 A the glancing angle was set at 3°. The detector used is a thin window flow proportional counter. The proportional counter is more stable and has better discriminating properties than the copper beryllium phototube. However, the window in the proportional counter limits its usefulness to about 200 A. The spectrometer is evacuated to vacuum of 5×10^{-7}. The x-ray chamber is all metal with metal O rings and is bakeable at 400°C. The x-ray chamber is evacuated with a vacIon pump to reduce target contamination. The K emission band of carbon has been obtained with this instrument and is compared with that obtained by Chalklin.[1] The M emission band of Mo and Nb have also been obtained.

[1] F. C. Chalklin, Proc. Roy. Soc. (London) **A194**, 42 (1948).

R2. X-Ray Measurement of the Atomic Scattering Factors of Copper and Iron. BORIS W. BATTERMAN,* *Bell Telephone Laboratories.*—Present measurements on cold-worked powder specimens of iron and copper show that the ratio of atomic scattering factors of the lowest order reflections of these metals is, within experimental error, the value calculated from the free atom wave functions. Using rock salt as an external standard, the scattering factors of these reflections agree with the free atom values within an error corresponding to the contribution of approximately one free-atom-3*d* electron. From their measurements of atomic scattering factors of single crystals, Weiss and DeMarco[1] have concluded that metallic iron has 2.3 3*d* electrons compared with 6 for the free atom. These results have not been confirmed in the current work.

* Present address: IBM Research Laboratory, Poughkeepsie.
[1] R. J. Weiss and J. J. DeMarco, Revs. Modern Phys. **30**, 59 (1958).

R3. Atomic Displacements in Copper-Rich Metallic Solid Solutions. W. W. WEBB, *Union Carbide Corporation.*—Amplitudes of atomic displacements due to lattice vibrations and "size" effects in selected copper-rich solid solutions have been determined from measurements of relative integrated intensities of x-rays Bragg diffracted from randomly oriented polycrystalline samples. Experimental tests of some of the assumptions of the pertinent theory of "size" effects[1,2] substantiated its adequacy as a basis for the present measurements, but the results obtained are at variance with the predictions of models based on elasticity theory. Computation of a pseudo-Debye-Waller factor, $\exp(-2B\sin^2\theta/\lambda^2)$, from intensity measurements at 90°K and at 300°K permit the application of an appropriate lattice vibration model to separate the total rms amplitude of atomic displacements, given by the measured values of $2B$ into static ("size" effect) and dynamic (lattice vibration) contributions. Values of static and dynamic displacements and characteristic temperatures will be presented and discussed.

[1] K. Huang, Proc. Roy. Soc. (London) **A190**, 102 (1947).
[2] B. S. Borie, Acta Cryst. **10**, 89 (1957).

R4. Small Angle X-Ray Intensities from Multiple Scattering.* B. E. WARREN, *MIT.*—In powder samples containing crystals with random orientation, a relatively strong small-angle intensity is produced by multiple scattering. The intergrain contribution comes from an hkl reflection in one grain followed by the same hkl reflection in a second grain. The intragrain contribution results from an hkl reflection followed by a $\bar{h}\bar{k}\bar{l}$ reflection of the reflected beam in the same grain. The intergrain contribution is independent of grain size and falls off as $1/2\theta$. The intragrain contribution is strongly dependent on the grain size L, and is of the form $L^4\exp[-KL^2(2\theta)^2]$. For Co$K\alpha$ radiation and a copper sheet of thickness $t=1/\mu$, at a scattering angle $2\theta=1°$, the computed intensities in electron units per atom are as follows: intergrain scattering $I(eua)=26$; intragrain scattering $I(eua)=300$, 2200, 3100, 1650, 370, 45 for grain sizes $L=100$, 200, 300, 400, 500, 600 A, respectively. The effect of cold work in the sample will be discussed.

* Research sponsored by the U. S. Atomic Energy Commission.

R5. Photon Absorption by Valence Band Electrons in Aluminum.* W. M. NEUPERT, D. E. BEDO, AND D. H. TOMBOULIAN, *Cornell University.*—A normal incidence vacuum spectrograph has been modified primarily for the study of (1) secondary structures in the photon absorption by valence electrons, and (2) M emission and absorption spectra of K, Ca, and a few of the neighboring transition metals. The instrument covers the spectral region extending from 300 to 1200 A, corresponding to incident photon energies of 40 to 10 ev. The resolution at the high-energy end is better than 0.1 ev. An important feature of the design is the feasibility of producing absorbing layers directly within the chamber and keeping them essentially free from contamination during an exposure. The instrument has been used to carry out measurements on Al foils and to explore the fine structure in the absorption on the low-energy side of the $L_{2,3}$ edge. In the curve which represents the absorption of the photons by valence electrons, secondary maxima are observed at incident photon energies of 14.8, 16.8, 20.0, 23.0, 27.4, and 31.0 ev. These will be compared with data deduced from the fine structure present on the high-energy side of the $L_{2,3}$ edge and also with electron energy eigen losses.

* Supported in part by the Office of Ordnance Research, U. S. Army.

R6. Optical Constants of Aluminum.* H. MENDLOWITZ, *National Bureau of Standards.*—It will be shown that the optical constants of aluminum from the near ultraviolet (2500 A) to the near infrared (5 μ) can be described in terms of the Drude formula,

$$\epsilon(\omega)=1-\frac{\omega_p^2\tau^2}{1+\omega^2\tau^2}+i\frac{\omega_p^2\tau}{\omega(1+\omega^2\tau^2)},$$

where $\epsilon(\omega)$ is the complex dielectric constant of the material, ω_p^2 is a constant determined by the density N of free electrons, ω is the circular frequency of the electromagnetic radiation, and τ is the relaxation time. The value for N is taken to correspond to 2.2 free electrons per atom and the value for τ is taken to be 1.2×10^{-15} sec. Deviations outside the aforementioned wavelength region will be discussed. Also the validity of these parameters will be compared with those obtained from experiments for wavelengths greater than 1 μ.

* Supported in part by the U. S. Atomic Energy Commission.

R7. Surface Reflectivity of Aluminum Subjected to Shocks. M. SOLOW, N. COLEBURN, R. WILEY, S. J. JACOBS, AND B.

DRIMMER, *U. S. Naval Ordnance Laboratory.*—While investigating the application of specular surface reflection[1,2] for the study of shock phenomena in metals and liquids by the change in surface direction produced by the shock, this Laboratory discovered an anomalous change in surface reflection not explainable by change in the surface direction. When a shock wave was normally incident on a polished metal surface, changes in the light reflection still occurred. Experiments on polished aluminum specimens mounted in vacuum and in water and subjected to plane shock waves of 250 kilobars showed a sudden and permanent decrease in reflected light. This change took place in less than 10^{-8} sec which is the time resolution of the observing smear camera. The specimens, recovered after being shocked, showed small tension cracks on the free surfaces. They also exhibited an increased hardness which increased with distance from the free surfaces. The experimental investigation supports the interpretation that the discontinuous and anomalous change in surface reflectivity is due to the mechanical change of the surface. A qualitative explanation is given in terms of solid-state theory which takes into account the effect of the very strong shock forces on the grain boundaries, impurity atoms, and dislocations in the lattice structure.

[1] W. A. Allen and C. L. McCary, Rev. Sci. Instr. **24**, 165 (1953).
[2] T. P. Cotter, thesis, Cornell University (September, 1953).

R8. Optical Properties of Nickel and Their Interpretation. S. ROBERTS, *General Electric Research Laboratory.*—Optical properties of an annealed and electropolished nickel bar were measured by polarimetric methods at 88°, 298°, and 473°K. The real and imaginary components of the dielectric constant are reported in the wavelength range from 0.365 to 2.65 μ. The results may be resolved into components attributable to free electrons and bound electrons following the classical treatment by Drude.[1] More than one free electron term is indicated, but a single term accounts for most of the dc conductivity. This is the only free electron term which depends significantly on temperature. Notwithstanding a 20:1 variation in dc conductivity, the change in optical properties *versus* temperature is very small. This may be explained by the hypothesis that the conductivity due to the principal class of free electrons and their relaxation time are both proportional to the same mean free path and hence are in a constant ratio. At longer wavelengths this analysis predicts a greater temperature dependence of optical properties. When so extrapolated, the author's results agree with the experimental data of Beattie and Conn[2] and with the temperature coefficients they observed.

[1] P. Drude, *The Theory of Optics* (Longmans Green and Company, New York, 1902), p. 398.
[2] J. R. Beattie and G. K. T. Conn, Phil. Mag. **46**, 989 (1955).

Post-Deadline Papers, If Any

WEDNESDAY MORNING AT 10:00

Room 6–120

(R. M. BOZORTH presiding)

Magnetism I

RA1. Low-Temperature Remanence, Molecular Field, and Approach to Absolute Magnetic Saturation of Holmium Metal. WARREN E. HENRY, *U. S. Naval Research Laboratory.*—The molecular exchange field and product $g'J'$ have been determined for the rare earth metal, holmium, by measuring the magnetization in continuous magnetic fields up to 75 000 gauss and at temperatures 295°K, 100°K, 4.2°K, and 1.3°K. The molecular field is determined by a method used previously.[1] This permits calculation of the exchange integral from experimental data. The product, $g'J'$ (g'=effective Landé splitting factor and J'=effective inner quantum number) is only 4.0 Bohr magnetons per atom of holmium in contrast to the expected 10 Bohr magnetons per atom as deduced from spectroscopic data and inferred from measurements reported in the literature. The discrepancy between the measured saturation magnetization and the inferred gJ product may be explained on the basis of crystalline electric field splitting. The zero field magnetization is 0.22 Bohr magneton per atom at 4.2°K and 0.42 Bohr magneton per atom of holmium at 1.3°K. There is a pronounced hysteresis effect in the liquid helium range; e.g., at 10 kilogauss, the magnetization in decreasing fields is 50% higher than in increasing fields. In the liquid helium range and in the 100°K range, $(\partial^2 M/\partial H^2)_T$ is positive and changes sign.

[1] W. E. Henry, Phys. Rev. **94**, 1146 (1954).

RA2. Magnetic Form Factor of Cobalt.* R. NATHANS, *Pennsylvania State University and Brookhaven National Laboratory,* AND A. PAOLETTI, *Comitato Nazionale Ricerche Nucleari, Italy, and Brookhaven National Laboratory.*—The magnetic form factor of the face-centered-cubic phase of metallic cobalt has been determined by using a polarized neutron beam spectrometer. The ratio of reflected intensities from a magnetized single crystal is measured for neutrons polarized parallel and antiparallel to the field on the crystal, giving p_{hkl}/b_{hkl}, where p_{hkl} and b_{hkl} are the magnetic and nuclear structure factors for the (hkl) reflection. Since b_{hkl} is known, the measurement yields p_{hkl}. Of particular interest in the data is the failure of the form factor values for the higher (hkl) reflections to fall on a smooth curve, in particular the (311) and (400) reflections. These deviations may be an indication of a departure from spherical symmetry for the $3d$ electrons. The form factor of the hexagonal phase is being measured to determine whether there are any differences because of the change in symmetry, and these results will be discussed.

* This work was performed under the auspices of the U. S. Atomic Energy Commission and the National Security Agency.

RA3. Dipolar-Type Anisotropy in Cubic Ferromagnets.* F. KEFFER AND T. OGUCHI, *University of Pittsburgh.*—A reevaluation has been made of Van Vleck's[1] second-order perturbation theory of dipolar-type anisotropy in cubic ferromagnets. In the low-temperature limit of strong correlation between the direction of neighbor spins, we find an anisotropy varying as the 10th power of the magnetization. The theory is somewhat analogous to the strong-correlation theory of quadrupolar anisotropy.[2] The physical explanation seems to be that, at low temperatures, the ferromagnet may be thought of as divided into regions in which the magnetization, and hence the axis of quantization for the perturbation theory, is tilted at slight random angles with respect to the over-all sample magnetization. This picture is the same as that of Zener's classical analysis. Impetus for this work was supplied by

Kasuya and by Charap and Weiss, who challenged, correctly, a spin-wave analysis[3] which purported to show a negligible temperature variation of dipolar anisotropy. We shall discuss the relation of this new 10th-power law to the essentially correct spin-wave theories of Kasuya and of Charap and Weiss.

* Work done at the Sarah Mellon Scaife Radiation Laboratory and supported by the U. S. Air Force through the Air Force Office of Scientific Research and Development Command.
[1] J. H. Van Vleck, Phys. Rev. **52**, 1178 (1937).
[2] F. Keffer, Phys. Rev. **100**, 1692 (1958).

RA4. Magnetic Anisotropy in Thin Films. E. L. Boyd, *IBM Research Laboratory, Poughkeepsie.*—The magnetic anisotropy of thin, single-crystal films of nickel, nickel-iron, and nickel-cobalt alloys has been determined by the torque method. The films were produced epitaxially by vapor deposition onto sodium-chloride single crystals. Anisotropy constants obtained from nickel and nickel-iron films were in good agreement with previous results obtained from bulk samples,[1] K_1 and K_2 being -39×10^3 and 40×10^3 erg/cc, respectively, in pure nickel films. The magnetic anisotropy of nickel-cobalt films with up to 40% cobalt is in qualitative agreement with the results of magnetization measurements made on bulk crystals.[2] The constant K_1 increases from a negative value in pure nickel to positive values with less than 10% cobalt. Further additions gradually cause K_1 to become negative again. The effects of heat treatment and strains in the films will be discussed.

[1] R. M. Bozorth and J. G. Walker, Phys. Rev. **89**, 624 (1953).
[2] L. W. McKeehan, Phys. Rev. **51**, 136 (1937).

RA5. Anisotropy Field, Anisotropy Torque, and Their General Analytical Expressions.* Henri Amar, *The Franklin Institute Laboratories.*—A description of magnetocrystalline anisotropy by an equivalent field has been used by Kittel[1] and Bickford,[2] and later by other investigators in the analysis of ferromagnetic resonance experiments. Kittel and Bickford calculated approximate expressions for the anisotropy field for several special cases. A discussion of the concept of equivalent field is here followed by a general and rigorous derivation. Let $\mathbf{e}_r$ (direction cosines $\alpha_1\alpha_2\alpha_3$) be a unit vector parallel to the magnetization density $\mathbf{I}$ of a ferromagnetic crystal. It is shown in general that a P.E. $U(\alpha_1\alpha_2\alpha_3)$ is equivalent to a uniquely defined torque $\mathbf{T}=\text{curl}\,U=\text{grad}\,U\times\mathbf{e}_r$ acting on $\mathbf{e}_r$, $\alpha_1\alpha_2\alpha_3$ being the differentiation variables. This leads to an anisotropy field $H'=-\text{grad}\,U+\lambda\mathbf{I}$ where the arbitrary scalar function $\lambda(\alpha_1\alpha_2\alpha_3)$ may be so chosen as to make the vectors $\mathbf{I}$, $\mathbf{H}'$, $\mathbf{T}$ mutually perpendicular. Besides their relevance to the analysis of ferromagnetic resonance experiments, these results may be applied to the calculation of the magnetization curve of single domain uniaxial or cubic crystals.

* This research was supported in whole by the U. S. Air Force monitored by the Air Force Office of Scientific Research and Development Command.
[1] C. Kittel, Phys. Rev. **73**, 155 (1948).
[2] L. R. Bickford, Phys. Rev. **78**, 449 (1950).

RA6. Pseudodipolar Anisotropy in Cubic Ferromagnets at Low Temperatures.* S. H. Charap† and P. R. Weiss, *Rutgers University.*—Previous calculations of K_1 using pseudodipolar coupling (spin $\frac{1}{2}$ per atom) are improved by a proper treatment of the exchange based on Dyson's[1] spin waves. Dipolar terms of the form $S^zS^\pm$ give rise to the entire low-temperature variation of K_1 from its ground-state value K_{10}. It turns out that $K_1\sim[M(T)]^8$ in this treatment as well as in a less rigorous calculation.[2] The important terms in the Van Peipe[3] ground-state expansion are examined and an approximate wave function is found to be the convergent form $\exp[\sum_{i,\Delta} S^-_{R_i}S^-_{R_i+\Delta}]\psi_0$, where ψ_0 is the state of complete alignment and $S^-_{R_i}$ reverses the spin located at $\mathbf{R}_i$. The value of K_{10} obtained by use of the first two terms of the expansion of this function (Van Peipe's wave function) is in agreement with that calculated by spin wave methods.

* Supported in part by Rutgers Research Council, the Office of Naval Research, and Radio Corporation of America.
† Present address: International Business Machines Research Laboratory.
[1] F. J. Dyson, Phys. Rev. **102**, 1217 (1956).
[2] T. Kasuya, J. Phys. Soc. Japan **11**, 944 (1956). There is an error of a factor on 2 in K_{10} in this paper.
[3] W. F. Van Peipe, Physica **5**, 465 (1938); P. Argyres and C. Kittel, Acta Met. **1**, 241 (1953).

RA7. (Abstract withdrawn).

RA8. Observation of Ferrimagnetic Resonance in YIG as a Function of Large Hydrostatic Pressure.* I. P. Kaminow,† William Paul, and R. V. Jones, *Harvard University.*—Recently it has been shown that the magnetocrystalline anisotropy of ferromagnetic insulators can be attributed to the crystalline electric field at the magnetic ion. The application of hydrostatic pressure to a cubic crystal reduces the lattice constant without destroying the symmetry. In this way, it is expected that one can vary the crystalline field parameters and, consequently, the cubic anisotropy. Ferrimagnetic resonance experiments on yttrium iron garnet indicate that K_1/M_s increases approximately 30%, K_2/M_s decreases 90%, and g_{eff} increases 1% at a pressure of 10 000 atmos. These changes are nonlinear functions of pressure with the largest change occurring below 2000 atmos. Bridgman's data for similar oxide crystals (mineral garnet and magnetite) indicate a volume reduction of 0.6% in 10 000 atmos with only small deviations from linearity. The mechanism for these large pressure shifts is not understood. In fact, the magnitude of the cubic field "a" term for ions in S states (such as Fe^{3+}) is itself a mystery. In addition, to a variation in the crystalline field with pressure, the shift could be associated with changes of spin-orbit coupling, exchange interaction, or ionic arrangement in the unit cell.

* Research supported by the U. S. Air Force.
† Bell Telephone Laboratories Communications Development Training Program Fellow.

RA9. Ferromagnetic Resonance in GdIG at High-Power Levels.* J. J. Green, *Harvard University* (introduced by R. V. Jones).—The nonlinear effects of ferromagnetic resonance were observed in single crystal GdIG at 77°K and 195°K as a function of crystallographic orientation. The interpretation of these effects is based on the Suhl-Anderson[1] theory and leads to an anisotropy in the spin wave line width ΔH_k, which is similar to the observed anisotropy in the uniform precession line width ΔH and the threshold field h_{crit}. In the hard direction [100], which has the narrowest line width and lowest threshold field, it is possible to observe a subsidiary absorption

which occurs at a power level in good agreement with the theory. Further instabilities appear in the resonance absorption above the initial threshold. Those appear as discontinuities in the slope of the curve of χ_{max}'' *versus* h_{rf}. The ratio of the rf field required for each higher instability to the initial threshold field h_{crit} appears to be a constant independent of crystal orientation and is in agreement with the constant found in similar observations on single crystal YIG.

* Research supported by a U. S. Air Force contract.
[1] H. Suhl, Phys. and Chem. Solids 1, 209 (1957).

RA10. Resonance Experiments on Polycrystalline Ferrites Using Circularly Polarized Radiation. J. RENÉ ZEENDER AND ERNST SCHLÖMANN, *Raytheon Manufacturing Company.*—If the saturation magnetization is much smaller than the anisotropy field the individual grains behave approximately independently. The structure of the absorption line is then primarily determined by the spreading of the resonance frequencies of individual grains caused by crystalline anisotropy. Absorption lines with several peaks and shoulders are observed under these conditions.[1] The peaks associated with grains, for which the free precession of the magnetization vector follows an ellipsoidal cone ([110] for cubic crystals), should be partially excited by both senses of circular polarization. The peaks associated with grains, for which the free precession follows a circular cone ([100] and [111] for cubic crystals), should be excited only by one sense of circularly polarized radiation. Experiments at x-band on various nickel-ferrite aluminates are in agreement with the theoretical predictions. They show that the secondary absorption peak is not due to the excitation of the exchange mode. The agreement between theory and experiment is rather poor in the case of various hexagonal compounds (Mg_3Y, Mg_2Z, and MgZnY). For these compounds the neglect of dipolar interaction, which is a basic approximation of the theory, is not well justified.

[1] E. Schlömann and J. R. Zeender, J. Appl. Phys. **29**, 341 (1958).

RA11. Neutron Scattering by Ferrimagnetic Spin Waves.* T. A. KAPLAN, *The Pennsylvania State University and Brookhaven National Laboratory.*—A calculation of the cross section for the scattering of neutrons by spin waves in a normal spinel has been made, based on previous results.[1] The formula for the acoustic mode ($\omega \to 0$ as $q \to 0$, ω and q the magnon frequency and propagation vector), with q small, disagrees with the previously published result.[2] The order of the singularlty occurring at $q=0$ is different in the antiferromagnetic limit. The singularity will be discussed in terms of the physical basis, given by Anderson,[3] for the amplitude divergence occurring in antiferromagnets. The agreement of our formula with experiment has been pointed out.[4,5] The results for the optical modes show that these should be observable with present intensities. Such experiments determining the optical as well as the acoustic frequencies should provide a quite direct measurement of the various exchange parameters.

* Work performed under the auspices of the U. S. Atomic Energy Commission and the National Security Agency.
[1] T. A. Kaplan, Phys. Rev. **109**, 782 (1958).
[2] B. N. Brockhouse, Phys. Rev. **106**, 859 (1957).
[3] P. W. Anderson, Phys. Rev. **86**, 694 (1952).
[4] B. N. Brockhouse, Phys. Rev. **111**, 1273 (1958).
[5] Riste, Blinowski, and Janik, J. Phys. Chem. Solids (to be published).

RA12. Magnetic Structure of Hausmannite, Mn_3O_4. J. S. KASPER, *General Electric Research Laboratory* (introduced by I. S. Jacobs).—The magnetic structure, as well as the crystal structure, of Mn_3O_4 has been determined by neutron diffraction studies on polycrystalline material at 4.2, 77, and 298°K. Above the ferrimagnetic transition temperature of 43°K, the unit cell is body-centered tetragonal, space group I^4/amd, with $a_0=5.75$ A°, $c_0=9.42$ A° as described in the literature. It is found, however, that the oxygen parameters are significantly different from the reported ideal values. As a result, the four oxygens closest to a *B*-site ion deviate from a square arrangement. For the magnetic structure, the unit cell is orthorhombic resulting from a doubling of a_0. The observed "magnetic intensities" agree well with those calculated for a model based on the formulation $(Mn^{2+})[Mn^{3+}Mn^{3+}]O_4$ with triangular arrangements of moments. The angle between the moments on *B* sites has been taken to be 130°, to give a value of 1.6 μ_B for the saturation moment in agreement with magnetic measurements. The direction of the moment on the *A* site (also the resultant of the moments on *B* sites) is parallel to [100]. The *B*-site moments are in planes parallel to (010). This triangular arrangement is in agreement with the conclusions drawn from the high-field magnetization study by Jacobs.

RA13. Kinetic Studies of Magnetic Annealing in Cobalt-Substituted Magnetite. WILFRED PALMER, *IBM Research Laboratory, Poughkeepsie.*—The uniaxial anisotropy energy density of a material susceptible to magnetic annealing may be written

$$W_U = -F \sum_i \alpha_i^2 \beta_i^2 - G \sum_{i>j} \alpha_i \alpha_j \beta_i \beta_j,$$

where α_i and β_i are the direction cosines of the measuring and annealing fields, respectively, and F and G are positive coefficients. In the present work, kinetic studies have been made of the variations of F and G during isothermal magnetic anneals of cobalt-substituted magnetites. The time dependences of F and G are different, and for a given annealing direction neither of these quantities approaches its final value exponentially. The rate in advanced stages of the anneal is slower than that required for an exponential approach derived from the initial rate. The departure from an exponential approach of the coefficient G is least pronounced in samples of low cobalt content. These observations are shown to be consistent with the model of magnetic annealing proposed by Penoyer and Bickford.[1]

[1] R. F. Penoyer and L. R. Bickford, Jr., Phys. Rev. **108**, 271 (1957).

RA14. Triangular Ferrimagnetic Arrangements in Chromium-Containing Spinels. I. S. JACOBS, *General Electric Research Laboratory.*—Chromium-containing spinels frequently have lower spontaneous magnetizations than predicted by the antiparallel arrangement (Néel) of *A*-site and *B*-site moments. Triangular ferrimagnetic arrangements (Yafet and Kittel) with angles between moments on one kind of site have been suggested. Magnetization measurements on the compounds $(MnFe_{2-t}Cr_tO_4)$ $(0 \leqslant t \leqslant 2)$, by Gorter, Lotgering, and Edwards support this suggestion. Also, neutron diffraction on $CuCr_2O_4$ by Prince is consistent with a triangular ferrimagnetic. However, neutron diffraction by Pickart on several ferrite-chromites yields no evidence for ordered triangular arrangements. Recent measurements[1] to 140 koe on $MO \cdot Mn_2O_3$ show that triangular arrangements are accompanied by a differential susceptibility at high fields, directly measuring the interaction between moments at angles within a site group. Similar measurements on $CuCr_2O_4$ and two ferrite-chromites ($t=1.0$ and 1.5) at 4.2°K[2] reveal high-field susceptibilities, with increases in magnetization of 50 to 100% over previously reported "saturation" values. The magnitudes of these susceptibilities may be reconciled with other estimates of the interactions. It is concluded that triangular ferrimagnetic arrangements are present, notwithstanding the absence of long-range order in the ferrite-chromites.

[1] I. S. Jacobs, Am. Inst. Elec. Engrs. Conference on Magnetism, Philadelphia, November, 1958; J. Appl. Phys. (to be published).
[2] Samples kindly provided by Dr. E. Prince and Dr. S. Pickart.

WEDNESDAY MORNING AT 9:30

Room 26–100

(H. MARKOVITZ presiding)

High-Polymer Physics II

Invited Papers

S1. Time Dependence of Fracture and Fatigue. BERNARD D. COLEMAN, *Mellon Institute.* (40 min.)

S2. Compressibility of Polymer Melts. B. MAXWELL, *Princeton University.* (40 min.)

S3. Theory of Rolling Friction for Spheres. D. G. FLOM AND A. M. BUECHE, *General Electric Company.*—A theory of rolling friction featuring the importance of elastic hysteresis losses is presented. A simple model of retarded elasticity is chosen to represent the physical properties of the material. A prediction resulting from the theory is that the coefficient of friction for a relatively hard sphere rolling on a softer base material should vary with speed so as to go through a maximum. This relationship resembles closely the variation of mechanical loss with frequency. The results are not restricted to rolling but also apply to well-lubricated sliding where shearing forces have been minimized. Although the theory is developed for a material with idealized physical properties, it nevertheless affords a basis for comparing real materials and for predicting their frictional properties in cases where deformation losses are predominant.

Business Session of the Division of High-Polymer Physics

WEDNESDAY MORNING AT 10:00

Room 4–370

(H. LEVINSTEIN presiding)

General Semiconductor Physics

SA1. Theory of Surface Conductance in Semiconductors. DANIEL R. FRANKL, *Sylvania Research Laboratories.*—Schrieffer's theory[1] of surface conductance in a semiconductor with diffusely scattering surface is extended to include near-intrinsic and accumulation layers by retaining the exact form of the space-charge potential. For the carriers attracted to the surface, Eq. (5) of reference 1 is solved in two regions, one governed by the b.c. of random scattering at the surface and the other by an appropriate b.c. at infinite depth. Following a suggestion of Garrett,[2] we compute the conductance change due to the band curvature, obtaining a convergent expression that comprises a term corresponding to the bulk mobility plus a correction term. Numerical evaluation of the latter is under way.

[1] J. R. Schrieffer, Phys. Rev. **97**, 641 (1955).
[2] C. G. B. Garrett (private communication).

SA2. $1/f$ Noise and Related Surface Effects in Thin Germanium Filaments.* A. U. MAC RAE AND H. LEVINSTEIN, *Syracuse University.*—The variation of $1/f$ noise in thin germanium filaments as a function of the surface potential, has been investigated by applying steady electric fields perpendicular to the specimen surface. A strong dependence of the noise on the surface potential was observed for inversion layers on p-type germanium, the noise minimum being coincident with the surface conductivity minimum. Noise measurements in the presence of different ambients indicate that the kind and number of slow surface states as well as the surface potential determine the magnitude of the noise. The noise always relaxes back to its original value with a $\log(t)$ dependence, after the application of a steady field to the surface. This is in contrast to the conductivity whose relaxation varies anywhere from $\log(t)$ to $\exp(t)$, depending on the ambient and temperature. When visible light is incident on the surface the noise increases. Temperature dependence measurements of the $1/f$ noise in gold-doped germanium whose resistance increases rapidly with decreasing temperature, indicate that it is the $1/f$ noise power which is independent of temperature when a constant voltage is applied across the filament.

* Supported by the Aerial Reconnaissance Laboratory, Wright Air Development Center.

SA3. Influence of Transverse Modes on Photoconductive Decay in Filaments. J. S. BLAKEMORE AND K. C. NOMURA, *Honeywell Research Center.*—The roles of high-order modes are discussed for decay of excess carriers in a semiconducting filament whose surfaces have a very large recombination velocity. A solution is given for the strength of the various modes following any duration of excess generation (i.e., illumination) and for a generation procedure which differs from spatial uniformity in any desired fashion. It is well known that high-order modes can exhibit behavior of strong surface recombination[1,2]; but examples are used here to demonstrate diffusive and possible surface generative characteristics of these modes in addition. A technique is described for minimizing the influence of the surface on the decay scheme; this is useful in measurements of bulk lifetime.

[1] W. Shockley, *Electrons and Holes in Semiconductors* (D. van Nostrand Company, Inc., Princeton, New Jersey, 1950), p. 230.
[2] D. T. Stevenson and R. J. Keyes, J. Appl. Phys. **26**, 190 (1955).

SA4. Transient Response of Semiconductor Diodes.* VICTOR A. J. VAN LINT, *General Dynamics Corporation.*—The minority-carrier lifetime in the base region of semiconductor diodes is usually measured by injecting excess carriers and observing some electrical property of the component as the excess carriers are trapped. Several different methods in use differ principally in the method of carrier injection and the

technique of measurement.[1-3] The investigations to be discussed have demonstrated that for a particular diode geometry and injection method, the various types of measurements can be related to each other and to a single calculated function. For example, carriers can be injected by passing a forward current through the diode, and the decay measured by observing the voltage across the diode after the circuit is opened. The results of this experiment can be simply related to the recovery time method, in which the diode is switched to a reverse condition. Formulas have been derived describing the transient behavior of two types of idealized diode (a planar diode of arbitrary base thickness, and a hemispherical junction in a semi-infinite base) under two types of injection (low-current injection and uniform injection).

* Supported in part by the U. S. Air Force Cambridge Research Center.
[1] B. Lax and S. F. Neustadter, J. Appl. Phys. **25**, 1148 (1954).
[2] R. H. Kingston, Proc. Inst. Radio Engrs. **42**, 829 (1954).
[3] M. Byczkowski and J. R. Madigan, J. Appl. Phys. **28**, 878 (1957).

SA5. Space-Charge-Limited and Temperature-Limited Injection of Charge Carriers in a Space-Charge-Depletion Region.* JEROME M. LAVINE, *Raytheon Manufacturing Company.*—The forward and reverse characteristics of both *p*- and *n*-doped contacts located in the space-charge-depletion region of a reverse biased silicon *p-n* junction will be compared with those of a metal point contact as observed by Matthei and Brand.[1] The floating potential of these doped contacts will also be described. A simple band model will be used to show that space-charge-limited injection of holes from a *p*-doped contact and of electrons from an *n*-doped contact occurs when these contacts are forward biased, in much the same manner as in the case of the *n-i-n* structure treated by Shockley and Prim.[2] The model shows, however, that the injection of electrons from a *p*-doped contact and of holes from an *n*-doped contact will not be space charge limited for most current densities provided that the contact is biased in reverse for majority carriers. In this case all of the carriers present in the contact will flow through the space-charge region in a manner analogous to temperature-limited flow in a vacuum diode.

* This work supported by the Bureau of Ships.
[1] W. G. Matthei and F. A. Brand, J. Appl. Phys. **28**, 513 (1957).
[2] W. Shockley and R. C. Prim, Phys. Rev. **90**, 573 (1953).

SA6. Interstitials and Phase Change, with Special Reference to Germanium. JEROME ROTHSTEIN, *Edgerton, Germeshausen and Grier, Inc.*—It is proposed that in diamond-type and other open lattices thermal generation of interstitials can occur at surfaces and other imperfections, migrating to the interior analogous to formation and migration of vacancies. Interstitialcies appear energetically favored over Frenkel and Schottky defects for several substances with denser high-temperature phase (e.g., melt) than low-temperature phase, and should engender pre-transition phenomena. In germanium, for example, many surface atoms bond to three nearest neighbors, not four as in the bulk; jumping of surface atoms to adjacent interstitial sites is geometrically similar to ammonia inversion. Further interstitialcy migration is possible by successive jumps of the same atom (if tagged and so distinguishable) or chains of jumps by different atoms. Interstitial clusters may form as directionality of atomic bonding orbitals and crystal structure suggest their relative stability, explaining observed coordination number eight and higher density of liquid. Sheets of interstitials could develop even earlier and provide slip planes and crystallite boundaries; loss of resistance to shear (melting) could thus occur with perhaps under 10% interstitials. Supercooling of melt, due to trapped interstitials, should be pronounced, particularly at high purity, as observed. As interstitials are donors, melt should be degenerate *n*-type conductor as observed.

SA7. Thermoelectric Power of Titanium Dioxide. H. P. R. FREDERIKSE AND W. R. HOSLER, *National Bureau of Standards.*—Rutile single crystals (obtained from the Linde Company) were reduced to different extent (weight loss 0.01–0.1%) or doped with pentavalent ions (Ta, Nb) by diffusion. Both treatments produce a light to dark blue color depending on the concentration of vacancies or foreign ions. The thermoelectric power Q (300–1200°K), resistivity ρ (4–1200°K), and the Hall coefficient R (~30–600°K) were measured as a function of temperature in the indicated ranges. The temperature dependence of the reduced and the doped samples is qualitatively the same above 78°K. The Hall mobility depends on the crystallographic direction, but varies little between samples (for $T>200$°K). Both the energy band picture and the localized level model were used in analyzing the thermoelectric data. From the band picture one obtains an effective mass of the order of 10–$80m_0$ in reasonable agreement with previous results.[1] The density of states is in both cases within an order of magnitude of the number of Ti ions. It is suggested that the conduction around room temperature takes place in a very narrow *3d* band of Ti.

[1] R. G. Breckenridge and W. R. Hosler, Phys. Rev. **91**, 793 (1953).

SA8. Analysis of the Effect of Radiation on the Thermoelectric Determination of Thermal Conductivity.* J. H. CAHN AND T. C. HARMAN,† *Battelle Memorial Institute.*—In this procedure,[1] a current is passed through a semiconducting sample having a large thermoelectric power, establishing a temperature gradient. The sample is suspended in a vacuum by thin current and thermocouple lead wires. This permits simple boundary conditions for energy transfer to the sample to be applied. The equations for radiative and conductive transfer can readily be solved when the temperature of the sample is everywhere near that of the ambient. The solution from which the thermal conductivity is calculated is expanded as a series in the ratio of radiative to thermally conducted power. The second order approximation appears to be accurate up to 1000°K.

* Sponsored in part by the Office of Naval Research.
† Now at Lincoln Laboratories.
[1] T. C. Harman, J. Appl. Phys. **29**, 1373 (1958).

SA9. Effect of Heat Treatment on Reverse Current in Silicon *p-n* Junctions.* A. L. HARRINGTON AND M. F. MILLEA, *Pacific Semiconductors, Inc.*—The effect of heat treatment on the reverse leakage in silicon *p-n* junctions has been investigated, using high-voltage silicon bar *p-n* junctions produced by the floating zone technique. The junctions were etched in a mixture of HNO_3 and HF, after which the reverse current at 600 v was less than 1 μa (0.3×0.3 cm^2 cross section). The junctions were heated to 1000°C in air for approximately 30 min and air cooled, and the same etch procedure was repeated. The resulting reverse current was more than 10 times higher after than before the heat treatment. Various experiments indicated that most of the increase in reverse current after heat treatment occurred at the surface. One is therefore led to propose that the surface properties which determine reverse current are a function of the bulk condition. The rate of cooling after heat treatment appeared to be of minor importance. When the heat treatment was performed in a vacuum, there was a smaller increase in reverse current. Heat treatments had no significant effect on etching rates, etch pit formation, or bulk resistivities. A model to account for these observations, involving bulk-surface interactions, will be discussed.

* This work was supported by contract with the U. S. Army Signal Engineering Laboratories.

SA10. Improvement in Floating Zone Method. W. G. PFANN, K. E. BENSON, AND D. W. HAGELBARGER, *Bell Telephone Laboratories.*—Stability of floating zones in solid

members other than round rods has been investigated experimentally and theoretically. By using suitably shaped *wide zones* the floating zone method can be extended to much larger, and also smaller, cross sections than are feasible for round rods. Zone shapes studied include: (a) open-end—a zone melted through the thickness and across the entire width of a vertical plate; (b) closed-end—a similar zone in which the extremes of the width are unmelted; (c) continuous—a zone of annular cross section in a vertical pipe; (d) disk—a round zone in a horizontal plate (which may be pressurized on the under side to support the zone). The maximum stable height l_m for types (b) and (c) is the same as for zones in round rods of large diameter[1] but does not necessarily decrease with plate thickness, whereas l_m for round-rod zones does decrease as the radius decreases.

[1] W. Heywang, Z. Naturforsch. **11a**, 238 (1956).

WEDNESDAY MORNING AT 10:00

Kresge Auditorium

(HARVEY BROOKS presiding)

Invited Papers of the Division of Solid-State Physics

T1. Some Recent Developments in Energy Band Theory. F. HERMAN, *RCA Laboratories.* (30 min.)

T2. New Method for Calculating Energy Bands in Crystals. J. C. PHILLIPS, *University of California, Berkeley.* (30 min.)

T3. Plane Wave Expansion Methods in the Calculation of Energy Bands. P. M. MARCUS, *Carnegie Institute of Technology.* (30 min.)

T4. Forbidden Functions in Crystals. P. E. KAUS, *RCA Laboratories.* (30 min.)

WEDNESDAY AFTERNOON AT 2:15

Kresge Auditorium

(J. K. GALT presiding)

Invited Papers of the Division of Solid-State Physics

U1. Electronic Structure of Indium. J. R. REITZ, *Case Institute of Technology.* (30 min.)

U2. Energy Band Structure of InSb as Indicated by Infrared Absorption. H. Y. FAN, *Purdue University.* (30 min.)

U3. Symmetry of *M* and *R* Centers in Alkali Halides. A. W. OVERHAUSER, *Ford Motor Scientific Laboratory.* (30 min.)

U4. Quadrupole Interactions in the Vibration Spectra of Diamond-Type Crystals. M. LAX, *Bell Telephone Laboratories.* (30 min.)

WEDNESDAY AFTERNOON AT 2:00

Room 6–120

(G. H. VINEYARD presiding)

Thermal Effects and Order-Disorder in Metals

UA1. Lattice Stability of Metals. II. Zinc, Copper, and Silver.* LARRY KAUFMAN, *Manufacturing Laboratories, Inc.* (introduced by J. Goodenough).—Thermodynamic analysis of the fcc (α) and bcc (β) solid solutions of the Ag-Zn and Cu-Zn systems has been carried out in which the differences in free energy between the α, β, and η (hcp) forms of zinc, and the α and β forms of copper and silver have been calculated as a function of temperature. It is now possible to formulate the conditions for α/liquid, β/liquid, and α/β equilibrium in both systems, compute the activity of zinc in the α and β phases of Cu-Zn and Ag-Zn, and the degree of short range order in bcc Cu-Zn and Ag-Zn. For zinc, the cohesive energy difference between the hcp and fcc form is 460 cal/mole while the cohesive energy difference between fcc and bcc zinc (fcc more stable) is 250 cal/mole. The average Debye θ values for hcp, fcc, and bcc zinc are 235, 219, and 212°K, respectively. The cohesive energy difference between the fcc and bcc forms of copper and silver are 1500 and 905 cal/mole, respectively, while the average Debye θ values are 315 and 276°K for copper, and 220 and 204°K for silver.

* This work has been supported by the Office of Naval Research.

UA2. Fusion Curves of Four Group VIII Metals to 100 000 Atmospheres. F. P. BUNDY AND H. M. STRONG, *General Electric Research Laboratory.*—The fusion curves for Ni, Pt, Rh, and Fe have been determined experimentally to 100 000 atmos pressure. Various thermocouple arrangements were used inside the pressure chambers to indicate temperatures

Detection of fusion was by abrupt changes in electrical resistance of the sample, or by temperature dwell due to latent heat change during slow heating or cooling. The fusion temperatures at 1 and 100 000 atmos, respectively, for the various metals were: Ni 1453°, 1670°±10°; Pt 1773°, 2070°±15°; Rh 1980, 2400°±15°; Fe 1532°, 1740°±15°. The experimental data for each metal could be fitted quite well with Simon-type fusion curves. The slopes of these curves at 1 atmos, together with the Clausius-Clapeyron relationship, yielded the volume changes upon melting. The $\Delta V/V_s$ values found were: Ni 0.06±0.01; Pt 0.08±0.01; Rh 0.12±0.03; Fe 0.03±0.005. The constants in the Simon's equations which matched the experimental data differed considerably from theoretical values, but a functional relationship appeared evident between Simon's exponent c and the Grüneisen constant γ.

UA3. Experimental Fusion Curve of Iron to 96 000 Atmospheres: Temperature of Earth's Core. H. M. STRONG, *General Electric Research Laboratory.*—Iron of 99.88% purity and contained in pure alumina or magnesia was melted under pressures up to 96 000 atmos. The occurrence of melting was detected by a temperature arrest caused by the latent heat of fusion or by an abrupt increase in electrical resistance at the melting point. Temperature was observed by a platinum, platinum-rhodium thermocouple. The initial slope of the fusion curve was about 330 atmos/deg, in agreement with the slope computed from the Clausius-Clapeyron equation. At 96 000 atmos the melting point was 1740°±15°C. Simon's fusion equation could be fitted to the experimental data and it was used to extrapolate the melting point to pressures corresponding to that existing at the surface of the Earth's core; *viz.*, 1.4×10^6 atmos. At this pressure the extrapolated melting point was 2340±200°C, considerably lower than earlier extrapolations given by Simon and by Gilvarry.

UA4. A Study of Order in Au_3Cu. F. M. D'HEURLE* AND PAUL GORDON, *Illinois Institute of Technology* (introduced by A. S. Nowick).—The order-disorder transformation of Au_3Cu has been studied by means of isothermal jacket microcalorimeters. At 100°C these instruments can detect a heat evolution of 0.002 calories per hour and about twice this amount at 200°C. Ordering kinetics have been interpreted with the help of x-ray diffraction. The critical temperature has been determined as 209±2°C. The absence of a latent heat at the critical temperature does not necessarily imply that the transformation should be classified as a high-order transformation. Rather it is believed that in spite of an apparent reversibility equilibrium conditions are not obtained. It has been found that quenched-in defects, presumably vacancies, can play a very important role in ordering transformations. They do not only contribute to the speed of the transformation, but also help in bringing the alloy closer to true equilibrium conditions than would be otherwise possible.

* Now at IBM Research Center, Yorktown Heights.

UA5. Stabilization Effects in Au-Cd Alloys.* H. K. BIRNBAUM,† W. CLASS, D. S. LIEBERMAN, AND T. A. READ, *University of Illinois.*—The β phase of the Au-Cd alloy system is an ordered CsCl type structure which exhibits two known diffusionless phase transformations. Annealed, slow-cooled alloys of a 47.5 atomic percent cadmium concentration, transfrom upon cooling at approximately 65°C to a twinned, orthorhombic structure (β'), whereas those of a 49 atomic percent cadmium concentration transform at approximately 32°C to a twinned, tetragonal structure (β''). Aging of alloys in the β phase just above the transformation temperature has the effect of stabilizing the β phase, i.e., the transformation is suppressed to a lower temperature. In addition, in 47.5 atomic % Cd alloys, stabilization can result in the complete suppression of the $\beta \rightarrow \beta'$ reaction, in which case the $\beta \rightarrow \beta''$ reaction occurs at approximately 33°C. Studies made of these stabilization effects through the use of x-ray diffraction, resistivity, dilatation, and hardness measurements, will be discussed.

* Work supported in part by the U. S. Atomic Energy Commission.
† Union Carbide Fellow, now at the Institute of Metals, University of Chicago.

UA6. Antiphase Domain Boundary in Ordered Structures. JOHN W. CAHN, *General Electric Research Laboratory,* AND RYOICHI KIKUCHI, *Wayne State University and Hughes Aircraft Company.*—The free energy and thickness of the antiphase domain boundaries have been computed for the Bragg Williams approximation and also for the quasi-chemical model for a variety of structures. For a beta-brass type structure, the domain boundary consists of a region in which the long-range order gradually changes sign, and in which the short-range order is diminished. The thickness of this region increases with increasing temperature, becoming infinite at the transition temperature. To a first approximation the free energy and thickness are independent of the orientation of the boundary in the lattice. For a Cu_3Au type structure, the free energy and thickness depend on orientation and have minimum values for ⟨100⟩ directions. If only nearest neighbors are considered then energy and thickness are zero for the ⟨100⟩ directions.

UA7. Neutron Diffuse Scattering Study of Short-Range Order in β-Brass.* D. T. KEATING, *Brookhaven National Laboratory.* AND C. B. WALKER, *University of Chicago.*—Measurements have been made of the diffuse scattering of monochromatic neutrons from two single crystals of β-brass, one of which was highly enriched with the isotope Cu^{65}. The enriched sample exhibited a considerably more intense short-range order scattering. The diffuse scattering was investigated along the [100] direction from the forward direction to scattering angles exceeding the position of the (100) superlattice reflection, for several temperatures above $T_c = 465$°C. The short-range order scattering was found to be sharply peaked near the superlattice position, indicating the local order to be correlated over longer distances than usually pictured. The intensity of this scattering was found to decrease markedly with increasing temperature, but to retain its characteristic sharpness. More precise data accumulated in both the [100] and [111] directions are being combined to determine the short-range order parameters for β-brass at 550°C.

* This work was done under the auspices of the U. S. Atomic Energy Commission and Office of Ordnance Research, U. S. Army.

UA8. X-Ray Study of G. P. Zones in Al-Ag Alloys. M. B. WEBB, *General Electric Research Laboratory.*—Al-Ag alloys, with compositions varying from 0.5 to 5.0 at. % Ag, were homogenized, quenched in brine, and aged at room temperature for a month. The small angle x-ray pattern was observed. The scattering curves for the more concentrated samples show a maximum at about 2°.[1] This maximum is less pronounced for more dilute samples, disappearing for 0.5 atomic %. Rather than considering the "complex" scattering entity of a Ag cluster surrounded by its depleted zone,[1] the scattering is interpreted in terms of simple spherical clusters of Ag atoms. The number of Ag atoms per cluster is roughly proportional to the Ag concentration and the number of clusters is relatively independent of concentration. For 0.5 atomic % Ag, the clusters contain about 10 atoms. The maxima in the scattering curves are interpreted as interparticle interference effects with a simple pair-distribution function of the clusters. This distribution is a plausible result of the competitive growth of Ag clusters.

[1] C. B. Walker and A. Guinier, Acta Met. 1, 568 (1953).

WEDNESDAY AFTERNOON AT 2:00

Room 10–250

(I. S. JACOBS presiding)

Magnetism II; Ferroelectricity

V1. Spin Wave Spectra for Canted Antiferromagnets and Ferromagnets.* R. ORBACH,† *University of California, Berkeley.*—The magnetic resonance conditions and the spin wave spectra are found for canted antiferromagnetic and ferromagnetic lattices, where the cant is produced by magnetocrystalline anisotropy fields which are noncolinear. The sublattices are thereby caused to cant towards each other in antiferromagnets and away from each other in ferromagnets. The cant of the antiferromagnetic sublattices may produce a net moment (weak ferromagnetism) but does not alter appreciably the usual antiferromagnetic spin wave spectrum in the presence of anisotropy. The static susceptibility parallel ($\chi_{\parallel}$) and at right angles ($\chi_{\perp}$) to the vector difference of the anisotropy fields is calculated, and is shown to be altered from the noncanted result. It is shown that in antiferromagnets with no apparent weak ferromagnetism, canted sublattices may still be present, and can be detected by a nonzero ratio of $\chi_{\parallel}$ to $\chi_{\perp}$ at 0°K. The ferromagnetic spin wave spectrum shows a sudden change from the normal spectrum as soon as one introduces the noncolinear anisotropy fields. An optical branch is formed and a high frequency $\mathbf{k}=0$ magnetic resonance is expected. This resonance is a consequence of the two sublattice character of the canted ferromagnet and may be termed an exchange resonance.

* Supported in part by the National Science Foundation.
† National Science Foundation Predoctoral Fellow.

V2. Nuclear Resonance in Antiferromagnetic MnF_2 under Hydrostatic Pressure.* T. KUSHIDA† AND G. B. BENEDEK, *Harvard University.*—We have studied the pressure dependence of the nuclear magnetic resonance frequency of the F^{19} nucleus in antiferromagnetic MnF_2 in zero external field at 35.7°K and 4.2°K. The pressure range at 35.7°K was from 1 to 1000 kg/cm², and at 4.2°K was from 1 to 100 kg/cm². Helium was used as the pressure transmitting medium. The resonance frequency ν was observed to increase linearly with pressure at each temperature with slopes given by $(d\nu/dP)_{35.7°K}=0.46\pm0.01$ kc/(kg/cm²), $(d\nu/dP)_{4.2°K}=0.30\pm0.30$ kc/(kg/cm²). These data may be analyzed in terms of the pressure dependence of the hyperfine coupling constants[1] $A=(2A_s^{\mathrm{I}}-A_s^{\mathrm{II}})$ between the manganese electrons and the flourine nucleus, and the pressure dependence of the Néel temperature (T_N). Such an analysis gives $(\partial \ln T_N/\partial P)=4.38\times10^{-6}$/(kg/cm²) and $(\partial \ln A/\partial P)=1.88\times10^{-6}$/(kg/cm²).

* Supported jointly by the ONR, U. S. Army Signal Corps and U. S. Air Force.
† Now at Hiroshima University, Japan.
[1] V. Jaccarino and R. G. Shulman, Phys. Rev. **107**, 1196 (1957).

V3. Note on Dilute Cu-Mn Alloys. H. SATO, *Ford Motor Scientific Laboratory.*—A dilute solution of Mn in Cu shows a peculiar property which is characterized by a possible antiferromagnetic transition at low temperatures but with a positive paramagnetic Curie point. It seems probable in this case that both ferromagnetic and antiferromagnetic interactions with different interaction ranges coexist.[1] Recently, Dekker worked out a simple statistical treatment from the assumption that the nearest neighbor interaction between Mn atoms is antiferromagnetic and the long range interaction is ferromagnetic. With this assumption, he further made a bold simplification and obtained a proper result.[2] This assumption is, however, quite contrary to the one which was anticipated from our calculation on a magnetically dilute system.[1] Furthermore, because of this simplification, it is not clear whether or not the assumption adopted is really a characteristic of the system. We have made an approximate calculation using the contrary assumption. Here, the nearest neighbor interaction is taken care of by a pair approximation of the "cluster-variation method" and the superposed long range interaction is replaced, on the average, by a molecular field. This calculation also leads to a correct result.

[1] Sato, Arrott, and Kikuchi, J. Phys. Chem. Solids (to be published).
[2] A. J. Dekker, Physica **24**, 697 (1958).

V4. Derivation of the Magnetostriction Energy for a Hexagonal Antiferromagnet. D. R. BEHRENDT, *National Aeronautics and Space Administration.*—Recently W. P. Mason[1] has derived the magnetostriction and anisotropic energies for hexagonal crystals. This work has been extended to include a two-sublattice antiferromagnetic hexagonal crystal through fourth rank and sixth rank tensors. The equations become particularly simple for a crystal in which the magnetic moments of the two sublattices are in the basal plane. Under certain conditions the magnetostriction energy contains a term which varies as the second power of the cosine of angle between the two sublattice magnetizations. This result can be compared with an interpretation[2] of the experimental magnetic properties of dysprosium[3] where it was found necessary to include a term of this form in the energy expression. The magnetostriction of dysprosium can then be estimated under the assumption that the magnetostriction forms the only contribution to the second power cosine term.

[1] W. P. Mason, Phys. Rev. **96**, 302 (1954).
[2] Liu, Behrendt, Legrold, and Good, Jr. (to be published).
[3] Behrendt, Legrold, and Spedding, Phys. Rev. **109**, 1544 (1958).

V5. Specific Heats of $NiCl_2\cdot6H_2O$ and $CoCl_2\cdot6H_2O$ between 1.4°K and 20°K.* W. K. ROBINSON AND S. A. FRIEDBERG, *Carnegie Institute of Technology.*—The specific heats of $NiCl_2\cdot6H_2O$ and $CoCl_2\cdot6H_2O$ have been measured from 1.4°K to 20°K. Lambda-type anomalies were observed at 5.34°K and 2.29°K for $NiCl_2\cdot6H_2O$ and $CoCl_2\cdot6H_2O$, respectively, due presumably to antiferromagnetic transitions. It has been possible to separate out the magnetic contribution to the specific heat and to calculate the total entropy gained in each transition. This quantity was found to be given accurately by $R\ln(2S+1)$ with $S=\frac{1}{2}$ for Co^{++} and $S=1$ for Ni^{++}. Short-range order is particularly pronounced in these substances, the fraction of the total entropy gained above the Néel point being 0.52 for $CoCl_2\cdot6H_2O$ and 0.40 for $NiCl_2\cdot6H_2O$. The results for $CoCl_2\cdot6H_2O$ are consistent with recent susceptibility data.[1] The observation of a cooperative transition in $NiCl_2\cdot6H_2O$ is consistent with the reported susceptibility[2] and proton resonance[3] findings and provides a reasonable basis for understanding these results.

* Work supported by the National Science Foundation and the Office of Naval Research.
[1] Haseda and Kanda, J. Phys. Soc. Japan **12**, 1051 (1957).
[2] Haseda and Date, J. Phys. Soc. Japan **13**, 175 (1958).
[3] Kim and Sugawara, J. Phys. Soc. Japan **13**, 968 (1958).

V6. Neutron Diffraction Investigations of Metallic Cerium at Low Temperatures. M. K. WILKINSON, H. R. CHILD, W. C. KOEHLER, AND E. O. WOLLAN, *Oak Ridge National Laboratory.*—Neutron diffraction investigations have been performed on metallic cerium in an attempt to clarify the anomalous

behavior which has been observed in previous specific heat[1] and magnetic susceptibility[2] measurements. The results from neutron scattering confirm recent x-ray experiments[3] which indicated that the difficulty in interpretation has arisen because the exact crystal structure of the samples has not been known. There are three crystallographic forms of cerium that exist between 450°K and 4°K, and the relative concentrations of the three phases is dependent both on the sample temperature and on the previous history of the sample. Neutron diffraction investigations on three specially prepared samples at various temperatures from 300°K to 4.2°K have been able to correlate the interesting magnetic behavior with the existing crystallographic conditions. These experiments indicate that there is a change in the electronic configuration of the cerium atoms when the collapsed face-centered-cubic phase is formed and that there is an antiferromagnetic transition in the hexagonal-close-packed phase at a temperature near 13°K.

[1] D. H. Parkinson and L. M. Roberts, Proc. Phys. Soc. (London) **B70**, 471 (1957).
[2] J. M. Lock, Proc. Phys. Soc. (London) **B70**, 566 (1957).
[3] McHargue, Yakel, and Jetter, ORNL-2422, 207 (1957).

V7. Neutron Diffraction Study of UMn_2. P. K. Iyengar* and B. N. Brockhouse, *Chalk River Laboratories.*—The susceptibility[1] of UMn_2 shows an anomaly at 260°K and peculiar hysteresis effects below about 200°K. Neutron diffraction patterns have been obtained at temperatures from 95°K to 296°K. The positions and intensities of the diffraction lines at 296°K were consistent with the known Cu_2Mg type cubic structure with $a=7.15$ A. At lower temperatures a gradual distortion of the cubic unit cell occurs which first becomes visible under the resolution used at about 220°K, then rapidly increases to about 175°K, and then increases more slowly to 95°K. The distortion results in a splitting of the 111 line into two components of nearly equal intensity, and of the 220 line into three components with intensities in the approximate ratio 1:4:1. The over-all intensities are independent of temperature to about 5%, no additional lines appear at the low temperatures, and no appreciable changes in the diffuse scattering occur. A magnetic field of 3000 Gauss had no visible effects. At 95°K the distorted (monoclinic) unit cell had nearly equal lattice parameters of 7.10 A and a base angle of 94°. The only possible evidence found for antiferromagnetism[1] was the fact that the measured jF^2 for the inner component of the split 111 line was about 10% larger than for the outer component.

* Guest scientist from the Atomic Energy Establishment, India, now returned.
[1] S. T. Lin and A. R. Kaufmann, Phys. Rev. **108**, 1172 (1958).

V8. Neutron Diffraction Studies of the Magnetic Ordering in $CrCl_3$ and $FeCl_3$. J. W. Cable, M. K. Wilkinson, and E. O. Wollan, *Oak Ridge National Laboratory.*—Neutron diffraction investigations have been performed on anhydrous $CrCl_3$ and $FeCl_3$ at temperatures from 4.2° to 298°K to determine the existence of magnetic ordering in these hexagonal layer-type structures. Antiferromagnetic reflections were observed from polycrystalline $CrCl_3$ below 17°K, and these reflections suggest a magnetic structure in which the magnetic moments are aligned parallel within each hexagonal layer and the moments in adjacent layers are antiparallel. $FeCl_3$ becomes antiferromagnetic below 16°K but the magnetic structure is very complex and involves antiferromagnetic coupling within the hexagonal layers. The atomic moments were determined from the paramagnetic scattering, and in both compounds these values correspond to spin-only values for the respective ions in agreement with results obtained from previous magnetic measurements.[1]

[1] Starr, Bitter, and Kaufmann, Phys. Rev. **58**, 977 (1940).

V9. Hydrostatic Pressure Effects on Ferroelectrics. I. Tri-glycine Sulfate. F. Jona and G. Shirane, *Westinghouse Research Laboratories.*—The effect of hydrostatic pressure on the ferroelectric properties of tri-glycine sulfate has been investigated. Up to 2550 atmos, the transition point increases linearly with increasing pressure with a slope of $dT/dp=2.5_5 \times 10^{-3}$ degree/atmos. The Curie-Weiss law, $\epsilon_b=C/(T-T_0)$, is unaffected by pressure except for the shift in transition temperature ($C\cong 2900$ deg). The spontaneous polarization P_s increases with increasing pressure. At room temperature, for example, ($T=23.5$°C), a pressure of 2550 atmos increases P_s by approximately 5%. However, within the range of approximately 50 degrees below the transition, the plot of P_s *versus* reduced temperature T/T_c (where T_c=transition point) yields a single curve for any value of pressure ranging up to 2550 atmos.

V10. Chemical Composition, Homogeneity, and Phase Conditions in Vacuum Deposited $BaTiO_3$ Films.* William M. Becker, *The National Cash Register Company.*—Thin films of $BaTiO_3$ have been formed by methods similar to those of Feldman.[1] X-ray fluorescent spectrography has been utilized to determine the chemical composition of both the vapor phase and the film layers. The analysis shows initial excessive barium enrichment of the vapor when stoichiometric material is evaporated, thus leading to large concentration gradients in the films. Layers with over-all Ba/Ti mole ratios greater than 1 are usual with stoichiometric evaporants. TiO_2 enrichment is required to obtain ratios less than 1. Subsequent air bakeouts of the films at high temperatures result in preferential volatilization of barium. For near-stoichiometric composition in films deposited on platinum, an unoriented tetragonal $BaTiO_3$ phase is found, but other titanates and a number of oxides also appear to be present. Change of evaporating techniques to minimize concentation gradients, and the use of sapphire and rutile substrates do not affect this result.

* Supported in whole or in part by the U. S. Air Force, monitored by the Computer Research Branch, Aeronautical Research Laboratory, Wright Air Development Center.
[1] C. Feldman, Rev. Sci. Instr. **26**, 463 (1955).

V11. Domain Nucleation and Reversal in $BaTiO_3$. S. Triebwasser and E. F. Hahn, *IBM Research Laboratory, Poughkeepsie.*—Current models of switching in single crystal ferroelectrics consider two basic processes. First, it is assumed that by some mechanism nuclei of reversed polarization form[1] and then proceed to grow principally in the direction of the applied field. After a "tube" of reversed polarization has grown through the thickness of the crystal, it proceeds to grow by sidewise domain wall motion. Recent experiments by Miller[2] have demonstrated the latter process conclusively in $BaTiO_3$ in the slow switching (seconds) region. Experiments on $BaTiO_3$ have been performed in which switching transients in the 1–1000 μsec range have been interrupted and the domain pattern examined by etching techniques. Liquid mercury, LiCl solution, evaporated gold, and evaporated silver electrodes were used. Results indicate that for metal electrodes, liquid or evaporated film, during a large part of the switching process very few reversed domains penetrate through the thickness of the crystal, but extensive sidewise growth does take place. On the other hand LiCl solution electrodes yield results fairly consistent with the earlier model of switching discussed above.

[1] R. W. Landauer, J. Appl. Phys. **28**, 227 (1957).
[2] R. C. Miller, Phys. Rev. **111**, 736 (1958).

Invited Paper

V12. Radiation Effects in Ferroelectrics: Tryglycine Sulfate. A. G. Chynoweth, *Bell Telephone Laboratories.* (30 min.)

WEDNESDAY AFTERNOON AT 2:00

Room 4–270

(E. M. CONWELL presiding)

Invited Paper

VA1. Collision Ionization in Semiconductors. M. C. STEELE, *RCA Laboratories.* (30 min.)

Transport Phenomena in Semiconductors

VA2. Hall Effect in *P*-Type Germanium at High-Electric Fields. J. ZUCKER AND E. M. CONWELL, *Sylvania Research Laboratories.*—The Hall coefficient of a semiconductor, as is well known, depends not only upon the number of free carriers, but also upon the details of scattering processes and band structure. To observe the dependence on the latter in the "hot carrier" range, measurements of Hall coefficient were taken on *p*-type germanium as a function of electric field intensity up to 7000 volts/cm at liquid nitrogen and room temperatures. The voltage was applied in pulses to avoid heating the sample. A null method was developed for measuring the pulse heights. For low magnetic fields and room temperature the Hall constant of a high resistivity *p*-type sample was found to decrease 35% as the electric field increased from the Ohm's law region to 7000 v/cm. This does not imply an increase in carrier concentration since the sample was in the exhaustion region, and precautions had been taken to minimize injection and prevent surface breakdown. Most of the decrease can be attributed to the changes that take place in the light hole band beyond a few kT,[1] specifically the decrease in curvature of this band and the increasing anisotropy of the light hole constant energy surfaces.

[1] E. O. Kane, J. Phys. Chem. Solids **1**, 82 (1956).

VA3. Hot Carrier Ionization of Impurities in Ge at 78°K.* D. M. BROWN AND RALPH BRAY, *Purdue University.*—Neutral impurities having shallow levels (~0.01 ev) can be ionized by hot carriers at relatively low fields ($\leq$10 v/cm) and low temperatures ($\leq$20°K). The present work utilizes impurities with deeper levels to obtain carrier freeze out, and permit ionization studies at 78°K. Ionization has been obtained with a variety of compensated Zn-doped germanium samples, ranging in resistivity from 0.6 to 640 ohm-cm at 78°K, corresponding to freeze out of 60 to 99.95% of the extrinsic carriers. The absence of contact effects is assured by the reproducibility of the results with changes in contacts and sample geometry. Comparative measurements with germanium samples having similar mobilities, but negligible freeze out, permit separation of carrier concentration from mobility changes. Ionization effects begin at $E<100$ v/cm for the purer samples. As E is increased to 5000 v/cm, only *gradual* increases in carrier concentration, ultimately by factors of 2 to 15, are observed, indicating relatively inefficient ionization. Rise times of current are below the response time of the oscilloscope (7 mμsec), implying very short majority carrier lifetimes. There is surprisingly little or no rise in mobility from reduction of impurity scattering at high fields, even for the most impure samples ($\mu_L/\mu_I \approx 10$).

* Work supported by U. S. Signal Corps contract.

VA4. Pressure Dependence of "Hot-Electron" Effects. S. H. KOENIG, *IBM Watson Laboratory,* M. I. NATHAN, *IBM Research Laboratories, Poughkeepsie,* AND WILLIAM PAUL AND A. C. SMITH, *Harvard University.*—The pressure dependence of the high-field "tensor" electrical conductivity has been investigated in *n*-type germanium. The sample geometry was chosen to give optimum transfers voltage for a longitudinal current.[1] At 77°K, the shape of the current-ongitudinal voltage characteristics is independent of pressure up to the maximum pressure of 7000 kg per cm² and for electric field to 500 v/cm. At 195°K, and more so at 300°K' the saturation (high field) current decreases with increasing pressure up to 10 000 kg per cm² more rapidly than the low field mobility. Above 15 000 kg per cm², at 300°K, the conductivity remains linear to progressively larger electric field. These data are consistent with an interpretation involving *interband* scattering to the (100) minima in a higher conduction band. The transverse or anisotropy voltage is somewhat more complicated. At 77°K for field less than 3000 v/cm, the anisotropy[1] decreases with increasing pressure. For higher field the reverse is true. Possible mechanisms for this will be discussed.

[1] Sasaki, Shibuya, and Mizuguchi, J. Phys. Soc. Japan **13**, 456 (1958).

VA5. Piezoresistance of *N*-type Germanium.* H. FRITZSCHE, *University of Chicago.*—The piezoresistance of the conduction band of As and Sb doped Ge has been measured as a function of uniaxial tensile stress between 7°K and 300°K. The results obtained with current and stress oriented along [110] are in good agreement with the Adams[1]-Herring[2] model which ascribes the effect to the strain-induced change in the relative populations of the different valleys. The terms in the piezoresistance of second and higher order in stress depend on the strain-induced shift of the Fermi-level and hence on the detailed structure[3] and strain dependence[4] of the lowest donor states. The experiments yield an upper limit of 6×10^{-4} ev for the energy difference Δ between the onefold and the threefold "*ls*"-like states of Sb in Ge. For As in Ge the onefold state is found to be the ground state with 4.5×10^{-3} ev$>\Delta>Z\times10^{-3}$ ev.

* Work supported in part by a National Science Foundation Grant and a U. S. Atomic Energy Commission contract.
[1] E. N. Adams, Chicago Midway Lab. Tech. Rep. (ML-TN-P8).
[2] C. Herring, Bell System Tech. J. **34**, 237 (1955).
[3] W. Kohn and J. M. Luttinger, Phys. Rev. **98**, 915 (1955).
[4] P. J. Price, Phys. Rev. **104**, 1223 (1956).

VA6. Effect of Hydrostatic Pressure on Piezoresistance Effects in Germanium. M. POLLAK AND R. W. KEYES, *Westinghouse Research Laboratory.*—An apparatus for the measurement of piezoresistance has been successfully operated under hydrostatic pressures in excess of 10^4 atmos. The apparatus applies a small alternating shear stress, which is produced by an electromagnet, to the sample, and is essentially the same as that previously described by one of the authors. We have used the apparatus to measure the effect of hydrostatic pressure on π_p/π_n, the ratio of the large piezoresistance coefficients of *p*- and *n*-type germanium, at 300°K. π_p/π_n decreases slightly with increasing pressure, and at 10^4 atmos is about 3% less than its value at one atmosphere. A model of the changes produced in the energy bands of germanium by hydrostatic pressure has been developed by several workers at Harvard University. The theory of the piezoresistance of this model, including effects of scattering between the [111] and [100] bands, has been worked out and will be used to interpret the experimental result.

VA7. Transverse Magnetoresistance of Zn Doped Ge at 4.2°K in the Prebreakdown Region.* P. KELLEY AND R. J. KEYES, *MIT.*—Zn doped Ge at 4.2°K exhibits a large trans-

verse magnetoresistance which is extremely sensitive to the magnitude and direction of the magnetic field. Depending on crystal orientation relative to H, changes in resistance of approximately three orders of magnitude increasing and decreasing, can be observed when H is varied from 0 to 4000 gauss. When the magnetic field is held constant and the sample is rotated in the plane perpendicular to the electric field, variations of three orders of magnitude also occur. To study the connection between the anisotropy and crystal structure a sample was cut so that the electric field could be applied along the [111] axis. Since the crystal has three-fold rotational symmetry about the [111] axis, one should expect to observe the same symmetry in conduction *vs* angle when the magnetic field is rotated in the transverse plane. For large magnetic and electric fields this symmetry was observed.

* The work reported here was performed at Lincoln Laboratory, a technical center operated by Massachusetts Institute of Technology with the joint support of the U. S. Army, Navy, and Air Force, under contract.

VA8. Effect of Light on Impurity Conduction in Germanium.* A. L. McWHORTER, *MIT.*—The effect of light on the conductivity of p-type compensated germanium at 4.2°K has given additional support to the hopping model of impurity conduction proposed by Conwell[1] and Mott.[2] Neglecting activation energy, the model gives a conductivity of the form $Af(1-f)\exp(-BN_A^{-1/3})$, where A and B are (calculated) constants and f is the fractional occupancy of the acceptors (N_D/N_A at equilibrium). The direct effect of light is to produce hole-electron pairs, but at low-intensity levels most of these carriers become trapped, decreasing f. Thus if $N_D/N_A<\frac{1}{2}$, the impurity conductivity should initially decrease; while if $N_D/N_A>\frac{1}{2}$, it should initially increase, pass through a maximum, and then decrease as the light intensity is gradually increased. These predictions have been verified in several samples (N_A ranging from 2×10^{15} to 10^{16} cm^{-3}, compensation from 15 to 90%), although in some the effects are partially masked by the untrapped carriers. General agreement was obtained with the theoretical conductivity in this impurity range, as was also reported by Blakemore.[3]

* The work reported here was performed at Lincoln Laboratory, a technical center operated by Massachusetts Institute of Technology with a joint support of the U. S. Army, Navy, and Air Force, under contract.

[1] E. M. Conwell, Phys. Rev. **103**, 51 (1956).
[2] N. F. Mott, Can. J. Phys. **34**, 1356 (1956).
[3] J. S. Blakemore, Bull. Am. Phys. Soc. Ser. II, **3**, 328 (1958).

VA9. Photomagneto-mechanical Effects in Ge. ARNOLD R. MOORE AND JOHN O. KESSLER, *RCA Laboratories.*—A new and very sensitive apparatus has been used to measure the change in force exerted on Ge specimens by an inhomogeneous magnetic field when the specimens are illuminated by high intensity light. The force changes are due to several types of circulating current effects (PEM effect), as well as due to a change in the magnetic susceptibility. The method of resolution of the observed force into its proper components will be discussed. Observations concerning the normal photomagneto-mechanical effect[1] will be discussed in terms of its dependence on the temperature, light intensity, and wavelength of the incident radiation. A new effect of this general type has been observed and its characteristics will also be described. The new effect occurs when the carrier diffusion velocity v_d is outward from the interior of the specimen. Inside-out diffusion-velocities result either from the use of penetrating light ($\lambda>1.6\ \mu$) and high recombination surfaces, or from suitable masking of the specimen. In the former case the geometry is the same as in the normal PEM effect, with $|\mathbf{v}_d\times\mathbf{H}|=v_dH$; in the latter, the usually considered $\mathbf{v}_d$ may be parallel to $\mathbf{H}$. The masking then provides a strong secondary perpendicular component. Whereas the normal effect produces a magnetic moment in the direction of the magnetic field, the new interior, or IPEM, effect produces a magnetic moment in the opposite direction.

[1] Aigrain and Garreta, Compt. rend. **238**, 1573 (1954).

VA10. Light-Induced Magnetic Susceptibility Changes in Ge. JOHN O. KESSLER AND ARNOLD R. MOORE, *RCA Laboratories.*—The change in the magnetic susceptibility, χ, of Ge under high-intensity illumination has been observed by means of the apparatus described in the previous paper. These measurements were carried out in the vicinity of room temperature on near intrinsic samples in which the number of the light-injected pairs ($5\times10^{13}\leq\Delta n\leq7\times10^{14}$/cm^3) outweighs the equilibrium number. These are the first measurements of the contribution to the χ of pairs in this temperature range and at such relatively low pair concentration. The preliminary results of these measurements indicate the presence of a hitherto unsuspected component of χ, which is apparently connected with correlations among the charge carriers. The magnitude of the effect is approximately 400 times that expected from the extrapolation of previous experimental results or of the Landau-Peierls diamagnetism, where the carrier contribution to χ is taken as a simple sum of the χ contributions of the individual carriers, including both holes and electrons. The relationship between the observed light-induced χ, the carrier density, and the recombination statistics will be discussed.

VA11. Some Electrical Properties of V_2O_3. F. J. MORIN, *Bell Telephone Laboratories.*—An abrupt change in the electrical conductivity at the Néel temperature ($T_N=170$°K) was reported[1] to occur in sintered, polycrystalline V_2O_3 samples. Now, with single crystals, this behavior is confirmed. Stoichiometric V_2O_3 is a metal above T_N, and below T_N a semiconductor. When a crystal is made nonstoichiometric, it becomes a semiconductor both above and below T_N, the change in conductivity at the transition is reduced and the transition shifts to a lower temperature. In either case, the conductivity change is accompanied by a temperature hysteresis of about 15°K. A model has been proposed[2] to explain these results.

[1] M. Foex, J. recherches centre natl. recherche sci. Labs. Bellevue (Paris) **21**, 237 (1952).
[2] F. J. Morin, Bell System Tech. J. **37**, 1047 (1958).

WEDNESDAY AFTERNOON AT 2:00

Room 26–100

(R. S. STEIN presiding)

High-Polymer Physics III

Invited Papers

Y1. Structural Features of High Polymers Determined by Dynamic Mechanical Tests. L. E. NIELSEN, *Monsanto Chemical Company.* (40 min.)

Y2. Nuclear Magnetic Relaxation of Polyethylene. D. C. DOUGLASS, *Bell Telephone Laboratories.* (40 min.)

Y3. Nuclear Magnetic Resonance and Thermal Expansion in Polyethylene as a Function of Crystallinity, Branching, and Temperature.* N. FUSCHILLO AND J. A. SAUER, *Pennsylvania State University.*—Molecular motion in four polyethylenes with different concentrations of side branches and varying percent-crystallinity have been studied using proton magnetic resonance and volume expansion techniques. The NMR line shapes are analyzed by means of line width, second moment and intensity ratio determinations and activation energies for segmental reorientation and diffusion ascertained. The thermal expansion data are analyzed by the method of Price.[1] For the two samples of highest crystallinity the contributions to the narrow line component of the complex NMR line shape arise almost exclusively from the disordered regions of the polyethylene until temperatures close to the crystalline melting temperature are approached. Over a wide temperature range, both the NMR intensity ratio and the density percent-crystallinity show a similar variation with temperature. The distinction between ordered and disordered regions in the specimens of low crystallinity is much less clearly shown by the NMR method. This is caused by a less perfect crystalline order associated with the presence of side branches and the consequent onset of significant crystalline melting at temperatures as low as 310°K.

* Supported in part by the U. S. Atomic Energy Commission.
[1] F. P. Price, J. Chem. Phys. **19**, 973 (1951).

Y4. Nuclear Magnetic Resonance and Thermal Expansion in Isotactic Polypropylene, Polybutene, and Polypentene.* J. A. SAUER, A. E. WOODWARD, AND N. FUSCHILLO, *Pennsylvania State University.*—Molecular motion has been studied by both proton spin magnetic resonance and volume dilatometry on the same specimen for samples of isotactic polypropylene and isotactic polybutene and by volume expansion alone for isotactic polypentene. Multiple specimen techniques previously described[1] are used from 77°K to 450°K for NMR measurements and from 160°K to the melting point for the dilatometric determinations. Both the NMR and dilatometric results are characterized by definite transition regions, corresponding to the onset of segmental and branch point motion in the amorphous and in the crystalline regions of these polymers. It is shown from both the NMR and thermal expansion analysis that for the polypropylene sample, the crystallinity changes vary little with temperature to within a few degrees of the well-defined melting region and that segmental motion is relatively restricted in the crystalline regions until this temperature range is approached. In contrast, the polybutene specimen exhibits a change in crystallinity over a much broader range of temperatures. These results suggest a less perfect ordering in the crystalline regions of the isotactic polybutene sample.

* Supported in part by the U. S. Atomic Energy Commission.
[1] Fuschillo, Krautkopf, and Sauer, Bull. Am. Phys. Soc., Ser. II, **3**, 131 (1957).

Y5. Molecular Motion in Some Glassy Polymers. W. P. SLICHTER AND ELAINE R. MANDELL, *Bell Telephone Laboratories.*—Molecular motion in several glassy polymers has been examined by proton magnetic resonance methods over the temperature range 77–400°K, and has been interpreted in terms of the detailed behavior of molecular chains and substituents. Comparisons are made between transitions seen by proton resonance and glass transitions seen by other models. Powles' observations[1] on polymethyl methacrylate are largely borne out, though at low temperatures the second moment of the resonance shows smaller values than those reported earlier.[1] The differences among samples are interpreted in terms of variations in the degree of stereospecific structure. In polymethyl alpha-chloroacrylate, the low-temperature values of the second moment are much smaller than expected. These depressed values are ascribed to rotation of methyl groups about the threefold axes. In polycyclohexyl methacrylate, the bulkiness of the ester group evidently inhibits motion in the chain branches and leads to the low-temperature value of the second moment predicted for motionless chains.

[1] J. G. Powles, J. Polymer Sci. **22**, 79 (1956).

Y6. Secondary Dielectric Dispersion in Polyvinyl Chloride. MARTIN G. BROADHURST, SHELDON G. TURLEY,* AND EDWIN R. FITZGERALD, *The Pennsylvania State University.*—Measurements of complex dielectric constant ($\epsilon^* = \epsilon' - i\epsilon''$) at frequencies from 50 to 50 000 cps and at temperatures from −100 to +65°C have been made on samples of polyvinyl chloride (polymerized at ~50°C) in order to establish the detailed nature of the secondary dispersion occurring in this polymer. This broad disperison, first reported by Fuoss,[1] occurs in the vicinity of 0°C at audio-frequencies. The loss factor *vs* frequency maxima become broader and higher with increasing temperature and shift to higher frequencies; thus the curves will not superpose with horizontal shifting along the frequency axis and the method of reduced variables does not apply. Linear thermal expansion data and mechanical loss tangent measurements in the same temperature range were also obtained. Mechanical loss tangent *vs* temperature curves show broad maxima in roughly the same temperature region as dielectric loss tangent *vs* temperature curves at corresponding frequencies. Results have also been obtained on samples of polyvinyl chloride polymerized at approximately −20 and 5°C where a reduction in the secondary dielectric dispersion appears to result from the increased crystallinity of the samples.

* Present address: Dow Chemical Company, Midland, Michigan.
[1] R. M. Fuoss, J. Am. Chem. Soc. **63**, 369 and 378 (1941).

THURSDAY MORNING AT 9:30

Room 26–100

(W. P. SLICHTER presiding)

High-Polymer Physics IV

Invited Papers

Z1. Infrared Studies of Amorphous Polymers. S. KRIMM, *University of Michigan.* (40 min.)

Z2. Amorphous Orientation in Semicrystalline Polymers. R. S. STEIN, *University of Massachusetts.* (40 min.)

Z3. An Empirical Method for Estimating the Degree of Crystallinity of Native Cellulose Using the X-Ray Diffractometer. L. SEGAL, J. J. CREELY, A. E. MARTIN, JR.,* AND C. M. CONRAD, *Southern Regional Research Laboratory*† (introduced by Rollin S. Orr).—An empirical method for determining the crystallinity of native cellulose was studied with an x-ray diffractometer using the focusing and transmission techniques. The influence of fluctuations in the primary radiation and in the counting and recording processes have been determined. The intensity of the 002 interference and the amorphous scatter at $2\theta=18°$ was measured. The percent of crystalline material in the total cellulose was expressed by an x-ray "crystallinity index." This was done for cotton cellulose decrystallized with aqueous solutions containing from 70% to nominally 100% ethylamine. The x-ray "crystallinity index" was correlated with acid hydrolysis crystallinity, moisture regain, density, leveling-off degree of polymerization values, and infrared absorbence values for each sample. The results indicate that the crystallinity index is a time-saving empirical measure of relative crystallinity. The precision of the crystallinity index in terms of the several crystallinity criteria is given. Based on over 40 samples for which acid hydrolysis crystallinity values were available the standard error was 6.5%.

* Present address: Courtaulds (Alabama), Inc., Mobile, Alabama.
† One of the laboratories of the Southern Utilization Research and Development Division, Agricultural Research Service, U. S. Department of Agriculture.

Z4. Diffusivities and Solubilities of Methane in Polyethylene. J. L. LUNDBERG, M. B. WILK, AND MARILYN J. HUYETT, *Bell Telephone Laboratories.*—The diffusivities and solubilities of methane in polyethylene have been measured in the 125° to 230°C and 60- to 670-atmos region. Liquid polyethylene constrained in a fritted glass (or steel) cylinder is placed in a pressure vessel. The system is charged with gas and closed. Pressure changing with time is observed as the gas is sorbed by the polyethylene. The number of moles of gas external to the polymer is calculated for each observation. Solubilities are calculated from molecular data extrapolated to zero and infinite times. Diffusivities are calculated by fitting to the experimental points a close approximation to the infinite sum solution of the diffusion equation for radial diffusion in an infinite cylinder. A method for fitting nonlinear curves based upon least squares is used on a high-speed computer. Data for the methane-polyethylene system are compared to diffusivities and solubilities of nitrogen in polyethylene in the same temperature-pressure region.

Z5. Improved Semi-Automatic Histogram Plotter. R. H. KELSEY AND E. E. HANSON,* *Firestone Tire and Rubber Company.*—An improved instrument for constructing particle size distribution diagrams from electron micrographs is described. Its use permits the measurement of large numbers of particles rapidly and with low observer fatigue. The magnification of the image to be measured may be chosen to make the instrument error less than the resolution of the electron microscope. The device consists of a measuring unit in the form of a pair of dividers, controlling a servo system which automatically classifies the particles and plots the histogram as an array of steel balls in a slotted matrix. Adjustments for zero and span are provided, and the total number of particles measured is recorded.

* Deceased.

THURSDAY AFTERNOON AT 2:00

Room 26–100

(E. R. FITZGERALD presiding)

High-Polymer Physics V

ZA1. Origin of Alleged Deviations from the Theoretical Stress-Strain Isotherm for Rubber Networks. A. CIFERRI AND P. J. FLORY, *Mellon Institute.*—The molecular theory of rubber elasticity yields the relationship for simple elongation $\tau=G(\alpha-1/\alpha^2)$ where τ is the equilibrium stress referred to the initial cross section, α is the relative length, and G is a parameter proportional to the number of cross linkages per unit volume and dependent upon temperature. Improved agreement with experiment is claimed through use of the relation $\tau=2C_1(\alpha-1/\alpha^2)+2C_2(1-1/\alpha)^3$. To gain further evidence for the theoretically inexplicable C_2 term, stress-elongation measurements have been performed on networks of poly (-dimethylsiloxane), poly (-ethyl acrylate), natural rubber, polyisobutylene, and ploy (-methylmethacrylate) under a wide range of experimental conditions. Results may be summarized as follows: (1) the apparent value of C_2 varies markedly from one material to another; (2) it decreases with increase in temperature above the glass transition point; (3) its value depends on the time allowed for equilibration; (4) C_2 is markedly reduced if the sample is permanently swollen by a diluent, or if it is subjected to swelling and deswelling at each tension; (5) in general, the apparent value of C_2 correlates with the magnitude of the hysteresis displayed by the sample under the conditions employed. These results indicate that the C_2 term originates from the difficulty of attaining elastic equilibrium and that, under ideal experimental conditions, its value should be negligible, if not zero.

Invited Papers

ZA2. Elasticity of Networks Comprising Real Polymer Chains. P. J. FLORY, *Mellon Institute.* (40 min.)

ZA3. Effect of Hindrance to Rotation on the Statistics of Polymer Chains. C. A. J. HOEVE, *Mellon Institute.* (20 min.)

ZA4. Theory of the Helix-Coil Transition in Polypeptides and Polynucleotides. B. H. ZIMM, *General Electric Company.* (40 min.)

SUPPLEMENTARY PROGRAMME

SP1. Self-Consistent Field Theory for Incomplete Shells.*† C. C. J. ROOTHAAN, *University of Chicago.*—By a rigorous application of the variation principle, SCF equations have been derived for those cases where the total energy can be expressed as

$$E=2\sum_k H_k+\sum_{kl}(2J_{kl}-K_{kl})+f[\sum_m H_m+\tfrac{1}{2}\sum_{mn}(aJ_{mn}+bK_{mn})+\sum_{km}(2J_{km}-K_{km})];$$

k and l refer to the orbitals of a doubly occupied shell, m and n to a partially occupied shell; f is the fractional occupation number, and a and b are constants characteristic of the state. Two alternative forms were obtained for the SCF equations, one where the effective Hamiltonians for the complete and incomplete shells are different, and one where they are the same. In both cases the "orbital energy matrix" is diagonal; the orbitals are proper symmetry orbitals, and the two sets of orbitals are connected by a unitary transformation. The cases to which the present theory applies include *all* atomic states arising from the configuration p^n; *all* molecular states arising from the configurations π^n, δ^n, etc.; and the *ground state* of any combination of half-occupied shells, e.g., the $4s)3d)^{6,7}S$ ground state of Cr.

* Work supported in part by Wright Air Development Center, U. S. Air Force, and the National Science Foundation.
† To be given at the end of Session QA if the chairman rules that time permits.

SP2. Theory of Flow Orientation and Fracture Strength of Linear Polymers.*† C. C. HSIAO, *University of Minnesota.*—An analysis is given to describe the effect of large flow orientation on the variation of the fracture strength of a model linear high-polymer solid. For the simple state of uniaxial orientation the fracture strength in the direction of orientation and that perpendicular to the direction of orientation are evaluated as functions of the strain change and the strength of unoriented material. The results indicate an increase of strength in the direction of orientation and a decrease of strength perpendicular to the direction of orientation as the degree of orientation increases.

* Supported in part by the U. S. Atomic Energy Commission.
† To be given at the end of Session K if the Chairman rules that time permits.

SP3. Stretch Orientation and Mechanical Breakdown of Polystyrene and Polyethylene.*† C. C. HSIAO, *University of Minnesota.*—For samples of oriented amorphous polystyrene and partial crystalline polyethylene the fracture strengths for different degrees of uniaxial orientation are determined and are found to agree fairly well with certain previous theoretical predictions.

* Supported in part by the U. S. Atomic Energy Commission.
† To be given at the end of Session K if the Chairman rules that time permits.

Author Index to Papers Presented at the 1959 Cambridge Meeting

Adawi, I.—A3
Adrian, F. J.—KA1
Alers, G. A.—B2, B4
Allard, J. G.—FA2
Allen, Leland C.—A9
Allgaier, R. S.—BA12
Amar, Henri—RA5
Amdur, I.—CA3
Ames, L.—CA9
Amsterdam, M. F.—A12
Anderson, P. W.—G2, L2
Andrew, J. F.—B11
Anspaugh, Bruce E.—C4
Argyres, P. N.—IA5
Arndt, R.—JA1
Arnold, George W.—JA3, JA4
Arrott, A.—DA4
Artman, Robert A.—J8
Azároff, Leonid V.—P13

Baker, G. S.—B10, P2
Balluffi, R. W.—Q4
Barkow, A. G.—D7
Barnes, R. G.—NA9
Bass, R.—Q5
Batterman, Boris W.—R2
Bauerle, J. E.—BA8
Becker, J. H.—BA9
Becker, William M.—V10
Bedo, D. E.—R5
Behrendt, D. R.—V4
Benedek, G. B.—V2
Benson, K. E.—SA10
Berner, R.—B9
Berry, B. S.—B8
Beshers, D. N.—P11
Bienvenue, L. L.—P3
Binder, D.—K10
Biondi, Manfred A.—G3
Birnbaum, H. K.—UA5
Blakemore, J. S.—SA3
Blatt, F. J.—Q11
Blewitt, T. H.—C1, C2, C3, G12
Bloembergen, N.—L1, NA1, NA10
Boltax, A.—C10
Bovarnick, Bennett—CA11
Bowers, R.—BA8
Bowlden, H. J.—F8
Boyd, E. L.—RA4
Boyle, W. S.—O5
Bragg, Robert H.—P13
Braunstein, R.—BA1
Bray, Ralph—VA3
Brebrick, R. F.—BA12
Broadhurst, Martin G.—Y6
Brockhouse, B. N.—V7
Bron, W. E.—FA5
Brown, D. M.—VA3
Brown, R. G.—HA1
Brown, Richard N.—BA2, F4
Brueckner, K. A.—IA3
Bruemmer, Martha—I3
Bube, Richard H.—BA11, F12
Bueche, A. M.—S3
Bundy, F. P.—UA2
Butler, J. W.—H9, H11
Button, Kenneth J.—F5, I4

Cable, J. W.—V8
Cahn, J. H.—SA8
Cahn, John W.—UA6
Carlson, R. O.—F1
Castle, Barbara J.—KA4
Chandrasekhar, B. S.—O7
Charap, S. H.—RA6
Child, H. R.—V6
Childs, W. J.—H6
Chraplyvy, Z. V.—IA4
Chrenko, R. M.—NA13
Christensen, R. L.—CA9
Chupp, E. L.—D9
Chynoweth, A. G.—V12
Ciferri, A.—ZA1
Class, W.—UA5
Cohen, Leslie—H2
Cohen, Morrel H.—A4, J2, O1
Coleburn, N.—R7
Coleman, Bernard D.—K2, S1
Collins, Frank—CA1
Coltman, R. R.—C1, C2, C3, G12
Compton, W. Dale—FA4, JA3, JA4
Conrad, C. M.—Z3
Conwell, E. M.—VA2
Cooper, John N.—G6, G7
Corbett, J. W.—C8, EA10, JA7
Cornish, A. J.—BA8
Cowen, J. A.—NA5
Crawford, B. L., Jr.—HA3
Creely, J. J.—Z3
Crittenden, E. C., Jr.—G6, G7
Crut, M.—H1
Curtis, L. J.—Q11
Czyzak, S. J.—P7

Daniels, W. B.—B5
Darby, J. B., Jr.—Q4
Das, Y. C.—K12
Davies, J. A.—EA7
Davis, P. W.—BA5
DeSorbo, Warren—G9, Q8
DeVries, K. L.—B10
De Wit, G.—P5
d'Heurle, F. M.—UA4
Diehl, J.—B9, C3
Dienes, G. J.—EA4
Dixon, Jack R.—BA3
Douglass, D. C.—Y2
Dreeben, Arthur B.—F12
Dresselhaus, G.—A5
Drimmer, B.—R7
DuMond, J. W. M.—D9

Edwards, D. F.—I3
Edwards, T. H.—HA1
Efremov, N.—IA7
Ehrenreich, H.—A4
Eisen, F. H.—JA10
Elliott, D. D.—D8
Etzel, H. W.—FA2
Eubank, H. P.—D10
Eyges, L.—IA5

Fairbank, William M.—G13
Fan, H. Y.—F7, JA8, JA9, U2
Fernandez-Bertram, Jose—HA6
Fessenden, R. W.—KA2
Fink, R. W.—H3
Fisher, David E.—D1, D2
Fisher, P.—F7
Fitzgerald, Edwin R.—Y6
Flom, D. G.—S3
Flory, P. J.—ZA1, ZA2
Foner, S.—DA1
Ford, G. C.—D3
Ford, K. W.—H7, H8
Frankl, Daniel R.—SA1
Frederikse, H. P. R.—SA7
Fred, Mark—M2
Freeman, A. J.—E3
Friedberg, S. A.—V5
Friedman, A. N.—O6
Fritzsche, H.—VA5
Fuschillo, N.—Y3, Y4

Garber, M.—Q11
Garfunkel, M. P.—G3
Garrett, D. L.—Q1
Gavenda, J. D.—O3
Geil, P. H., Jr.—K8
Gelles, I. L.—F2
Gerritsen, H. J.—NA3
Gibbs, J. H.—N6
Gibbs, P.—B10, P1, P2
Gilbert, T. L.—IA6
Girifalco, L. A.—EA5, EA11
Goldburg, Walter I.—NA4
Goodenough, John B.—A11
Goodman, Gordon—M2
Goodman, L. S.—H6
Gordon, D. I.—C14
Gordon, Paul—UA4
Gouterman, Martin—M1
Granato, A.—P4
Green, A. E. S.—H7, H8
Green, J. J.—RA9
Green, Mino—CA7
Greene, Lawrence C.—J5
Greenfield, I. G.—C7
Grimes, Hubert H.—Q9
Grone, A. R.—Q6
Gwinn, William D.—HA6

Hagelbarger, D. W.—SA10
Hahn, E. F.—V11
Hall, H. T.—B10
Hall, J. J.—O6
Ham, Frank S.—A8
Ham, Joe S.—K3, K4
Hammill, H.—B12
Hammond, G. L.—BA12
Hanson, E. E.—Z5
Harman, T. C.—SA8
Harrington, A. L.—SA9
Harris, D. W.—EA10
Harrison, S. E.—NA3
Hass, Marvin—EA3
Hatch, Albert J.—H10
Hatcher, R. D.—EA4
Hause, C. D.—HA4
Henry, Warren E.—RA1
Herman, F.—T1
Herring, Conyers—LA1
Hickmott, J. T.—HA9
Hickmott, T. W.—CA8

Hijikata, Katsunori—HA5
Hildebrand, B.—D6
Hines, R. L.—JA1
Hoeve, C. A. J.—ZA3
Hofmann, J. A.—NA8
Holland, M. G.—F9
Holliday, J. E.—R1
Holstein, T.—O2
Hopfield, J. J.—I2
Hopkins, I. L.—N2
Hosler, W. R.—SA7
Hrostowski, H. J.—NA12
Hsiao, C. C.—K12, K13, SP2, SP3
Hudson, R. C.—FA11
Hultsch, R. A.—NA9
Huntington, H. B.—Q6
Huyett, Marilyn J.—Z4

Ingham, H. S., Jr.—FA8
Iyengar, P. K.—V7

Jacobs, I. S.—RA14
Jacobs, S. J.—R7
Jehle, Herbert—QA8, QA9
Jewell, R.—D9
Johnson, E. G.—K11
Johnson, P. D.—FA7
Jona, F.—V9
Jones, R. V.—RA8
Jones, W. H., Jr.—NA9

Kabler, M. N.—FA10
Kaelble, D. H.—K11
Kaiser, R. H.—NA12
Kamber, K.—P8
Kaminow, I. P.—RA8
Kane, G.—D7
Kanter, Manuel A.—O9
Kaplan, T. A.—RA11
Kasper, J. S.—RA12
Kauffman, J. W.—C12, Q7
Kaufman, Larry—UA1
Kaus, P. E.—T4
Kear, B. H.—P12
Keating, D. T.—UA7
Keffer, F.—RA3
Keith, H. D.—K5, K6
Kelley, P.—VA7
Kelsey, R. H.—Z5
Kernohan, R. H.—C9
Kessler, John O.—VA9, VA10
Keyes, R. J.—VA7
Keyes, R. W.—VA6
Kieffer, L. J.—H6
Kikuchi, Ryoichi—UA6
King, W. T.—HA3
Kingston, David L.—J5
Kirkland, W. K.—K10
Kjeldaas, T., Jr.—O2
Klabunde, C. E.—C1, C2, C3, G12
Kleiner, Walter H.—F4, I5
Kleinman, L.—A7
Klick, Clifford C.—FA3, FA4
Klokholm, E.—Q3
Knox, K.—NA11
Koehler, J. S.—P5
Koehler, W. C.—V6
Koenig, S. H.—O6, VA4
Kohn, H. L.—C12
Kohn, Walter—A6
Kolos, W.—QA2, QA6
Komura, Yukitomo—KA7
Koster, G. F.—NA2
Kretschmar, George G.—BA10
Krimm, S.—Z1
Kropschot, R. H.—Q11
Kunzler, J. E.—O5
Kushida, T.—V2

Lampert, Murray A.—I6
Landel, Robert F.—N1
Lauer, James L.—CA5
Lavine, Jerome M.—SA5
Lax, Benjamin—BA2, F4, F5, I4
Lax, M.—U4
Layer, H. P.—FA11
Lern, Arthur J.—G6, G7
Levin, E. R.—EA9
Levinstein, H.—BA4, SA2
Levy, Paul W.—JA6
Lewis, H. R.—NA3
Lieberman, D. S.—UA5
Lind, Edward L.—BA11
Linz, Arthur, Jr.—J4
Lockett, Andrew M., III—IA3
Loeb, A. L.—CA2
Long, Donald—F6
Longmire, M. S.—CA3
Ludwig, G. W.—F1, F3
Lundberg, J. L.—Z4
Lundqvist, Stig—EA1
Lundsten, R. H.—C14

Mackinnon, E. M.—IA4
Mac Rae, A. U.—SA2
Mahanty, J.—EA8
Mahendroo, P. P.—NA7
Maki, Gilda—CA6
Malenka, B. J.—IA2
Mallard, W. C.—Q5
Mandel, Gerald—CA1
Mandell, Elaine R.—Y5
Mann, Glen A.—HA4
Mapother, D. E.—G10
Maradudin, A. A.—EA6, EA7, EA8, G5
Marcus, P. M.—T3
Marcus, R. A.—QA7
Marezio, M.—O11
Margolis, B.—IA1
Mark, Hans—D9
Marshall, W.—E2
Martin, A. E., Jr.—Z3
Mason, E. A.—CA3
Matsuo, T.—D11
Matthias, Bernd—G1
Maxwell, B.—S2
Maxwell, K. H.—CA7
McCaldin, J. O.—F14
McClure, J. W.—O8
McDaniel, R. E.—D7
McLean, A. D.—QA4
McWhorter, A. L.—VA8
Meakin, J. D.—P9, P10, Q3
Mendlowitz, H.—R6
Merrifield, R. E.—KA5
Meshii, M.—Q7
Meyer, Horst—M3
Meyer-Berkhout, U.—H7, H8
Millea, M. F.—SA9
Mitchell, D. L.—BA4
Moffitt, William—M1, M2
Moore, Arnold R.—VA9, VA10
Morin, F. J.—VA11
Morse, R. W.—O3, O4
Mrozowski, S.—K9
Mulliken, R. S.—QA1
Muschlitz, E. E., Jr.—CA4
Myers, John—F6

Nathan, M. I.—VA4
Nathans, R.—RA2
Neighbours, J. R.—B2, B4
Nelson, C. M.—JA2, JA5
Nethercot, A. H.—DA3
Neumark, G. F.—J6
Neupert, W. M.—R5
Newman, R.—NA13
Nielsen, L. E.—Y1
Nisennoff, M.—JA8
Nixon, J. D.—I7
Noggle, T. S.—C13, D12
Noll, Walter—K2
Nolle, A. W.—NA7
Nomura, K. C.—SA3
Nowick, A. S.—FA5, Q2
Nudelman, S.—HA9

O'Dell, F. W.—D4, D6
Offenbacher, E. L.—EA9
O'Friel, Z.—D7
Oguchi, T.—RA3
Okada, J.—B11
Olsen, T.—O4
Orbach, R.—V1
Otter, F. A.—G10
Overbeek, J. T. G.—CA2
Overhauser, A. W.—U3
Overstreet, R.—BA7

Padden, F. J., Jr.—K5, K6
Palmer, Wilfred—RA13
Paoletti, A.—RA2
Paré, V. K.—C6
Parker, Paul M.—NA5
Patterson, D. A.—FA6
Paul, William—F9, RA8, VA4
Pearlstein, Edgar A.—C4
Peretti, J.—G5
Pershan, Peter S.—NA6
Peters, C. W.—I3
Pfann, W. G.—SA10
Philippoff, Wladimir—N4
Phillips, J. C.—A7, EA2, T2
Poliak, M.—VA6
Pool, M. L.—H5
Potter, Roy F.—BA10
Pratt, G. W., Jr.—E1
Pratt, P. L.—P12
Price, P. J.—A2
Primak, William—O9
Pugh, E. W.—C11

Rabin, Herbert—FA3
Ramaswamy, M. K.—H4
Ramdas, A. K.—JA9
Ransil, Bernard J.—QA5
Read, T. A.—UA5
Redman, J. K.—C2, C3, G12
Reitz, J. R.—U1
Reynolds, D. C.—P7

Reynolds, J. H.—D3
Richards, P. L.—G4
Rimai, L.—NA10
Riste, T.—E4
Rivlin, R. S.—N5
Roberts, S.—R8
Robinson, W. K.—V5
Romer, Robert H.—G13
Roothaan, C. C. J.—QA2, QA3, QA6, SP1
Rosendorff, S.—IA1
Rosenstock, Herbert B.—A13
Rotenberg, Manuel—IA3
Roth, Laura M.—I5
Rothstein, Jerome—SA6
Ryan, F. M.—C11

Sack, R. A.—K1, QA2
Sagalyn, P. L.—NA8
Sah, C. T.—J1
Saltsburg, Howard—J7
Sands, M.—D8
Sato, H.—B4, G11, V3
Satterthwaite, C. B.—G8
Sauer, J. A.—Y3, Y4
Scace, R. I.—F3
Schaeffer, Oliver A.—D1, D2
Schindler, A. I.—O10
Schissel, P. O.—CA10
Schlömann, Ernst—RA10
Schmidlin, Frederick W.—G6, G7
Schmunk, Richard E.—B6
Schnitzel, R.—B7
Schoen, Alan—Q10
Scobie, J.—H3
Scott, R. G.—K8
Segal, L.—Z3
Sello, H.—J1
Seraphim, D. P.—Q2
Sery, R. S.—C14
Shapiro, M. M.—D4, D6
Sharma, B. L.—H5
Shilliday, T. S.—BA5
Shirane, G.—V9
Shoemaker, Clara B.—KA7
Shoemaker, David P.—KA7
Shulman, R. G.—NA11
Sinai, J. J.—QA4
Sirlin, A.—IA1
Slichter, W. P.—Y5
Slifkin, L. M.—FA10, FA11, Q5
Smith, A. C.—VA4
Smith, Charles S.—B6
Smith, G. M.—CA4
Smith, L. B.—O8
Smith, R. J.—O10
Smith, W. V.—F2
Smoluchowski, R.—C11, FA8, FA9
Sochard, I. I.—BA9
Solow, M.—R7
Sommer, A. H.—BA6
Sorokin, P. P.—F2
Sosin, A.—P3
Spicer, W. E.—BA6
Statz, H.—NA2
Steele, M. C.—VA1
Stein, R. S.—Z2
Stewart, John W.—KA6
Stiegler, J. O.—D12
Stiller, B.—D4, D6
Strandberg, M. W. P.—HA7
Strong, H. M.—UA2, UA3
Sugihara, T. T.—D11
Swan, Paul R.—K7
Symons, N. K. J.—K8

Tannenwald, L. M.—H12
Tauber, G. E.—A1
Terhune, R. W.—I3
Tesk, J. A.—C12
Thomas, D. G.—I1
Thompson, D. O.—C6
Thomson, Robb—P6
Tobin, Ralph—H2
Tomboulian, D. H.—R5
Tomizuka, C. T.—Q1, Q4
Toupin, R. A.—B1
Townes, R. L.—K10
Tremere, D. A.—J1
Triebwasser, S.—V11
Tsubomura, H.—HA8
Turley, Sheldon G.—Y6
Turnbull, David—J2, Q8
Tweet, A. G.—F13
Tyler, W. W.—F10

Ulrich, A. J.—H11

Vanfleet, H. B.—P2
Van Lint, Victor A. J.—SA4
Van Vleck, J. H.—M4
Volkin, H. C.—KA3

Waddel, R. C.—D4
Waldorf, D. L.—B3
Walker, C. B.—O11, UA7
Walker, R. M.—C8, JA8
Wall, N. S.—H1
Wallis, R. F.—EA6, F8
Walsh, Walter, M., Jr.—DA2
Walter, N. M.—K6
Ward, J. B.—C12
Warren, B. E.—R4
Watkins, G. D.—JA7
Waugh, J. S.—KA2
Webb, M. B.—UA8
Webb, W. W.—R3
Wechsler, M. S.—C9
Weeks, R. A.—JA2, JA5
Weiss, A. W.—QA3
Weiss, P. R.—RA6
Weizer, V. G.—EA11
Wentz, R. P.—N2
Wert, C.—P8
White, J.—BA6
Whitmore, Frank C.—K4
Wiegand, D. A.—FA1, FA9
Wiersema, P. H.—CA2
Wigen, P. E.—NA5
Wiley, R.—R7
Wilk, M. B.—Z4
Wilkinson, M. K.—V6, V8
Wilkinson, P. G.—HA2
Williams, Ferd E.—F11, FA7
Williams, W. S.—CA10
Wilsdorf, H. G. F.—C7, P9, P10
Wilson, E. Bright, Jr.—M5
Wittke, J. P.—NA3
Wobschall, D. C.—B11, B12
Wolga, G. J.—HA7
Wollan, E. O.—V6, V8
Wood, J. H.—A10
Wood, Lawrence A.—N3
Woodbury, H. H.—F1, F3
Woodward, A. E.—Y4
Wyckoff, H. W.—K6
Wyluda, B. J.—NA11

Yagoda, Herman—D5
Yahia, J.—BA7
Yos, Jerrold—QA8
Young, D. A.—J3
Young, F. W., Jr.—C5

Zatzick, M. R.—D10
Zeender, J. René—RA10
Zilsel, P. R.—I7
Zimm, B. H.—ZA4
Zimmerman, J. E.—G11
Zinn, John—HA6
Zucker, J.—VA2
Zwerdling, Solomon—F5, I4

Preliminary Announcement of the 1959 Spring Meeting at Washington

THERE is a surprise in this year's announcement of the Spring meeting. There is nothing novel about the city (Washington), nor the dates, which are Thursday, Friday, and Saturday, April 30, May 1 and 2. The scientific sessions, however, will be held in the Willard and Raleigh hotels, in the Departmental Auditorium and in the Department of Commerce Auditorium, all in downtown Washington.

This innovation—or rather, return to the practices of years ago—is compelled by our faithfulness to our traditional dates, those that follow immediately upon the meeting of the National Academy of Sciences. Alas, this is the very time of year when Washington is most popular, and conventions larger and more opulent than ours are competing with ours for space. Our Local Committee is doing its best to stabilize our arrangements for the future, and its best is something that few can rival and no one can surpass.

Room reservations are to be made by writing to the Willard Hotel, 14th and Pennsylvania Avenues NW, Washington, D. C. You *must* mention that you are a member of this Society coming to its meeting!! The Willard engages to provide rooms in other hotels after its allotment to our members is fully booked: you may designate the hotels of your choice.

Deadline is Friday, February 20. Abstracts are to be sent to Karl K. Darrow, Secretary, American Physical Society, Columbia University, New York 27, New York. Re-read the instructions for the preparation of abstracts (page 206). After excessively numerous warnings, we now reject abstracts of which only carbons are submitted.

Proceedings of the American Physical Society

Minutes of the Divisional Meeting of the Division of Fluid Dynamics Held in San Diego, California, November 24, 25, 26, 1958

THE 1958 Divisional Meeting was held in the Hotel San Diego, San Diego, California, during the three days preceding Thanksgiving. The arrangements for the meeting were made by the Programme Committee consisting of W. M. Elsasser (*Chairman*), R. J. Emrich (*Secretary*), J. C. Evvard, F. N. Frenkiel, and E. A. Frieman, and by a highly conscientious staff from the Scripps Institution of Oceanography helping W. M. Elsasser. The scientific program included 5 invited and 68 contributed papers. The 247 registered participants attending the meeting included 209 from out of town.

The delightful city of San Diego and the existence of many attractions other than scientific in the vicinity served to make the three days pleasant, but the full programme (including an evening session on Monday) did not allow unscheduled time to bask on the La Jolla beach. The meeting was conducted (perhaps for the last time) without resorting to parallel sessions, and the attendance of all the participants to hear each paper with stimulating discussions following prevailed as at past Divisional Meetings. All sessions were held in the Continental Room of the Hotel San Diego, and informal contacts in the adjoining halls and lobbies were practicable, many, and profitable. The banquet of the Division on Tuesday night was well attended and honored the several local laboratories conducting research in the physics of fluids. F. N. Frenkiel, Chairman of the Division, presided and introduced Roger Revelle who presented a stimulating lecture on the opportunities man has to understand the two great fluid bodies—the sea and the atmosphere.

Raymond J. Emrich, *Secretary*
Division of Fluid Dynamics

Monday Morning at 9:00

(R. J. Emrich presiding)

A1. High-Energy Molecular Beams from Shock Wave Heated Sources.* H. W. Liepmann and B. Sturtevant, *California Institute of Technology.*—By reflecting a shock wave from a solid boundary one can prepare a sample of gas at high temperatures and pressure. This gas can be used as source for an intermittent high-energy molecular or plasma beam by simply adding a small orifice to the reflecting wall and processing the resulting beam in the standard fashion. To take a conservative example heating argon at 10 μ pressure with a $M=10$ shock wave results in a beam of about 1-ev energy with about 10^{20} particles/cm^2 sec. Thus standard molecular beam techniques can be extended to beams with at least 25

times more energy than beams from conventional ovens. The intermittent characteristic of the beam is not necessarily a drawback, but sometimes even advantageous in simplifying the pumping requirements. Performance and preliminary results obtained in such a device will be discussed.

* Carried out under the sponsorship of the Office of Naval Research.

A2. Strength of a Shock Wave Transmitted through an Orifice.* L. MONROE AND A. ROSHKO, *California Institute of Technology* (introduced by H. W. Liepmann).—If a shock wave in a shock tube impinges on a partition containing a hole, the wave is partially reflected and partially transmitted. Measurements were made of the strength of the shock transmitted through small holes, for various strengths of the incident shock. Calculations of the transmitted shock strength based on a one-dimensional model of the flow[1,2] agree well with the experimental results. For strong shocks, departure from perfect gas behavior has a strong effect on the flow through the orifice, but the strength of the transmitted shock is practically the same as for a perfect gas.

* Sponsored by Office, Chief of Ordnance, and the Office of Ordnance Research.
[1] D. S. Dosanjh, NACA, N.N. 3680 (1956).
[2] W. J. Franks and J. Gordon Hall, J. Aeronaut. Sci. **24**, 917 (1957).

A3. Measurements of Free Charge Density in Shock Tube Flows.* ROBERT G. JAHN, *California Institute of Technology*, AND FRED A. GROSSE, *Lehigh University*.—The electrical properties of the gas behind a head-on reflection of a Mach 6 shock wave in nitrogen have been studied in a $1\frac{3}{8}$-in. cylindrical shock tube using platinum film probes on the inner wall, and a microwave absorption technique. The films record two classes of signal: a current conduction through the ionized gas, and an electrostatic response which can also be detected outside of a nonconducting shock tube section. A microwave beam, incident transversely on a similar nonconducting tube section, is partially reflected at the charged gas surface, and the transmitted portion is further attenuated by bulk absorption within the conducting gas. The total attenuation can be related theoretically to the electron density, yielding a time-ionization profile whose maximum is in qualitative agreement with the thin-film conductivity measurements.

* Supported by the Office of Naval Research.

A4. Unexplained Weakened Regular Reflection in Shock Tubes.* EDWARD M. LITTLE, *U. S. Navy Electronics Laboratory*.—Regular reflection of shocks from an oblique reflector in a shock tube agree with steady state theory except for the case where the rarefaction from the corner overtakes the reflected shock. We call this case "weakened regular reflection." For the case when the rarefaction overtakes only part of the reflected shock, it bends it backward as it should, due to weakening. However, in the case where it overtakes the whole of the reflected shock, it is bent forward, strange to say. For Mach reflection the angle of the reflected shock disagrees with steady state theory by as much as 5 to 10 deg as shown previously be L. G. Smith. This is the direction that weakening would cause. No general theory has been worked out yet for these transient shock reflections. The pictures were taken by the "circular schlieren" technique. The shock tube was 8 by 8 in. Shock weakness was 0.77 to 0.86. This experimental work was done at the Naval Ordnance Laboratory, Silver Spring, Maryland.

* This is a part, expanded, of a paper at the meeting of the American Physical Society at the University of Virginia, December 28–30, 1949. Abstracted in Phys. Rev. **77**, 573 (1950).

A5. Refraction of Shock Waves in a Nonuniform Ocean. MAURICE HOLT, *Brown University* (introduced by W. H. Reid).—In an ocean the temperature is approximately constant in a shallow layer near the surface; below this layer the temperature decreases with depth. As a result when an explosion is initiated at a point in the nonuniform part of the ocean marked refraction effects occur. These are especially noticeable in the shadow zone formed below the boundary between the uniform and nonuniform regions. Near the source of the explosion the pressure pulse has the usual shape of initial peak followed by exponential decay. In the shadow zone, however, the pulse shape is changed and the initial pressure jump at the head of the wave is followed by a further continuous increase to a maximum behind the front. This complicates the calculation of peak pressures in the shadow zone. To explain the effect the refraction of a plane shock wave moving into a region of transverse temperature gradient is investigated. Calculation of the disturbed field behind the refracted shock confirms the observed behavior in the shadow zone.

A6. Rates of Ionization in Shock Layers.* M. H. BORTNER, *M. S. V. D. General Electric Company* (introduced by S. M. Scala).—Rates and times of ionization of atomic and molecular species of the atmosphere have been calculated for several typical sets of boundary conditions employing collision theory methods of homogeneous chemical kinetics. Original calculations were made assuming instantaneous atom-molecule equilibrium considering all imaginable ion-forming reactions. The reaction forming NO^+ from the uncharged atoms was found to be by far the most important. Practically all other ions are formed by a charge transfer reaction involving NO^+. The times required to form equilibrium concentrations of ions and electrons by this mechanism were found to be of the order of microseconds or less. Later calculations did not assume instantaneous atom-molecule equilibrium but rather incorporated dissociation reactions. A system of atom-forming reactions was combined with the aforementioned ionization reactions. For this mechanism it was found that the times involved are somewhat longer. At any instant the concentrations of ions are virtually the equilibrium concentrations corresponding to local concentrations of atoms and molecules. However, the atoms and molecules are not at equilibrium since the atom-forming reactions are comparatively slow. Thus the rate of approach of ion concentrations toward true equilibrium is rate-controlled by the atom-forming reactions.

* Supported by the Ballistic Missile Division of the U. S. Air Force.

A7. Stagnation Point Heat Transfer in a Partially Ionized Gas. RICHARD W. RUTOWSKI, *Lockheed Aircraft Corporation* (introduced by D. Bershader).—Recent developments in the theory of heat transfer to the stagnation point of a hypervelocity blunt body[1] relate the rate of heat transfer to the enthalpy gradient across the boundary layer, and include the effects of dissociation and diffusion. In our experiment interest centers on blunt body heat transfer in a partially ionized gas. Measurements have been made on a model using shock-heated argon. Measured rates of heat transfer are compared with theoretically predicted rates. Finally, there will be a discussion of additional signals, including a possible mechanism therefore, which indicates a flow of electrons from the body to the gas for sufficiently strong shocks.

[1] L. Lees, Jet Propulsion **26**, 259 (1956), and J. A. Fay and F. R. Riddell, J. Aeronaut. Sci. **25**, 73 (1958).

A8. Two-Dimensional Structure of Gaseous Detonation Waves.* J. A. FAY AND G. OPEL, *Massachusetts Institute of Technology*.—Schlieren photographs of oxy-hydrogen and oxy-acetylene detonation waves at initial pressures between 1 atmos and 1 mm of mercury show marked departures from a one-dimensional flow. At the higher pressures a standing wave pattern indicates that the burned gas flow is supersonic with respect to the front, which is slightly convex to the oncoming

flow. At lower pressures, where the thickness of the combustion zone is clearly discernable, the front is irregular and distorted. At the lowest pressures a regular cellular structure with a clearly defined wavelength can be seen in the oxy-acetylene mixtures. This pattern may be related to the phenomenon of spinning detonation. A theory is presented to explain the behavior of the detonation wave at about atmospheric pressure by accounting for boundary layer growth on the tube wall. This theory is consistent with velocity measurements showing the effects of tube diameter and initial pressure.

* Supported by Project Squid.

A9. Calculation of Reaction Profiles behind Steady-State Shock Waves. II. Strong Shock Waves in Air. RUSSELL E. DUFF, *Los Alamos Scientific Laboratory*, AND NORMAN DAVIDSON, *California Institute of Technology*.—The steady-state reaction profile behind shock waves in air has been calculated by a numerical procedure described previously.[1] Initial conditions were chosen which correspond to a pressure of 1 mm Hg before the shock and temperatures after vibrational equilibration and before chemical reaction of 10 000°K and 7000°K (shock Mach numbers of approximately 14.9 and 12.2). The chemical reactions considered were $O+N_2 \rightleftarrows NO+N$ and $N+O_2 \rightleftarrows NO+O$ as well as the dissociations of O_2, N_2, and NO. The rate constants used were based on recent experimental determinations. The calculations show that the reaction kinetics of air at high temperatures is very complicated. None of the usual simplifying kinetic assumptions is strictly admissible, although to within an order of magnitude, the dissociation reactions for N_2 and O_2 are out of equilibrium to the same extent over the last 90% of the temperature change behind the shock. In both cases the transient NO concentration far exceeds its equilibrium value. At the lower shock temperature the N concentration also shows a relatively small transient maximum. In both cases the direct dissociation of N_2 makes a negligible contribution to progress of the over-all reaction.

[1] R. E. Duff, J. Chem. Phys. **28**, 1193 (1958).

A10. Shock Wave Structure in the Hypersonic Flight Regime.* S. C. LIN AND J. D. TEARE, *Avco Research Laboratory* (introduced by A. Kantrowitz).—The approach to thermal equilibrium behind strong shock waves in multicomponent gases, such as air, involves many intercoupling chemical processes. These include not only relaxation of internal energy modes of individual components, but also exchange reactions linking the dissociation and ionization of one chemical species to another. Because of the large number of available reaction paths, it is necessary to compare the relative importance of various paths for any situation before the histories of approach to equilibrium can be determined. Otherwise a few missing links in the reaction chains can result in misleading conclusions, as evidenced by some of the previous work on the subject. In the present paper, the relative importance of several reaction paths leading to dissociation and ionization of oxygen, nitrogen, and nitric oxide is examined in light of the most recent specific rate information. Numerical results for temperature, density, and chemical composition profiles behind steady normal shock waves in air are presented for various velocity-altitude regimes. The thermal effect of interaction between molecular vibrational relaxation and other processes is included. The results, which readily demonstrate the important role of exchange reactions, are compared with earlier works and with recent shock tube experiments. The significance of these results in high-altitude hypersonic flight is discussed.

* Sponsored by the Ballistic Missile Division, Air Research and Development Command, U. S. Air Force.

A11. Rotational and Vibrational Relaxation in Diatomic Gases.* J. G. PARKER, *Applied Physics Laboratory, The Johns Hopkins University*.—Calculations of rotational and vibrational relaxation times for gases composed of homonuclear diatomic molecules have been carried out. The treatment is based totally on classical physics so that the results obtained are valid at temperatures sufficiently high that quantum-mechanical effects may be ignored. Results of this analysis indicate that the number of collisions required to attain equilibrium rotationally Z_R is independent of temperature, depending only on molecular constants, while the number involved in the equillbrium of vibration Z_V is decidedly temperature dependent. The theoretical expression for Z_V contains the same molecular constants appearing in the formula for Z_R, so that a connection between Z_V and Z_R may be established. Comparison of theory and experiment is made for the gases chlorine, nitrogen, and oxygen.

* Supported by the Bureau of Ordnance, Department of the Navy.

A12. Adiabatic Functions for Real Gases at High Temperatures. ADOLF R. HOCHSTIM, *Convair, San Diego*.—Adiabatic gammas for air were tabulated by the author. These functions, together with ratio of enthalpy to internal energy, reduce for an ideal cold gas to the constant ratio of specific heats. It was found that for an isentropic expansion in partially dissociated and ionized air in equilibrium, the result in using variable gammas can be approximated to a good degree by the use of at least two different constant gammas and constant ratio of enthalpy to internal energy. These constants were taken from stagnation point. The following inequality relation of gammas was found to hold for high-temperature gases:

$$\frac{C_P}{C_V} \geq \left(\frac{\partial \ln P}{\partial \ln \rho}\right)_S \geq \left(\frac{\partial \ln T}{\partial \ln \rho}\right)_S + 1 \geq \left[1 - \left(\frac{\partial \ln T}{\partial \ln P}\right)_S\right]^{-1} > 1.$$

MONDAY AFTERNOON AT 2:30

(P. P. WEGENER presiding)

B1. Steady Rotational Flow of a Heavy Incompressible Fluid. CARL ECKART, *Scripps Institution of Oceanography*. (30 min.)

B2. Onset of Thermal Convection in a Radiating Atmosphere.* EDWARD A. SPIEGEL, *University of California* (introduced by John A. Crawford).—A radiative heat transfer equation[1] is introduced into the study of the convective instability of a horizontal, radiating fluid layer. The development generally parallels the classical work of Rayleigh[2] and its extensions by Pellew and Southwell.[3] Thus the Boussinesq approximations are introduced and the investigation therefore only applies to layers whose thickness is much less than one scale height. An equation of marginal stabillty is derived and it is seen that convection may arise when a nondimensional quantity analagous to the Rayleigh number exceeds a certain critical value. Critical values of the instabillty parameter and wavelengths of the most unstable cellular disturbances are

computed for several optical thicknesses of the layer by means of a variational principal. Approximate expressions are also derived from the physical interpretation of the instability parameter as a ratio of buoyancy force to viscous force.

* Partially supported by the Office of Naval Research.
[1] E. A. Spiegel, Astrophys. J. **126**, 202 (1957).
[2] Lord Rayleigh, Phil. Mag. **32**, 529 (1916).
[3] A. Pellew and R. V. Southwell, Proc. Roy. Soc. (London) **A176**, 312 (1940).

B3. Nonlinear Convective Effects in a Constrained Fluid. G. VERONIS, *Woods Hole Oceanographic Institution* (introduced by W. V. R. Malkus).—An investigation is undertaken into the finite amplitude behavior of a rotating layer of fluid heated uniformly from below and cooled from above. The rotation is a constraint which effectively stabilizes the fluid, i.e., the vertical temperature gradient necessary for instability to infinitesimal perturbations is larger in the case of the rotating fluid than it is for the nonrotating fluid. However, after instability the finite amplitude motions which occur can reduce the constraint of rotation. Indeed, this destabilizing effect can be so strong that in some cases the fluid will become unstable to finite amplitude disturbances for a value of the external (eigen) parameter lower than that which corresponds to instability due to infinitesimal perturbations. In the present problem viscosity is necessary for the release of potential energy. The analysis indicates that this energy releasing role of viscosity is necessary for the occurrence of a finite amplitude instability.

B4. Axisymmetric Free-Convection Temperature Field along a Vertical Thin Cylinder.* FRANCIS R. HAMA, JOHN V. RECESSO, AND JEAN CHRISTIAENS, *University of Maryland*.—With a view to studying the effect of strong transverse curvature on boundary-layer problems, the axisymmetric free-convection problem along a vertical thin cylinder is investigated theoretically as well as experimentally. A theory is developed as an extension of the Pohlhausen solution of a thick axisymmetric laminar boundary layer by Mark and by Glauert and Lighthill. Experiments consist of a thermocouple survey of the temperature field over an electrically heated brass cylinder of $\frac{1}{4}$-in. diam and 10-ft height and an interferometric study of the density field over a bare tungsten wire of 0.02-in. diam and 5-ft height. The thermal-layer thicknesses are about five and fifty times the radii of the cylinders, respectively. Experimental results of the local heat-transfer coefficient are in excellent agreement with the theory. This, in turn, justifies the theories of laminar boundary layer along a thin cylinder.

* Supported by the U. S. Air Force Office of Scientific Research.

B5. On Free Surface Oscillations in a Rotating Liquid. J. W. MILES, *University of California* (introduced by S. A. Schaaf).—The disturbed motion of a liquid having a free surface in a vertical, rotating, circular cylinder and an equilibrium distribution of velocity corresponding to rigid body rotation is studied in linear approximation. It is shown that a vertical gradient of velocity necessarily generates vorticity, whence the disturbed motion cannot remain irrotational. (Earlier studies of this problem were based on shallow water theory, in which approximation the disturbed motion can remain irrotational.) The natural frequencies for the free surface oscillations are studied in some detail for a deep tank (say depth$\gg$diameter), and it is found that one effect of rotation is to split the pairs of frequencies (that would have been of equal magnitude and opposite sign) for the nonrotating liquid. In addition, new resonant frequencies are found that have no counterpart for a nonrotating liquid and for which the motion does not fall off exponentially with depth. The results are applied to forced, transverse oscillations of the tank, and explicit solutions are given for three special cases.

B6. Distribution of Particle Velocities in Ocean Waves.* J. P. RUINA, B. L. HICKS, N. KNABLE, AND G. S. NEWELL, *University of Illinois*.—Sea clutter was observed by the Control Systems Laboratory with an airborne, coherent, X-band radar for a variety of sea states. The power spectrum of the clutter may be interpreted as the distribution of radial velocities of the scatterers within the illuminated patch. The scatterers consist probably of the small waves and also, for heavy enough sea states, of the material associated with whitecaps. The sea clutter data collected by CSL can best be summarized by the equation $\Delta_0 = DH_{\frac{1}{3}}/T_m$ where Δ_0, D, $H_{\frac{1}{3}}$, and T_m refer, respectively, to the half-width of the velocity distribution, a dimensionless constant equal to 11 ± 1, the "significant wave height", and the period corresponding to the maximum of the energy spectrum plotted against frequency. The half-width was also found to be approximately proportional to wind speed. Less than one-half of the observed width of the velocity distribution can be attributed to the (orbital) *particle* velocity of the water, as computed from the Neumann spectrum. The contribution to the width made by drift and white cap velocities is unknown. Range-frequency displays of the clutter spectra also yield several kinds of information about the sea surface, though of a more qualitative nature.

* Performed under a Joint Services contract administered by the Signal Corps.

B7. Energy Spectrum of Small Wind Waves.* B. L. HICKS AND E. A. HUBER, *University of Illinois*.—Analysis of available experimental data in the range of frequencies $f = 0.5$ to 12 cps indicates that, for large enough values of the average wind speed V or average fetch F, the spectral energy density $\varphi^\alpha f^{-5}$ and is independent of V and F. For small values of V or F, $\varphi^\alpha f^q V^3 F^{1.5}$ where $q > 0$. In the former case the acceleration of gravity is the only physical parameter that affects φ. In the latter case, a second parameter must enter, presumably, a viscosity. Both the position of the maximum of the spectrum and the wave energy $E = \int_0^\alpha \varphi(f) df$ appear to vary slowly with V and F throughout the range of these variables (1–15 ft/sec and 50–2000 ft). In the past it has been believed that the energy of the (longer) wind waves on the ocean "saturates," for a given wind speed, if the fetch is increased sufficiently. No such "saturation" of the energy of the small waves has been observed. For capillary wind waves ($f > 16$ cps), preliminary CSL data agree with $\varphi^\alpha f^{-5/2}$, which is the dependence expected if the spectrum depends only upon (coefficient of surface tension)/(density). When white caps occur, however, much larger wave energies are observed than in the absence of white caps. The several possible explanations of this effect have not yet been tested.

* Performed under a Joint Services contract administered by the Signal Corps.

B8. Contribution to the Theory of Viscous Lifting. J. F. OSTERLE, *Carnegie Institute of Technology* (introduced by S. Corrsin).—A recent paper[1] revives interest in the problem of viscous lifting by describing experiments conducted on a lifting device consisting of a continuous belt rising vertically out of a reservoir of liquid. A film of the liquid is drawn up by the belt, presumably by the action of viscosity. In these experiments the flow in the film was regulated by means of an adjustable obstruction. It was found that as the obstruction is gradually removed the flow increases up to a certain critical value at which time the film springs free from the obstruction and no further increase in flow is possible. The author offers no explanation for this flow limit except to note that it is equal to the flow which would obtain in a free film. This paper presents a detailed analysis of the flow past the obstruction from which it is possible to predict the limiting flow. Surface tension effects are neglected and the results for the cutoff flow appear to be somewhat low.

[1] J. J. van Rossum, Appl. Sci. Research 7, Sec. A, No. 2–3 (1958).

B9. Critical Heat Flux in Pool Boiling.* T. K. SLAWECKI, *M. S. V. D. General Electric Company* (introduced by J. Farber).—Hydrodynamic stability of the vapor-liquid interface in the transition region of pool boiling has been analyzed theoretically. The resulting stability criteria were used to obtain equations for the Leidenfrost point (onset of film boiling) and the maximum heat flux point. These equations agree in form to the empirical equations used in the past to correlate experimental heat transfer data and those derived by means of dimensional differential analysis.

* Supported by the Ballistic Missile Division of the U. S. Air Force.

B10. Spark Stabilization by a Gas Vortex.* C. COBB, J. CHAMBERS, AND V. BLACKMAN, *Giannini Research Laboratory.*—A rotating mirror camera and a Kerr cell camera have been used to study photographically the buildup of a spark channel in a gas vortex. The spark is initiated by discharging either a low inductance capacitor or a length of coaxial cable between electrodes at either end of a cylindrical chamber which is one-half inch in diameter and from one inch to one-eighth inch in length. The coaxial cable can give a square current pulse with a duration of up to 3 μsec. The vortex is formed by injecting gas tangentially into the cylindrical chamber through an orifice in the wall and allowing the gas to escape through an axial orifice in the electrodes. The pressure distribution has been determined over a wide range of inlet and outlet conditions by means of movable pressure taps. Radial pressure gradients are as high as 4000 psi/inch with a minimum pressure on the axis of 3 psia when the flow exhausts into atmospheric pressure. Photographs will be presented to illustrate the stabilizing influence of the vortex. This arrangement is also being used to study the propagation of a cylindrical shock into a known pressure gradient.

* This work was supported by the U. S. Air Force Office of Scientific Research.

B11. Shock Stand-Off Distance in Slip Flow. S. A. SCHAAF AND E. S. MOULIC, *University of California.*—The stand-off distance of detached shocks in front of spheres and cylinders in supersonic flow at very low Reynolds numbers has been investigated by means of the after glow and free molecule probe techniques in the Berkeley low-density wind tunnel. For moderately rarefied flow, there is a shock zone followed by an essentially inviscid region and finally a boundary layer on the surface of the sphere or cylinder. Under these conditions, the center of the shock zone stands off from the boundary layer displacement thickness by the usual distance as given by inviscid theory. For more highly rarefied flows, the shock zone and the boundary layer merge in the vicinity of the forward stagnation point. For highly rarefied flows the shock wave disappears.

MONDAY EVENING AT 8:00

(D. W. KERST presiding)

C1. Recent Theoretical Developments in Plasma Stability. MARSHALL ROSENBLUTH, *General Atomic.* (30 min.)

C2. Aerodynamic Facilities Utilizing Electric Arc Techniques. RONALD SMELT, *Lockheed Aircraft Corporation.* (30 min.)

TUESDAY MORNING AT 9:00

(G. B. SCHUBAUER presiding)

D1. Transition to Turbulence in Circular Couette Flow. DONALD COLES, *California Institute of Technology.* (30 min.)

D2. Expansion of the Turbulent Velocity Field in Ideal Random Functions. I. ARMAND SIEGEL AND WILLIAM C. MEECHAM, *University of Michigan.*—We apply a fundamental suggestion of Wiener[1] in statistical turbulence theory to homogeneous isotropic fields. Let x be the four-dimensional radius vector in space-time. The ideal random function in four dimensions, $A_i(x)$, is defined as follows. Its integral over any space-time region is Gaussianly distributed with variance equal to the four-dimensional volume of the region, and is statistically independent of the similar integral over any non-overlapping region. (This is the rigorously undefined space-time derivative of the four-dimensional Wiener random function.) Then the expansion

$$U_i(\mathbf{x}) = U_{0i}(\mathbf{x}) + \int K_{i\alpha}(\mathbf{x}-\mathbf{x}_1)A_\alpha(\mathbf{x}_1)d\mathbf{x}_1 + \int\int K_{i\alpha\beta}(\mathbf{x}-\mathbf{x}_1, \mathbf{x}-\mathbf{x}_2)A_\alpha(\mathbf{x}_1)A_\beta(\mathbf{x}_2)d\mathbf{x}_1 d\mathbf{x}_2$$

provides a formal representation more than general enough to encompass the stationary homogeneous velocity fields studied in turbulence theory. The field is in this way defined through the ordinary (i.e., not random) functions $K_{i\alpha}$, $K_{i\alpha\beta}\cdots$. The successive terms are, for nearly Gaussian distributions, successively decreasing corrections; the series is the functional analog of a power series.

[1] N. Wiener, *Fifth International Congress for Applied Mechanics* (John Wiley and Sons, Inc., New York, 1939).

D3. Expansion of the Turbulent Velocity Field in Ideal Random Functions. II.* WILLIAM C. MEECHAM, *University of Michigan,* AND ARMAND SIEGEL, *Boston University.*—The pressure term in the Navier-Stokes equations for incompressible flow is first eliminated. The velocity field for a member of the ensemble is then written in terms of a "power" series of ideal random functions (see preceding abstract). The necessary restrictions for the determination of the ordinary functions K in the expansion are obtained either by constructing correlation tensors following the method of von Karman-Howarth or from the Navier-Stokes equations directly. When only the lowest order nonvanishing terms are retained, one finds Chandrasekhar's[1] equation (obtained by him using a different method). This result is to be expected since the velocity field

to lowest order obeys a joint-normal distribution. The present method gives a systematic technique for the correction of the Chandrasekhar result. It is interesting to note that the first term also gives the first hypothesis used by Kraichnan[2] in his work on the theory of turbulence.

* This research was supported jointly by the U. S. Air Force Office of Scientific Research and by Project Michigan, a Department of Army sponsored project of The University of Michigan.

[1] S. Chandrasekhar, Proc. Roy. Soc. (London) **A229**, 1 (1955).
[2] R. H. Kraichnan, Phys. Rev. **109**, 1407 (1958).

D4. Visualization of the Transition to Turbulence in a Free-Convection Boundary Layer. E. R. G. ECKERT, G. P. HARTNETT, AND T. F. IRVINE, JR., *University of Minnesota* (introduced by J. R. Winckler).—It had been established by E. R. G. Eckert and E. Soehngen that the initial phases of the transition process in a free-convection boundary layer can be clearly observed through a Zehnder-Mach interferometer. Wavelength, velocity, and frequency of the instability waves were established in this way. The later phases of transition-rollup into vortices and breakup into irregular turbulent fluctuations—which because of their three-dimensional character cannot be observed with the interferometer—have now been studied by injection of smoke threads into the boundary layer. A film will be shown on these studies which include natural transition as well as transition tripped by a two-dimensional roughness element. The film shows clearly how the instability waves roll up into vortices with axis normal to the flow direction. Further downstream vortices with an axis parallel to the flow direction appear randomly, which process introduces three-dimensionality. The final breakup into turbulence appears to be quite rapid. Numerical evaluations concern the value of the critical Grashof number as influenced by a roughness element.

D5. Extended Applications of Hot-Wire Anemometry to High-Speed Turbulent Boundary Layers.* M. V. MORKOVIN AND R. E. PHINNEY, *The Johns Hopkins University* (introduced by L. S. G. Kovasznay).—A hot-wire anemometer represents a nonlinear system consisting of the flow-field, the wire, and the associated instrumentation. The method of extracting information from a heated thin wire, cooled by an unsteady compressible flow, based on the concept of local linearization around each operating point of the system, was extended to wires in yaw and to constant-temperature systems. An X probe was designed and used for boundary-layer measurements from which the Reynolds stress and the energy flux can be obtained. The results appeared to be consistent with plausible extrapolations of low-speed concepts. Procedures for measurements with single normal wires were clarified and improved. The satisfactory agreement between results of measurements with sleeved and bare wires made both of tungsten and platinum−10% rhodium, with a variety of holders, provided further verification of the rather complicated methods of measurement and interpretation. The techniques were applied to the study of the fluctuation structure of a thick, fully developed, turbulent boundary layer at $M_1=1.77$. With the aid of a technique for partial calibration *in situ*, it was established that previously inferred maxima of fluctuations in the supersonic region do not exist.

* This work was sponsored by the U. S. Air Office of Scientific Research.

D6. Similarity Spectra in Isotropic Turbulence Using Kovasznay's Transfer Function. W. H. REID, *Brown University*, AND D. L. HARRIS, *David Taylor Model Basin*.—Similarity solutions are given for the energy spectrum and transfer function in the initial period of decay for a range of values of the Reynolds number using the transfer theory suggested by Kovasznay. Because of the simple form of the theory, the solution can be obtained in closed form for all values of the Reynolds number, and this exact solution is useful for some analytical purposes. To obtain detailed results, however, it is more convenient to employ numerical methods. It is found, for example, that the skewness factor S of $-\partial u_1/\partial x_1$ varies only between $3.93K_K$ for $R_\lambda=0$ and $2.86K_K$ for $R_\lambda=\infty$, where K_K is the arbitrary constant occurring in the theory. A comparison is also made between the present results and those obtained by using Heisenberg's transfer theory.

D7. Experiment on Transition from Turbulent to Laminar Pipe Flow. MERWIN SIBULKIN, *Convair Scientific Research Laboratory*.—A ¼-in. diam tube, a relatively short diffuser, and a 1-in. diam tube were connected in series. The direction of flow was from the smaller to the larger tube. The air flow rate was set so that while fully developed turbulent flow existed in the smaller tube, the Reynolds number in the larger tube was below critical. The subject of the experiment was to observe the effects of this lower than critical Reynolds number on the initially turbulent flow. Two diffusers, a 3° half-angle cone and a 90° sudden expansion were used to try to separate expansion from Reynolds number effects. Measurements were made of the mean velocity and longitudinal velocity fluctuations on the tube centerline as a function of distance downstream of the diffuser and of pipe Reynolds number. It was found that the ratio of centerline velocity to mean flow velocity $u_c/\bar{u}$ increased with downstream distance indicating that the velocity distribution was changing from the relatively flat turbulent profile toward the parabolic laminar profile, $u_c/\bar{u}=2$. Similarly, the turbulent velocity fluctuations decayed downstream of the diffuser. Both measurements showed that laminar pipe flow was approached more rapidly at lower Reynolds numbers.

D8. Systematic Approximation of the Linear Boltzmann Equation.* E. P. GROSS AND E. A. JACKSON, *Brandeis University*.—A systematic procedure is proposed for approximating the linear Boltzmann equation. The Nth approximation replaces the symmetric portion of the collision kernal, $K(c,c_1)$,[1] by a bilinear series of orthonormal velocity polynomials of order N or less. In low-order approximation the present method provides a justification of the linearized form of the equation Bhatnagar, Gross, and Krook used to approximate the Boltzmann equation. This equation has been extended by Krook and Fishman, and applied to a number of problems by them and Gross, Jackson, and Ziering. Jackson showed, using this equation, that the distribution function for the Couette flow problem is a nonanalytic function of the velocity at low densities, and as a result, the flow velocity is a nonanalytic function of the mean free path λ [being of the form $(x/\lambda)\log(x/\lambda)$]. This result is not obtained by the standard method of approximating the distribution function by a polynomial expansion, as in the Chapman-Enskog or Grad schemes. The present method will likewise make it possible to treat much more accurately low-density gas dynamics, high-frequency sound propagation, and boundary value problems.

* Research supported by the U. S. Air Force Office of Scientific Research.

[1] S. Chapman and T. G. Cowling, *The Mathematical Theory of Non-Uniform Gases* (Cambridge University Press, New York, 1953), Sec. 7.6.

D9. On the Linearization of Boltzmann's Equation in Relation to Adiabatic and Isothermal Behavior.* J. M. BURGERS, *University of Maryland*.—To linearize Boltzmann's equation the collision terms on the right-hand side are replaced by a simplified expression,[1] and the distribution function for the velocities is split into an undisturbed part F_0 and a small disturbance (for convenience a single type of monatomic molecule is taken). As restoring term on the right-hand side a Maxwellian distribution is used, not $=F_0$, but with a number density, mean flow velocity, and mean temperature to be found from the condition that the conservation equations must be satisfied. Such linearized equations are applied to the behavior

of a gas subjected to a periodic impressed force field. When the conservation conditions are worked out, a result is obtained which can be adapted to adiabatic or to isothermal behavior, depending on ratios formed out of the collision frequency and wave number of the impressed force, and mean molecular speed. For an impressed electric field the relative change in number density is not always given by $\pm e\varphi/kT$ (φ: potential).

* Partial outcome of work supported by the U. S. Air Force Office of Scientific Research.

[1] M. Krook, Phys. Rev. **99**, 1896 (1955); E. P. Gross and M. Krook, Phys. Rev. **102**, 593 (1956).

D10. Simplified Solution of the Orr Sommerfeld Equation. R. BETCHOV, *Douglas Aircraft Company.*—The stability of an incompressible boundary layer along a flat plate can be studied by simple means. An inviscid approximation is obtained first. It is then completed by a viscous correction at the wall and a correction at the critical layer. Friction at the wall is the cause of a process of diffusion and transport of vorticity. The effective transport velocity changes sign at the critical layer, and this has an essential effect on the repartition of vorticity. At the critical layer the friction redistributes the vorticity of the inviscid motion, and the net effect is that of a special row of vortices. The inviscid solution and the two viscous effects are superposed in accordance with the boundary conditions. This leads to approximate expressions for the eigenvalues or for the solution itself. In general, the inviscid motion is indifferent, the process of vorticity diffusion is destabillzing, and the special row of vortices at the critical layer is stabilizing.

D11. On the Second Approximation to the Stress and the Heat Flux in a Gas.* HSUN-TIAO YANG, *University of Southern California.*—The classical expressions for the second approximation to the stress and the heat flux in a gas are those of Burnett. More recent work in the kinetic theory of gases consists of Grad's thirteen-moment equations and Ikenberry-Truesdell's iterates. The Burnett equations may be deduced from the latter two systems, which are, therefore, more general. All these three approaches are approximating the Boltzmann equation by partial differential equations for the flow variables. Another way is to approximate the Boltzmann equation directly by replacing the collision integral by a simple collision term. This results in the simplified partial differential equation of Bhatnagar, Gross, and Krook for the molecular distribution function. The second approximation to the stress based on this simplified collision equation is obtained by Burgers and that to the heat flux is obtained here. It is shown that these second approximations based on the simplified collision equation are compared favorably with those based on the full Boltzmann equation.

* Supported by the Office of Scientific Research.

TUESDAY AFTERNOON AT 2:30

(MARSHALL ROSENBLUTH presiding)

E1. On the Stability of Plasma in Static Equilibrium. M. D. KRUSKAL AND C. R. OBERMAN, *Project Matterhorn, Princeton University.*—Criteria useful for the investigation of the stability of a system of charged particles are derived from the Boltzmann equation in the small m/e limit. These criteria are obtained from the examination of the variation of the energy due to a perturbation, when subject to the general constraint that all regular, time-independent constants of the motion (including the energy) have their equilibrium values. The first-order variation of the energy vanishes trivially, and the second-order variation yields a quadratic form in the displacement variable ξ (which may be introduced because of the well-known properties of this limit). The positive-definiteness of this form is a sufficient condition for stability. Several theorems are stated comparing stability under the present theory with that under conventional hydromagnetic fluid theories where heat flow along magnetic lines of force is neglected. Generalizations can be made to systems where the effect of collisions is included.

E2. Hydromagnetic Stability of a Streaming Cylindrical Plasma. N. J. ZABUSKY, *California Institute of Technology.*—Dispersion relations are found for three related problems in which the effects of *mass motion* are considered. The equilibrium configuration about which small amplitude perturbations were studied consisted of a dissipationless fluid flowing in an infinite cylinder, which also contains a uniform longitudinal field. Problem (1) is an extension of earlier work,[1] where the plasma is bound by a current sheet and includes electromagnetic radiation and compressibility effects. Problems (2) and (3) assume that the plasma is bound by a nonconducting compressible medium and has the equilibrium magnetic field $\mathbf{B}=(O,B_{\theta a}r/r_a,B_{za})$ and equilibrium velocity $\mathbf{V}=(O,V_{\theta a}r/r_a,V_{za})$. In (2) incompressibility is assumed, while in (3) the assumption of compressibility is made [V, $V_A=B/(\mu_0\rho_p)^{\frac{1}{2}}$ < sonic speed] so that a matrix-perturbation expansion can be made about the incompressible solution. The effects of the moving boundary are included. It was found convenient to use the hydromagnetic pressure, $p+B^2/2\mu_0$ as the basic dependent variable and to use the hydromagnetic equations in a symmetric form similar to that given by Elsasser (1954). These equations were extended to a quasi-symmetrical form for treating the compressible medium.

[1] Kruskal and Schwarzschild, Proc. Roy. Soc. (London) **A223**, 354 (1954).

E3. Stabilization of a Pinch by an Alternating Magnetic Field. ERICH S. WEIBEL, *Space Technology Laboratories* (introduced by E. B. Turner).—This paper presents an analysis of the stability of a plasma column which is confined by a longitudinal magnetostatic field on which is superimposed an oscillating transverse magnetic field. The fields are produced by suitably energized conductors wound on a cylinder which is coaxial to the plasma and surrounds it. The plasma is assumed to be perfectly conducting and its interior is field free. It is found that this confinement is stable.

E4. Plasma Oscillations of a Large Number of Electron Beams. JOHN DAWSON, *Project Matterhorn, Princeton University.*—Electrostatic plasma oscillations of a large number of electron beams are investigated. The problem of approximating a continuous velocity distribution by means of a large number of beams is considered in detail. It is found that the beams are always unstable. However, the larger the number of beams used in the approximation the slower are the growth rates of most of the modes. The velocity distribution may be said to be stable if the growth rates of all unstable modes go to zero as the number of modes go to infinity; otherwise it is unstable. The limiting results are in agreement with those of Landau.[1] This treatment is closely related to the normal mode treatment of the Boltzmann equation given by Van Kampen.[2]

[1] L. Landau, J. Phys. U.S.S.R. **10**, 25 (1946).
[2] N. G. Van Kampen, Physica **21**, 949–963 (1955).

E5. Plasma Containment in a Toroidal Configuration by a dc-rf Field Combination. V. JOSEPHSON, *Space Technology Laboratories* (introduced by E. B. Turner).—A basic requirement for an economic fusion reactor is an efficient means of hot plasma containment for a time sufficient for the fusion reaction to be completed. A plasma confined by a combination of a dc longitudinal electric field surrounded by an rf transverse field with this field greater than the longitudinal field is stable as shown by E. S. Weibel.[1] Since the extreme difficulty of coupling rf power to a low impedance load such as a plasma is the chief obstacle in the above confinement method, it would be ideal to bypass this coupling problem by generating the rf power immediately around the load. Preliminary studies indicate that it is feasible in the following manner. A "pinched" plasma is produced in a toroidal discharge tube by application of a "slow" electric field. This assembly is located inside of a klystron-type cavity which serves as the catcher cavity of a klystron or Resnatron type amplifier. Here, rf power (with the desired transverse field around the plasma) is generated by interaction with a bunched electron beam. Although the efficiency of such a system will probably be low, the usual power transfer loss in conventional power systems is bypassed here, making this system still attractive as a plasma containment mechanism.

[1] Paper E3 presented at his meeting.

E6. Transient Temperature Variations during the Self-Heating of a Plasma by Thermonuclear Reactions.* HOWARD D. GREYBER, *M. S. V. D. General Electric Company.*—The ion and electron temperature variations in an idealized controlled thermonuclear reactor burning various ratios of deuterium and tritium are calculated. The variation in the fraction of energy deposited to the nuciear and electron gases with temperature is specifically included. One qualitative result is that it would be unsafe to assume nuclear temperature always equal to or greater than electron temperature for a nuclearly reacting plasma with tritium concentration greater than 10%.

* Research done at University of California Radiation Laboratory, Livermore, California, and supported by the U. S. Atomic Energy Commission.

E7. Distortion of Axisymmetric, Poloidal Magnetic Fields by Uniform Flow of a Conducting Fluid. BURTON D. FRIED, *Space Technology Laboratories.*—In magnetohydrodynamic flow problems, distortion of the magnetic field depends on $R_M=4\pi\sigma vL/c^2$ while perturbation of the flow involves $Q=R_MB^2/8\pi\rho v^2$. Large field distortions with small flow perturbations are possible if $R_M\gg1$, $Q\ll1$. For uniform flow in an axisymmetric poloidal field ($B_\theta=0$) with external current density $J_\theta(r,z)$ the exact vector potential $A=A_\theta$ is given by $A(r,z)=\int_0^\infty dr'\int_{-\infty}^\infty dz' r' G(r',z';r,z)J_\theta(r',z')$ with Green's function

$$G=(4\pi I/c)\int_0^\infty dx x J_1(xr)J_1(xr')(\beta^2+4x^2)^{-\frac{1}{2}} \times \exp\{-\tfrac{1}{2}|z-z'|[(\beta^2+4x^2)^{\frac{1}{2}}\pm\beta]\}$$

where $\beta=4\pi\sigma v/c^2$ and the upper sign is for $z>z'$, the lower for $z<z'$. The integrand $\to 0$ exponentially for large x, facilitating numerical quadrature. The resulting fields for the case of a single turn coil and for a semi-infinite solenoid will be shown. [For $\beta=0$ and $J_\theta=\delta(z)\delta(r-a)$, A reduces to the classical formula for a single turn coil.]

E8. Velocities in Small Tubes of Electrically Excited Shock Waves in Deuterium. E. JOHN EASTMOND AND EUGENE B. TURNER, *Space Technology Laboratories.*—A device, developed in this laboratory, for attaining very high temperatures in hydrogen and deuterium plasmas requires the injection of an ionized gas of known characteristics, the calculation of which requires a knowledge of the shock velocity. The shock waves were produced by electrical discharge systems similar to those described by Josephson.[1] The energy was stored in a 3.2-μf low-inductance capacitor charged to 30 kv. The breakdown of a triggered spark switch allowed a maximum current of 150 000 amp to flow in a 3-in. diam tapered discharge tube with a close-fitting coaxial return. The shock velocities were measured with an image-converter streak camera in small tubes of $\frac{1}{2}$-, $\frac{3}{4}$-, and 1-in. diam which projected about one tube diameter through an end plate on the tapered tube. The shock velocities, which ranged from 4 cm/μsec at 12-μ to 7.5 cm/μsec at 200-μ pressure, were higher in the larger diameter tubes—especially at the lower pressures, and were only slightly less than those in a 3-in. diam tube using the same tapered-discharge-tube drivers.

[1] V. Josephson, J. Appl. Phys. **29**, 30 (1958).

E9. Plasma Propulsion by a Rapidly Varying Magnetic Field.* MILTON M. KLEIN, *M. S. V. D. General Electric Company.*—An investigation has been made of the motion of a plasma under the action of a magnetic field from a rapidly varying current carried by a circular coil. For the case where the plasma is assumed completely diamagnetic velocities in the range 10^6 cm/sec to 10^7 cm/sec may be attained for a frequency of 1 Mc and a maximum current of order 10^4 amp. The efficiency of transfer of energy from the magnetic field to the plasma is in the range 5 to 10%. Numerical solutions for the diamagnetic case have been obtained in similarity form from which information for a particular physical situation may easily be obtained. For the case where the plasma is not assumed diamagnetic, the gas is partially ionized by the magnetic field and forms a current sheath which moves forward into the neutral gas. Preliminary calculations indicate that the rate at which neutrals move into the sheath is much greater than the rate at which neutrals are ionized. Neutrals therefore accumulate in the sheath, and are partially lost by diffusion through the sheath with a consequent decrease in the amount of plasma being accelerated.

* Supported by the Ballistic Missile Division of the U. S. Air Force.

E10. Shock Tube Driver with a Plasma Jet Supply.* GORDON L. CANN, *California Institute of Technology* (introduced by C. B. Millikan).—A plasma jet that will operate from a 100-kw (300-v) dc power source has been designed and constructed. Helium gas is heated in the jet and fed directly into the driver of a shock tube. An operating cycle of about 10 sec is required to raise the pressure in the driver from 1 mm of Hg to 100 psi. The electrodes are not water-cooled and do not show any appreciable burning after 5 or more runs. Preliminary experiments indicate that the gas in the driver can be heated fairly uniformly in this way to a temperature higher than could be obtained by heating the whole driver structure. This development is aimed at obtaining driver performance comparable or better than that obtained from combustion shock tube drivers.

* Supported by the Office, Chief of Ordnance, and the Office of Ordnance Research.

E11. Structure of Hydromagnetic Shock Waves in a Cold Plasma. LEVERETT DAVIS,* R. LUST, AND A. SCHLUTER, *Max-Planck-Institut fur Physik, Gottingen.*—The steady, time-independent flow normal to a magnetic field of a cold (no thermal motions) quasi-neutral gas consisting of ions and electrons is investigated neglecting collisions but not neglecting the inertial effects associated with the electric current. When the particle trajectories do not make loops, a rigorous solution of the resulting nonlinear equations may be expressed in terms of elliptic functions. Both wave trains and solitary waves are found, all solutions being symmetrical about maxima and minima in the field strength. The wavelengths are of the order of the gyro-radius. The relation of these

waves to hydromagnetic shock waves in low density, cool plasmas is considered and it is concluded that the entire shock will have a thickness determined by the product of the mean time between collisions and the gas velocity with respect to the shock front. This region will be occupied by a wave train whose structure has dimensions of the order of the gyroradius but which differs from the waves considered above in that they are nonstationary in any frame of reference.

* National Science Foundation Fellow. Permanently at California Institute of Technology.

E12. Low-Temperature Plasma Tunnel Using Mercury Vapor and Radio-Frequency Excitation. H. U. ECKERT, *Convair Scientific Research Laboratory.*—In an effort to avoid the high-temperature problems of arc tunnels and the time limitations of shock tubes, production of a strong electrodeless discharge in the divergent portion of a Laval nozzle is discussed as an alternate method for generating plasma flow. This eliminates cooling of the throat and flow contamination by electrode material. While most of the energy from the excitation field will go to the electron component the main body of the gas can still be heated sufficiently to counteract cooling and possible liquefaction of the flow during expansion. One can, therefore, use a vaporized liquid instead of a permanent gas as testing medium and operate the tunnel on the two-phase principle thus eliminating the need for large vacuum pumps. The most suitable liquid appears to be mercury because it is monatomic in the gas phase, has the desired vapor pressure range in a convenient temperature range, is comparatively easy to ionize, and is noncorrosive. A small tunnel built upon these considerations and some phenomena observed in its operation will be described.

TUESDAY EVENING AT 8:00

(F. N. FRENKIEL presiding)

Banquet of the Division of Fluid Dynamics

After-dinner speaker: ROGER REVELLE, **Man between Two Oceans**

WEDNESDAY MORNING AT 9:00

(W. C. GRIFFITH presiding)

F1. Similarity Parameters for Surface Melting of a Blunt-Nosed Body in a High-Velocity Gas Stream. LESTER LEES, *California Institute of Technology.*—By employing a simple model for the two-phase boundary layer produced by surface melting, "scaling laws" are obtained for the regime in which vaporization does not occur at the gas-liquid interface. When the liquid is fairly viscous, the gas boundary layer is virtually independent of the liquid-film. The temperature rise across this film depends not only on the local heat transfer rate, but also on the difference in total enthalpy across the gas boundary layer. Thus, tests in rocket exhaust jets may not simulate vaporization or film instability phenomena that could occur in flight. A preliminary study of the effect of mass addition to the gas phase shows that the amount of heat "blocked" by this process is also sensitive to the total enthalpy difference across the gas boundary layer. The possible increase in effective heat capacity with vaporization at the gas-liquid interface is quite substantial at a flight velocity of 20 000 ft/sec, amounting to a factor of about 5 for the laminar boundary layer at the forward stagnation point, and about 2 for a turbulent gas boundary layer at the body sonic point. This phenomenon can also be analyzed along the lines of the present study.

F2. Pressure Distributions on Blunt-Nosed Cones in Low-Density Hypersonic Flow.* L. TALBOT, S. A. SCHAAF, AND F. C. HURLBUT, *University of California.*—Pressure distributions were measured on a family of spherically blunted cones in the Mach number range $3.7<M<5.8$, and for Reynolds numbers based on nose radius and free stream conditions in the range $200<\mathrm{Re}<5000$. These data were compared with GALCIT measurements on similar cones at the same Mach numbers but at Reynolds numbers $6\times10^4<\mathrm{Re}<1.6\times10^5$. It was found that even at the low Reynolds numbers of the present tests the pressure distributions were given satisfactorily by modified Newtonian theory on the spherical portions of the cone, followed by a transition to the Kopal value on the conical portion. The transition zone between Newtonian pressure distribution and the Kopal value appears to be somewhat longer than the corresponding GALCIT pressure distribution, and there was slightly less over-expansion in this region. These differences may be attributable to viscous effects.

* This work was supported by the Bell Aircraft Corporation.

F3. Experiments on Supersonic Blunt-Body Flows.* JAMES M. KENDALL, JR., *Jet Propulsion Laboratory* (introduced by P. P. Wegener).—Recently, progress has been made in the theoretical calculation of the inviscid flow between the detached shock wave and the surface of a blunt body traveling at supersonic speed. Detailed experimental data are needed for comparison. Experiments have been made in the supersonic wind tunnels of the Jet Propulsion Laboratory on spheres, disks, and blunted cones over the Mach number range 1.8 to 5.0 in air. Surface pressures, shock wave shape and detachment distance, certain velocity gradients, the sonic line location, and some streamline paths were determined. The sonic line is found as the trace of the termination point of a weak shock generated by a probe ahead of the model. For a sphere, good agreement between theory[1] and experiment is found.

* Supported by the Department of the Army, Ordnance Corps, and the Department of the Air Force.

[1] M. D. Van Dyke, J. Aeronaut. Space Sci. **25**, 485 (1958).

F4. Supersonic Nozzle Flow of a Chemically Reacting Gas Mixture with Finite Reaction Rates.* PETER P. WEGENER, *Jet Propulsion Laboratory.*—Stationary supersonic nozzle flow of a mixture of nitrogen and nitrogen-dioxide at low concentration and measurements of the rate of recombination to nitrogen-tetroxide by optical methods have been discussed

previously.[1] Further experiments and analysis are described in this paper for flows where the reactant concentration is raised to 5% by volume, and the heat of reaction affects the flow markedly. It is again observed that the flow parameters have values between those predicted for either frozen flow or flow in chemical equilibrium. By measuring effective area and static pressure distributions, it is possible to determine all flow parameters from the one-dimensional equations of motion. Reactant concentrations and reaction rate constants found in this manner agreed with those determined independently by absorption measurements.

* Supported by the Department of the Army, Ordnance Corps, and the Department of the Air Force.
[1] P. Wegener, J. Chem. Phys. **28**, 724 (1958).

F5. Observations of Shock Tube Performance at Low Initial Pressure. RUSSELL E. DUFF, *Los Alamos Scientific Laboratory*.—An electron beam densitometer has been used to investigate the behavior of a conventional 1¾-in. i.d. shock tube operating at initial pressures of the order of 1 mm Hg. Most of the experiments were performed in argon with shock Mach numbers ranging between 1.2 and 7.0. The most striking observation was that the duration of flow before the arrival of the contact surface was proportional to initial pressure and independent of expansion chamber length. At an initial pressure of 0.5 mm Hg the observed duration varied between 600 μsec at $M_S=1.2$ and 20 μsec at $M_S=7.0$. The diaphragm pressure ratio required to produce a shock of velocity $M_S=1.6$ varied from 200 at an initial pressure of 0.25 mm Hg to 20 at an initial pressure of 50 mm Hg. For a given diaphragm pressure ratio the shock velocity decreased with tube length in a highly nonlinear manner. The density behind the shock wave was observed to increase significantly before the arrival of the contact surface under all conditions. This surprising shock tube behavior is believed related to severe laminar boundary layer development behind the shock wave at low initial pressures.

F6. Interferometric Study of Shock Tube Boundary Layers.* JOHN R. ASBRIDGE, *Lehigh University* (introduced by R. J. Emrich).—The boundary layers growing on the walls of a shock tube behind an advancing shock wave have been studied with a Mach-Zehnder interferometer. The investigation has been carried out in a ⅜-in.×4-in. shock tube, with the interferometer looking at the boundary layers on the 4-in. walls. Density profiles have been determined in the laminar, transitional, and turbulent boundary layer areas of flow for a number of shock strengths and initial densities. These profiles are compared with those predicted by Mirels. Effects due to roughness, and in particular, to joints in the tube, are considered in some detail. Free stream density variations are recorded, and in some cases, rapidly increasing free stream density is observed to be coincident with boundary layer transition.

* Supported by the Office of Naval Research.

F7. Vaporization Processes in the Hypersonic Laminar Boundary Layer.* S. M. SCALA AND G. L. VIDALE, *M. S. V. D. General Electric Company*.—In a paper on heat and mass transfer effects, Nusselt[1] credited Stefan with having first recognized the importance of diffusion in problems involving evaporation. Hence, some of the general aerophysical aspects of evaporation and sublimation have been known for approximately seventy-five years; however, the detailed investigation of the aerothermochemical aspects has remained as a field of contemporary research. During hypersonic flight, the net aerodynamic heat transfer into the surface of a vaporizing material depends critically upon the thickening of the boundary layer, due to the injection process, and the heat absorbing capacity of the chemical species evolved during vaporization. An analysis of the phenomenon is presented in which the pertinent laminar boundary layer equations for diffusion, convection, and thermal exchange are solved, subject to the appropriate physico-chemical constraints arising from the kinetics of vaporization. Utilizing these numerical solutions, one may estimate the behavior of an arbitrary material, subject to hypersonic flight conditions, provided only that one has an independent knowledge of certain minimum physico-chemical data. In addition, a universal solution is given, utilizing the least number of independent parameters, which defines the flight regimes where the vaporization process is diffusion controlled, kinetically limited, or both.

* Supported by the Ballistic Missile Division of the U. S. Air Force.
[1] W. Nusselt, ZAMM **10**, 105–121 (April, 1930).

F8. Transport and Thermodynamic Properties in a Hypersonic Laminar Boundary Layer.* SINCLAIRE M. SCALA AND CHARLES W. BAULKNIGHT, *M. S. V. D. General Electric Company*.—An accurate determination of the heat transfer and surface shear forces in a hypersonic laminar boundary layer depends upon the solution of the boundary layer equations at the surface of the vehicle. This requires, as auxiliary data, the transport and thermodynamic properties of the fluid medium. At the temperatures normally encountered in hypersonic flight, there is a paucity of experimental data, and hence these properties must be estimated using empirical models for the potential energy function which represents the molecular interactions between the chemical species present in the gas. Caclulations have therefore been made of the transport and thermodynamic properties of the components of dissociated air, utilizing the formulas of statistical mechanics, the Lennard-Jones 6:12 model for the molecular species where appropriate, and the rigid sphere model for the atomic species. These data were utilized in performing boundary layer analyses. Some typical results are presented here for the case in which dissociated air was treated as a binary mixture of "air atoms" and "air molecules."

* Supported by the Ballistic Missile Division of the U. S. Air Force.

F9. Experiment on the Stability of the Hypersonic Laminar Boundary Layer.* A. DEMETRIADES, *California Institute of Technology* (introduced by L. Lees).—The hydrodynamic stability of the laminar boundary layer over a sharp-lipped flat plate at zero incidence at a Mach number of 5.8 has been investigated with the aid of a hot-wire anemometer. Artificial disturbances of a periodic nature were created near the leading edge of the plate, and their amplification or decay was studied as a function of stream-wise distance, tunnel supply pressure, and disturbance frequency. It was found that for distinct ranges of the Reynolds number and the disturbance frequency such disturbances amplify, as also observed in the laminar boundary layer at lower Mach numbers. A "line of maximum amplification" was also discovered, but the selectivity of the hypersonic layer was found to be much lower than that of the subsonic layer, indicating that the disturbance amplification rates were very low in the present case. The wavelengths of the disturbances receiving maximum amplification are found to be one order of magnitude greater than the local boundary layer thickness.

* Carried out under the sponsorship of the Office Chief of Ordnance, and the Office of Ordnance Research, U. S. Army.

F10. Calculation of Perturbations in One-Dimensional Flow Fields and Some Applications. HAROLD MIRELS, *Lewis Research Center, NASA* (introduced by J. C. Evvard).—A general method is presented for determining perturbations of one-dimensional flows. The perturbations may be due to steady, or unsteady, mass addition, heat addition, body forces, and area variation. (Disturbances due to unsteady wall boundary layers are included.) The method consists of first writing

the flow field associated with an elemental mass source, heat source, body force, etc. The net disturbance at a point, due to an arbitrary spatial and temporal distribution of sources, is then found by integrating these elemental solutions along characteristic lines. Emphasis is placed on describing the application of the method to a variety of flow problems. These include finding (a) perturbations of a fluid for which the basic (unperturbed) flow is uniform; (b) perturbations of a fluid for which the basic flow contains a discontinuity (such as a shock wave, contact surface, flame front, etc.); and (c) perturbations of a fluid for which the basic flow contains several "centered" discontinuities (such as shock flows, piston driven shocks, burning initiated at a closed end, etc.). The present paper is an elaboration and extension of the method previously used by the author (NACA TN 3712) to determine attenuation in a shock tube.

F11. Transformations between Two-Dimensional and Axially Symmetric Real Gas Boundary Layers. JOSEPH J. SHEPPARD, JR., *Convair Scientific Research Laboratory* (introduced by M. F. Romig).—Relations are derived from first principles to transform the boundary layer equations for steady axially symmetric laminar flow of a compressible, viscous, heat conducting, real gas into the boundary layer equations for an equivalent two-dimensional flow. The resulting transformation is nearly identical to that first presented by Mangler for the special case of a perfect gas with constant properties. Real gas effects, including binary dissociation or ionization are included in the present transformation. No restrictions are placed on the variation of fluid properties with temperature and pressure. Relations for cases involving transpiration and mass transfer cooling are presented. Local thermodynamic equilibrium is assumed in the derivation. Applicability of the relations to special nonequilibrium cases is discussed. Quantitative rules defining the range of validity of the transformation are presented. A similar transformation for axially symmetric compressible turbulent boundary layers is presented. The latter does not require an assumption concerning the details of the turbulent dissipation process.

F12. Laminar Flow in the Entrance Region of a Porous Pipe.* H. L. WEISSBERG, *Oak Ridge Gaseous Diffusion Plant.*—The equation of motion for steady, incompressible, axially symmetric flow in a pipe with uniform wall suction or injection is expressed in terms of a "dimensionless stream function," $F(\zeta,\eta)=\psi(x,r)/\psi(x,a)$ where ψ is the usual stream function, x and r are cylindrical polar coordinates, a is the radius of the pipe, $\zeta=1-[2Rx/(aN)]$, $\eta=(r/a)^2$. R and N are Reynolds numbers which specify the flows through the pipe wall and through the inlet, respectively. This equation, which includes as a special case the equation previously obtained[1,2] for similar (affine) velocity profiles, is greatly simplified by passing to the limit which is approached as N increases. Nonsimilar, ζ-dependent solutions are approximated by a generalization of the method applied by Morduchow to the ζ-independent equation of Yuan[2] and Finkelstein. The results show the manner in which the condition of similarity of the velocity profiles is approached for a prescribed (e.g., parabolic) inlet profile. They also indicate the development of reverse flow at the wall of the pipe in the range of R values for which no similar solutions have been found.

* Work supported by the U. S. Atomic Energy Commission.

[1] A. S. Berman, Report K-944, Oak Ridge Gaseous Diffusion Plant, Union Carbide Nuclear Company, Oak Ridge, Tennessee, (1952).

[2] S. W. Yuan and A. B. Finkelstein, Trans. Am. Soc. Mech. Engrs. **78**, 719 (1956).

WEDNESDAY AFTERNOON AT 2:30

(W. M. ELSASSER presiding)

G1. Experimental Measurements in Controlled Fusion Research. MARK HEALD, *Project Matterhorn, Princeton University.* (30 min.)

G2. Electrohydrodynamic Properties of Satellites. L. KRAUS, *Convair-San Diego* (introduced by J. W. Bond).—The linearized theory of the interaction of a charged body in a plasma, as described by Kraus and Watson, indicates that for a small body moving at satellite velocities in the ionosphere, interesting electrohydrodynamic effects may be expected. The phenomena of interest are the drag, the increased ionization in the wake, and the angle of the wake. A parameter analysis of these phenomena permits us to assess these effects. It is found that the drag effect is negligibly small compared to neutral drag for altitudes below about 400 km. However, above 500 km this situation is reversed. For low perigee satellites, the charge drag effect may, therefore, be neglected. The increase in ionization above ambient in the wake appears to be quite large and may be detectable by low-frequency radar. The cone angle is only a few degrees. This angle increases and the ionization density in the wake decreases if the electron temperature is considerably higher than the ion temperature. Parameters consistent with satellite data have been chosen. If the surface potential of a satellite is raised by some internal means, the effects on the drag and the wake ionization can be increased considerably and offer an interesting tool for upper atmospheric investigations.

G3. Structure of Correlation in Plasma with an External Field. C. M. TCHEN, *National Bureau of Standards.*—As an extension of the Boltzmann equation, the kinetic equation for plasma is derived in the form of a generalized Fokker-Planck equation by including an external electric field. The method is based on the system of equations of Bogoliubov, Born, Green, Kirkwood, and Yvon. The binary and triple correlations are considered. The friction and diffusion coefficients are calculated in terms of the interaction law, and involve the external field. Such an occurrence of the external field in the collision terms cannot be predicted from the Boltzmann theory. The new kinetic equation is applied to the analysis of the "runaway" phenomenon of electrons.

G4. Magneto-Convection in a Viscous Fluid of Infinite Electrical Conductivity. W. V. R. MALKUS, *Woods Hole Oceanographic Institution.*—The nonlinear interactions of magnetic and motion fields are studied in nonrotating and rotating cellular convection. No external magnetic fields are imposed on the fluid system. A determination is made of the stable magnetic fields associated with the steady-state convection when the electrical resistance is zero. The viscosity and thermal diffusivity which determine the amplitude of the fields are retained in the analysis. It is found that the most stable magnetic field is that one which alters the momentum transport in a manner which permits an optimum rate of release of potential energy. For the nonrotating systems with small Prandtl number the stable state is one of detailed local equi-

partition of magnetic and kinetic energy. For the rotating system the stable state can be one of vastly greater magnetic energy than kinetic energy. The possible relation of these results to geomagnetism, solar convection, and interstellar turbulence is explored.

G5. Conductivity Measurements at Magnetic Reynolds Numbers Greater than Unity. E. B. TURNER AND E. JOHN EASTMOND, *Space Technology Laboratories.*—Measurements were made of the electrical conductivities of deuterium plasmas behind shock waves with velocities of 2.5 to 10 cm per microsecond in a ¼-in. diameter Vycor tube. The shock waves were produced by electrical discharge tubes described by Eastmond and Turner.[1] A field coil, which produced a dc field of a few hundred gauss, was used with a search coil similar to that described by Lin, Resler, and Kantrowitz.[2] Since magnetic Reynolds numbers greater than unity are attained by the plasma one cannot assume that the magnetic field is undistorted by the passage of the shock wave. The quantities $V_p/I\sigma u_2 U$ and $\varphi/I\sigma u_2$ are no longer constant but can be expressed as functions of the magnetic Reynolds number only which was determined experimentally by shooting metallic slugs of various conductivities and velocities through the coil. V_p and φ are the voltage peak and flux change through the search coil. The integrated signal from the search coil, which is proportional to the flux change, gives a more accurate measurement and a clearer representation of the conductivity changes in the nonuniform region behind the shock waves. Results showed rough agreement with Spitzer's theory.

[1] Paper E8 presented at this meeting.
[2] Lin, Resler, and Kantrowitz, J. Appl. Phys. **26**, 95 (1955).

G6. Interaction between a Strong Shock and an Inhomogeneous Magnetic Field.* M. SCHEIBE, *University of Maryland* (introduced by D. Bershader).—An investigation of the interaction between the ionized gas flow behind a strong shock and an inhomogeneous magnetic field has been conducted using pulsed fields of up to 65 000 gauss. Appreciable interactions were obtained despite the fact that the tube walls were nonconducting and the ($\mathbf{V}\times\mathbf{B}$) lines did not close in the gas. The inhomogeneity of the field provided the mechanism by which the induced currents formed closed circuits. Although the interaction was three-dimensional, the flow pattern qualitatively agreed with a one-dimensional treatment. Secondary shocks were formed in the field region and the incident shock strength was decreased upon transmission through the field. The expansion wave accompanying the decrease in shock strength was observed. An observed three-dimensional effect was the rapid readjustment of the transmitted shock to approximately its original strength after passing out of the field region. Comparison of the position of the secondary shock in the field with the values of $\rho/\sigma B^2$ seemed to indicate that the conductivity σ was a tensor rather than a scaler. This is due to the fact that currents were set up parallel to the flow as well as transverse to it.

* Work supported by the Air Research and Development Command.

G7. Magnetic Channeling and Reflection of High-Velocity Shocks. S. L. LEONARD, V. JOSEPHSON, G. E. MASEK, AND J. R. PENNING, *Space Technology Laboratories.*—High-velocity shock waves in hydrogen have been used in laboratory experiments to produce complete ionization, high conductivity, and high temperature. The application for which the plasma is intended requires minimum contamination in the plasma and high temperatures for a finite time. Therefore, it is desirable to (1) isolate the shocks from material walls to eliminate wall material contamination, and (2) to reflect the shock back through the plasma to reduce mass motion of the plasma and to continue heating it. A shock tube assembly, as described by Eastmond and Turner,[1] has been used to drive $M\sim 60$ shocks into Vycor tubes ¼-in. and ¾-in. i.d., around which have been placed axial magnetic channeling and reflection fields. Smear camera measurements have been made on shock velocity, channeling, and reflection as functions of magnetic field strengths. In addition, time resolved spectroscopy has been used to study the nature of the luminosity observed.

[1] Paper E8 presented at this meeting.

G8. On the Turbulent Flow of an Electrically Conducting Stream in the Presence of a Magnetic Field.* L. G. NAPOLITANO, *Polytechnic Institute of Brooklyn* (introduced by Antoni Ferri).—The paper is concerned with the study of the turbulent boundary layer over a flat plate when the fluid is electrically conducting and a magnetic field is present. It is assumed that the fluid has constant properties and that linearization with respect to the magnetic Reynolds number is permissible. A suitable two-layer model of the hydromagnetic turbulent boundary layer is then postulated and the energy transfer mechanism occurring therein is described. Solutions are obtained for the two layers in terms of a "magnetic parameter" ξ, and are then joined by following an extension of the Clauser approach.[1] Both the modified law of the wall and skin friction law are thus determined. The cases considered pertain to magnetic fields fixed relative to the plate and/or to the free stream. Solutions are given to within a first approximation in the magnetic parameter ξ and the corresponding results are presented and discussed.

* Work supported by the Air Research and Development Command.
[1] F. H. Clauser, Advances in Appl. Mech. **IV** (1956).

G9. Catastrophic Pitting of Meteorite Bodies.* ROBERT H. JOHNSON, *General Electric Research Laboratory.*—A very violent instability has been observed in the shock layer flow field associated with the hypersonic helium flow over blunt bodies with surface cavities. Experiments in the helium tunnel of the General Electric Research Laboratory at Mach numbers of 22 and 25 have shown that cavities of various sizes and shapes on the surface of blunt bodies cause the detached shock wave to oscillate and change shape with time. The mechanism of this instability appears to involve the formation within the cavity of vortices which are subsequently ejected from the cavity. Cavity shapes more conducive to vortex formation such as hemispherical holes have resulted in the least stable flows. Conversely, cavity shapes are not amenable to vortex growth such as a conical hole result in a more stable flow over the body. Experiments using the hydraulic analogy for compressible gas flow have illustrated the nature of this oscillatory flow. The violent action of the vortex within the cavity can account for some of the deeper pits observed in many meteorites. That is, the vortex ejection presents a mechanism for increasing the depth of a given cavity on a meteoric body during flight into the earth's atmosphere.

* Supported by the Ballistic Missile Division of the U. S. Air Force.

G10. Aerodynamic Mechanism of Pit Formation in Ablating Bodies. D. T. WILLIAMS, *University of Florida.*—Pits in meteorites have been tentatively identified as being caused by bound vortices in the boundary layers on their surfaces.* A series of experiments were carried out in which pits were formed on the surfaces of salt cakes pushed through a lake. The markings and locations of the pits were so similar to those on meteorites as to support the conculsion that the pitting in both instances has the same origin—erosion by bound vortices in the boundary layer. The effect of initial shape of the ablating salt cakes, and of differences in ablating materials lead to the following conclusions. (a) Pits form only where a positive pressure gradient exists, directed mainly downstream, but with a component normal to the flow velocity. (b) Small differences in material composition cause relatively large differences in tendency to pit during ablation.

(c) The detailed mechansim of pit formation appears to require the accumulation of vorticity in a bound vortex, like that presumed to occur in a vortex tube.

* Paper in process of publication as a *Smithsonian Contribution to Astrophysics.*

G11. Propagation of Chemical Reaction Zones in an Oxidant-Metal Dust Mixture. J. HERSHKOWITZ AND F. R. SCHWARTZ, *Picatinny Arsenal.*—High-speed photographic observations have been made of the propagation of chemical reaction in 8½ in. long columns of granular mixtures of potassium perchlorate and atomized aluminum. The mixture was loose loaded into a hole ⅜ in. in diameter bored along the axis of a 2-in. diam Lucite rod and was initiated by an electric detonater. A light emitting zone about 1 inch long propagates along the column at 820 m/sec. Behind this zone there is a dark region which is followed at a slower rate by an afterburning cloud. Preliminary experiments have been conducted on the effects of column diameter, confinement, oxidant-metal dust ratio, particle size, density, and adding explosive to the mixture. A tentative theory to explain the results has been formulated in which the initial chemical reaction is a surface or "fines" phenomena, the dark space is due to energy "sinks," and the after-burning represents combustion of the remaining mixture. Significance of the results will be discussed and plans for future work outlined.

SUPPLEMENTARY PROGRAMME

H1. Effect of Compressibility on Thermodynamic and Flow Properties for Partially Dissociated and Ionized Gases. ADOLF R. HOCHSTIM, *Convair, San Diego.*—It was found that compressibility $z=Pv/RT$ plays an important role in high-temperature thermodynamics and in flow properties. Specific heats and adiabatic gammas exhibit minima and maxima at some specific values of compressibility. The same holds true for partial derivatives of internal energy and compressibillty with respect to density and temperature. For air, $z\sim1.21$ corresponds to almost completely dissociated oxygen, $z\sim2.0$ to almost completely dissociated oxygen and nitrogen, $z\sim4.0$ to almost completely (singly) ionized oxygen and nitrogen. At these points, specific heats and difference in specific heats have minima and adiabatic gammas maxima. The ratio of densities across normal shock as a function of velocity at constant ambient density exhibits inflection points at the mentioned compressibilities. It was shown that the frequent assumption in hypersonic flow problems, namely, $\gamma'=H/E$ = constant, where H is the enthalpy and E the internal energy, leads to the result that all other adiabatic gammas are constant and equal to γ' and that the compressibility z is constant on an isentrope, e.g., for diatomic gas without virial contributions the above assumption implies that the degree of dissociation is constant on an isentrope. The dependence of thermodynamic properties on compressibility offers very attractive possibilities for numerical fit to high-temperature thermodynamics of multicomponent mixtures.

H2. On the Instability of a Plasma with Anisotropic Distribution of Ion Velocities in a Magnetic Field. EUGENE GUTH, *Oak Ridge National Laboratory.*—Gross[1] gave a theory of the small-amplitude oscillations of an ionized gas, including the effects of temperature motions using the linearized form of the Boltzmann-Maxwell equations proposed by Vlasov. This theory was improved by Sen[2] by employing the Laplace transformation method as used by Landau.[3] The plasma oscillations are found to be unstable in frequency bands around multiples of the gyro-frequency. Vedyonov and Sagdeyev[4] considered the magnetohydrodynamic oscillations taking account of the magnetic self-field, which was neglected by Gross (as an effect of order v/c). Attention is called to an extension of the work of Gross and Sen by Harris (to be published). The interrelations of these investigations will be discussed together with the relation of the hydrodynamic to the kinetic approach.

[1] E. P. Gross, Phys. Rev. **82**, 232 (1951).
[2] H. K. Sen, Phys. Rev. **88**, 816 (1952).
[3] L. Landau, J. Phys. U.S.S.R., **10**, 25 (1946).
[4] Volume III of the four presentation volumes on *The Physics of Plasmas* distributed by the U.S.S.R. at the Second Geneva Conference, September 1958; cf. also the short summary in Sec. 3 of the Geneva paper Nr-2214 by Sagdeyev *et al.*; note that Sec. 2 is just a rederivation of results obtained earlier by Rosenbluth and Longmire, Ann. Phys. (N. Y.) 1, 120 (1957), but Rosenbluth and Longmire did not consider the topics dealt with in Sec. 3 by Sagdeyev *et al.*

Errata to Minutes of the Conference on Weak Interactions at Gatlinburg which were published in the Bulletin, Series II, Volume 4, No. 1, Part 1

E8, by Eugene Guth. In line 11 from the end, instead of "give the misleading impression" read "state." Also, omit the last 2 sentences at the end and read instead "The two-component neutrino is here considered—as usual—*the limiting case of a Dirac neutrino.* If the two-component equation is considered *a limiting case of a Majorana neutrino*, then $C=1$ and $CP=P=T$ as claimed by Case, McLennan, and Serpe."

MEETINGS AND DEADLINES FOR 1959

Place	*Meeting dates*	*Deadline date*
Austin, Texas	March 6–7	past
Cambridge, Massachusetts	March 30, 31, April 1	past
Washington, D. C.	April 30, May 1–2	February 20
Milwaukee, Wisconsin	June 18–20	April 17
Honolulu*	August 27–29	July 1
Chicago	November 27–28	September 25
Pasadena*	December 28–30	October 23

* Abstracts for the Honolulu and Pasadena meetings are to be sent to W. A. NIERENBERG, University of California, Berkeley 4, California, and must reach his office not later than the corresponding deadline date.

Abstracts for the other meetings listed above are to be sent to KARL K. DARROW, American Physical Society, Columbia University, New York 27, New York, and must reach his office not later than the corresponding deadline date. Take note that abstracts mailed the day before deadline day often fail to arrive in time: the last postal delivery of the day usually comes to our office before 2 P.M. Allow at least two days for abstracts sent by airmail from points east of the Mississippi, and longer for those sent from farther west. Abstracts postmarked (at the point of dispatch) on deadline day are instantly rejected, and telegrams heralding their arrival are fruitless except in revenue to the telegraph company. Special delivery is usually useless and sometimes worse than useless; read the story recounted on page 127 of this Bulletin. *The privilege of contributing papers of meetings of the American Physical Society is restricted to the members of the Society and to nonmembers whose papers are sponsored by members.*

RULES AND INSTRUCTIONS FOR THE PREPARATION OF ABSTRACTS

The Council has ordered that abstracts shall be not longer than two hundred (200) words or the equivalent thereof. In reckoning equivalence, a footnote is equated to ten words; each line in a table to ten words; a "display" formula—one that requires a line to itself—is an expensive luxury equated to forty words.

Two copies of each abstract must be sent to the appropriate office. They must be typewritten; *one must be an original*, the other may be an original or a carbon copy. *Carbon copies will not be accepted in lieu of originals:* they smear. *Abstracts must be double-spaced:* single-spaced manuscripts are too crowded to permit the editorial markings to be made with ease and clearness. *Each abstract must be confined to a single page:* if it is too long for a single page it is too long to be printed. If we receive an abstract typed on two pages, we print only its first page. *Write each abstract as a single paragraph:* the suppression of paragraphs costs time and labor to the editors. *Do not use very thin paper;* a sheet of very thin paper may cause extraordinary trouble when mixed with sheets of reasonable thickness. *Telegraphed abstracts are refused.* The American Institute of Physics will bless you if you type first the title of your abstract in lower-case with capitalized initials, then your name in capitals, then the name of your institution in lower-case underlined. Issues of the *Bulletin* are always appreciably delayed because the editors have to do what the authors should have done.

Remember the rule of the Council that, if an author submits more than one abstract, all but one must go onto the Supplementary Programme. In enforcing this rule, an abstract is credited to the author whose name appears first in the by-line.

It has now become an expensive business to make any change in an abstract, even the smallest, after the abstract has gone to press. By order of our Council "A change in an abstract will be permitted only at the discretion of the Secretary or his deputy, and only if TEN DOLLARS is enclosed with the letter in which the change is requested." As heretofore, an abstract will not be withdrawn from proof unless the asker sends ten dollars with his request.

AMERICAN PHYSICAL SOCIETY

MARCH 30 - APRIL 1, 1959

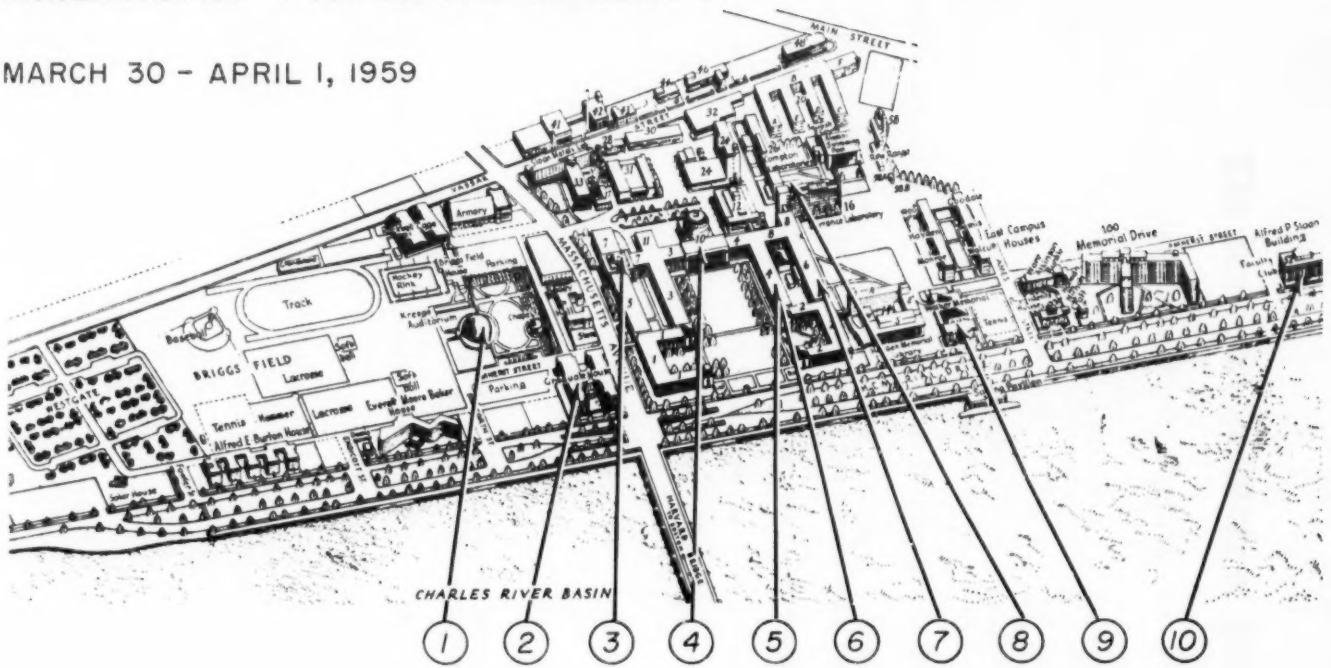

1 · KRESGE AUDITORIUM AND LITTLE THEATRE

2 · GRADUATE HOUSE

3 · REGISTRATION, BUILDING 7 LOBBY

4 · ROOM 10 - 250

5 · ROOM 4 - 270

6 · ROOM 4 - 370

7 · ROOM 6 - 120

8 · ROOM 26 - 100

9 · WALKER MEMORIAL

10 · FACULTY CLUB

The American Institute of Physics

OFFICERS OF THE SOCIETY FOR 1959

President	G. E. UHLENBECK	University of Michigan
Vice-President	V. F. WEISSKOPF	Massachusetts Institute of Technology
Secretary	K. K. DARROW	Bell Telephone Laboratories (*retired*) (Office at Columbia University)
Treasurer	S. L. QUIMBY	Columbia University
Managing Editor	S. A. GOUDSMIT	Brookhaven National Laboratory

Past Presidents now on Council: W. F. G. Swann, E. P. Wigner, H. D. Smyth, and J. W. Beams.

Elected Members now on Council: S. K. Allison, N. F. Ramsey, Walker Bleakney, W. K. H. Panofsky, W. A. Fowler, Charles Kittel, Harvey Brooks, and Charles Hard Townes.

Local Secretary for the Pacific Coast	W. A. NIERENBERG	University of California, Berkeley
Deputy Secretary	W. W. HAVENS, JR.	Columbia University

Please cut along this line

(To be sent to Professor John C. Slater, Massachusetts Institute of Technology, Cambridge 39, Massachusetts)

I expect to attend the banquet of Tuesday evening, March 31. My party will comprise ..... persons.

I expect to attend the social hour of Monday afternoon, March 30. My party will comprise ..... persons.

If you want to be sure of having tickets, send with this form a check (made out to American Physical Society) for $3.00 multiplied by the number of banquet reservations plus $1.50 multiplied by the number of reservations for the social hour. Your tickets will be held in your name at the desk.

Name.....